



IRON(III) PHOSPHATE CATALYZED SYNTHESIS OF β-AMIDO CARBONYL COMPOUNDS

Farahnaz K. Behbahani^{[a]*}, Sara Naeini^[b], Saeed Suzangarzadeh^[b]

Keywords: iron(III) phosphate (FePO₄); β-acetamido carbonyl compounds; catalyst; synthesis

Aldehydes have been used in a one-pot reaction with enolizable ketones, acetonitrile, benzonitrile and acetyl chloride in the presence of FePO₄ at room temperature to form the corresponding β-acetamido ketones in very good yields. Three new compounds and rare β-amido ketones are reported additionally. The use of readily available FePO₄ as a catalyst renders this process quite simple and convenient.

Corresponding Authors

Tel: +98 026 34418145

Fax: +98 026 34418156

E-Mail: Farahnazkargar@yahoo.com

[a] Department of chemistry, Karaj Branch, Islamic Azad University, Karaj, Iran.

[b] Department of Chemistry, Shahr-E-Rey Branch, Islamic Azad University, Tehran, Iran.

Introduction

β-Acetamido ketone skeletons exist in a number of biological and pharmaceutical compounds makes them valuable building blocks^{1,2} and there have been intensive attempts to synthesize β-amido ketones. The best-known route for the synthesis of these compounds is the Dakin–West reaction,³ which involves the condensation of an α-amino acid with acetic anhydride in the presence of a base to afford the β-acetamido ketones.⁴ Another procedure for the formation of these compounds from condensation of enolizable ketones, an aryl aldehyde, and acetyl chloride in nitriles in the presence of heterogeneous and homogeneous acid catalysts have been reported by Nabid and Tabatabaei⁵ and others references therein. Recently, Fe(ClO₄)₃⁶ and CuSO₄·5H₂O⁷ was also reported by our research group.

In addition to mentioned above, FePO₄ is cheap, safe and available reagent⁸ that has also been employed for the selective oxidation of CH₄ to CH₃OH⁹ and benzene to phenol¹⁰ one-pot synthesis of dihydropyrimidinones and thiones¹¹, one-pot three component synthesis of 2,4,5-trisubstituted imidazoles¹², acetylation alcohols and phenols¹³ and tetrahydropyranation alcohols and phenols.¹⁴ In this communication we wish to report synthesis of β-amido

ketones with enolizable ketones, acetonitrile, benzonitrile and acetyl chloride in the presence of FePO₄ at room temperature (Scheme 1).

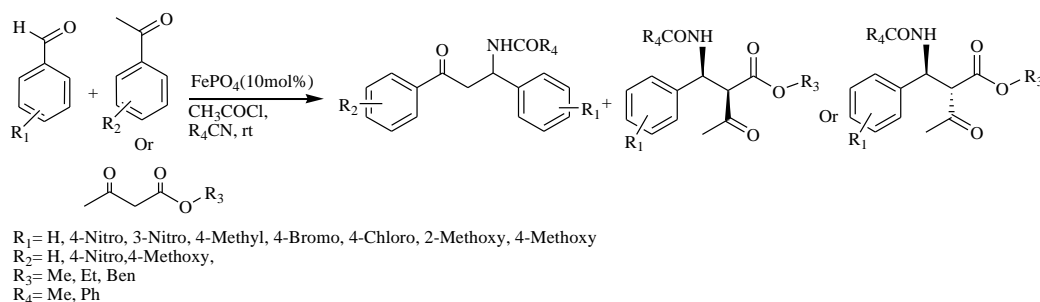
Results and discussion

At the first, the reaction of benzaldehyde, acetophenone, acetyl chloride and acetonitrile was studied in the absence of catalyst. The reaction was not completed even after 24 h. Obviously, the catalyst is an effective component for this reaction.

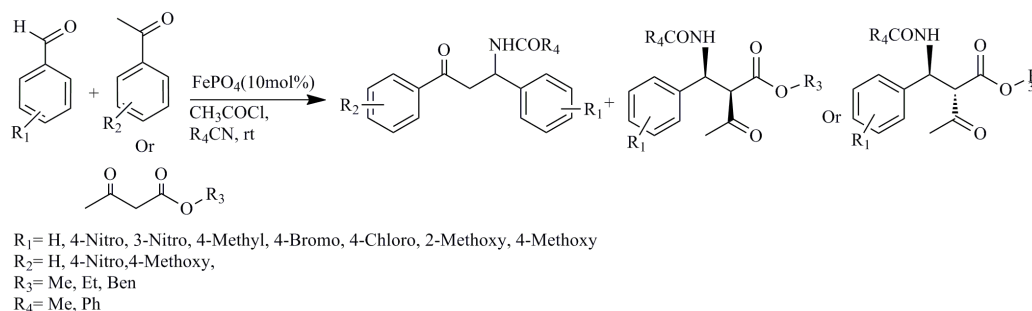
In a model reaction, with benzaldehyde (5.0 mmol), acetophenone (5.0 mmol), AcCl (1.5 mmol), acetonitrile (1.0 ml) and FePO₄ (0, 2, 5, 10, 15 mol %) stirred at room temperature without solvent. The conversion was completed at appreciated time in table 1. The product was obtained using 10 mol% of FePO₄ in 92% yield. Thus the entry 4 of Table 1 was selected and the reactions were continued under optimized conditions.

Table 1. The Optimization of FePO₄ for the synthesis of N-(3-oxo-1,3-diphenylpropyl) acetamide (**1**)

| Entry | Catalyst, mol % | Time, h | Yield, % |
|-------|-----------------|---------|----------|
| 1 | 0 | 48 | 10 |
| 2 | 2 | 30 | 50 |
| 3 | 5 | 9 | 65 |
| 4 | 10 | 4.5 | 92 |
| 5 | 15 | 4.5 | 92 |



Scheme 1



Scheme 2

Table 2. FePO₄-catalyzed synthesis of β-amido ketones

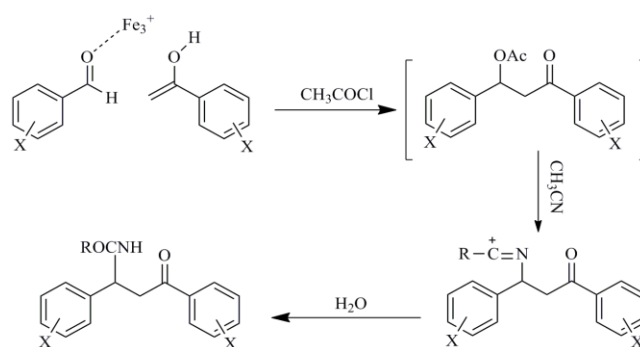
| Entry | R ₁ | R ₂ | R ₃ | R ₄ | Time, h | Yield, % | M.p., °C, Found | Reported ^{ref.} |
|-----------------|-------------------|-------------------|----------------|---|---------|----------|-----------------|--------------------------|
| 1 | H | H | | Me | 6 | 92 | 105-107 | 105-107 ⁷ |
| 2 | H | H | | Ph | 6 | 92.5 | 152-154 | 153-154 ⁷ |
| 3 | 4-NO ₂ | H | | Me | 6 | 91 | 147-148 | 148-149 ⁷ |
| 4 | 3-NO ₂ | H | | Me | 6.5 | 85 | 137-139 | 140-139 ⁷ |
| 5 | 4-Br | H | | Me | 5 | 94 | 148-149 | 147-148 ⁷ |
| 6 | 4-Cl | H | | Me | 4 | 90 | 178-179 | 180-182 ⁷ |
| 7 | 4-Cl | H | | Ph | 4 | 93 | 131-132 | 131-133 ⁷ |
| 8 | 4-Cl | | OMe | Me | 3.5 | 88 | 109-110 | 110-112 ⁷ |
| 9 | 4-Cl | 4-NO ₂ | | Me | 8 | 85 | 119-120 | 121-122 ¹⁵ |
| 10 | 2-Cl | H | | Me | 7 | 92 | 133-135 | 135-136 ¹⁴ |
| 11 | 2-NO ₂ | H | | Me | 8 | 91 | 145-147 | 148-150 ¹⁵ |
| 12 | 2-OMe | 4-NO ₂ | | Ph | 4 | 85 | 136-138 | 138-140 ⁷ |
| 13 ^a | 4-Cl | 4-Br | | Ph | 8 | 85 | 119-120 | - |
| 14 ^a | 4-NO ₂ | H | | 4-CH ₃ C ₆ H ₄ | 4 | 85 | 158-160 | - |
| 15 ^a | 4-NO ₂ | 4-Br | | Ph | 2.5 | 98 | - | - |

a) new compounds

To prove the generality of the optimized reaction conditions, the variety of aldehydes with electron-donating and electron-withdrawing groups on the aromatic ring and enolizable ketones such as acetophenone, 4-nitro acetophenone, benzyl, ethyl and methyl acetoacetate were also subjected to Dakin-West reaction in the presence of FePO₄ as a catalyst. The results showed that the naturality of groups didn't affect upon the reaction time and yields (Table 2). In all contents, complete conversion was observed after appropriate time and the products were isolated in very high yields. β-Acetamido ketones were also prepared from β-keto esters by the reaction of aromatic aldehydes, acetonitrile and acetyl chloride in the presence of FePO₄. Interestingly, it was also found that the products of entries 13, 14, and 15 have not previously been prepared and so they were new compounds.

A mechanism may be postulated as shown below (Scheme 2). The mechanism¹⁶ may involve the enolic form of the ketone which attacks the activated aldehyde to provide a β-acetoxy ketone. The acetyl group is displaced by alkyl/aryl nitrile followed by water addition leads to provide the product.

To show the fairly advantages of using FePO₄ as a catalyst in the synthesis of (1), our protocol was compared with previously reported methods (Table 3). From the results given in Table 3, the advantages of this work are evident regarding the yields of the reactions which are very important in chemical industry especially when it is combined by easy separation.



Scheme 3.

Experimental

Melting points were measured by using the capillary tube method with an electro thermal 9200 apparatus. IR spectra were recorded on Bruker FT-IR spectrometer did scanning between 4000–400 cm⁻¹. ¹H NMR and ¹³CNMR spectra were obtained on Bruker DRX-300MHz NMR instrument. Mass spectra were taken on an Agilent 5973 Network Mass Selective Detector instrument.

Synthesis of β- acetamido ketone and esters: General procedure. A mixture of ketone or ethyl, and methyl acetoacetate (5.0 mmol), aldehyde (5.0 mmol) and acetyl

Table 3 The synthesis of (1) using variety of catalysts was compared.

| Entry | Catalyst | Mol % or g | Time, h | Temp., °C | Yield, % ^{Ref.} |
|-------|---|------------|---------|-----------|--------------------------|
| 1 | Montmorillonite K-10 | 2 g | 7 | 70 | 80 ¹⁷ |
| 2 | Silica-sulfuric acid | 78 | 1.08 | 80 | 91 ¹⁸ |
| 3 | Sc(OTf) ₃ | 10 | 30 | r.t | 82 ¹⁶ |
| 4 | Cu(OTf) ₂ | 10 | 30 | r.t | 64 ¹⁶ |
| 5 | Bi(OTf) ₃ | 10 | 30 | r.t | 69 ¹⁶ |
| 6 | I ₂ | 10 | 4.5 | r.t | 85 ¹⁹ |
| 7 | BiCl ₃ or BiOCl | 20 | 7 | r.t | 92 ²⁰ |
| 8 | LiClO ₄ | 100 | 0.5 | r.t | 59 ²¹ |
| 9 | InCl ₃ | 100 | 0.5 | r.t | 19 ²¹ |
| 10 | ZrOCl ₂ .8H ₂ O | 20 | 5 | r.t | 90 ²² |
| 11 | Amberlyst-15 | 0.2g | 6 | r.t | 89 ²³ |
| 12 | H ₆ P ₂ W ₁₈ O ₆₃ | 7 | 1 | 80 | 85 ²⁴ |
| 13 | FeCl ₃ .6H ₂ O | 10 | 8 | r.t | 88 ²⁵ |
| 14 | CuO | 50 | 20 | 80 | 40 ²⁶ |
| 15 | Fe ₂ O ₃ | 50 | 20 | 80 | 65 ²⁶ |
| 16 | CdO | 50 | 18 | 80 | 35 ²⁶ |
| 17 | TiO ₂ | 50 | 18 | 80 | 20 ²⁶ |
| 18 | ZnO | 50 | 6 | 80 | 90 ²⁶ |
| 19 | Heteropoly acid | 0.7 | 0.41 | 80 | 86 ²⁴ |
| 20 | ZnO | 50 | 6 | 80 | 90 ²⁷ |
| 21 | NH ₂ SO ₃ H | 5 | 1.41 | r.t | 90 ²⁸ |
| 22 | Co(HSO ₄) ₂ | 20 | 0.9 | r.t | 92 ²⁹ |
| 23 | Zn(HSO ₄) ₂ | 20 | 0.5 | r.t | 90 ²⁹ |
| 24 | ZnO bulk | 10 | 4 | r.t | 55 ²⁵ |
| 25 | ZnO nanoparticles | 10 | 1 | r.t | 83 ²⁵ |
| 26 | PANI-H ₂ SO ₄ | 20 | 1 | 50 | 90 ⁵ |
| 27 | Fe(ClO ₄) ₃ .6H ₂ O | 1 | 3.5 | 80 | 77 ⁶ |
| 28 | Mg(HSO ₄) ₂ | 20 | 0.83 | r.t | 89 ³⁰ |
| 29 | MgCl ₂ | 20 | 20 | r.t | 30 ³⁰ |
| 30 | Zr(HSO ₄) ₂ | 20 | 0.5 | r.t | 90 ³⁰ |
| 31 | ZrCl ₄ | 20 | 5 | r.t | 80 ³⁰ |
| 32 | CeSO ₄ | 20 | 3.5 | 85 | 83 ²⁵ |
| 33 | Mn(bpdo) ₂ Cl ₂ /MCM-41 | 10 | 7 | r.t | 96 ³¹ |
| 34 | CeCl ₃ .7H ₂ O | 10 | 13 | r.t | 82 ³² |
| 35 | FePO ₄ | 10 | 4.5 | r.t | 92 ^{This work} |

chloride (1.5 mmol) in 1 ml of acetonitrile/benzonitrile was treated with a catalytic amount of FePO₄ (10 mol%) at room temperature. The progress of the reaction was monitored by TLC. Upon completion of the reaction, a mixture of crushed ice (50 ml) was added to the reaction mixture. The precipitated solid was filtered off. The residue was washed with water (20 ml) and the crude product recrystallized from ethyl acetate/n-hexane.

Physical and spectra data for new compounds

N-(3-(4-bromophenyl)-1-(4-chlorophenyl)-3-oxopropyl)-benzamide (entry 13): Yield=85%, M.p= 119-120 °C, white solid; IR (KBr) 3295, 3059, 1688, 1655, 1603, 1585, 1069, 1096, 815 cm⁻¹; ¹H NMR (CDCl₃) δ: 3.47 (dd, 1H, J=7.8Hz and J=13.45Hz, CH₂), 3.83 (dd, 1H, J=8.7Hz and J=15.25Hz, CH₂), 5.71 (m, 1H, CH), 7.26 (m, 1H, NH), 7.39 (d, 2H, J=8.3Hz, ArH), 7.64 (d, 2H, J=8.31Hz, ArH), 7.57 (d, 2H, J=8.22Hz, Ar), 7.88 (d, 2H, J=8.32Hz, Ar), 7.73 (m, 5H, ArH). ¹³C NMR (CDCl₃) δ: 199, 167, 149, 146,

136, 134, 131, 128, 127, 120, 52, 48 ppm; MS m/z: 443[M⁺], C₂₂H₁₇BrClNO₂.

4-methyl-N-(1-(4-nitrophenyl)-3-oxo-3-phenylpropyl)-benzamide (entry 14): Yield=85%, M.p=158-160 °C, white solid; IR (KBr) 3306, 3061, 2956, 2922, 1687, 1624, 1545, 1356, 833, 754 cm⁻¹; ¹H NMR (CDCl₃) δ: 2.39 (s, 3H, CH₃), 3.50 (dd, 1H, J=4.74 and 4.59Hz, CH₂), 3.84 (dd, 1H, J=16.87Hz, CH₂), 5.71 (m, 1H, CH), 7.32-7.34 (m, 1H, NH), 7.26 (d, 2H, J=6.84Hz, ArH), 7.46 (d, 2H, J=6.78Hz, ArH), 7.56-7.67 (m, 5H, ArH), 7.73 (d, 2H, J=7.05Hz, ArH), 7.91 (d, 2H, J=6.93Hz, ArH) ppm; ¹³C NMR (CDCl₃) δ: 200, 167, 149, 146, 142, 136, 133, 131, 127, 120, 52, 44, 24 ppm; MS m/z: 388[M⁺], C₂₃H₂₀N₂O₄.

N-(3-(4-bromophenyl)-1-(4-nitrophenyl)-3-oxopropyl)-benzamide (entry 15): Yield=98%, M.p=191-192 °C, light yellow solid; IR (KBr) 3309, 3058, 2924, 1688, 1629, 1522, 1347, 1581, 1074, 848, 817 cm⁻¹; ¹H NMR (CDCl₃) δ: 3.55 (dd, 1H, J=12.04Hz, CH₂), 3.88 (dd, 1H, J=12.74Hz, CH₂), 5.83 (m, 1H, CH), 7.26-7.55 (m, 1H, NH), 7.47 (d, 1H,

$J=7.28\text{Hz}$, ArH), 7.60 (d, 5H, $J=7.8\text{Hz}$, ArH), 7.52-7.78 (m, 5H, ArH), 7.84 (d, 1H, $J=7.04\text{Hz}$, ArH), 8.16 (d, 1H, $J=7.02\text{Hz}$, ArH) ppm; ¹³C NMR (CDCl₃) δ: 199, 166, 148, 145, 134, 133, 130, 127, 126, 120, 50, 45 ppm; MS m/z : 77[C₉H₁₄], 105[C₁₀H₁₄O], 155[C₉H₁₃Br], 185[C₁₀H₁₃BrO], 349[C₁₈H₂₁BrN₂O₃], 452[M⁺], 454[M+2]⁺, C₂₂H₁₇BrN₂O₄.

Conclusion

In conclusion, the new simple catalytic process can produce, under mild conditions, an effective multicomponent transformation of enolizable ketones, acetonitrile, benzonitrile and acetyl chloride in the presence of FePO₄ at room temperature to form the corresponding β-acetamido ketones in high yields. The reaction system can be successfully applied to a variety of aryl aldehydes to synthesize a wide variety of new β-acetamido ketones.

References

- Casimir, J. R.; Turetta, C.; Ettouati, L.; Paris, J., *Tetrahedron Lett.*, **1995**, 36, 4797.
- Godfrey, A. G.; Brooks, D. A.; Hay, L. A.; Peters, M.; McCarthy, J. R.; Mitchell, D., *J. Org. Chem.*, **2003**, 68, 2623.
- Dakin, H. D.; West, R., *J. Biol. Chem.*, **1928**, 78, 745.
- Buchanan, G. L., *Chem. Soc. Rev.*, **1988**, 17, 91.
- Nabid, M. R.; Tabatabaei Rezaei, S., *J. Appl. Catal. A: Gen.*, **2009**, 366, 108.
- Heravi, M. M.; Behbahani, F. K.; Daraie, M.; Oskooie, H. A., *Mol. Divers.* **2009**, 13, 375.
- Behbahani, F. K.; Doragi, N.; Heravi, M. M., *Synth. Commun.*, **2012**, 1, 42.
- TAP report for Iron (III) phosphate July. **2004**.
- Otsuka, K.; Wang, Y., *J. Appl. Catal. A.*, **2001**, 145, 222.
- Ren, T., an, L., Zhang, X., Suo, J., *J. Appl. Catal. A.*, **2003**, 11, 244.
- Heravi, M. M.; Behbahani, F. K.; Zadsirjan, V.; Oskooie, H. A., *Heterocyclic Commun.*, **2006**, 12, 369.
- Behbahani, F. K.; Yektanezhad, T.; Khorami, A. R., *Heterocycles* **2010**, 81, 2313.
- Behbahani, F. K.; Frahani, M.; Oskooie, H. A., *Korean J. Chem. Soc.*, **2011**, 55, 633.
- Behbahani, F. K.; Farahani, M., *Lett. Org. Chem.* **2011**, 8, 431.
- Shinu, V. S.; Sheeja, B.; Purushothaman, E.; Bahulayan, D., *Tetrahedron Lett.* **2009**, 50, 4838.
- Pandey, G.; Singh, R. P.; Garg, A.; Singh, V. K., *Tetrahedron Lett.* **2005**, 46, 2137.
- Yakaiah, T.; Lingaiah, B. P. V.; Reddy, G. V.; Narsaiah, B.; Rao, P. S., *Arkivoc* **2007**, XIII, 227.
- Khodaei, M. M.; Khosropour, A. R.; Fattahpour, P. A., *Tetrahedron Lett.* **2005**, 46, 2105.
- Das, B.; Reddy, K. R.; Ramu, R.; Thirupathi, P.; Ravikanth, B., *Synlett*, **2006**, 1756.
- Ghosh, R.; Maiti, S.; Chkraborty, A., *Synlett*, **2005**, 115.
- Khan, A. T.; Parvin, T.; Choudhury, L. H., *Tetrahedron Lett.*, **2007**, 63, 5593.
- Ghosh, R.; Maiti, S.; Chkraborty, A.; Chkraborty, S.; Mukherjee, A. K., *Tetrahedron Lett.*, **2006**, 62, 4059.
- Das, B.; Reddy, K. R., *Helv. Chim. Acta.*, **2006**, 89, 3109.
- Heravi, M. M.; Ranjbar, L.; Derikvand, F.; Bamoharram, F. F., *Catal. Commun.*, **2007**, 8, 289.
- Mirjafary, Z.; Saeidian, H.; Sadeghi, A.; Matloubi Moghaddam, F., *Catal. Commun.*, **2008**, 9, 229.
- Maghsoodlou, M. T.; Hassankhani, A.; Shaterian, H. R.; Habibi_khorasania, S. M.; Mosaddegh, E., *Tetrahedron Lett.*, **2007**, 48, 1729.
- Nagarapu, L.; Kantevari, S.; cheemalapati, V. N.; Apuri, S.; Kumari, N. V., *J. Mol. Catal. A: Chem.*, **2007**, 264, 22.
- Heravi, M. M.; Ranjbar, L.; Derikvand, F.; Bamoharram, F. F., *J. Mol. Catal. A: Chem.*, **2007**, 276, 226.
- Momeni, A. R.; Sadeghi, M.; Hadizadeh, M., *Turk. J. Chem.*, **2009**, 33, 751.
- Momeni, A. R.; Sadeghi, M., *Appl. Catal. A: Gen.*, **2009**, 357, 100.
- Heravi, M. M.; Behbahani, F. K.; Malakooti, K., *Synthetic Commun.*, **2010**, 40, 1180.
- Khan, A. T.; Choudhury, L. H.; Parvin, T.; Ali, A., *Tetrahedron Lett.*, **2006**, 47, 8137.

Received: 07.04.2013.

Accepted: 08.06.2013.



CERRIC AMMONIUM NITRATE (CAN) CATALYSED SYNTHESIS OF PYRANO[2,3-*d*]PYRIMIDINE-2,4,7-TRIONES IN AQUEOUS MEDIUM UNDER SONICATION VIA ONE-POT THREE COMPONENT REACTON

Anshu Dandia^{[a]*}, Shyam L. Gupta^[a] and Sumit Bhaskaran^[a]

Keywords: Pyrano[2,3-*d*]pyrimidine, 1,3-dimethyl barbituric acid, ceric ammonium nitrate (CAN), ultrasound irradiation.

A green, environmentally benign, facile and efficient one-pot three-component reaction of benzaldehyde, barbituric acid and mel drum's acid for the synthesis of 5-phenyl-5,6-dihydro-1*H*-pyrano[2,3-*d*]pyrimidine-2,4,7(3*H*)-trione derivatives using ceric ammonium nitrate (CAN) as a catalyst in aqueous medium under ultrasonic irradiation is described. 1,3-dimethyl barbituric acid gives slightly lower yield as compared to barbituric acid and takes longer time to complete the reaction. Excellent yields, no need of base, and simple workup procedure are the prominent features of this protocol.

Corresponding Authors

Tel.: +91-9414073436

E-Mail: dranshudandia@yahoo.co.in

[a] Centre of Advanced Studies, Department of Chemistry,
University of Rajasthan, Jaipur-302004 India

INTRODUCTION

Organic synthesis performed through multicomponent reactions is an attractive area of research in organic chemistry. Multicomponent reactions (MCRs)¹⁻³ can be defined as convergent chemical processes where three or more reagents are combined in such a way that the final product retains significant portions of all starting materials. They offer a highly atom-economic and efficient way of generating complex molecules in fewer numbers of steps, often with minimal byproducts. One-pot MCRs often shorten reaction periods, giving higher overall chemical yields than multiple-step syntheses, and therefore can reduce the use of energy and manpower.⁴ The combination of multicomponent reactions (MCRs) and nonconventional solvents like water has become a new research direction, which enables simultaneous growth of both MCRs and green solvents toward ideal organic synthesis.⁵⁻⁶ The use of water as a green solvent in organic reactions has improved not only the aspect of the reactions from the viewpoint of green and sustainable properties, but also the synthetic efficiency by stabilizing the catalyst, changing the reaction selectivity or facilitating product isolation.⁷

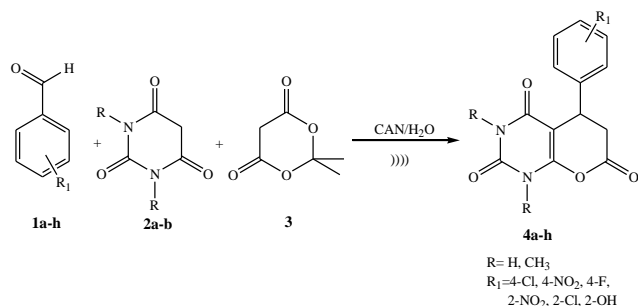
The fused pyrimidines are an important class of compounds as chemotherapeutic agents in attracting attention of medicinal chemists for their antibacterial⁸, antiviral⁹ and cytotoxic¹⁰ properties. The pyrano-fused pyrimidines showed a broad range of biological activities, such as antitubercular, antimicrobial,¹¹⁻¹² antiplatelet,¹³ antifungal,¹⁴ antiviral,¹⁵ analgesic as well as anticonvulsant activities and also showed effects against amphetamine induced stereotypy and on potentiation of pentobarbitone sodium hypnosis.¹⁶ Moreover, all the compounds which have a uracil moiety in the skeleton of an organic molecule

showed antitumor, antibacterial, bronchodilator, vasodilator, antihypertensive, cardiotoxic, hepatoprotective, and antiallergic activities; some of them also exhibit antimalarial, analgesic, antifungal, and herbicidal properties.¹⁷⁻¹⁹ Because of these biological activities, these compounds have distinguished themselves as heterocycles of profound chemical and biological significance. Thus, the synthesis of these molecules has attracted considerable attention²⁰ but all these methods suffered from drawbacks such as longer reaction time, use of hazardous organic solvents and reagents, use of conventional conditions etc. Recently Pasha *et al.*²¹ reported a methodology for the synthesis of pyranopyrimidine under microwave irradiation but in this method base is needed for the completion of reaction. Thus, the search for new catalyst and methods is still of growing importance and interest.

Ultrasound irradiation has been utilized to accelerate a number of synthetically useful reactions during the last few years. Thus, a large number of organic reactions can be carried out under ultrasonic irradiation in high yields, short reaction time and mild conditions.²²⁻²³ Cavitation is the formation, growth and collapse of bubbles in an irradiated liquid. This effect induces very high local pressure and temperature inside the bubbles and enhances mass transfer and turbulent flow in the liquid.²⁴ Sonochemistry shares sustainable chemistry with aims such as the use of less hazardous chemicals and solvents, reduced energy consumption and increased product selectivity.²⁵

Cerium (IV) ammonium nitrate (CAN) is one of the most interesting oxidants in organic synthesis since it is stable in different solvents and is commercially available.²⁶ Recently, ceric ammonium nitrate (CAN) received considerable attention as an inexpensive, nontoxic and readily available catalyst for catalyzing various organic transformations not only based on its electron transfer capacity but also with its Lewis acidic property.²⁷ It has many advantages such as solubility in water, inexpensiveness, eco-friendly nature, simplicity in handling, high reactivity and easy work-up procedures.²⁸

As a part of our ongoing research program on the development of green methodologies in the synthesis of biological important compounds using readily available, inexpensive, and environment friendly catalysts,²⁹ herein, we report a facile, and rapid one-pot three-component route to the synthesis of 5-aryl-5,6-dihydro-1*H*-pyrano[2,3-*d*]pyrimidine-2,4,7-triones by the reaction of aromatic aldehydes **1a-h**, barbituric acid **2a-b** and meldrum's acid **3** in the presence of CAN as the Lewis catalyst under ultrasonic irradiation in aqueous medium (Scheme 1).



Scheme 1. Synthesis of pyrano[2,3-*d*]pyrimidine-2,4,7-trione derivatives

RESULTS AND DISCUSSION

Initially, in order to optimize the reaction conditions, we choose the reaction of 4-chlorobenzaldehyde **1a**, barbituric acid **2a** and meldrum acid **3** in the presence of 10 mol % CAN in different solvents using ultrasonic irradiation (Table 1) but we found that the best conversion was observed when the reaction was performed in water (Table 1, Entry 6). The use of other solvents such as ethanol, methanol, toluene, acetonitrile and CH₂Cl₂ gave poor to moderate yields (Table 1, Entry 1-5).

Table 1. Effect of solvent on the synthesis of 5-(4-chlorophenyl)-5,6-dihydro-1*H*-pyrano[2,3-*d*]pyrimidine-2,4,7(3*H*)-trione (**4a**)^a

| S. No. | Solvents | Time, min | Yield, %* |
|--------|---------------------------------|-----------|-----------|
| 1 | Acetonitrile | 105 | 58 |
| 2 | Toluene | 135 | 42 |
| 3 | Methanol | 68 | 68 |
| 4 | Ethanol | 54 | 72 |
| 5 | CH ₂ Cl ₂ | 120 | 58 |
| 6 | Water | 30 | 94 |

^aReactions are performed on a 2 mmol scale of the reactants and 10 mol% of CAN under ultrasonic irradiation; *Isolated Yield

Further, we focused on systematic evaluation of different catalysts for the model reaction of 4-chlorobenzaldehyde **1a**, barbituric acid **2a** and meldrum acid **3** in water under ultrasonic irradiation. In order to confirm the effective involvement of catalyst during this transformation, we carried out the model reaction without any catalyst. In the absence of catalyst, the reaction was incomplete even after 4 hr of sonication (Table 2, entry 1) and Knoevenagel adduct was the only product. Further use of K₂CO₃ as a catalyst doesn't seem to increase the yield (22%, Table 2, entry 2). Now, a wide range of catalysts were employed including *p*-TSA, sulfamic acid, L-proline and CAN to improve the yield of product (Table 2). The results are summarized in

Table 2 which showed that in presence of CAN the desired product was obtained in 94% yield within 30 min. Therefore, this catalyst appears to be superior to any of the other catalysts tested.

Further, in order to optimize the amount of CAN for the synthesis of the target compounds, we started the study by treating a mixture of 4-chlorobenzaldehyde **1a**, barbituric acid **2a** and meldrum acid **3** in the presence of different amounts of CAN under ultrasonic irradiation (Table 2; entries 6, 7, 8) but we found that 10 mol % of CAN gave the best result in terms of time of completion and the product was obtained in 94% yield (Table 2; entry 7).

Table 2. Influence of various catalysts on the synthesis of 5-(4-chlorophenyl)-5,6-dihydro-1*H*-pyrano[2,3-*d*]pyrimidine-2,4,7(3*H*)-trione (**4a**)^a

| S. No. | Catalyst | Time, min | Yield, %* |
|--------|--------------------------------|-----------|-----------|
| 1 | - | 240 | NR |
| 2 | K ₂ CO ₃ | 150 | 22 |
| 3 | <i>p</i> -TSA | 110 | 58 |
| 4 | Sulfamic acid | 124 | 62 |
| 5 | L-proline | 80 | 73 |
| 6 | CAN (5 mol %) | 62 | 82 |
| 7 | CAN (10 mol %) | 30 | 94 |
| 8 | CAN (15 mol %) | 30 | 93 |

^aReactions are performed on a 2 mmol scale of the reactants in water under ultrasonic irradiation; NR – No reaction; *Isolated Yield

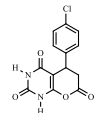
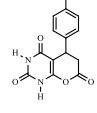
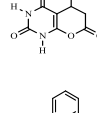
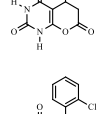
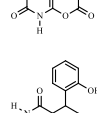
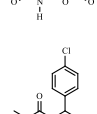
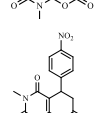
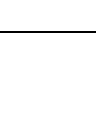
To test the generality of this reaction, a series of aromatic aldehydes with both electron-donating and electron-withdrawing substituents were reacted with meldrum acid and barbituric acid under the optimized reaction conditions, and the results are summarized in Tables 3. Results indicated that a series of aromatic aldehydes were successfully employed to prepare the corresponding product in excellent yields and there is no major effect on the yield of product by electron donating/withdrawing substituents.

Further, we used 1,3-dimethyl barbituric acid in place of barbituric acid and interestingly we found that the reaction proceeds at slower rate as compared to barbituric acid in terms of time and product yield. This was because the acidity of methylene proton of 1,3-dimethylbarbituric acid is lower (pK_a=7.1)²⁹ than barbituric acid (pK_a=4.01)³⁰ and the carbanion formation is difficult than barbituric acid and this is the reason why reaction proceeds with slower rate.

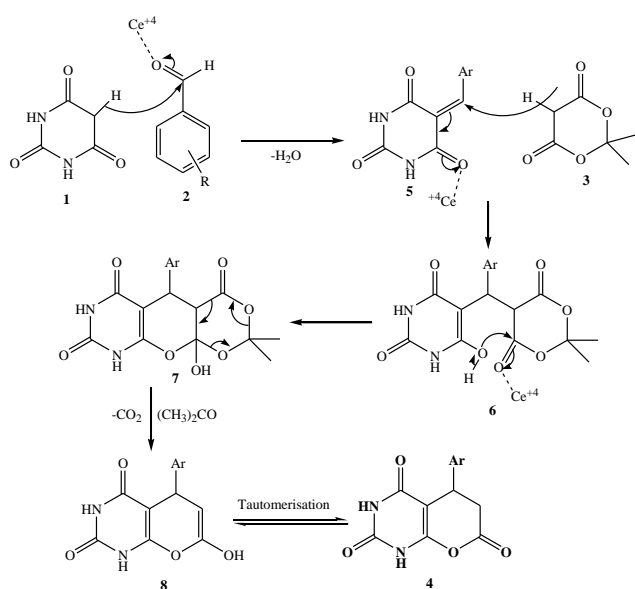
The pure products were obtained simply by recrystallization from ethanol without involving any chromatographic purification. All the synthesized compounds are new and were characterized by IR, ¹H NMR, ¹³C NMR and mass analysis.

Mechanistically, the formation of the product is expected to involve the formation of a Knoevenagel adduct **5** by the condensation between **1** and **2** and this condensation is facilitated by the coordination of Ce⁺⁴ ion with carbonyl oxygen. Further the Michael addition is also facilitated by the coordination of Ce⁺⁴ between **3** and **5** to give **6**, which cyclise to give tricyclic intermediate **7**, which in turn releases acetone and carbon dioxide and gave compound **8** which tautomerises into final compound **4** (Scheme-2).

Table 3. Synthesis of compounds 4a-h

| S.No. | R | R ₁ | Time, min | Yield, %* | | Mp (°C) |
|-------|-----------------|-------------------|-----------|-----------|--|---------|
| 4a | H | 4-Cl | 30 | 94 |  | 284-286 |
| 4b | H | 4-NO ₂ | 26 | 96 |  | 250-252 |
| 4c | H | 4-F | 31 | 94 |  | 264-266 |
| 4d | H | 2-NO ₂ | 27 | 95 |  | 216-218 |
| 4e | H | 2-Cl | 29 | 95 |  | 242-244 |
| 4f | H | 2-OH | 32 | 94 |  | 290-292 |
| 4g | CH ₃ | 4-Cl | 40 | 83 |  | 304-306 |
| 4h | CH ₃ | 4-NO ₂ | 37 | 86 |  | 318-320 |

*Isolated yield

**Scheme 2.** Plausible Mechanism**EXPERIMENTAL SECTION**

Melting points were recorded on a Toshniwal apparatus and are uncorrected. The purity of compounds was checked on thin layers of silica gel in various non-aqueous solvent systems e.g. n-hexane: ethyl acetate (7:3), benzene:ethyl acetate (9:1), benzene:dichloromethane (8:2). IR spectra (KBr) were recorded on Shimadzu FT IR-8400s spectrophotometer and ¹H-NMR and ¹³C-NMR spectra were recorded on a Bruker DRX-300 instrument at 300 and 75, respectively in DMSO-*d*₆ relative to tetramethylsilane as an internal reference. Mass spectrum of representative compound was recorded on Waters Xevo Q-ToF spectrometer at 70 eV. Elemental microanalyses were carried out on a Carlo-Erba 1108 CHN analyzer.

Ultrasound irradiation was provided by ultrasonic processor probe (Processor SONOPROS PR-1000MP, OSCAR ULTRASONICS with power input 230V, 50 Hz, 4 Amps and power variac 0-230V and 3Amps) operating at 20 kHz, 750W with 6mm/12 mm tip diameter probes.

General Procedure for the Synthesis of 5-aryl-5,6-dihydro-1*H*-pyrano[2,3-*d*]pyrimidine-2,4,7-triones derivatives (4a-h)

A mixture of benzaldehyde **1a-h** (2 mmol), barbituric acid **2a-b** (2 mmol), meldrum's acid **3** (2 mmol), and CAN (10 mol %) in 20 ml water was introduced in a heavy walled pear-shaped two-necked flask with non-standard taper outer joint. The flask was attached to a 12mm tip diameter probe and the reaction mixture was sonicated for the specified period at 50% power of the processor and in a 4 s pulse mode till a solid product separates out. Completion of the reaction was monitored by TLC using n-hexane: ethyl acetate (7:3) as an eluant. All the reactions were invariably completed in 25-40 min. Upon completion, the reaction, the solid product was filtered washed with water, dried and recrystallised from ethanol.

Spectral characterizations**5-(4-Chlorophenyl)-5,6-dihydro-1*H*-pyrano[2,3-*d*]pyrimidine-2,4,7(3*H*)-trione (4a)²¹**

Mp 284-286°C; IR (KBr): ν 3388, 3294, 2968, 1738, 1686, 1588, 1174 cm^{-1} ; ¹H NMR (300 MHz, DMSO-*d*₆): δ 11.36 (s, 1H, NH), 11.15 (s, 1H, NH), 7.97 (d, *J* = 8.4 Hz, 2H, Ph), 7.77 (d, *J* = 8.4 Hz, 2H, Ph), 4.35 (t, *J* = 6.9 Hz, 1H, CH), 3.38 (d, *J* = 6.9 Hz, 2H, CH₂); ¹³C NMR (75 MHz, DMSO-*d*₆): δ 164.1, 161.8, 158.6, 156.2, 143.5, 132.1, 125.8, 123.5, 121.0, 120.4, 92.7, 32.4, 23.1. Anal. Calcd for C₁₃H₉ClN₂O₄: C, 53.35; H, 3.10; N, 9.57%. Found: C, 53.21; H, 3.19; N, 9.72%; ESI (ms) 293 [M+H]⁺

5-(4-Nitrophenyl)-5,6-dihydro-1*H*-pyrano[2,3-*d*]pyrimidine-2,4,7(3*H*)-trione (4b)²¹

Mp 250-252°C; IR (KBr): ν 3384, 3296, 2974, 1742, 1680, 1586, 1170 cm^{-1} ; ¹H NMR (300 MHz, DMSO-*d*₆): δ 11.45 (s, 1H, NH), 11.27 (s, 1H, NH), 8.12 (d, *J* = 8.4 Hz, 2H, Ph), 7.62 (d, *J* = 8.4 Hz, 2H, Ph), 4.39 (t, *J* = 7.2 Hz, 1H, CH), 3.40 (d, *J* = 6.9 Hz, 2H, CH₂); ¹³C NMR (75 MHz, DMSO-*d*₆): δ 166.5, 163.1, 157.8, 154.9, 147.6, 133.2, 126.7, 124.5, 122.1, 120.7, 92.0, 32.1, 23.4. Anal. Calcd for C₁₃H₉N₃O₆: C, 51.49; H, 2.99; N, 13.86%. Found: C, 51.38; H, 3.15; N, 13.98%; ESI (ms) 304 [M+H]⁺

5-(4-Fluorophenyl)-5,6-dihydro-1*H*-pyrano[2,3-*d*]pyrimidine-2,4,7(3*H*)-trione (4c)²¹

Mp 264-266°C; IR (KBr): ν 3402, 3290, 2982, 1735, 1687, 1589, 1176 cm^{-1} ; ¹H NMR (300 MHz, DMSO-*d*₆): δ 11.43 (s, 1H, NH), 11.21 (s, 1H, NH), 8.04 (d, *J* = 8.4 Hz, 2H, Ph), 7.28 (d, *J* = 8.4 Hz, 2H, Ph), 4.36 (t, *J* = 7.2 Hz, 1H, CH), 3.38 (d, *J* = 7.2 Hz, 2H, CH₂); ¹³C NMR (75 MHz, DMSO-*d*₆): δ 168.7, 163.4, 158.2, 155.4, 146.5, 133.8, 128.5, 127.8, 119.2, 92.3, 31.4, 24.6. Anal. Calcd for C₁₃H₉FN₂O₄: C, 56.53; H, 3.28; N, 10.14%. Found: C, 56.38; H, 3.17; N, 10.28%; ESI (ms) 277 [M+H]⁺

5-(2-Nitrophenyl)-5,6-dihydro-1*H*-pyrano[2,3-*d*]pyrimidine-2,4,7(3*H*)-trione (4d)²¹

Mp 216-218°C; IR (KBr): ν 3396, 3284, 2992, 1742, 1692, 1584, 1180 cm^{-1} ; ¹H NMR (300 MHz, DMSO-*d*₆): δ 11.37 (s, 1H, NH), 11.18 (s, 1H, NH), 7.84-7.92 (m, 2H, Ph), 7.28-7.36 (m, 2H, Ph), 4.42 (t, *J* = 7.2 Hz, 1H, CH), 3.36 (d, *J* = 7.2 Hz, 2H, CH₂); ¹³C NMR (75 MHz, DMSO-*d*₆): δ 165.7, 162.7, 154.4, 152.5, 147.1, 136.7, 129.2, 127.2, 122.7, 121.4, 91.8, 31.7, 23.8. Anal. Calcd for C₁₃H₉N₃O₆: C, 51.49; H, 2.99; N, 13.86%. Found: C, 51.36; H, 3.14; N, 13.70%; ESI (ms) 304 [M+H]⁺

5-(2-Chlorophenyl)-5,6-dihydro-1*H*-pyrano[2,3-*d*]pyrimidine-2,4,7(3*H*)-trione (4e)²¹

Mp 242-244°C; IR (KBr): ν 3402, 3286, 2972, 1742, 1692, 1584, 1170 cm^{-1} ; ¹H NMR (300 MHz, DMSO-*d*₆): δ 11.34 (s, 1H, NH), 11.21 (s, 1H, NH), 7.72-7.78 (m, 2H, Ph), 7.30-7.35 (m, 2H, Ph), 4.37 (t, *J* = 7.2 Hz, 1H, CH), 3.35 (d, *J* = 6.9 Hz, 2H, CH₂); ¹³C NMR (75 MHz, DMSO-*d*₆): δ 164.7, 162.2, 156.1, 154.5, 143.9, 132.4, 126.5, 124.2, 121.7, 119.8, 92.3, 31.8, 23.9. Anal. Calcd for C₁₃H₉ClN₂O₄: C, 53.35; H, 3.10; N, 9.57%. Found: C, 53.51; H, 3.23; N, 9.39%; ESI (ms) 293 [M+H]⁺

5-(2-Hydroxyphenyl)-5,6-dihydro-1*H*-pyrano[2,3-*d*]pyrimidine-2,4,7(3*H*)-trione (4f)²¹

Mp 290-292°C; IR (KBr): ν 3592, 3396, 3298, 2974, 1738, 1688, 1586, 1172 cm^{-1} ; ¹H NMR (300 MHz, DMSO-*d*₆): δ 11.48 (s, 1H, NH), 10.17 (s, 1H, NH), 7.94-8.02 (m, 2H, Ph), 7.67-7.75 (m, 2H, Ph), 4.34 (t, *J* = 7.2 Hz, 1H, CH), 4.15 (s, 1H, OH), 3.33 (d, *J* = 6.9 Hz, 2H, CH₂); ¹³C NMR (75 MHz, DMSO-*d*₆): δ 170.3, 163.6, 156.8, 153.7, 136.1, 129.7, 127.1, 125.4, 122.4, 118.1, 91.8, 33.2, 24.2. Anal. Calcd for C₁₃H₁₀N₂O₅: C, 56.94; H, 3.68; N, 10.22%. Found: C, 57.12; H, 3.56; N, 10.32%; ESI (ms) 275 [M+H]⁺

5-(4-Chlorophenyl)-1,3-dimethyl-5,6-dihydro-1*H*-pyrano[2,3-*d*]pyrimidine-2,4,7(3*H*)-trione (4g)

Mp 304-306°C; IR (KBr): ν 1742, 1690, 1596, 1182 cm^{-1} ; ¹H NMR (300 MHz, DMSO-*d*₆): δ 7.98 (d, *J* = 8.4 Hz, 2H, Ph), 7.81 (d, *J* = 8.4 Hz, 2H, Ph), 4.33 (t, *J* = 7.2 Hz, 1H, CH), 3.36 (d, *J* = 6.9 Hz, 2H, CH₂), 2.99 (s, 6H, 2xCH₃); ¹³C NMR (75 MHz, DMSO-*d*₆): δ 164.9, 161.2, 159.3, 157.9, 144.9, 133.8, 126.1, 122.6, 121.5, 121.3, 92.3, 32.0, 27.4, 23.5. Anal. Calcd for C₁₅H₁₃ClN₂O₄: C, 56.17; H, 4.09; N, 8.73%. Found: C, 56.31; H, 4.398; N, 8.85%. ESI (ms) 321 [M+H]⁺

1,3-Dimethyl-5-(4-nitrophenyl)-5,6-dihydro-1*H*-pyrano[2,3-*d*]pyrimidine-2,4,7(3*H*)-trione (4h)

Mp 318-320°C; IR (KBr): ν 1740, 1694, 1590, 1178 cm^{-1} ; ¹H NMR (300 MHz, DMSO-*d*₆): δ 8.12 (d, *J* = 8.4 Hz, 1H, Ph), 7.67 (d, *J* = 8.4 Hz, 1H, Ph), 4.36 (t, *J* = 7.2 Hz, 1H, CH), 3.41 (d, *J* = 7.2 Hz, 2H, CH₂), 2.98 (s, 6H, 2xCH₃);

¹³C NMR (75 MHz, DMSO-*d*₆): δ 166.1, 162.5, 157.4, 155.2, 147.3, 132.8, 127.5, 124.2, 121.8, 120.1, 91.6, 32.6, 27.7, 23.2. Anal. Calcd for C₁₅H₁₃N₃O₆: C, 54.38; H, 3.96; N, 12.68%. Found: C, 54.53; H, 3.83; N, 12.85%. ESI (ms) 332 [M+H]⁺

CONCLUSION

In conclusion, we have developed an efficient and straightforward procedure for the synthesis of pyrano[2,3-*d*]pyrimidine-2,4,7-trione derivatives under ultrasonic irradiation in aqueous medium using ceric ammonium nitrate as a mild, readily available, inexpensive, and efficient catalyst. Good functional group tolerance, broad scope of usable substrates, excellent yields and short routine are the prominent features of the present sonocatalyzed methodology. This method provides several advantages such as environmentally benign, excellent yields, no need of base, and simple workup procedure. Slower reaction of 1,3-dimethyl barbituric acid due to its low acidity of methylene proton.

ACKNOWLEDGEMENTS

Financial assistance from the CSIR [02(0143)/13/EMR-II], New Delhi is gratefully acknowledged. We are also thankful to the Central Drug Research Institute (CDRI), Lucknow and IIT Delhi for the spectral analyses.

REFERENCES

- ¹(a) Orru, R. V. A., de Greef, M., *Synthesis* **2003**, 1471; (b) Tejedor, D., González-Cruz, D., Santos-Expósito, A., Marrero-Tellado, J. J., de Armas, P., García-Tellado, F., *Chem.-Eur. J.* **2005**, *11*, 3502.
- ²(a) Dömling, A., *Chem. Rev.* **2006**, *106*, 17; (b) Toure, B. B., Hall, D. G., *Chem. Rev.* **2009**, *109*, 4439.
- ³Verónica, E., Mercedes, V., Menéndez, J. C., *Chem. Soc. Rev.* **2010**, *39*, 4402.
- ⁴*Multicomponent Reactions*; Zhu, J., Bienaymé, H., Ed.; Wiley-VCH: Weinheim **2005**.
- ⁵Gu, Y., *Green Chem.*, **2012**, *14*, 2091
- ⁶Andrade, C. K. Z., Alves, L. M., *Curr. Org. Chem.* **2005**, *9*, 195.
- ⁷(a) Simon, M.-O., Li, C.-J., *Chem. Soc. Rev.* **2012**, *41*, 1415; (b) Butler, R. N., Coyne, A. G., *Chem. Rev.* **2010**, *110*, 6302; (c) Kobaayshi, S., *Pure Appl. Chem.* **2007**, *79*, 235.
- ⁸Holla, B. S., Kalluraya, B., Sridhar, K. R., Drake, E., Thomas, L. M., Bhandary, K. K., Levine, M. J., *Eur. J. Med. Chem.* **1994**, *29*, 301.
- ⁹Molina, P., Aller, E., Lorenzo, Á., López-Cremades, P., Rioja, I., Ubeda, A., Terencio, M. C., Alcaraz, M. J., *J. Med. Chem.* **2001**, *44*, 1011.
- ¹⁰(a) Chobe, S. S., Dawane, B. S., Tumbi, K. M., Nandekar, P. P., Sangamwar, A. T., *Bioorg. Med. Chem. Lett.* **2012**, *22*, 7566; (b) Di Parsia, M. T., Suarez, C., Vitolo, M. J., Marquez, V. E., Beyer, B., Urbina, C., Hurtado, I., *J. Med. Chem.* **1981**, *24*, 117.
- ¹¹Kamdar, N. R., Haveliwala, D. D., Mistry, P. T., Patel, S. K., *Eur. J. Med. Chem.* **2010**, *45*, 5056.
- ¹²(a) Abdel Fattah, M. E., Atta, A. H., Abdel Gawad, I. I., Mina, S. M., *Orient. J. Chem.* **2004**, *20*, 257; (b) Ghorab, M. M., Hassan, A. Y., *Phosphorus, Sulfur Silicon Relat. Elem.* **1998**, *141*, 251.
- ¹³Bruno, O., Brullo, C., Ranise, A., Schenone, S., Bondavalli, F., Barocelli, E., Ballabeni, V., Chiavarini, M., Tognolini, M., Impicciatore, M., *Bioorg. Med. Chem. Lett.* **2001**, *11*, 1397.
- ¹⁴Aklualia, V. K., Bala, M., *Indian J. Chem., Sect. B* **1996**, *35B*, 742.
- ¹⁵Shamroukh, A. H., Zaki, M. E. A., Morsy, E. M. H., Abdel-Motti, F. M., Abdel-Megeid, F. M. E., *Arch. Pharm.* **2007**, *340*, 236.
- ¹⁶Joshi, K. C., Jain, R., Sharma, K., *J. Indian Chem. Soc.* **1988**, *45*, 202.
- ¹⁷(a) *The pyrimidines*; Fenn, D., Ed.; Wiley: New York **1994**; (b) Heber, D., Heers, C., Ravens, U., *Pharmazie* **1993**, *48*, 537; (c) Grivasky, E. M., Lee, S., Sigal, C. W., Duch, D. S., Nichol, C. A., *J. Med. Chem.* **1980**, *23*, 327; (d) Broom, A. D., Shim, J. L., Anderson, G. L., *J. Org. Chem.* **1976**, *41*, 1095.
- ¹⁸Ghorab, M. M., Hassan, A. Y., *Phosphorus, Sulfur Silicon Relat. Elem.* **1998**, *141*, 251; (b) Furuya, S., Ohtaki, T., *Eur. Patent* **1994**, 6,085,65; (c) Coates, W. J., *Eur. Patent* **1990**, 3,510,58.
- ¹⁹(a) Kitamura, N., Onishi, A., *Eur. Patent* **1984**, 1,635,99; (b) Davoll, J., Clarke, J., Elslager, E. F., *J. Med. Chem.* **1972**, *15*, 837; (c) Levitt, G., *U. S. Patent* **1982**, 4,339,267.
- ²⁰(a) Bo, J., Li-Yuan, X., Xing-Han, W., Man-Su, T., Yin-Ping, L., Shu-Jiang, T., *Tetrahedron Lett.* **2012**, *53*, 1261; (b) Aly, H. M., Kamal, M. M., *Eur. J. Med. Chem.* **2012**, *47*, 18; (c) Kamdar, N. R., Haveliwala, D. D., Mistry, P. T., Patel, S. K., *Eur. J. Med. Chem.* **2010**, *45*, 5056; (d) Elinson, M. N., Ilovaisky, A. I., Merkulova, V. M., Demchuk, D. V., Belyakov, P. A., Ogibin, Y. N., Nikishin, G. I., *Electrochimica Acta* **2008**, *53*, 8346; (e) Majumdar, K. C., Chattopadhyay, S. K., *Can. J. Chem.* **2006**, *84*, 469; (f) Majumdar, K. C.; Jana, N. K.; Bandyopadhyay, A.; Ghosh, S. K., *Synth. Commun.* **2001**, *31*, 2979.
- ²¹Azzam, S. H. S., Pasha, M. A., *Tetrahedron Lett.* **2012**, *53*, 7056.
- ²²(a) Wilkes, J. S., *Green Chem.* **2002**, *4*, 73; (b) Cravotto, G., Fokin, V. V., Garella, D., Binello, A., Boffa, L., Barge, A., *J. Comb. Chem.* **2010**, *12*, 13; (c) Cravotto, G., Cintas, P., *Chem. Soc. Rev.* **2006**, *35*, 180; (d) Pizzuti, L., Martins, P. L. G., Ribeiro, B. A., Quina, F. H., Pinto, E., Flores, A. F. C., Venzke, D., Pereira, C. M. P., *Ultrason. Sonochem.* **2010**, *17*, 34.
- ²³(a) Singh, B. S., Lobo, H. R., Pinjari, D. V., Jarag, K. J., Pandit, A. B., Shankarling, G. S., *Ultrason. Sonochem.* **2013**, *20*, 633; (b) Jarag, K. J., Pinjari, D. V., Pandit, A. B., Shankarling, G. S., *Ultrason. Sonochem.* **2011**, *18*, 617; (c) Mason, T. J., *Ultrasonic* **1992**, *30*, 192; (d) Cravotto, G., Cintas, P., *Angew. Chem. Int. Ed.* **2007**, *46*, 5476.
- ²⁴(a) Mason, T. J., Lorimer, J. P., *Chem. Soc. Rev.* **1987**, *16*, 239; (b) Li, J. T., Wang, S. X., Chen, G. F., Li, T. S., *Curr. Org. Synth.* **2005**, *2*, 415; (c) Cravotto, G., Cintas, P., *Chem. Soc. Rev.* **2006**, *35*, 180.
- ²⁵(a) Nasir Baig, R. B., Varma, R. S., *Chem. Soc. Rev.* **2012**, *41*, 1559; (b) Albogami, A. S., Saleh, T. S., Zayed, E. M., *Ultrason. Sonochem.* <http://dx.doi.org/10.1016/j.ultsonch.2013.03.003>
- ²⁶(a) Nair V., Deepthi, A., *Chem. Rev.* **2007**, *107*, 1862; (b) Nair, V., Panicker, S. B., Nair, L. G., George, T. G., Augustine, A., *Synlett* **2003**, 156.
- ²⁷(a) Tapaswi, P. K., Mukhopadhyay, C., *Arkivoc* **2011**, (*x*), 287; (b) Sridharan V., Menendez, J. C., *Org. Lett.* **2008**, *10*, 4303; (c) Chang, M.-Y., Wu, T.-C., Lin C.-Y., Hung, C.-Y., *Tetrahedron Lett.* **2006**, *47*, 8347.
- ²⁸(a) Sadek, K. U., Alnajjar, A., Mekheimer, R. A., Mohamed, N. K., Mohamed, H. A., *Green and Sustainable Chem.* **2011**, *1*, 92; (b) Mekhalifa, A., Mutter, R., Heal, W., Chen, B., *Tetrahedron* **2006**, *62*, 5617.

- 28(a) Dandia, A., Parewa, V., Gupta, S. L., Rathore, K. S., *J. Mol. Catal. A: Chem.* **2013**, 373, 61; (b) Dandia, A., Jain, A. K., Bhati, D. S., Laxkar, A. K., *Tetrahedron* **2013**, 69, 2062; (c) Dandia, A., Parewa, V., Rathore, K. S., *Catal. Commun.* **2012**, 28, 90; (d) Dandia, A., Parewa, V., Jain, A. K., Rathore, K. S., *Green Chem.* **2011**, 13, 2135; (e) Dandia, A., Jain, A. K., Sharma, S., *Tetrahedron Lett.* **2012**, 53, 5859.
- ²⁹Washburn, E. W., (Eds.) *International Critical Tables*; New York, McGraw-Hill **1929**, 6, 261.
- ³⁰Ballard, B. B., Nelson, E., *J. Pharmacol. Exp. Ther.* **1962**, 135, 120.

Received: 03.05.2013.
Accepted: 08.06.2013.



SPECTROSCOPIC CHARACTERIZATION OF INTERACTION WATER-SOLUBLE CATIONIC PORPHYRAZINE AND ANIONIC SURFACTANTS WITH DIFFERENT ALKYL CHAIN LENGTH

Hamid Dezhampناه^{[a]*} and Roghaye Firouzi^[a]

Keywords: Water-soluble porphyrazine; Surfactant; Premicellar aggregate; Micellized monomer, Anionic surfactant; hydrophobic interaction.

Interactions of cationic tetrakis (N, N', N'', N'''- tetramethyltetra-3, 4-pyridinoporphyrazinatozinc (II) [Zn (tmtpa)] with various anionic micelles of surfactants n- alkyl sulfonate and sulfate (n=11, 12, 14) have been investigated spectrophotometrically at 25 °C in premicellar and postmicellar region. The results have shown that with increasing the alkyl chain length of surfactants, the maximum absorbance of Zn (tmtpa) shifted to a higher wavelength and binding affinity of Zn (tmtpa) to anionic micelles increases. This confirms that the surfactant micelle, which has a longer alkyl hydrocarbon chain, enables greater solubilization of porphyrazine. Thus, the hydrophobic interaction of the porphyrazine with micelles increases in the order: C₁₁H₂₃SO₃Na < C₁₂H₂₅SO₄Na < C₁₄H₂₉SO₃Na..

* Corresponding Authors

Tel:+ 98-131-3243630-5

Fax: + 98-131-3233262

E-Mail: h.dpanah@guilan.ac.ir, h_dpanah@yahoo.com

[a] Laboratory of physical Chemistry, Department of Chemistry, Faculty of Science, University of Guilan P.O. Box 1914, Rasht 0098, Iran:

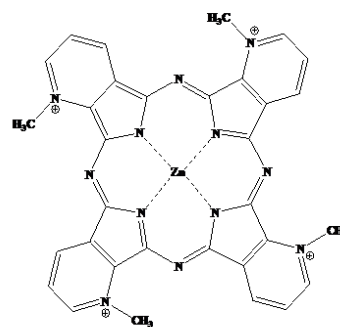
length; sodium 1-decansulfonate (C₁₁H₂₃SO₃Na), sodium dodecylsulfate (C₁₂H₂₅SO₄Na), sodium tetradecylsulfonate (C₁₄H₂₉SO₃Na) surfactants in aqueous solutions. Spectrophotometric method is used to investigate this interaction at the concentration below and above their critical micelle concentration (CMC).

Introduction

The aggregation of porphyrin and metalloporphyrin provides an insightful information in understanding the fundamental processes of living organisms and has been extensively studied in order to explain the biosynthetic formation and biological activity of naturally occurring compounds.¹ Under appropriate conditions with controlled ionic strength and protonation, porphyrins form highly ordered aggregates, namely J- or H-aggregates. J-aggregate is side-by-side arrangement of the porphyrin rings with absorption band red-shift, while H-aggregate is face-to-face arrangement of the porphyrins with absorption band blue-shift compared with porphyrin monomer. In the aggregation complex, the adjacent porphyrin molecules interact by hydrophobic interaction or electrostatic attraction.^{2,3}

Cationic tetra-azaporphyrins, or porphyrazines, represent an alternative and highly developed class of cationic porphyrinic compounds. Macrocycles hasted on the porphyrazine core, including phthalocyanines, but the replacement of the meso methylene carbons of porphyrins with nitrogen in porphyrazines creates profound differences.⁴ For example, porphyrazines absorb more strongly at longer wavelengths, a critical feature in biological and medical applications.^{4,5}

The objective of the current work is to understand and characterize the role of the hydrophobicity on the interaction between tetrakis(N,N',N'',N'''-tetramethyltetra-3,4-pyridinoporphyrazinatozinc(II) [Zn(tmtpa)] (scheme 1) and a series of anionic surfactants with different alkyl chain



Scheme 1. The structure of tetrakis (N, N', N'', N'''- tetramethyltetra-3, 4- yridinoporphyrazinatozinc(II) [Zn (tmtpa)]

Materials

The Zn (tmtpa) was prepared and purified according to literature methods.⁶ Sodium 1-decansulfonate, sodium dodecylsulfate, sodium tetradecylsulfonate were Sigma chemicals and were used without further purification. All experiments were run in phosphate buffer of pH=7.2. spectrophotometric measurements a series of dye-surfactant solution by constant concentration of porphyrazine (1×10⁻⁵ M) and various concentration of surfactant was prepared and the absorption spectra of these solutions were recorded at 25 ± 0.1 °C. The absorbances were measured on the double beam absorbance spectrophotometer Cary 500 scan UV-vis, using a matched pair of quartz cells (1 cm path length) at 25.0 °C. The mixed solutions were prepared instantly and the absorbance was measured after thermostation.

Results and discussions

The UV-vis absorption spectra of Zn (tmtppa) in aqueous solution in the presence and the absence of $C_{14}H_{29}SO_3Na$ are displayed in Figures 1A and 1B. It is observed that the addition of $C_{14}H_{29}SO_3Na$ changes the position, width, and intensity of the absorption spectra of Zn (tmtppa) at different ratio of $[C_{14}H_{29}SO_3Na]/[Zn(tmtppa)]$ (R). The interaction process can be divided into two successive stages. At the first stage ($R = 0-52.5$), with the increase of the concentration of $C_{14}H_{29}SO_3Na$, remarkable hypochromicity accompanied by broadening of Q -band is observed. At $R = 52.5$, was observed, which is blue shifted compared to the monomer peak at 681 nm. The occurrence of 53nm blue shift and significant decreasing of Q -band indicate the aggregation of porphyrazine. We assume that a new type Zn (tmtppa) - $C_{14}H_{29}SO_3Na$ aggregate formed in the solution, which can be classified as H-aggregate.

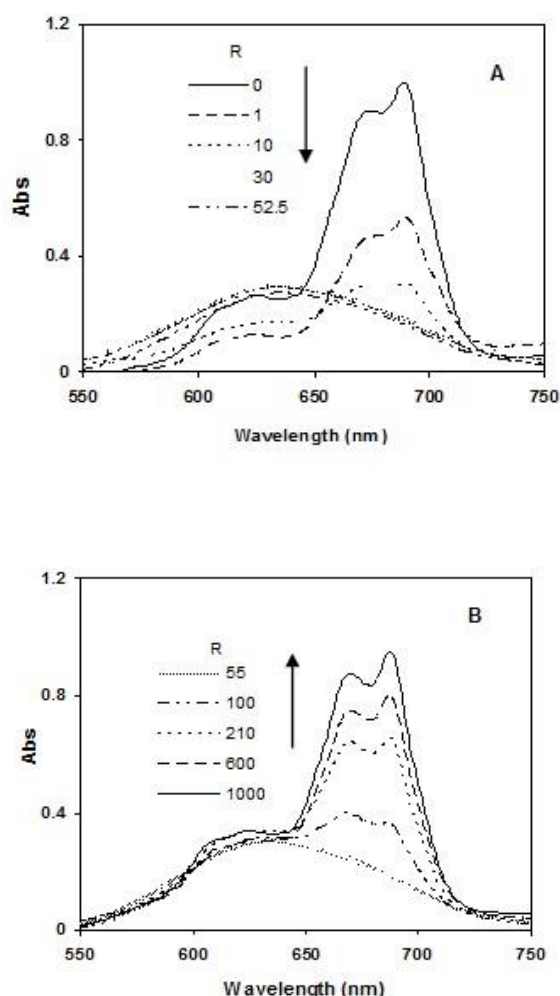


Figure 1. The UV-vis spectra of Zn(tmtppa) in the presence of various $C_{14}H_{29}SO_3Na$ concentrations: (A) at low concentrations; (B) at high concentrations.

In the second stage ($R > 52.5$), when $R = 55-1000$, a gradual hyperchromicity and red shift of Q -band can be observed. The structure of J -aggregate changes slightly along with increase in the concentration of $C_{14}H_{29}SO_3Na$ ($R > 55$). When $R = 1000$, the hyperchromicity and red-shift of Q -band to 678 nm, suggesting that the aggregates are broken partially after

further interaction with $C_{14}H_{29}SO_3Na$. We assume that the porphyrazine-surfactant complex formed at high concentration of $C_{14}H_{29}SO_3Na$, which is much lower than the CMC of $C_{14}H_{29}SO_3Na$, is the micellized monomer. The intensity and position of Q band (681 nm) is almost unchanged until R is more than 1000, which implies that almost all Zn (tmtppa) molecules become micellized monomer. Similar spectral change was observed in the case of the others surfactants.

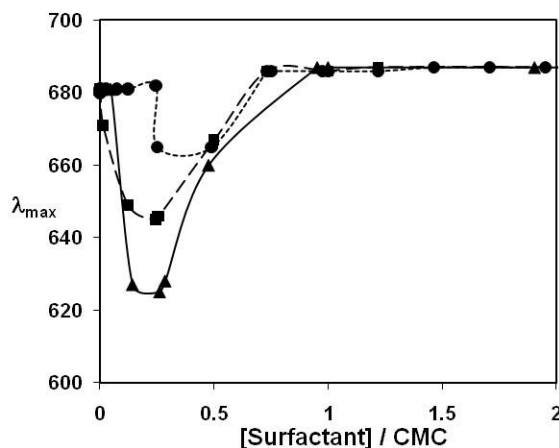


Figure 2. The Wavelength absorbance change of 1×10^{-5} mol/L Zn(tmtppa) (below and above the CMC) with the concentration of $C_{11}H_{23}SO_3Na$ (●), $C_{12}H_{25}SO_4Na$ (■) and $C_{14}H_{29}SO_3Na$ (▲).

The absorbance change of 1×10^{-5} mol L^{-1} Zn(tmtppa) (below and above the CMC) with the concentration of $C_{11}H_{23}SO_3Na$, $C_{12}H_{25}SO_4Na$ and $C_{14}H_{29}SO_3Na$ are shown in Figure 3. The absorbance of Zn(tmtppa) initially decreased with increasing the surfactant concentrations well below the CMC and reached a minimum value and then increased again with further increasing of surfactant concentrations above the CMC. This indicates that the bound Zn(tmtppa) to micelles increases with the lengthening of the alkyl chains of the surfactants. This implies an increase in equilibrium distribution of the porphyrazine molecules that are transferred into the micellar phase more favorably with the increase in their hydrophobicity, as observed also in other cases.⁷

Acknowledgment

We gratefully acknowledge the Research Council of University of Guilan for supporting this work.

References

- ¹Ibrahim, H. Kasselouri, A. You, C. Maillard, P., Rosilio, V., Pansu, R., Prognon, P. *J. Photochem. Photobiol. A: Chem.*, **2011**, 217(1), 10.
- ²Paulo, P. M. R.; Costa, S. M. B., *Photochem. Photobiol. Sci.*, **2003**, 2, 597.
- ³Gouterman, M. In: *The porphyrins*, Vol. 3, Dolphin D. (Ed.) Academic Press: New York, **1978**;
- ⁴Suchetti, C. A. Durantini, E. N., *Dyes Pigments* **2007**, 74, 630.
- ⁵Thamae M. and Nyokong, T., *J. Electroanal. Chem.*, **1999**, 470, 126.

⁶Schenning, A. P. H. J., Hubert, D. H. W. Feiters, M. C. Nolte, R. J. M., *Langmuir*, **1996**, *12*, 1572.

⁷Maiti, N. C. Mazumdar, S. Perisamy, N., *J. Phys. Chem. B*, **1998**, *102*, 1528.

Received: 22.05.2013.

Accepted: 11.06.2013.



SYNTHESIS, STRUCTURE, AND MAGNETIC BEHAVIOR OF $[\text{Cu}_2(\text{PYRAZINE})_3(\text{CH}_3\text{O})_2](\text{ClO}_4)_2$

Benjamin L. Solomon^[a], Christopher P. Landee^[b], Jerry P. Jasinski^[c],
Mark M. Turnbull^{[a]*}

Keywords: Pyrazine, Copper(II), Synthesis, X-ray Structure, Magnetism.

Reaction of copper perchlorate with sodium nitrite and pyrazine in methanol gives rise to the compound $[\text{Cu}_2(\text{pyrazine})_3(\text{CH}_3\text{O})_2](\text{ClO}_4)_2$ (**1**). This complex has been characterized through IR, combustion analysis, single crystal X-ray diffraction, and temperature dependent magnetic susceptibility measurements. Compound **1** crystallizes in the triclinic space group P-1 with the copper coordination geometry being nearly square pyramidal. The Cu(II) ions are bridged by the methoxide ions to form a dimeric structure. Compound **1** exhibits an extended 3-D network with pyrazine rings forming sheets of the copper dimers, and bridging those sheets to form a distorted honeycomb. Magnetic susceptibility measurements show a strong antiferromagnetic exchange within the methoxy-bridged copper dimers with $2J \sim -880$ K.

* Corresponding Authors

Fax: +1-508-793-8861

E-Mail: mturnbull@clarku.edu

[a] Carlson School of Chemistry and Biochemistry, Clark University, 950 Main Street, Worcester, Massachusetts 01610

[b] Department of Physics, Clark University, 950 Main Street, Worcester, Massachusetts 01610

[c] Department of Chemistry, Keene State College, 229 Main Street, Keene, New Hampshire 03435

INTRODUCTION

Transition metal ions form interesting and diverse coordination complexes that vary widely in structure with a change of ligand, or ion. To study this phenomenon many different families of Cu(II) complexes have been made to establish the effects of modification of the structure and electronic effects on the packing motif.¹⁻⁴ Copper(II), with its single unpaired electron and almost negligible internal magnetic field, as indicated by a g factor close to 2.00,⁵ is an exemplary choice to study quantum magnetic interactions.

Pyrazine is an interesting ligand for research in the realm of copper(II) coordination chemistry due to the second donor nitrogen in the 4 position, making pyrazine a possible bidentate ligand.^{6,7} The bidenticity of pyrazine can also create an efficient pathway for spin exchange and subsequent magnetic interactions.^{8,9} Pyrazine is a much weaker base than the well-studied monodentate ligand pyridine¹⁰ (pyrazine $pK_a = 1.1$; pyridine $pK_a = 5.2$).¹¹ The weaker basicity of pyrazine decreases the favorability of the ligand deprotonating another species in the solution, allowing for the synthesis of unique complexes compared to when pyridine is the ligand. Pyrazine complexes can also have varied dimensionalities depending on the stoichiometry of the starting materials.¹²

We are involved in a project to produce families of two-dimensional quantum Heisenberg antiferromagnets (2D-QHAF).^{13,14} A recent report of $[\text{M}(\text{pyrazine})_2\text{NO}_2]\text{ClO}_4$, where M is Co(II) or Cu(II), by Gao *et al.*¹⁵ is of interest to our group due to the similarities in structure to some high temperature superconductors.¹⁶ Our attempts to grow single crystals of the copper complex using the published synthesis proved ineffective. However, during those attempts, we

encountered a novel pyrazine/methoxide-bridged, three-dimensional coordination polymer. Here we present the synthesis, crystal structure, and magnetic properties of $[\text{Cu}_2(\text{pyrazine})_3(\text{CH}_3\text{O})_2](\text{ClO}_4)_2$ (**1**).

EXPERIMENTAL

Pyrazine and copper perchlorate hexahydrate were purchased from Aldrich Chemical Company and used without further purification. Sodium nitrite was purchased from Fisher Scientific and used without further purification. IR spectra were recorded as KBr pellets on a Perkin-Elmer Spectrum 100. X-Ray powder diffraction was carried out on a Bruker AXS-D8 X-ray Powder Diffractometer. Elemental analysis was carried out by Marine Science Institute, University of California, Santa Barbara, CA 93106.

Synthesis of $[\text{Cu}_2(\text{pyrazine})_3(\text{CH}_3\text{O})_2](\text{ClO}_4)_2$ (**1**)

Copper perchlorate hexahydrate (3.625 g, 9.9 mmol), sodium nitrite (0.686 g, 9.94 mmol), and pyrazine (1.595 g, 19.9 mmol) were placed in three separate 30 mL beakers and dissolved in 5 mL of methanol, 5 mL of methanol, and 5 mL of water, respectively. All three beakers were placed in a 1000 mL beaker. The large beaker was slowly filled with methanol to a level of 0.8 cm over the rim of the smaller beakers and four drops of HClO_4 were added to the solution. The 1000 mL beaker was then covered with parafilm. After 15 days, black needles (0.268 g, 6.44 % yield) had formed on the top of the sodium nitrite-containing beaker, with a green powder (0.760 g, 18.27 % yield) at the bottom of the beaker. Black prisms (0.492 g, 11.83 % yield) had formed on the bottom of the 1000 mL beaker. The products were isolated by vacuum filtration, washed with cold methanol, and air-dried. The needles and prisms both became a green color upon powdering, meaning the crystals are a very dark green. All three proved to be **1**, as indicated by identical IR spectra. Attempts to synthesize (**1**) by other methods using varying ratios of starting materials and differing orders of addition proved unsuccessful. IR (KBr, ν in cm^{-1}): 3108 (w), 3056 (vw), 2931 (vw), 2824 (w), 1426 (m), 1105 (s), 1085 (s), 1061 (m), 831 (w), 813 (w), 804 (w), 622 (m), 552 (w), 506 (w), 474 (w). CHN found (calculated): C 26.3 (26.8), H 2.90 (2.89), N 13.0 (13.4).

X-ray Structure Analysis

Data for **1** was collected on an Agilent Technologies Gemini Eos CCD-Xray Diffractometer using the CrysAlis Pro software package with MoK α radiation ($\lambda = 0.71073 \text{ \AA}$) via ω -scans at 173(2) K employing a graphite monochromator. Cell parameters were determined and refined using CrysAlisPro¹⁷ and absorption corrections were made using SADABS.¹⁸ The structure was solved by direct methods and refined via least-squares analysis using SHELXS97-2.¹⁹ All non-hydrogen atoms were refined anisotropically. Hydrogen atoms were added in calculated positions and refined using a riding model with fixed isotropic thermal parameters. Crystallographic information and details of the data collection can be found in Table 1.

Table 1. X-ray data for **1**.

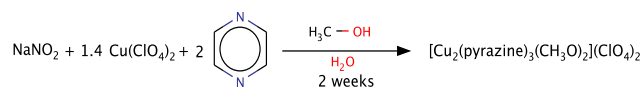
| | |
|---|--|
| Empirical Formula | C ₁₄ H ₁₈ N ₆ O ₁₀ Cl ₂ Cu ₂ |
| Formula weight (g mol ⁻¹) | 628.32 |
| T (K) | 173(2) |
| Wavelength (Å) | 0.71073 |
| Crystal System | Triclinic |
| Space Group | P-1 |
| a (Å) | 7.7047(7) |
| b (Å) | 9.0747(8) |
| c (Å) | 9.1003(11) |
| α (°) | 60.124(11) |
| β (°) | 82.573(9) |
| γ (°) | 85.277(7) |
| V (Å ³) | 546.96(10) |
| Z | 1 |
| Crystal Size (mm) | 0.30 x 0.25 x 0.20 |
| Absorption coefficient (mm ⁻¹) | 2.254 |
| F (0,0,0) | 316 |
| θ_{min} , θ_{max} | 3.50, 27.87 |
| Index Ranges | -10 < h < 9 -11 < k < 8 -11 < l < 11 |
| Reflections collected | 5849 |
| Independent reflections | 2993 |
| Restraints/parameters | 0/155 |
| Final R index [I > 2 σ (I)] | 0.0413 |
| R index (all data) | 0.0427 |
| Largest peak/hole (e/Å ³) | 1.95(near Cu1)/-0.51 |

Magnetic Susceptibility Data Collection

Magnetic data was collected using a Quantum Design MPMS-XL SQUID magnetometer. Finely ground samples of the crystals were packed in gelatin capsules. The moment was measured using magnetic fields from 0 to 50 kOe at 1.8 K. Several data points were collected as the field was brought back to 0 kOe to check for hysteresis; none was observed. Magnetization was then measured from 1.8 to 310 K in a 1 kOe field. The contributions from the sample holder were measured independently and subtracted from the data set. The data was also corrected for the temperature independent paramagnetism of the Cu(II) ion (60×10^{-6} emu/molOe) and for the diamagnetism of the constituent atoms (-226.5×10^{-6} emu/molOe) taken from Pascal's constants.⁵

RESULTS AND DISCUSSION

Reaction of one equivalent of sodium nitrite, 1.4 equivalents of copper perchlorate, and two equivalents of pyrazine in methanol and water over the course of two weeks produced black crystals of $[\text{Cu}_2(\text{pyrazine})_3(\text{CH}_3\text{O})_2](\text{ClO}_4)_2$ (**1**) in 11.83% yield.

Scheme 1. Preparation of compound **1**.

Attempts to prepare the complex by a variety of other methods, varying concentrations, solvents, and omitting the NaNO₂ proved unsuccessful. Although there is no nitrite ion in the final product, it is clear that its presence is required for successful preparation of **1**. We presume that the role of the nitrite ion is that of base/buffer to allow deprotonation of the methanol (most likely as a coordinated methanol molecule). Nitrite is a somewhat stronger base than pyrazine (pK_a HNO₂ = 3.3)²⁰ and thus more suited to that role.

Crystal Structure Analysis

Compound **1** crystallizes in the triclinic space group P-1. The asymmetric unit is shown in Figure 1. A crystallographic inversion center lies at (0.5, 0.5, 0.5) with respect to the Cu(II) ion, producing a methoxy-bridged dimer (Figure 2). Selected bond lengths and angles are given in Table 2.

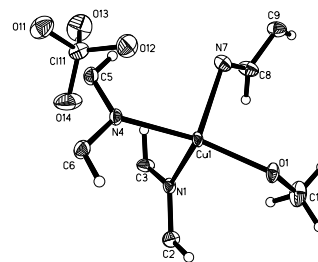
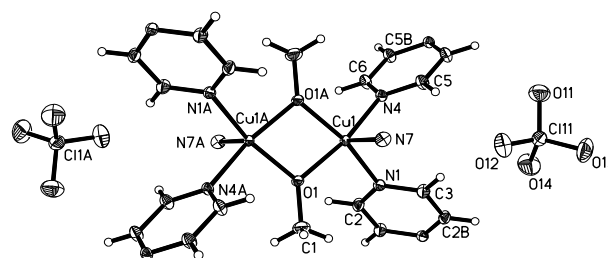
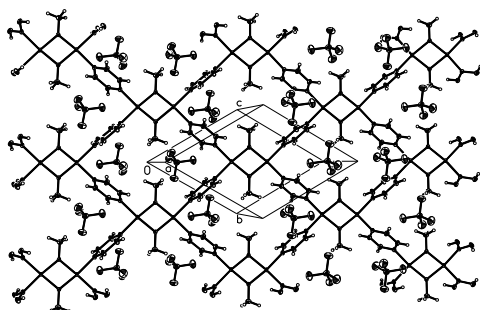
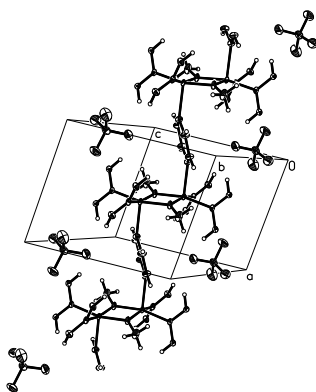
Figure 1. Thermal ellipsoid plot of the asymmetric unit of **1** showing 50% probability ellipsoids. H atoms were placed in calculated positions and are not labeled.Figure 2. Thermal ellipsoid plot showing the dimeric core of **1** (50% probability ellipsoids). Only the nitrogen atoms of the N7/N7A pyrazine rings are shown for clarity.

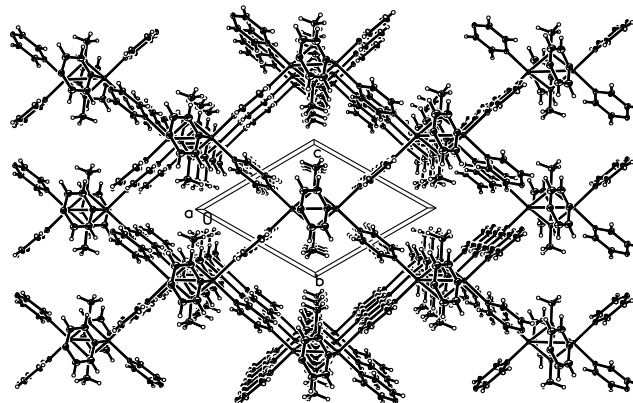
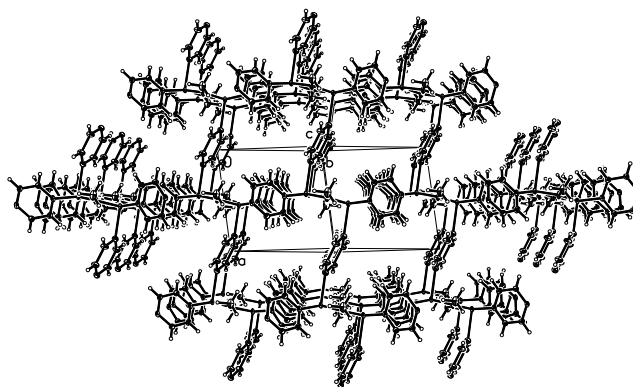
Table 2. Selected bond lengths (Å) and angles (°) for **1**.

| | | | |
|--------|----------|-------------|----------|
| Cu1-O1 | 1.928(3) | Cu1-O1-Cu1A | 101.7(1) |
| Cu1-N1 | 2.015(3) | O1A-Cu1-O1 | 78.33(1) |
| Cu1-N4 | 2.007(3) | O1-Cu1-N4 | 165.6(1) |
| Cu1-N7 | 2.255(3) | O1A-Cu1-N4 | 94.9(1) |
| O1-C1 | 1.431(5) | O1-Cu1-N1 | 94.4(1) |
| | | O1A-Cu1-N1 | 162.8(1) |
| | | N4-Cu1-N1 | 88.5(1) |
| | | O1-Cu1-N7 | 94.7(1) |
| | | O1A-Cu1-N7 | 93.5(1) |
| | | N4-Cu1-N7 | 98.5(1) |
| | | N1-Cu1-N7 | 102.7(1) |

The Cu ion has a nearly square pyramidal geometry as indicated by an Addison parameter (τ) of 0.05.²¹ The Cu(II) ion lies 0.257 (2) Å above the N1-N4-O1-O1A mean plane. The three symmetry-independent pyrazine rings lie across crystallographic inversion centers located at (0.5, 0.5, 1) for the N1 ring, (0.5, 1, 0.5) for the N4 ring, and (1, 0.5, 0.5) for the N7 ring. The N1 and N4 pyrazine rings are unremarkable^{22,23} and connect the copper dimers together to form a sheet parallel to the *bc*-plane (Figure 3). The N1-Cu1 vector lies 15.8(2)° below the copper-oxygen plane while N4-Cu1 vector is inclined 12.9(1)° in the same direction. The N7 pyrazine ring is on the opposite face and the Cu1-N7 bond is canted 5.4(1)° from the normal to the copper-oxygen plane (Figure 4). The N7-pyrazine ring occupies the axial site of the square pyramidal structure and the Cu1-N7 bond is ~0.25 Å longer than the Cu1-N1 and Cu1-N4 bonds as expected.

**Figure 3.** Sheet formed by methoxy-bridged copper dimers. The N7 pyrazine rings are removed for clarity.**Figure 4.** Links between sheets of dimers formed by the N7 pyrazine rings. The N1 and N4 pyrazine rings are removed for clarity.

This combination of the sheet formed by the N1 and N4 pyrazine rings, and the N7 pyrazine ring nearly normal to the Cu(II) ion gives rise to a 3D distorted honeycomb structure (Figures 5 and 6). The ClO_4^- ions occupy the holes of the distorted honeycomb, balancing the charge of the Cu(II) ion, and are nearly tetrahedral and otherwise unremarkable.

**Figure 5.** Packing structure of **1** viewed parallel to the *a* axis. Perchlorate ions have been removed for clarity.**Figure 6.** Packing structure of **1** viewed parallel to the *bc*-face diagonal. Perchlorate ions have been removed for clarity.

Similar covalently bonded networks of copper dimers bridged by alkoxy ligands have been synthesized. The compound $[\text{Cu}_2(\mu\text{-}(6\text{-oxyquinoline}))(\text{PPh}_3)_2]$ forms copper-oxygen dimers comparable to those found in **1**, but bridge via the oxyquinoline ligands to give chains of dimers.²⁴ A 2-D sheet is formed by the coordination polymer $[\text{Cu}_2(\text{salicylate})_2(\text{pyrazine})(\text{H}_2\text{O})_2]$.²⁵ Two copper atoms and two deprotonated phenolic oxygen atoms form copper-oxygen dimers that are linked by pyrazine units to yield a zigzag chain. Further dimensionality is added to the complex by the carboxyl groups of the salicylates, which bridge the zigzag chains to give a 2-D sheet. However, the Cu(II) ions have an octahedral geometry, unlike the square pyramidal geometry in **1**.

The two short and one long Cu-N bonds found in **1** are present in the polymer $[\text{Cu}_2(\text{monoethanolamine})_2(\text{pyrazine})_2](\text{CF}_3\text{SO}_3)_2$ ²⁶ to give a 3-D structure akin to **1**. The two short Cu-N bonds belong to the pyrazine that forms the 2-D sheets of copper dimers and the amino group that resides in the monoethanolamine ligand. The long Cu-N

bond is to the axial pyrazine ring that links the 2-D sheets of copper dimers together to form a 3-D structure as in **1**. As opposed to **1**, the coordination of the 2-D sheet is built through one ligand instead of two, as the monoethanolamine bridges one half of the dimer to itself by the formation of a five-membered ring. Related compounds have been synthesized that yield analogous structures such as $[\text{Cu}_2(\text{propanolamine})_2(4,4'\text{-bipyridine})_2](\text{ClO}_4)_3$ ²⁷ and $[\text{Cu}_2(\text{ethanolamine})_2(\text{bis}(4\text{-pyridyl})\text{ethylene})_2](\text{ClO}_4)_2$.²⁸

Magnetic Study

Magnetic susceptibility data were collected for compound **1** from 1.8 to 310 K in a 0.1 T field (Figure 7). Compound **1** is a strong antiferromagnet that has a maximum susceptibility well above room temperature. The data were fit to the Bleaney-Bowers equation (where ρ represents a paramagnetic impurity, and $N\alpha$ represents the temperature independent paramagnetism, see below).²⁹ The best data fit yields $2J = -880 (\pm 170)$ K, $g = 2.1 (\pm 1.7)$, and $\rho = 0.009 (\pm 0.005)$. The large errors in these fitted values arise due to the limited data available for the magnetic contribution of the dimer since the maximum in χ occurs well above room temperature (and the limit of our instrument). Thus, these values are presented as rough approximations only.

$$\chi_m = \frac{2N\beta^2 g^2}{3kT} \left[1 + \frac{1}{3} \exp\left(-\frac{2J}{kT}\right) \right]^{-1} (1 - \rho) + \frac{(N\beta^2 g^2)\rho}{4kT} + N\alpha$$

Eqn.1.

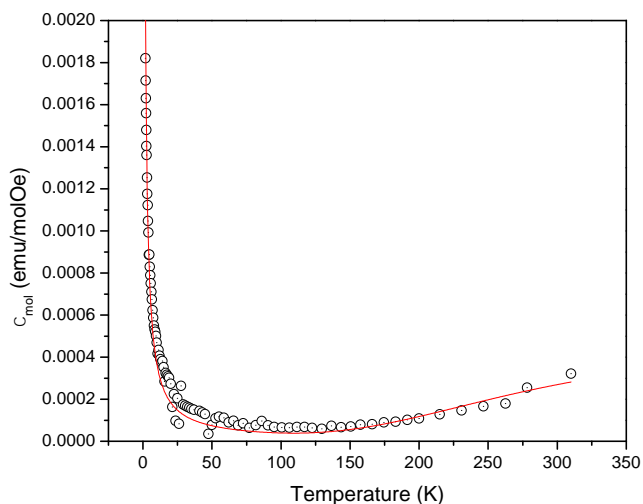


Figure 7. χ_m vs. T plot for **1** in a 0.1 T field. The solid line represents the best fit to a dimer model with a paramagnetic impurity term and was calculated from equation 1.

At room temperature, compound **1** exhibits a χT product of 0.053 emuK/molOe, well below the expected value of above 0.375 emuK/molOe for an $S = \frac{1}{2}$ ion with $g = 2.00$. This suggests very strong exchange. This was supported by the M vs. H data, which showed a saturation magnetization of 36.7 emu/mol at 5 T and 1.8 K. For a Cu(II) ion, a saturation magnetization near 6000 emu/mol is expected,⁵ implying that the response being measured at low temperature is not due to the bulk sample, but rather due to a paramagnetic impurity. The sharp increase in susceptibility

at lower temperatures also agrees with the presence of a trace paramagnetic impurity.

Copper dimers bridged by alkoxy,^{30,31} phenoxy,^{32,33} or hydroxy^{34,35} groups are part of a family of antiferromagnetic compounds with strong exchange. The value of the Cu-O-Cu angle ranges from $99.1(1)^\circ$ ($\{[2-(1-(2\text{-dimethylaminoethylamino})\text{ethyl})\text{-phenoxy}]\text{Cu}(\text{NCCCN})\}_2; 2J = -530 \text{ K}\}$ ³² to $103.9(2)^\circ$ ($\{[\text{Cu}(\text{Me}(6\text{-R-2-pyridylmethyl})-(2\text{-pyridyl})\text{benzylamine})\text{MeO}]\}_2(\text{ClO}_4)_2; 2J = -1840 \text{ K}\}$ ³¹ in these compounds, which all have maximum molar susceptibilities above room temperature. The magnitude of the 2J parameter has been related to the Cu-O-Cu angle,^{33,36} with larger angles exhibiting a larger exchange.^{37,38} The Cu-O-Cu angle of **1** is $101.7(1)^\circ$, agreeing with a maximum molar susceptibility occurring at greater than room temperature. Exchange may also occur within and between the layers of copper dimers through the pyrazine rings, but the very strong exchange within the dimers prevents any observation of that exchange.

ACKNOWLEDGEMENTS

Financial assistance from the NSF (IMR-0314773) and the Kresge Foundation toward the purchase of the MPMS-XL SQUID magnetometer are greatly appreciated. The Bruker D8-Advance powder X-ray Diffractometer was purchased with the assistance of funds from the Kresge Foundation and PCISynthesis, Inc. BLS is grateful for the PCISynthesis, Inc. Summer Research Fellowship. JPJ acknowledges the NSF MRI program (grant No. CHE-1039027) for funds to purchase the X-ray diffractometer.

APPENDIX. Supplementary Data

CCDC (940687) contains the supplementary crystallographic data for **1**. This data can be obtained free of charge via from <http://www.ccdc.cam.ac.uk/conts/retrieving.html>, or from the Cambridge Crystallographic Data Centre, 12 Union Road, Cambridge CB2 1EZ, UK; fax: (+44) 1223-336-033; or e-mail: deposit@ccdc.cam.ac.uk.

REFERENCES

- Adhikary, C., Koner, S., *Coord. Chem. Rev.* **2010**, 254, 2933.
- Herringer, S. N., Turnbull, M. M., Landee, C. P., Wikaira, J. L., *J. Coord. Chem.* **2009**, 62, 863.
- Tremelling, G. W., Foxman, B. M., Landee, C. P., Turnbull, M. M., Willett, R. D., *Dalton Trans.* **2009**, 47, 10518.
- Zhao, J.P., Hu, B.W., Sanudo, E., Yang, Q., Zeng, Y.F., Bu, X.H., *Inorg. Chem.* **2009**, 48, 2482.
- Carlin, R. L., *Magnetochemistry*, Springer-Verlag, **1986**.
- Otieno, T., Rettig, S., Thompson, R., Trotter, J., *Can. J. Chem.* **1989**, 67, 1964.
- Otieno, T., Gipson, A. M., Parkin, S., *J. Chem. Crystallog.* **2002**, 32, 81.
- Leznoff, D. B., Xue, B.-Y., Stevens, C. L., Storr, A., Thompson, R. C., Patrick, B. O., *Polyhedron* **2001**, 20, 1247.
- Manson, J. L., Huang, Q.Z., Lynn, J. W., Koo, H.J., Whangbo, M.H., Bateman, R., Otsuka, T., Wada, N., Argyriou, D. N., Miller, J. S., *J. Amer. Chem. Soc.* **2001**, 123, 162.
- Tomasik, P., Ratajewicz, Z., Newkome, G. R., Strekowski, L., *Pyridine-metal complexes*, John Wiley & Sons, **1985**.

- ¹¹ Keyworth, D., *The J. Organ. Chem.* **1959**, *24*, 1355.
- ¹² Carlucci, L., Ciani, G., Proserpio, D. M., Sironi, A., *J. Amer. Chem. Soc.* **1995**, *117*, 4562.
- ¹³ Gale, A. J., Landee, C. P., Turnbull, M. M., Wikaira, J. L., *Polyhedron* **2012**, *52*, 986.
- ¹⁴ Abdalrahman, M., Landee, C. P., Telfer, S. G., Turnbull, M. M., Wikaira, J. L., *Inorg. Chim. Acta* **2012**, *389*, 66.
- ¹⁵ Liu, T., Chen, Y.H., Zhang, Y.J., Wang, Z.M., Gao, S., *Inorg. Chem.* **2006**, *45*, 9148.
- ¹⁶ Monthoux, P., Balatsky, A., Pines, D., *Phys. Rev. B* **1992**, *46*, 14803.
- ¹⁷ CrysAlisPro Oxford Diffraction Ltd., Version 1.171.35.19 (release 27-10-2011 CrysAlis171.NET).
- ¹⁸ Sheldrick, G.M., SADABS v 2.01: An empirical absorption correction program, Bruker AXS Inc., Madison, WI (1999).
- ¹⁹ Sheldrick, G. M., *Acta Cryst. A* **2008**, *64*, 112.
- ²⁰ Schwartz, S. E., White, W. H., *Adv. Environ. Sci. Eng.* **1981**, *4*, 1.
- ²¹ Addison, A. W., Rao, T. N., Reedijk, J., van Rijn, J., Verschoor, G. C., *J. Chem. Soc., Dalton Trans.* **1984**, 1349.
- ²² Ramírez, J., Stadler, A.M., Rogez, G., Drillon, M., Lehn, J.M., *Inorg. Chem.* **2009**, *48*, 2456.
- ²³ Albrecht, A. S., Landee, C. P., Slanic, Z., Turnbull, M. M., *Mol. Cryst. Liq. Cryst.* **1997**, *305*, 333.
- ²⁴ Ponikiewski, L., Shi, W., Rothenberger, A., *Z. Anorg. Allg. Chem.* **2008**, *634*, 1770.
- ²⁵ Long-Guan, Z., Kitagawa, S., *J. Inorg. Organomet. Polym.* **2002**, *12*, 23.
- ²⁶ Marin, G., Kravtsov, V., Simonov, Y. A., Tudor, V., Lipkowski, J., Andruh, M., *J. Mol. Struct.* **2006**, *796*, 123.
- ²⁷ Tudor, V., Marin, G., Kravtsov, V., Simonov, Y. A., Lipkowski, J., Brezeanu, M., Andruh, M., *Inorg. Chim. Acta* **2003**, *353*, 35.
- ²⁸ Marin, G., Tudor, V., Kravtsov, V. C., Schmidtman, M., Simonov, Y. A., Müller, A., Andruh, M., *Cryst. Growth Des.* **2005**, *5*, 279.
- ²⁹ Bleaney, B., Bowers, K., *Proc. R. Soc. London, Ser. A.* **1952**, *214*, 451.
- ³⁰ Garcia, A. M., Manzur, J., Garland, M. T., Baggio, R., Gonzales, O., Pena, O., Spodine, E., *Inorg. Chim. Acta* **1996**, *248*, 247.
- ³¹ Rojas, D., García, A. M., Vega, A., Moreno, Y., Venegas-Yazigi, D., Garland, M. T., Manzur, J., *Inorg. Chem.* **2004**, *43*, 6324.
- ³² Biswas, A., Drew, M. G., Ribas, J., Diaz, C., Ghosh, A., *Inorg. Chim. Acta* **2011**, *379*, 28.
- ³³ Thompson, L. K., Mandal, S. K., Tandon, S. S., Bridson, J. N., Park, M. K., *Inorg. Chem.* **1996**, *35*, 3117.
- ³⁴ Massoud, S. S., Louka, F. R., Xu, W., Perkins, R. S., Vicente, R., Albering, J. H., Mautner, F. A., *Eur. J. Inorg. Chem.* **2011**, *50*, 3469.
- ³⁵ Cvetkovic, M., Batten, S. R., Moubaraki, B., Murray, K. S., Spiccia, L., *Inorg. Chim. Acta* **2001**, *324*, 131.
- ³⁶ Crawford, V. H., Richardson, H. W., Wasson, J. R., Hodgson, D. J., Hatfield, W. E., *Inorg. Chem.* **1976**, *15*, 2107.
- ³⁷ Merz, L., Haase, W., *J. Chem. Soc., Dalton Trans.* **1980**, *6*, 875.
- ³⁸ Melnik, M., *Coord. Chem. Rev.* **1982**, *42*, 259.

Received: 13.06.2013.

Accepted: 21.06.2013.



CORROSION RESISTANCE OF COMMERCIAL ALUMINIUM IN SIMULATED CONCRETE PORE SOLUTION IN PRESENCE OF CURCUMIN EXTRACT

Susai Rajendran^{[a,d]*}, K. Duraiselvi^[b], P. Prabhakar^[c], M. Pandiarajan^[d]
M. Tamilmalar^[e] and R. Joseph Rathish^[f]

Keywords: concrete corrosion, aluminium, simulated concrete pore solution, curcumin, green inhibitor.

The corrosion resistance of commercial aluminium (95% pure) in simulated concrete pore solution (SCPS) prepared in natural sea water has been evaluated in the absence and presence of curcumin extract and Zn^{2+} . It is observed that Aluminium is more corrosion resistance in SCPS than in sea water. When curcumin extract is added to SCPS, the corrosion resistance of Al increases. However, in the presence of curcumin - Zn^{2+} system, the corrosion resistance of Al in SCPS decreases.

Corresponding Authors

- [a] Department of Chemistry, Corrosion Research centre, RVS School of Engineering and Technology, Dindigul 624005, India. E.mail: srmjoany@sify.com
- [b] Department of Chemistry, Karpagam University, Coimbatore, E.mail: Duraiselvik@gmail.com
- [c] Department of Chemistry, APA College of Arts and Culture, E.mail: nivedhaprabhakar@rediffmail.com
- [d] Corrosion Research Centre, PG and Research, Department of Chemistry, GTN Arts College, Dindigul- 624005, India. E.mail: pandiarajan777@gmail.com.
- [e] Department of Chemistry, B.S Abdur Rahman Univeristy, Vandalur, Chennai, Tamil Nadu, India. E-mail: manomalar_84@yahoo.co.in
- [f] PSNA College of Engineering and Technology, Dindigul, India, Email: rathishjoseph@gmail.com

Introduction

Corrosion of reinforcing steel bars (rebars) in concrete is a serious and significant problem from both the economics and structural integrity standpoints. Many are the approaches that can be used to mitigate corrosion of reinforcing steel, among which, protective coatings and sealers, cathodic protection, concrete realkalization and corrosion inhibitors are commonly employed. The use of corrosion inhibitors is probably more attractive from the point of view of economics and ease of application.¹ The application of corrosion inhibitors in reinforced concrete is possible by adding it to the mixing water during the concrete preparation or by applying it to the external surface of hardened concrete. In this last case, the inhibiting compound should diffuse through the concrete cover and reach the rebar in a sufficiently high concentration to protect steel against corrosion. Reviews of the most commonly used corrosion inhibitor types in concrete repair systems² and the various possible mechanisms of inhibition have been recently published.³ Over the last years, the use of organic inhibitors, as an alternative to the more commonly employed calcium nitrite-based inhibitors, has been increasing. Organic inhibitors offer protection by adsorbing and

forming a protective film on the steel surface. Usually, there is a polar group in the organic molecule that adsorbs on the metal and a nonpolar hydrophobic chain oriented perpendicular to this surface. These chains act, on the one hand, by repelling aggressive contaminants dissolved in the pore solution, and on the other, by forming a tight film (barrier) on the metallic surface. Duprat and Dabosi⁴ examine the effect of various aminoalcohols as corrosion inhibitors of carbon steel in 3% NaCl solutions. The efficiency of the inhibitor increases when only one of the hydrogen atoms of the amino group is substituted, as the remaining one induces hydrogen bonds formation between surface-chelated molecules. In the case of 2-ethylamino-ethanol,⁵ the inhibitive action in 3% NaCl solutions was interpreted both by its stabilisation effect on the prepassive ferrous hydroxide films and by its adsorption through surface chelate formation onto bare metal sites. The effect of pH on the inhibitive efficiency was also investigated.

Contradictory results have been recently reported when testing corrosion inhibitors in simulated pore solutions and in mortars.⁶⁻⁸ Elsener et al.⁶ studied the efficiency of an inhibitor based on alkylamines on steel corrosion in mortars and in calcium hydroxide solutions. In mortars, there is no apparent inhibition of pitting or a decrease in corrosion rate (CR), but the initiation of the corrosion process appears to be delayed. The beneficial effect decreases on carbonated mortars. In a recent publication of these same authors,⁷ the discrepancy between the observed high diffusion rate of the migrating corrosion inhibitor (MCI) in mortar and the lack of corrosion inhibition was rationalised by the fact that only the diffusion of the volatile phase was measured. Migration of the nonvolatile component (carbonic acids) through concrete was not proved and assumed to be slow. Thus, the inefficiency detected in concrete, as compared to solutions, should be related to the inability of the nonvolatile components to reach the steel bars. In turn, Mammoliti et al.⁸ assumed that the difference in the inhibitors efficiency tested in concrete or in synthetic pore solutions is the result of the dependence of the inhibition mechanism on chemical reactions within the cement phase.

The present work is undertaken to evaluate the corrosion resistance of commercial aluminium (95 % pure) in natural sea water (Table 1) and to evaluate the corrosion resistance of aluminium in simulated concrete pore solution (SCPS) prepared in natural sea water in the absence and presence curcumin extract and Zn^{2+} . The outcome of the present study will be useful to the concrete corrosion technologists.

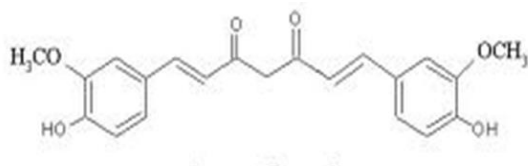
Materials and Methods

Metal specimens

Aluminium: commercial aluminium (95 % pure) was used in the present study.

Preparation of curcumin extract

10 g of turmeric powder was boiled with 50 ml of distilled water. The suspended impurities were removed by filtration .The filtrate was made up to 100 ml .It was used as inhibitor in the presence of Zn^{2+} . The structure of curcumin is shown in Scheme 1.



Scheme 1. Structure of curcumin

Simulated concrete pore solution (SCPS)

A saturated solution of $Ca(OH)_2$ is considered as simulated concrete pore solution.⁹ SCPS was prepared in natural sea water.

Table 1. Physicochemical parameters of sea water

| Parameters | Value |
|----------------|---|
| pH | 7.66 |
| Conductivity | 44200 $\mu\text{ohm}^{-1} \text{cm}^{-1}$ |
| Chloride | 6050 ppm |
| Sulphate | 2616 ppm |
| TDS | 30940 ppm |
| Total Hardness | 2800 ppm |
| Calcium | 120ppm |
| Sodium | 6300 ppm |
| Magnesium | 600 ppm |
| Potassium | 400 ppm |

Weight Loss Method

Aluminium specimens were immersed in 100 ml of the medium containing various concentrations of the inhibitor in the absence and presence of Zn^{2+} for 1 day. The weight of the specimens before and after immersion was determined using a Shimadzu balance, model AY62. The corrosion products were cleaned with Clarke's solution¹⁰. The inhibition efficiency (IE , in %) was then calculated using the equation:

where

W_1 = corrosion rate in the absence of the inhibitor.

W_2 = corrosion rate in the presence of the inhibitor.

$$IE = 100 \left[1 - \frac{W_2}{W_1} \right] \quad (1)$$

Potentiodynamicpolarization

Polarization studies were carried out in a CHI– Electrochemical workstation with impedance, Model 660A. A three-electrode cell assembly was used. The working electrode was aluminium (exposed area is 1 cm^2). A saturated calomel electrode (SCE) was the reference electrode and platinum was the counter electrode. From the polarization study, corrosion parameters such as corrosion potential (E_{corr}), corrosion current (I_{corr}) and Tafel slopes (anodic = b_a and cathodic = b_c) and linear polarization resistance (LPR) were calculated.

Results and Discussion

Analysis of Weight loss method

Corrosion rate of aluminium immersed in simulated concrete pore solution (SCPS) prepared in natural seawater, in the absence and presence of curcumin extract and Zn^{2+} are given in Table 2. The inhibition efficiencies are also given in this Table.

Table 2. Inhibition efficiencies of inhibitors in controlling corrosion of aluminium in SCPS prepared in sea water. Immersion period: 1day

| System | CR (mdd) | IE % |
|---|----------|------|
| Sea water | 32 | ---- |
| SCPS prepared in sea water | 6.4 | 80 |
| SCPS +Curcumin 6 ml | 0.64 | 98 |
| SCPS + Curcumin 6 ml + Zn^{2+} 50 ppm | 2.56 | 92 |

When aluminium is immersed in sea water, the corrosion rate is 32 mdd. When Aluminium is immersed in SCPS prepared in sea water the inhibition efficiency is 97 %. When 6 ml of curcumin extract is added the inhibition efficiency increases to 99 %. When 50 ppm of Zn^{2+} is added to the curcumin system, the inhibition efficiency decreases to 92 %. However, this corrosion rate is lower than that observed in presence of sea water.

Corrosion resistance of commercial aluminium in simulated concrete pore solution (SCPS) prepared in natural sea water(Table 1), in the absenceand presence of an aqueous extract of turmeric powder (curcumin) and Zn^{2+} has been evaluated by polarization study.Polarization study has been used to evaluate the corrosion resistance of metals .If corrosion resistance increases ,linear polarization resistance (LPR) value increases and corrosion current(I_{corr}) decreases.¹¹⁻²⁰.The polarization curves of aluminium immersed in various environments are shown in Figs. 1 to 4.

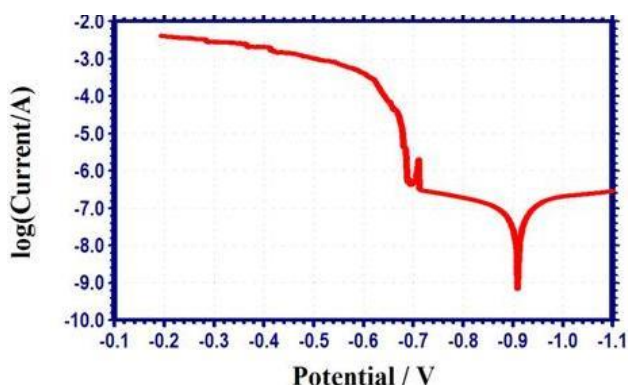


Figure 1. Polarization curve of aluminium immersed in natural sea water

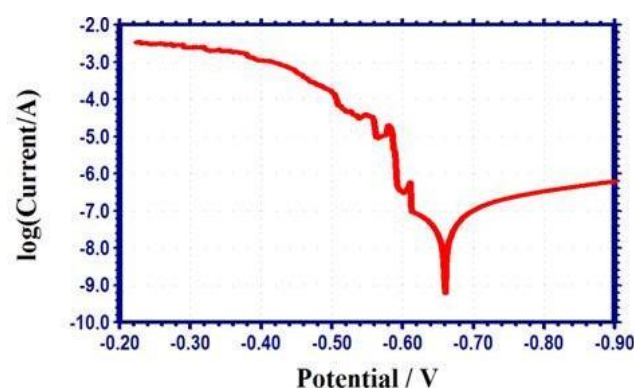


Figure 2. Polarization curve of aluminium immersed in simulated concrete pore solution (SCPS) prepared in sea water

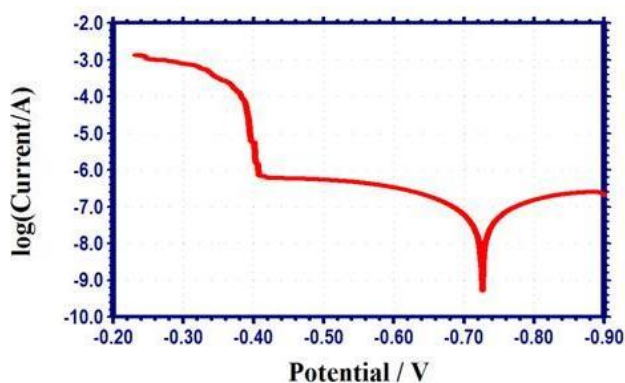


Figure 3. Polarization curve of aluminium immersed in SCPS and curcumin extract 6 ml

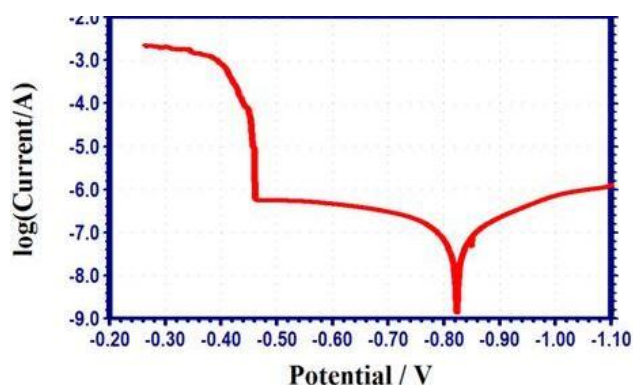


Figure 4. Polarization curve of aluminium immersed in SCPS + Curcumin extract 6 ml + Zn^{2+} 50 ppm.

Analysis of Polarization Study

The corrosion parameters, namely corrosion potential (E_{corr}), Tafel slopes (b_c =cathodic ; b_a =anodic), Linear polarization resistance (LPR) and corrosion current (I_{corr}) values are given in Table 3.

Aluminium in sea water

The polarization curves of aluminium in natural sea water is shown in Fig 1. The corrosion parameters are given in Table 2. It is seen that the corrosion potential is -909 mV vs SCE in the potential range of -0.7 volts to -1.1 V the two arms of the polarization curve are very similar. However breakdown potential is observed at -699 mV vs SCE. The passive film, is broken and corrosion current increases suddenly. Then, at -697 mV vs SCE, passive film is reformed. Hence corrosion current decreases. However, at -622 mV vs SCE, the passive film is broken and the corrosion current increases sharply. The passive film formed is oxides of aluminium. The breakage of passive film is due to the presence of aggressive ions such as chloride, present in sea water. When aluminium is immersed in natural sea water, the LPR value is $338005 \Omega \text{ cm}^2$ and the corrosion current is $2.424 \times 10^{-7} \text{ A cm}^{-2}$.

Aluminium in simulated concrete pore solution prepared is natural sea water

When aluminium is immersed in SCPS prepared in sea water, the corrosion potential is shifted to the anodic side, from -909 to -660 mV vs SCE (Fig 2). This is due to formation of a passive film formed on the metal surface. The film probably consists of aluminium oxide. The anodic Tafel slope is smaller than the cathodic Tafel slope.

That is the rate of change of current with potential is less during the anodic sweep than during the cathodic sweep. However, the passive film is broken at -607 mV vs SCE. As the potential is shifted to the anodic side, passive film is formed again at potential -605 mV vs SCE. Then again break down potential appears at -543 mV vs SCE. This trend is repeated as the potential is shifted to the anodic side. This indicates that the passive film produced on aluminium is disturbed when the potential is shifted to more anodic side. However the passive film is quite stable in the potential range of -606 to -641 mV SCE. It is observed from Table 2, that in presence of SCPS, aluminium is more corrosion resistant than in sea water. This is supported by the fact, that when aluminium is immersed in SCPS, the LPR value increases from 338005 to $418966 \Omega \text{ cm}^2$ and the corrosion current decreases from 2.424×10^{-7} to $2.938 \times 10^{-8} \text{ A cm}^{-2}$.

Influence of Curcumin on the resistance of aluminium in SCPS

Various inhibitors such as calcium nitrite,²¹ molybdate,²² sodium nitrite,²³ have been added to improve the corrosion resistance of metals in SCPS. The influence of a natural product, which is less toxic, namely, an aqueous extract of curcumin (extract from turmeric powder) on the corrosion resistance of aluminium in SCPS has been evaluated by polarization study (Fig. 3).

Table 3. Corrosion Parameters of aluminum immersed in simulated concrete pore solution (SCPS) prepared in sea water, in presence and absence of curcumin and Zn²⁺, obtained from polarization study.

| System | E_{corr} , mV* | b_a , mV** | b_c , mV** | LPR, ohm cm ² | I_{corr} , A cm ⁻² |
|-----------|------------------|--------------|--------------|--------------------------|---------------------------------|
| Sea water | -909 | 474 | 313 | 338005 | 2.424x10 ⁻⁷ |
| SCPS | -660 | 219 | 33 | 418966 | 2.938x10 ⁻⁸ |
| SCPS +A | -726 | 234 | 183 | 451237 | 9.894x10 ⁻⁸ |
| SCPS+B | -823 | 175 | 255 | 340564 | 1.324x10 ⁻⁷ |

A=Curcumin 6 ml, B=Curcumin 6 ml+ Zn²⁺ 50 ppm,*mV vs SCE; **mV in one decade

It is observed that when curcumin is added to SCPS, the corrosion potential is shifted to the cathodic side. However it is in the anodic region when compared with the corrosion potential in sea water alone. The LPR Value increases from 418966 to 451237 Ω cm² indicating that aluminium in SCPS is more corrosion resistant in presence of curcumin than in its absence, due to the formation of Al³⁺-curcumin complex apart from the formation of aluminium oxide film formed on the metal surface. However, the increase in the value of corrosion current warns that the protective film is porous and flow of electron can take place from the metal to the environment. In the anodic region it is observed that the breakdown potential appears from -380 to -403 mV vs SCE. Interestingly, it is observed that the passive film is stable in a wide range of potential, namely, from -400 to -600 mV vs SCE.

Influence of Curcumin -Zn²⁺ system on the corrosion resistance of aluminium in SCPS

In the corrosion inhibition study, it has been observed that the corrosion inhibition efficiency increases in the presence of inhibitor -Zn²⁺ system.²⁴⁻³⁰ This concept has been tried in the case of corrosion resistance of aluminium in concrete solution. The corrosion resistance has been evaluated by polarization study (Fig 4.). It is observed that in presence of curcumin -Zn²⁺ system, the corrosion potential shifts to the cathodic side (-823 mV vs SCE). However this is anodic side, when compared with corrosion potential of aluminium in sea water, LPR value decreases from 451237 to 340564 Ω cm² and the corrosion current increases from 9.894x10⁻⁸ to 1.324x10⁻⁷ A cm⁻². This indicates that the corrosion resistance of Al in SCPS decreases in presence of curcumin -Zn²⁺ system. However this is more corrosion resistant, when compared with sea water alone. Hence it is concluded that addition of Zn²⁺ must be avoided when curcumin is added as an inhibitor in concrete environment. This is due to the fact that Zn²⁺, when added to SCPS (which is an alkaline solution, pH=13.2) it is precipitated as Zn(OH)₂ in the bulk of the solution. Usually Zn²⁺ forms a weak complex with the inhibitors and transports the inhibitor towards the metal surface from the bulk of the solution. However under the present experimental condition, such a transport of inhibitor from the bulk of the solution towards the metal surface is prevented. Hence the corrosion resistance of aluminium in SCPS decreases, in presence of curcumin-Zn²⁺ system. However it is observed from Fig 4, that the film formed on the metal surface is stable in the potential range of -459 to -700 mV vs SCE. The break down potential is in the range of -395 to -458 mV vs SCE.

Conclusion

The corrosion resistance of commercial aluminium (95% pure) in simulated concrete pore solution (SCPS) prepared in natural sea water has been evaluated in the absence and presence of curcumin extract and Zn²⁺. It is observed that Aluminium is more corrosion resistant in SCPS than in sea water. When curcumin extract is added to SCPS, the corrosion resistance of Al increases. However, in the presence of curcumin -Zn²⁺ system, the corrosion resistance of Al in SCPS decreases.

Scope for the further study:

A systematic study in various concentrations of curcumin extract and Zn²⁺. The corrosion resistance of aluminium in SCPS prepared in sea water has been evaluated in presence of one concentration of curcumin extract (6 ml) and also one concentration of Zn²⁺ (50 ppm) will lead to very intensity results. The conclusion of the future study will be very useful to the concrete corrosion technologists

Acknowledgement

The authors are thankful to their Managements and St,Joseph's Research and Community Development Trust, Dindigul, India for their help and encouragement.

References

- Sastri, V. S., *Corrosion Inhibitors. Principles and Applications*, Wiley, England, 1998.
- Page, C. L., Ngala, V. T., Page, M. M., *Mag. Concr. Res.*, 2000, 52, 25.
- Hansson, C. M., Mammoliti, L., Hope, B. B., *Cem. Concr. Res.* 1998, 28, 1775.
- Duprat, M., Dabosi, F., *Corros.*, 1981, 37, 89.
- Duprat, M., Bui, N., Dabosi, F., *Corros.*, 1979, 35, 392-397.
- Elsener, B., Buchler, M., Stalder, F., Bohni, H., *Corros.*, 1999, 55, 1155.
- Elsener, B., Buchler, M., Stalder, F., Bohni, H., *Corros.*, 2000, 56, 727.
- Mammoliti, L., Hansson, C. M., Hope, B. B., *Cem. Concr. Res.* 1999, 29, 1583.
- Pandiarajan, M., Prabhakar, P., Rajendran, S., *Eur. Chem. Bull.*, 2012, 1(7), 238.

- ¹⁰Wranglen, G., *Introduction to Corrosion and Protection of Metals.*: Chapman & Hall, London., **1985**, 236.
- ¹¹Angelin Thangakani, J., Rajendran, S., Sathiyabama, J., Lydia Christy, J., Surya Prabha, A., Pandiarajan, M., *Eur. Chem. Bull.*, **2013**, 1(5), 265-275.
- ¹²Vijaya, N., Peter Pasgal Regis, A., Rajendran, S., Pandiarajan, M., Nagalakshmi, R., *Eur. Chem. Bull.*, **2013**, 2(5), 275-278.
- ¹³Agila Devi, S., Susai Rajendran, Jeyasundari, J., Pandiarajan, M., *Eur. Chem. Bull.*, **2013**, 2(2), 84.
- ¹⁴Rajendran, S., Anuradha, K., Kavipriya, K., Krishnaveni, A., and Angelin Thangakani, J., *Eur. Chem. Bull.*, **2012**, 1(12), 503.
- ¹⁵Nagalakshmi, R., Rajendran, S., Sathiyabama, J., Pandiarajan, M., Lydia Christy, J., *Eur. Chem. Bull.*, **2012**, 1(17), 238.
- ¹³Sahayam Raja, A., Nagalakshmi, R., Rajendran, S., Angelin Thangakani, J., Pandiarajan, M., *Eur. Chem. Bull.*, **2013**, 2(3), 130-136
- ¹⁴Shyamala Devi, B., Rajendran, S., *Eur. Chem. Bull.*, **2012**, 1(5), 150-157.
- ¹⁵Gowri, S., Sathiyabama, J., Rajendran, S., and Angelin Thangakani, J., *Eur. Chem. Bull.*, **2013**, 2(4), 214-219.
- ¹⁶Manimaran, N., Rajendran, S., Manivannan, M., John Mary, S., *Res. J. Chem. Sci.*, **2012**, 2(3), 52.
- ¹⁷Arockia Selvi, J., Rajendran, S., John Amalraj, A., Narayanasamy, B., *Port. Electrochim. Acta.*, **2009**, 27(1), 1.
- ¹⁸Ostoner, T. A., Justness, H., *Adv. Appl. Ceram.*, **2011**, 110, 131.
- ¹⁹Zhou, X., Yang, H.-Y., Wang, F- H., *Corros. Sci. Protect. Technol.* **2010**, 22, 343.
- ²⁰Zhu, Y., Lin, C., *Metallurg. Sinica*, **2010**, 46(2), 245.
- ²¹Johnsirani, V., Sathiyabama, J., Rajendran, S., Suriya Prabha, A., *ISRN Corros.*, **2012**, 2012, 1.
- ²²Gowri, S., Sathiyabama, J., Prabhakar, P., Rajendran, S., *Int. J. Res. Chem. Environ.*, **2013**, 3(1), 156.
- ²³Manivannan, M., Rajendran, S., *Res. J. Chem. Sci.* **2011**, 1(8), 42.
- ²⁴Wilson Sahayaraj, J., John Amalraj, A., Rajendran, S., Vijaya, N., *J. Chem.*, **2012**, 9(4), 1746.
- ²⁵Kavipriya, K., Sathiyabama, J., Rajendran, S., Krishnaveni, A., *Int. J. Adv. Engg. Sci. Technol.*, (IJAEST), **2012**, 2(2), 106.
- ²⁶Manivannan, M., Rajendran, S., *Asian J., Chem.*, **2012**, 24(10), 4713.
- ²⁷Muthumani, N., Rajendran, S., Pandiarajan, M., Lydia Christy, J., Nagalakshmi, R., *Port. Electrochim. Acta*, **2012**, 30(5), 307-315.

Received: 18.04.2013.

Accepted: 21.06.2013.



SYNTHESIS AND CHARACTERIZATION OF FORMAMIDINE DERIVATIVES FROM IMIDATE VIA DIFFERENT CATALYSTS

A. Yahyazadeh^{[a]*}, M. Hadisi Nea^[a] and S. Majnooni^[a]

Keywords: formamidine, imidate, sulfonic acid, aluminium chloride, anilinium chloride, silica sulfuric acid.

In this research, synthesis of (1E)-N'-((Z)-2-amino-1,2-dicyanovinyl)-N-(4-ethoxyphenyl)formamidine from imidate was investigated in the presence of different catalysts such as sulfonic acid (-SO₃H), P-Toluene sulfonic acid (PTSA), aluminium chloride (AlCl₃), ceric ammonium nitrate (CAN), anilinium chloride (C₆H₅NH₃⁺Cl⁻), Montmorillonite (K10), silica sulfuric acid (SiO₂-OSO₃H), silica-supported perchloric acid (HClO₄-SiO₂). Silica sulfuric acid exhibited high catalytic activity for this reaction and afforded excellent yields within a lesser time. Other formamidine derivatives were prepared from the reaction of imidate with amines in the presence of silica sulfuric acid under argon at room temperature.

Corresponding author*

Asieh Yahyazadeh

Fax: +98-131-3233262

E-Mail: yahyazadehphd@yahoo.com

[a] Department of Chemistry, College of Science, University of Guilan, Rasht, P. O. Box 41335-1914, Iran

Introduction

Amidines have long been regarded as valuable intermediates in the synthesis of heterocyclic compounds.^{1,2} Characteristic structural features of many natural substances would be very helpful for medicinal chemists because amidines are found in many bioactive natural products and identified as important pharmacophores.³⁻⁶ They possessing anti-degenerative⁷ anticancer^{8,9} anti-platelet¹⁰ and antimicrobial¹¹ activities. Amidine derivatives also act as serine protease inhibitors.¹² Very important compounds were prepared from amidines such as imidazole rings,¹³ purins^{14,15} quinazolines.¹⁶ Conventional strategies for amidine synthesis include the addition of metal amides or amines to nitriles, the addition of amines to imido ester intermediates, and the condensation of amides with amines in the presence of halogenating reagents.¹⁷ In this research, we have synthesized amidine derivatives from imidate in the presence of different catalysts.

Experimental

All chemicals and reagents were prepared from Sigma/Aldrich and Merck Chemical Companies. All solvents purified and dried using established procedures. Solvents were removed using rotary evaporator under reduced pressure. The ¹H NMR spectra were recorded on Bruker XL (400 MHz) instruments (with J-values given in Hz) and IR spectra on a Shimadzu IR-470 spectrophotometer. The melting points were measured on an Electro thermal digital melting point apparatus and are uncorrected.

General procedure for the preparation of imidate as precursor

Imidate was synthesized from the reaction of DAMN with trimethyl orthoformate (1:1) in dry dioxane under reflux for 2 hours. Methanol and dioxane were removed from reaction mixture by distillation as by-product. After cooling at room temperature and filtering, was added 2 mL n-hexane and allowed to stand in refrigerator for 48 hours. Precipitated yellow crystals were filtrated and were recrystallized in CH₂Cl₂ and Petroleum ether.

Imidate

Light yellow needles from petroleum ether/CH₂Cl₂ (92%) m.p: 132-133 °C; IR (KBr) v: 3450(NH₂), 3300 (NH₂), 2900 (C-H_{aliphatic}), 2225 (C≡N), 1640 (C=N), 1590 (N-H), 1380 (CH₃), 1260 (C-N), 1250 (C-O) cm⁻¹; ¹H NMR (CDCl₃) δ: 7.94 (s, 1H), 6.98 (s, 2H), 3.78 (s, 3H) ppm.

General procedure for the preparation of formamidine

A solution of synthesized imidate with amines was treated in the presence of catalyst amount in the dry ethanol under argon at room temperature. This reaction was continued until the reaction was completed. Residue was concentrated and dried under vacuum to give formamidine.

(1Z)-N'-((Z)-2-amino-1,2-dicyanovinyl)-N-(4-ethoxy phenyl) formamidine, 2a

Light green solid, (94 %) m.p: 148-150 °C; IR (KBr) v: 3480 (NH) 3300 (NH), 2980 (CH_{aromatic}), 2200 (C≡N), 1660 (N-H_{bend}), 1600 (C=C), 1560 (C=N), 1460 (CH_{3 bend}), 1360 (CH_{2 bend}), 1260 (C-N), 1160 (C-O), 820 (C-H_{bend}) cm⁻¹; ¹H NMR (CDCl₃): 9.83 (s, 1H), 7.70 (s, 2H), 6.87 (d, J=5Hz, 2H), 6.37 (s, 2H), 4.00 (s, J=7Hz, 2H), 3.35 (s, 1H), 1.32 (t, J=7Hz, 3H) ppm.

(1Z)-N-(4-methoxybenzyl)-N'-((Z)-2-amino-1,2-dicyanovinyl)-formamidine, 2b

Green solid, (87%) m.p: 150-152 °C; IR (KBr): 3480(NH), 3360 (N-H), 2950 (C-H), 2200 (C≡N), 1630 (N-H bend), 1600 (C=C), 1550 s (C=N), 1360 (CH₃ bend), 1260 (C-N), 1250 (C-O), 840 (C-H bend) cm⁻¹; ¹H NMR (CDCl₃): 7.97 (s, 1H), 7.71 (s, 1H), 7.26 (q, J = 5Hz, 2H), 6.99 (s, 1H), 6.96 (d, J = 10Hz, H), 6.06 (s, 2H, H), 4.48 (d, J = 5Hz, 2H), 3.81 (s, 3H) ppm.

(1Z)-N-(2-methoxybenzyl)-N'-((Z)-2-amino-1,2-dicyanovinyl)-formamidine, 2c

Cream solid, (86%) m.p: 148-150 °C; IR (KBr): 3400 (NH), 3300(NH), 3150(C-H aromatic), 2950(C-H aliphatic), 2200(C≡N), 1640(N-H bend), 1600(C=C), 1465(CH₃ bend), 850(C-H bend), Cm⁻¹; ¹HNMR (DMSO): 7.97(d, 1H), 7.71(d, J= 4.04 Hz, 1H), 7.27(q, J=5HZ, 2H), 7 (m, J=5 HZ, 1H), 6.91(m, J=10Hz, 1H), 6.06 (s, 2H), 4.47(d, J= 5Hz 2H), 3.81 (s, 3H) ppm.

(1Z)-N'-((Z)-2-amino-1,2-dicyanovinyl)-N-(2-methoxyphenyl)-formamidine 2d

Green solid, (90%) m.p: 138-140 °C; IR (KBr): 3380 (NH), 3330(NH), 3100(C-H aromatic), 2950(C-H aliphatic), 2200(C≡N), 1640(N-H bend), 1600(C=C), 1520 (C=N), 1460(CH₃ bend), 1280 (C-O), 860(C-H bend), Cm⁻¹; ¹HNMR (CDCl₃): 8.30 (s, 1H), 7.71 (s, 1H), 7.28 (d, J=1.2 Hz, 1H), 7.10 (m, J= 3.24 Hz, 1H), 7.01 (m, J = 7 Hz, 2H), 4.48 (s, 2H, H), 3.93 (s, 3H) ppm.

(1Z)-N'-((Z)-2-amino-1,2-dicyanovinyl)-N-(3,4-dimethoxyphenyl)formamidine 2e

Light green solid, (94%) m.p: 142-144 °C; IR (KBr): 3450 (NH), 3325 s (NH.), 3100 (C-H_{aromatic}) 2950 (C-H_{aliphatic}), 2210 (C≡N), 1630 (N-H bend), 1570 (C=C), 1510 (C=N), 1375 (CH₃ bend), 1260 (C-N), 1240 (C-O), 830 (C-H bend) cm⁻¹; ¹HNMR (DMSO): 9.85 (s, 1H), 7.75 (d, J= 7.3 Hz, 1H), 7.28 (m, 2H), 6.89 (d, J=8.5 Hz, 1H), 6.27 (s, 2H), 3.75(s, 3H), 3.72 (s, 3H) ppm.

(1Z)-N'-((Z)-2-amino-1,2-dicyanovinyl)-N-(3,4,5-trimethoxyphenyl)formamidine 2f

Green solid, (91%) m.p: 144-146 °C; IR (KBr): 3380 (NH), 3360 s (NH.), 2950 (C-H), 2200 (C≡N), 1680 (N-H bend), 1600 (C=C), 1500 (C=N), 1440 (CH₃ bend), 1280 (C-N), 1120 (C-O), 830 (C-H bend) cm⁻¹; ¹H NMR (CDCl₃): 9.16 (s, 1H), 8.54 (s, 1H), 6.89 (s, 2H), 6.31 (s, 2H), 3.96 (s, 6H, H), 3.94 (s, 3H, H).

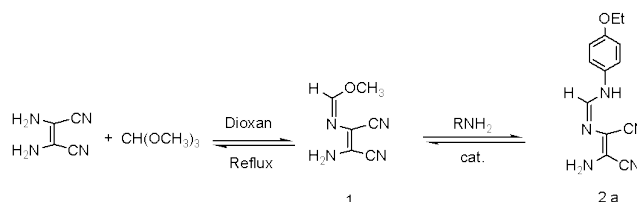
(1Z)-N-(2-chlorobenzyl)-N'-((Z)-2-amino-1,2-dicyanovinyl)-formamidine 2g

Green solid, (91%) m.p: 134-136 °C; IR (KBr): 3450 (NH), 3320 s (NH.), 3100 (C-H_{aromatic}) 2920 (C-H_{aliphatic}), 2200 (C≡N), 1620 (N-H bend), 1520 (C=N), 1440 (CH₃ bend), 1280 (C-N), 735 (C-H bend) cm⁻¹; ¹H NMR (DMSO): 8.17 (s, 1H),

7.75(d, J=2.8 HZ, 1H), 7.45 (s, 2H), 7.31 (t, J=2.8 HZ, 2H), 6.12 (s, 2H), 4.58 (d, J=4.4 HZ, 2H).

Result and discussion

The methods currently available for the preparation of amidines often involve multistep processes with long reaction times¹⁸ In this research, we focused our efforts to provide a convenient route for synthesis amidine from imidate at the least time with high yields. To reach this aim, initial, imidate was obtained from the reaction of diaminomaleonitrile (DAMN) with trimethyl orthoformate in refluxing dioxane. Synthesized imidate were reacted with 4-ethoxybenzylamine in the presence of different catalysts that have been shown in the Scheme 1. In this section of work, the main scope was investigation about the effect of different catalysts on the rate of reaction. Some of catalysts such as sulphonic acids such as p-toluenesulphonic acid (PTSA), AlCl₃, ceric ammonium nitrate (CAN),¹⁹ C₆H₅NH₃⁺Cl⁻,²⁰ K10, SiO₂-OSO₃H (SSA), HClO₄-SiO₂ were tested on reaction that have been shown in Table 1. This reaction without any catalyst took 20 days. The usage of other catalysts decreased the time of reaction about several days. It was observed that the reaction proceeded efficiently in the presence of silica sulfuric acid (SSA) at room temperature about 2 hours, giving formamidines in excellent yields. SSA was afforded from silica gel and chlorosulfonic acid as described previously.²¹



Catalyst: -SO₃H, PTSA, AlCl₃, CAN, C₆H₅NH₃⁺Cl⁻, K10, SiO₂-OSO₃H, HClO₄-SiO₂

Scheme 1: synthesis of (1E)-N'-((Z)-2-amino-1,2-dicyanovinyl)-N-(4-ethoxyphenyl)formamidine from imidate in the presence of different catalysts.

To demonstrate the generality of this method, we examined the reaction of imidate with various amines in the presence of SSA in dry ethanol under argon at room temperature (Scheme 2, Table 2). This method is effective for the preparation of formamidine derivatives from both electron-rich as well as electron-deficient.

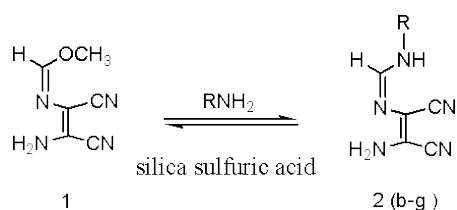
Table 1. Catalytic evolution for synthesis formamidine from imidate

| Entry | Catalyst | Time, days | Yield, % |
|-------|--|-------------|----------|
| 1 | No | 20 | 40 |
| 2 | -SO ₃ H | - | - |
| 3 | PTSA | 4 | 60 |
| 4 | AlCl ₃ | 7 | 48 |
| 5 | CAN | 8 | 50 |
| 6 | C ₆ H ₅ NH ₃ ⁺ Cl ⁻ | 3 | 67 |
| 7 | K10 | 1 | 70 |
| 8 | HClO ₄ - SiO ₂ | 3 | 58 |
| 9 | SiO ₂ -OSO ₃ H | 0.083 (2 h) | 87 |

Table 2. Synthesis of formamidine with the usage of amines and imidate in the presence of SSA

| Entry | compd. | Imidate | Amine | Formamidine | Time, min | M. P., °C | Yield, % |
|-------|--------|---------|-------|-------------|-----------|-----------|----------|
| 1 | 2a | | | | 120 | 148-150 | 94 |
| 2 | 2b | | | | 135 | 150-152 | 87 |
| 3 | 2c | | | | 130 | 148-150 | 86 |
| 4 | 2d | | | | 140 | 138-140 | 90 |
| 5 | 2e | | | | 110 | 142-144 | 94 |
| 6 | 2f | | | | 115 | 144-146 | 91 |
| 7 | 2g | | | | 165 | 134-136 | 91 |

In general, when R represented the electron with donor groups such as amino and ethoxy groups the yield and purity of the product were obviously better, and short reaction time was required.

**Scheme 2.** synthesis of formamidines from imidate in the presence of silica sulfuric acid.

All of synthesized compounds were characterized by TLC, IR, ¹H NMR. The IR vibrations of imidate showed NH₂ at about 3450 cm⁻¹, 3300 cm⁻¹ and the cyano at about 2225 cm⁻¹ and stretching vibration of C=N at about 1640 cm⁻¹. The other band were observed in expected place. Furthermore, ¹H NMR of imidate revealed proton of the N=CH as a singlet peak in the region of δ7.94 ppm. The protons of the NH₂ appeared in singlet pattern in δ 6.98 ppm. Protons of OCH₃ were seen as a singlet peak in the region of δ3.78 ppm.

The infrared spectrum of (2a-g) confirmed the presence of the NH₂ and C≡N stretching vibration within the region of 3300-3480 and 2200 cm⁻¹ and C=C appeared at about 1600 cm⁻¹. The ¹H NMR spectra showed proton of the NH in the range of δ8.17-9.83 ppm. Proton of N=CH was seen in

7.70-8.54. The protons of the aromatic rings were revealed in expected place. The protons of the NH₂ were seen at the region of δ 4-6.31ppm.

Conclusions

In conclusion, we tried to find efficient and new method for preparing formamidine. Different catalysts were tested to afford amidine from imidate. Effect of Catalysts on the rate of reaction was considered. Compared to other catalyst, SSA can decrease the time of reaction about several hours. So, SSA was chosen as best catalyst in this reaction and was examined on synthesis of different amidines. The Synthesis of all amidines in high yield only took about 2 hours.

Acknowledgment

We are grateful to the University of Guilan Research Council for the partial support of this work.

References

- Granik, V. G., *Russ. Chem. Rev.*, **1983**, 52, 377.
- Katritzky, A. R., Cai, C., Singh, S. K., *J. Org. Chem.*, **2006**, 71, 3375.
- Lange, U. E. W., Schiller, B., Baucke, D., Buschmann, E., Mack, H., *Tetrahedron Lett.*, **1999**, 40, 7067.

- ⁴Lee, M. Y., Kim, M. H., Kim, J., Kim, S. H., Kim, B. T., Jeong, I. H., Chang, S., Kim, S. H., Chang, S. Y., *Bioorg. Med. Chem. Lett.*, **2010**, 20, 541.
- ⁵Greenhill, J. V., Lue, P., *Prog. Med. Chem.*, **1993**, 30, 203.
- ⁶Dabak, K., *Turk. J. Chem.*, **2002**, 26, 547.
- ⁷Sondhi, S. M., Dinodia, M., Kumar, A., *Bioorg. Med. Chem.*, **2006**, 14, 4657.
- ⁸Sienkiewich, P., Bielawski, K., Bielawska, A., Palka, J., *Environ. Toxicol. Pharmacol.*, **2005**, 20, 118.
- ⁹Bielawska, A., Bielawski, K., Muszynska, A., *Farmaco.*, **2004**, 59, 111.
- ¹⁰Sielecki, T. M., Liu, J., Mousa, S. A., Racanelli, A. L., Hausner, E. A., Wexler, R. R., Olson, R. E., *Bioorg. Med. Chem. Lett.*, **2001**, 11, 2201.
- ¹¹Stephens, C. E., Tanius, E., Kim, S., Wilson, D. W., Schell, W. A., Perfect, J. R., Franzblau, S. G., Boykin, D. W., *J. Med. Chem.*, **2001**, 44, 1741.
- ¹²Liebeschuetz, J. W., Jones, S. D., Morgan, P. J., Marray, C. W., Rimmer, A. D., Roscoe, J. M. E., Waszkowycz, B., Welsch, P. M., Wylie, W. A., Young, S. C., Martin, H., Mahler, J., Brady, L., Wilkinson, K., *J. Med. Chem.*, **2002**, 45, 1221.
- ¹³Azmi, A. A., Elassar, A. Z. A., Booth, B. L., *Tetrahedron.*, **2003**, 59, 2749.
- ¹⁴Yahyazadeh, A., Habibi, F., **2007**. *E. J. Chem* 4, 372.
- ¹⁵Yahyazadeh, A., *Russ. J. Org. Chem.*, **2003**, 39, 1649.
- ¹⁶Loge, C., Testard, A., Thiery, V., Lozach, O., Blairvacq, M., Robert, J. M., Meijer, L., Besson, T., *Eur. J. Med. Chem.*, **2008**, 43, 1469.
- ¹⁷Charette, A. B., Grenon, M., *Tetrahedron Lett.*, **2000**, 41, 1677.
- ¹⁸Gielen, H., Alija, C. A., Hendrix, M., *Tetrahedron Lett.*, **2002**, 43, 419.
- ¹⁹Sadek, K. U., Alnajjar, A., Mekheimer, R. A., Mohamed, N. K., Mohamed H. A., *Green and Sustainable Chemistry.*, **2001**, 1, 92.
- ²⁰Yahyazadeh, A., Pourrostan, B., Rabiee, M., *JKCS.*, **2003**, 24, 1723.
- ²¹Salehi, P., Zolfigol, M. A., Shirini, F., Baghbanzadeh, M., *Curr. Org. Chem.*, **2006**, 10, 2171.

Received: 18.04.2013.

Accepted: 21.06.2013.



KINETICS AND MECHANISM OF THE OXIDATION OF SOME α -HYDROXY ACIDS BY QUINOLINIUM CHLOROCHROMATE

Neha Vyas^[a], Amit Daiya^[a], Anurag Choudhary^[a], Monica Sharma^[b] and Vinita Sharma^{[a]*}

Keywords: Correlation analysis; halochromates; α -hydroxy acids; kinetics; mechanism; oxidation; quinolinium chlorochromate.

The oxidation of glycolic (GA), lactic (LA), malic (ML) and a few substituted mandelic acids (MLA) by quinolinium chlorochromate (QCC) in dimethylsulphoxide (DMSO) leads to the formation of corresponding oxoacids. The reaction is first order each in QCC. Michaelis-Menten type of kinetics is observed with respect to the hydroxy acids. Reaction is failed to induce the polymerisation of acrylonitrile. The oxidation of α -deuteriomandelic acid (DMA) shows the presence of a primary kinetic isotope effect ($k_H/k_D = 5.75$ at 298 K). The reaction does not exhibit the solvent isotope effect. The reaction is catalysed by the hydrogen ions. The hydrogen ion dependence has the form: $k_{obs} = a + b[H^+]$. Oxidation of p-methyl mandelic acid has been studied in 19 different organic solvents. The solvent effect has been analysed by using Kamlet's and Swain's multiparametric equations. A mechanism involving a hydride ion transfer via a chromate ester is proposed.

Corresponding Authors

E-Mail: drvsharma29@gmail.com

[a] Department of Chemistry J.N.V. University, Jodhpur, 342 005, India

[b] Department of Chemistry, Modi Institute of Technology, Kota, Rajasthan, India

(PhCD(OH)COOH or DMA) was prepared by the method of Kemp and Waters.¹⁰ Its isotopic purity, ascertained by NMR spectra, was $95 \pm 5\%$. Due to the non-aqueous nature of the solvent, toluene p-sulphonic acid (TsOH) was used as a source of hydrogen ions. Solvents were purified by their usual methods.

Introduction

Selective oxidation of organic compounds under non-aqueous conditions is an important reaction in synthetic organic chemistry.^{1a} For this a number of different chromium(VI) derivatives have been reported.^{1b} Quinolinium chlorochromate (QCC) is one such compound used for the oxidation of phenylic alcohols and oximes.² α -Hydroxy acids may be oxidized either as alcohols, yielding corresponding oxoacids³ or they may undergo oxidative decarboxylation to yield a ketone.⁴ There seems to be no report available on the oxidation aspects using quinolinium chlorochromate (QCC). We have been interested in the kinetic and mechanistic aspects of the oxidation by complexed Cr(VI) species and several reports by halochromates have already been reported.⁵⁻⁸ In continuation of our earlier work with halochromates, we now report the kinetics and mechanism of oxidation of some hydroxy acids by QCC in DMSO as solvent. A suitable mechanism has also been proposed.

Experimental Section:

Materials

The hydroxy acids were commercial products of the highest purity available and were used as such. The preparation and specification of the substituted mandelic acids have been described earlier.⁹ QCC was prepared by reported method² and its purity was checked by an iodometric method. α -Deuteriomandelic acid

Product analysis

Product analyses were carried out under kinetic conditions i.e., with an excess of the reductant over QCC. In a typical experiment mandelic acid (MA, 7.6 g, 0.05 mol) and QCC (1.88 g, 0.01 mol) were dissolved in 100 ml of DMSO and was allowed to stand in dark for ≈ 24 h to ensure the completion of the reaction. It was then treated with an excess (250 ml) of a freshly prepared saturated solution of 2,4-dinitrophenylhydrazine in 2 mol dm⁻³ HCl and kept overnight in a refrigerator. The precipitated 2,4-dinitrophenylhydrazone (DNP) was filtered off, dried, weighed, recrystallised from ethanol and weighed again. The product was identical (mp and mixed mp) to an authentic sample of DNP of phenylglyoxylic acid. Similar experiments with the other hydroxy acids yielded the DNP of the corresponding oxoacids in 79 to 87% yields, after recrystallization. The oxidation state of chromium in completely reduced reaction mixtures, determined by an iodometric method, was 3.95 ± 0.10 .

Kinetic measurements

The pseudo-first order conditions were attained by keeping a large excess ($\times 15$ or greater) of the hydroxy acid over QCC. The temperature was kept constant to ± 0.1 K. The solvent was DMSO, unless specified otherwise. The reactions were followed by monitoring the decrease in the concentration of QCC spectrophotometrically at 352 nm for up to 80% of the reaction. No other reactant or product has any significant absorption at this wavelength. The pseudo-

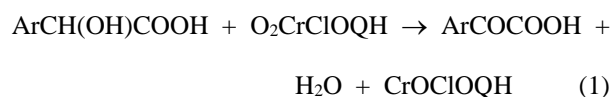
first order rate constants, k_{obs} , were computed from the linear least square plots of $\log[\text{QCC}]$ versus time. Duplicate kinetic runs showed that the rates were reproducible within $\pm 3\%$. The second order rate constants, k_2 , were calculated from the relation: $k_2 = k_{\text{obs}}/[\text{hydroxy acid}]$. All experiments, other than those for studying the effect of hydrogen ions, were carried out in the absence of TsOH.

Results

The rate and other experimental data were obtained for all the hydroxy acids studied. Since the results were similar, only representative data are reproduced here.

Stoichiometry

The oxidation of hydroxy acids resulted in the formation of the corresponding oxoacids. Product analysis and stoichiometric determinations indicated that the overall reaction could be written as below (1).

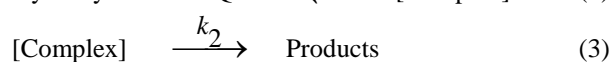
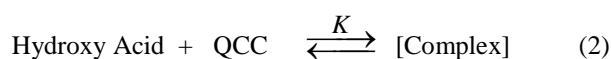


QCC undergoes a two-electron change. This is according to the earlier observations with other halochromates⁵⁻⁸ also.

Kinetics dependence/Rate Laws

The reactions are of first order with respect to QCC. Further, the pseudo-first order rate constant, k_{obs} is independent of the initial concentration of QCC.

Figure 1 depict a typical kinetic run. The reaction rate increases with increase in the concentration of the hydroxy acid but not linearly (Table 1). A plot of $1/k_{\text{obs}}$ against $1/[\text{Hydroxy acid}]$ is linear ($r > 0.995$) with an intercept on the rate-ordinate (Figure 2). Thus, Michaelis-Menten type kinetics are observed with respect to the hydroxyl acid. This leads to the postulation of following overall mechanism (2) and (3) and rate law (4).



$$\text{Rate} = \frac{k_2 K [\text{HA}][\text{QCC}]}{1 + K [\text{HA}]} \quad (4)$$

The dependence of reaction rate on the reductant concentration was studied at different temperatures and the values of K and k_2 were evaluated from the double reciprocal plots. The thermodynamic parameters of the complex formation and activation parameters of the decomposition of the complexes were calculated from the

values of K and k_2 respectively at different temperatures (Tables 3 and 4). Fig. 1 depict a typical kinetic run.

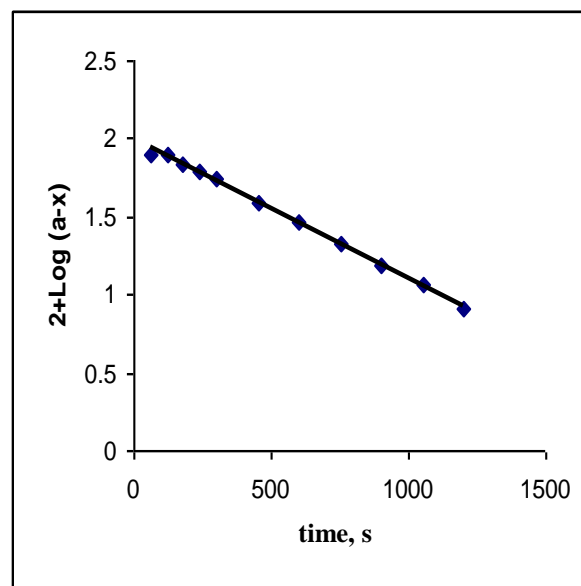


Figure1. Oxidation of Mandalic acids by QCC: A typical kinetic run

Induced Polymerisation of Acrylonitrile

The oxidation of hydroxy acids, by QCC, in an atmosphere of nitrogen failed to induce the polymerisation of acrylonitrile. Further, addition of acrylonitrile had no effect on the rate (Table 1).

Table 1. Rate constants for the oxidation of mandelic acid by QCC at 298 K

| $10^3 [\text{QCC}],$ mol dm^{-3} | $[\text{HA}],$ mol dm^{-3} | $10^4 k_{\text{obs}}, \text{s}^{-1}$ |
|--|--|--------------------------------------|
| 1.00 | 0.10 | 7.26 |
| 1.00 | 0.20 | 10.7 |
| 1.00 | 0.40 | 14.1 |
| 1.00 | 0.60 | 15.8 |
| 1.00 | 0.80 | 16.8 |
| 1.00 | 1.00 | 17.5 |
| 1.00 | 1.50 | 18.4 |
| 1.00 | 3.00 | 19.5 |
| 2.00 | 0.20 | 11.2 |
| 4.00 | 0.20 | 9.90 |
| 6.00 | 0.20 | 10.8 |
| 8.00 | 0.20 | 11.7 |
| 1.00 | 0.40 | 15.3* |

* contained $0.001 \text{ mol dm}^{-3}$ acrylonitrile

Effect of hydrogen ions

The reaction is catalysed by hydrogen ions. p-Toluene sulphonic acid (TsOH) was used as the source of hydrogen ions. The hydrogen ion dependence has the form $k_{\text{obs}} = a + b[\text{H}^+]$ (Table 2). The values of a and b , for p-methyl mandelic acid, are $18.4 \pm 0.19 \times 10^{-4} \text{ s}^{-1}$ and $28.5 \pm 0.33 \times 10^{-3} \text{ mol}^{-1} \text{ dm}^3 \text{ s}^{-1}$ respectively ($r^2 = 0.9995$).

Table 2. Effect of hydrogen ion concentration on the oxidation of mandelic acid by QCC

| | | | | | | |
|--|------|------|------|------|------|------|
| [H ⁺] | 0.10 | 0.20 | 0.40 | 0.60 | 0.80 | 1.00 |
| 10 ⁴ k _{obs} , s ⁻¹ | 21.1 | 24.3 | 29.7 | 35.1 | 41.4 | 46.8 |

[QCC] = 0.001 mol dm⁻³; [HA] = 1.00 mol dm⁻³; Temp. = 298 K**Table 3.** Formation constants for the decomposition of QCC–hydroxyacid complexes and thermodynamic parameters

| R | K, dm ³ mol ⁻¹ | | | | ΔH , kJ mol ⁻¹ | $-\Delta S$, J mol ⁻¹ K ⁻¹ | $-\Delta G$, kJ mol ⁻¹ |
|-------------------|--------------------------------------|-------|-------|-------|--------------------------------------|--|---------------------------------------|
| | 288 K | 298 K | 308 K | 318 K | | | |
| H | 6.17 | 5.40 | 4.73 | 4.05 | 12.5±0.4 | 18±1 | 7.16±0.3 |
| p-F | 5.80 | 5.10 | 4.32 | 3.60 | 13.8±0.6 | 24±2 | 6.81±0.5 |
| p-Cl | 5.94 | 5.25 | 4.52 | 3.80 | 11.9±0.3 | 17±1 | 7.03±0.3 |
| p-Br | 6.03 | 5.35 | 4.62 | 3.85 | 17.2±0.7 | 37±2 | 6.41±0.6 |
| p-Me | 5.88 | 5.15 | 4.41 | 3.76 | 14.7±0.5 | 27±1 | 6.79±0.4 |
| p-Pr ⁱ | 5.67 | 4.91 | 4.25 | 3.50 | 12.1±0.4 | 17±1 | 7.15±0.4 |
| p-OMe | 5.95 | 5.20 | 4.50 | 3.78 | 15.0±0.6 | 29±2 | 6.37±0.5 |
| m-Cl | 6.12 | 5.42 | 4.67 | 3.98 | 14.6±0.6 | 27±2 | 6.72±0.5 |
| m-NO ₂ | 6.05 | 5.31 | 4.62 | 3.90 | 14.7±0.7 | 27±2 | 6.78±0.5 |
| p-NO ₂ | 5.76 | 5.05 | 4.35 | 3.63 | 16.3±0.6 | 33±2 | 6.45±0.5 |
| GA | 5.82 | 5.12 | 4.39 | 3.68 | 13.4±0.5 | 23±2 | 6.75±0.4 |
| LA | 5.49 | 4.78 | 4.05 | 3.36 | 11.5±0.3 | 15±1 | 7.22±0.2 |
| MLA | 5.60 | 4.86 | 4.15 | 3.42 | 14.4±0.6 | 27±2 | 6.57±0.5 |
| DMA | 5.77 | 5.10 | 4.30 | 3.66 | 16.1±0.8 | 34±2 | 6.21±0.6 |

Kinetic isotope effect

To ascertain the importance of the cleavage of the C-H bond in the rate-determining step, the oxidation of α -deuteriomandelic acid (DMA) was studied. Results showed the presence of a substantial primary kinetic isotope effect (Table 4). The value of k_H/k_D is 5.85 at 298 K.

Effect of solvents

The rate of oxidation of mandelic acid was determined in nineteen different organic solvents. The choice of the solvents was limited by the solubility of QCC and reaction with primary and secondary alcohols. There was no noticeable reaction with the solvents chosen. The kinetics were similar in all the solvents. The values of formation constants K and decomposition constants of the complex, k_2 are recorded in Table 5.

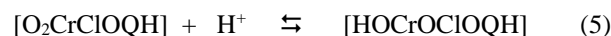
Discussion

A satisfactory linear correlation ($r^2 = 0.9600$) between the values the activation enthalpies and entropies of the oxidation of the hydroxy acids indicated the operation of compensation effect in this reaction.¹¹ The reaction also exhibited an excellent isokinetic effect, as determined by Exner's criterion.¹² An Exner's plot between $\log k_2$ at 288K and at 318 K was linear ($r = 0.9989$) (Figure 3). The value of isokinetic temperature is 881±17 K.

The linear isokinetic correlation implies that all the hydroxyl acids are oxidized by the same mechanism and the changes in rate are governed by the changes in both the enthalpy and entropy of the activation.

Reactive oxidizing species

The observed H⁺ dependence suggests that reaction follows two mechanistic pathways, one acid-independent and other acid-dependent. The acid catalysis may well be attributed to a protonation of QCC to give a stronger oxidant and electrophile.



Solvent effect

The rate constants of oxidation, k_2 , in eighteen solvents (CS₂ was not considered, as the complete range of solvent parameters was not available) were correlated in terms of the linear solvation energy relationship of Kamlet *et al.*¹³

$$\log k_2 = A_0 + p\pi^* + b\beta + a\alpha. \quad (6)$$

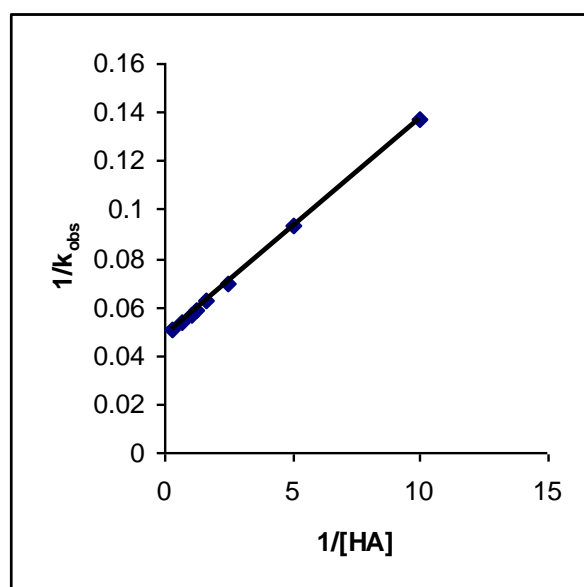


Figure 2. $1/k_{\text{obs}}$ vs $1/[\text{HA}]$: A double reciprocal plot

In this equation π^* represents the solvent polarity, β the hydrogen bond acceptor basicities and α is the hydrogen bond donor acidity. A_0 is the intercept term. It may be mentioned here that out of the 18 solvents, 12 have a value of zero for α . The results of correlation analyses in terms of a biparametric equation involving π^* and β , and separately with π^* and β are given below [(7 - 10)].

$$\log k_2 = -3.79 + 1.51(\pm 0.18)\pi^* + 0.23(\pm 0.15)\beta + 0.14(\pm 0.14)\alpha \quad (7)$$

$$R^2 = 0.8740; \quad sd = 0.16; \quad n = 18; \quad \psi = 0.39$$

$$\log k_2 = -3.82 + 1.56(\pm 0.17)\pi^* + 0.18(\pm 0.17)\beta \quad (8)$$

$$R^2 = 0.8647; \quad sd = 0.16; \quad n = 18; \quad \psi = 0.39$$

$$\log k_2 = -3.79 + 1.61(\pm 0.17)\pi^* \quad (9)$$

$$r^2 = 0.8495; \quad sd = 0.17; \quad n = 18; \quad \psi = 0.40$$

$$\log k_2 = -2.91 + 0.46(\pm 0.34)\beta \quad (10)$$

$$r^2 = 0.1036; \quad sd = 0.41; \quad n = 18; \quad \psi = 0.97$$

Here n is the number of data points and Ψ is the Exner's statistical parameter.¹⁴ Kamlet's¹³ triparametric equation explains ca. 87% of the effect of solvents on the oxidation. However, by Exner's criterion the correlation is not even satisfactory (cf. 7). The major contribution is of solvent polarity. It alone accounted for ca. 85% of the data. Both β and α play relatively minor roles.

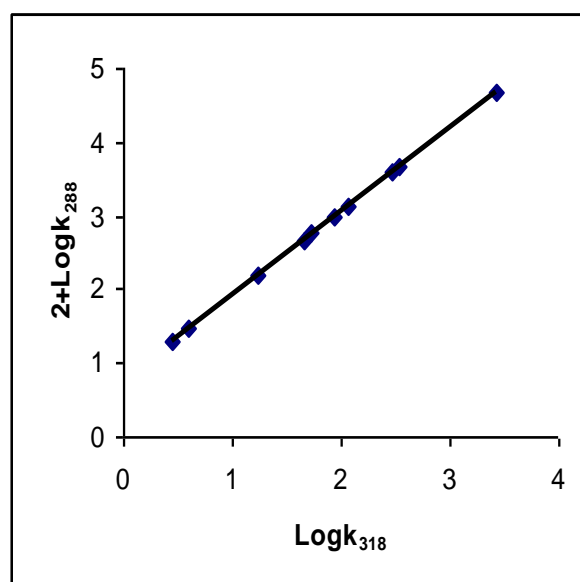


Figure 3. Exner's isokinetic relationship in the oxidation of HA by QCC

The data on the solvent effect were analysed in terms of Swain's equation¹⁵ of cation- and anion-solvating concept of the solvents also (11).

$$\log k_2 = aA + bB + C \quad (11)$$

Here A represents the anion-solvating power of the solvent and B the cation-solvating power. C is the intercept term. $(A + B)$ is postulated to represent the solvent polarity. The rates in different solvents were analysed in terms of (11), separately with A and B and with $(A + B)$.

$$\log k_2 = 0.59(\pm 0.05)A + 1.61(\pm 0.04)B - 3.97 \quad (12)$$

$$R^2 = 0.9971; \quad sd = 0.04; \quad n = 19; \quad \psi = 0.09$$

$$\log k_2 = 0.36(\pm 0.53)A - 2.87 \quad (13)$$

$$r^2 = 0.0270; \quad sd = 0.43; \quad n = 19; \quad \psi = 1.01$$

$$\log k_2 = 1.56(\pm 0.11)B - 3.78 \quad (14)$$

$$r^2 = 0.9212; \quad sd = 0.12; \quad n = 19; \quad \psi = 0.29$$

$$\log k_2 = 1.27 \pm 0.13(A + B) - 3.94 \quad (15)$$

$$r^2 = 0.8430; \quad sd = 0.17; \quad n = 19; \quad \psi = 0.41$$

Table 4. Rate constants for the decomposition of QCC–hydroxyacid complexes and activation parameters

| R | $10^4 k_2, \text{dm}^3 \text{mol}^{-1} \text{s}^{-1}$ | | | | ΔH^* kJ mol ⁻¹ | $-\Delta S^*$ J mol ⁻¹ K ⁻¹ | ΔG^* kJ mol ⁻¹ |
|-------------------|---|-------|-------|-------|--------------------------------------|--|--------------------------------------|
| | 288 K | 298 K | 308 K | 318 K | | | |
| H | 9.81 | 20.7 | 42.3 | 88.2 | 53.1±0.7 | 119±2 | 88.3±0.5 |
| p-F | 13.5 | 28.8 | 58.8 | 117 | 52.2±0.3 | 119±1 | 87.5±0.2 |
| p-Cl | 5.67 | 12.6 | 25.2 | 54.0 | 54.2±0.8 | 121±3 | 89.6±0.6 |
| p-Br | 4.68 | 10.8 | 21.6 | 45.9 | 54.9±0.7 | 118±2 | 90.0±0.6 |
| p-Me | 45.9 | 92.7 | 171 | 333 | 47.4±0.6 | 126±2 | 84.6±0.5 |
| p-Pr ⁱ | 39.6 | 79.2 | 153 | 297 | 48.5±0.5 | 123±1 | 85.0±0.4 |
| p-OMe | 468 | 882 | 1440 | 2610 | 40.5±0.9 | 130±3 | 79.1±0.7 |
| m-Cl | 1.53 | 3.42 | 7.83 | 17.1 | 58.9±0.9 | 114±2 | 92.7±0.6 |
| m-NO ₂ | 0.29 | 0.68 | 1.71 | 3.87 | 63.7±0.9 | 111±3 | 96.7±0.7 |
| p-NO ₂ | 0.20 | 0.49 | 1.17 | 2.79 | 64.3±0.7 | 122±2 | 90.1±0.6 |
| GA | 4.68 | 9.81 | 20.7 | 43.2 | 53.9±0.7 | 112±2 | 97.6±0.6 |
| LA | 6.75 | 14.4 | 29.7 | 62.1 | 53.7±0.6 | 120±2 | 89.2±0.5 |
| MLA | 5.76 | 12.6 | 25.2 | 54.9 | 54.2±0.9 | 119±3 | 89.6±0.8 |
| DMA | 1.63 | 3.54 | 7.55 | 16.3 | 55.8±0.7 | 124±2 | 92.6±0.6 |
| k_H/k_D | 6.06 | 5.85 | 5.60 | 5.41 | | | |

The rates of oxidation of *p*-methylmandelic acid in different solvents showed an excellent correlation in Swain's equation (cf. 11) with the cation-solvating power playing the major role. In fact, the cation-solvation alone accounts for *ca.* 99 % of the data. The correlation with the anion-solvating power was very poor. The solvent polarity, represented by (*A* + *B*), also accounted for *ca.* 84 % of the data. In view of the fact that solvent polarity is able to account for *ca.* 84 % of the data, an attempt was made to correlate the rate with the relative permittivity of the solvent. However, a plot of log k_2 against the inverse of the relative permittivity is not linear ($r^2 = 0.2882$; $sd = 0.56$; $\Psi = 0.91$).

Correlation Analysis of Reactivity

The rate of oxidation of substituted mandelic acids correlated well with Brown's σ^+ values,¹⁶ the reaction constant being negative (Table 6). The correlation with Hammett's σ values was not very significant. The large negative reaction constants and correlation with σ^+ values indicate a carbo-cationic reaction centre in the transition state.

Mechanism

Absence of any effect of added acrylonitrile on the reaction discounts the possibility of a one-electron oxidation, leading to the formation of free radicals. The presence of a substantial kinetic isotope effect in the oxidation of mandelic acid¹⁷ confirms the cleavage of the α -C-H bond in the rate determining step. The large negative reaction constant together with the excellent correlation with Brown's σ^+ values¹⁶ point to a highly electron-deficient carbon centre in the transition state. The transition state thus approaches a carbocation in character. This is supported by the solvent effect also. Greater role played by the cation-solvating power of the solvents supported the postulation of a carbocationic transition state. Therefore, the correlation analysis of substituent and solvent effects on the oxidation of mandelic acid supports the mechanism involving a hydride-ion transfer via a chromate ester.

Table 5. Effect of solvents on the oxidation of *p*-methyl mandelic acid by QCC at 308 K

| Solvents | $K, \text{dm}^3 \text{mol}^{-1}$ | $10^5 k_2, \text{s}^{-1}$ |
|------------------------|----------------------------------|---------------------------|
| Chloroform | 6.13 | 25.7 |
| Toluene | 4.72 | 8.32 |
| 1,2-Dichloroethane | 5.45 | 30.2 |
| Acetophenone | 5.44 | 44.7 |
| Dichloromethane | 5.85 | 35.5 |
| THF | 5.77 | 14.8 |
| DMSO | 5.15 | 92.7 |
| <i>t</i> -Butylalcohol | 5.84 | 14.1 |
| Acetone | 5.88 | 27.5 |
| 1,4-Dioxane | 4.93 | 15.5 |
| DMF | 4.95 | 56.2 |
| 1,2-Dimethoxyethane | 5.31 | 9.77 |
| Butanone | 6.03 | 20.4 |
| CS ₂ | 4.74 | 5.25 |
| Nitrobenzene | 5.40 | 41.7 |
| Acetic acid | 4.70 | 5.89 |
| Benzene | 6.22 | 10.5 |
| Ethyl acetate | 5.67 | 13.2 |
| Cyclohexane | 5.41 | 1.45 |

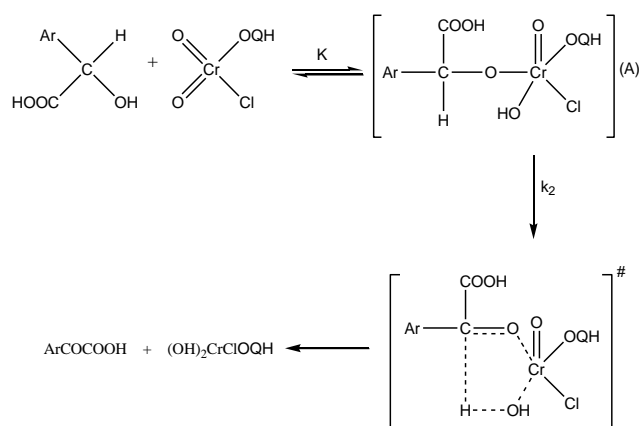
Table 6: Temperature dependence of the reaction constant

| Temp., K | 288 | 298 | 308 | 318 |
|----------|-----------|------------|------------|----------|
| ρ^* | - | -2.09±0.02 | -1.98±0.01 | - |
| | 2.16±0.01 | | | 190±0.02 |
| r^2 | 0.9999 | 0.9998 | 0.9999 | 0.9989 |
| sd | 0.006 | 0.007 | 0.008 | 0.006 |
| Ψ | 0.01 | 0.02 | 0.01 | 0.04 |

Kwart and Nickle¹⁸ have shown that a study of the dependence of the kinetic isotope effect on temperature can be gainfully employed to resolve this problem. The data for protio- and deuteriomandelic acids, fitted to the familiar expression $k_H/k_D = A_H/A_D \exp(E_a/RT)$ ^{19,20} show a direct correspondence with the properties of a symmetrical transition state in which the activation energy difference (E_a) for k_H/k_D is equal to the zero-point energy difference for the respective C-H and C-D bonds (≈ 4.5 kJ/mol) and the

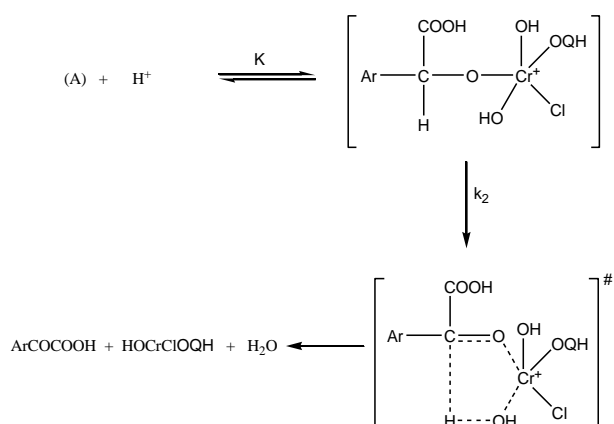
frequency factors and the entropies of activation of the respective reactions are nearly equal. Bordwell²¹ has documented a very cogent evidence against the occurrence of concerted one-step biomolecular processes by hydrogen transfer and it is evident that in the present studies also the hydrogen transfer does not occur by an acyclic biomolecular process. It is well established that intrinsically concerted sigmatropic reactions, characterized by transfer of hydrogen in a cyclic transition state, are the only truly symmetrical processes involving a linear hydrogen transfer.²² Littler²³ has also shown that a cyclic hydride transfer, in the oxidation of alcohols by Cr(VI), involves six electrons and, being a Huckel-type system, is an allowed process. Thus the overall mechanism is proposed to involve the formation of a chromate ester in a fast pre-equilibrium and then a decomposition of the ester in a subsequent slow step via a cyclic concerted symmetrical transition state leading to the product (Scheme 1 and 2). The observed negative value of entropy of activation also supports a polar transition state.

Acid-independent Path (Scheme - 1)



The observed negative entropy of activation also supports it. As the charge separation takes place, the charged ends become highly solvated. This results in an immobilization of a large number of solvent molecules, reflected in the loss of entropy.

Acid-dependent Path (Scheme - 2)



It is of interest to compare the mode of oxidation of hydroxy acids by PCC,²⁴ PFC²⁵ MCC²⁶ and QCC. The oxidation by PFC and QCC exhibited a similar kinetic picture i.e. Michaelis-Menten type kinetics with respect to hydroxy acids. While the oxidation by PCC and MCC, showed a first order kinetics. The rate laws, hydrogen ion

dependence and kinetic isotope effect are similar in both the cases. In the oxidations by PFC and QCC excellent correlations were obtained in terms of Swain's equation with the cation solvating power of the solvents playing the major role. In all the three oxidations the polar reactions are negative.

Conclusion

The reaction is proposed to proceed through a hydride-ion transfer via a chromate ester in the rate determining step. It has also been observed that hydride-ion transfer is also supported by the cation-solvating power of the solvents. Both deprotonated and protonated forms of QCC are the reactive oxidizing species.

Acknowledgement

Thanks are due to the UGC, New Delhi, India for financial support in the form of MRP and to Professor Kalyan K. Banerji, Dean, Sciences, National Law University, Mandore, Jodhpur, for his critical suggestions.

References

- Mehrotra, R. N., *Eur. Chem. Bull.*, **2013**, 2(10), 758; Banerji, J., Banerji, K. K.; Kotai, L., Sharma, D., Sharma, P. K., *J. Ind. Chem. Soc.*, **2011**, 88(12), 1879; Kotai, L., Gacs, I., Sajo, I. E.; Sharma, P. K.; Banerji, K. K., *Trends Inorg. Chem.*, **2009**, 11, 25; Banerji, J., Kotai, L., Banerji, K. K., *Ind. J. Chem. Sect. A*, **2009**, 48A(6), 797; Shukla, R., Kotai, L., Sharma, P. K.; Banerji, K. K., *J. Chem. Res. (S)*, **2003**(4), 184; Shukla, R., Sharma, P. K., Kotai, L., Banerji, K. K., *Proc.- Indian Acad. Sci. Chem. Sci.*, **2003**, 115(2), 129; Dubey, R., Kotai, L., Banerji, K. K., *J. Chem. Res. (S)*, **2003**(2), 56; Kumar, A., Mishra, P., Kotai, L., Banerji, K. K., *Ind. J. Chem. Sect. A*, **2003**, 42A(1), 72; Kotai, L., Kazinczy, B., Keszler, A., Holly, S., Gacs, I., Banerji, K. K., *Z. Naturforsch. B: Chem. Sci.*, **2001**, 56(8), 823. Sankhla, R., Kothari, S., Kotai, L., Banerji, K. K., *J. Chem. Res. (S)*, **2001**(4), 127; Banerji, J., Kótai, L., Sharma, P. K., Banerji, K.K., *Eur. Chem. Bull.* **2012**, 1(5), 135; Purohit, T., Banerji, J., Kotai, L., Sajo, I., Banerji, K. K., Sharma, P. K., *J. Ind. Chem. Soc.*, **2012**, 89, 1045; Meena, A. K., Daiya, A., Sharma, A., Banerji, J., Sajo, I. E., Kotai, L., Sharma, V., *Int. J. Chem. (Mumbai)* **2012**, 1, 55.
- Corey, E. J., Suggs, W. J. *Tetrahedron Lett.*, **1975**, 2647; Guziec, F. S., Luzio, F. A. *Synthesis*, **1980**, 691; Bhattacharjee, M. N., Choudhuri, M. K., Dasgupta, H. S., Roy, N., Khathing, D. T. *Synthesis*, **1982**, 588; Balasubramanian, K., Prathiba, V. *Indian J. Chem.*, **1986**, 25B, 326; Pandurangan, A., Murugesan, V., Palamichamy, P. *J. Indian Chem. Soc.*, **1995**, 72, 479; Panchariya, P., Purohit, T., Swami, P., Malani, N., Kotai, L., Prakash, O., Sharma, P. K. *Int. J. Chem. Sci.*, **2012**, 10, 557; Ashgar, B. M., Mansoor, S. S.; Malik, V. S., *Eur. Chem., Bull.*, **2013**, 2(8), 538-544; Panchariya, P., Vadera, K., Malani, N., Prasadrao, P., Kotai, L., Sharma, P. K., *J. Chem. Asia*, **2011**, 2(4), 225.;
- Singh, J., Kalsi, P. S., Jawanda, J. S., Chhabra, B. R., *Chem & Ind*, **1986**, 751.
- Banerji, K. K., *J. Chem. Res., (S)* **1978**, 193.
- Levesley, P., Waters, W.A., *J. Chem. Soc.*, **1955**, 215.
- Malani, N., Baghmar, M., Sharma, P. K., *Int. J. Chem. Kinet*, **2009**, 41, 65.
- Vadera, K., Sharma, D., Agarwal, S., Sharma, P. K., *Indian J. Chem.*, **2010**, 49A, 302.
- Vadera, K., Patel, M., Vyas, S., Purohit, P., Panchariya, P., Sharma, P. K., *Int. J. Chem. Sci.*, **2011**, 9(3) 1094.

- ⁸ Sharma, D., Panchariya, P., Purohit, P., Sharma, P.K., *Oxid. Commun.*, **2012**, 35(4) 821.
- ⁹ Vogel, I. A., *A text book of practical organic chemistry*, Longmans, London, **1956**, 776.
- ¹⁰ Kemp, T. J., Waters, W. A., *J. Chem. Soc.*, **1964**, 1192.
- ¹¹ Liu L., Guo, W. E. , *Chem Review*, **2001**, 101, 673.
- ¹² Exner, O. *Collect. Chem. Czech. Commun.*, **1977**, 38, 411.
- ¹³ Kamlet, M. J., Abboud, J L. M., Abraham, M. H., Taft, R. W. *J. Org. Chem.*, **1983**, 48, 2877.
- ¹⁴ Exner, O. *Collect. Chem. Czech. Commun.*, **1966**, 31, 3222.
- ¹⁵ Swain, C. G., Swain, M. S., Powel, A. L., Alunni, S. *J. Am. Chem. Soc.*, **1983**, 105, 502.
- ¹⁶ Brown, H. C., Okamoto, Y., *J. Am. Chem. Soc.*, **1958**, 80, 4079.
- ¹⁷ Asopa, R., Bhatt, P., Banerji, K. K., *Indian J. Chem*, **1992**, 31A, 706.
- ¹⁸ Kwart, H., Nickel, J. H. *J. Am. Chem. Soc.*, **1973**, 95, 3394.
- ¹⁹ Kwart, H., Latimer, M. C., *J. Am. Chem. Soc.*, **1971**, 93, 3770.
- ²⁰ Kwart, H., Slutsky, J. *J. Chem. Soc. Chem. Commun.*, **1972**, 1182.
- ²¹ Bordwell, F. G., *Acc. Chem. Res.*, **1974**, 5, 374.
- ²² Woodward, R. W., Hoffmann R. *Angew. Chem. Int. Ed Eng*, **1969**, 8, 781.
- ²³ Littler, J. S., *Tetrahedron*, **1971**, 27, 81.
- ²⁴ Banerji, K. K., *J. Chem. Res.*, **1978**, (S), 193; (M) 2561.
- ²⁵ Asopa, R., Agarwal, S., Banerji, K. ., *Proc. Indian Aca. Sci., Chem. Sci.*, **1991**, 104, 563.
- ²⁶ Swami, P., Yajurvedi, D., Mishra, P., Sharma, P. K., *Int. J. Chem. Kinet*, **2010**, 42, 50.

Received: 11.05.2013.

Accepted: 21.05.2013.



ADSORPTION OF MALACHITE GREEN DYE FROM AQUEOUS SOLUTION ONTO IRAQI RAW AL-HUSSAINIYAT CLAY

Saadiyah Ahmed Dhahir^{[a]*}, Enaas Abdul-Hussein^[a], Sanaa Tareq Sarhan^[a], and Noor Faraj^[a]

Keywords: adsorption, malachite green, Langmuir model, Freundlich model, thermodynamic, clay adsorbent

The adsorption of Malachite Green (MG) cationic dye on Al-Hussainiyat clay was first studied in a batch system for various dye concentrations. The adsorption was studied as a function of contact time, adsorbent dose, pH, and temperature under batch adsorption technique. The concentration of the solution before and after adsorption was measured spectrophotometrically. The equilibrium data fit with Langmuir and Freundlich models of adsorption and the linear regression coefficient R^2 was used to elucidate the best fitting isotherm model. Different thermodynamic parameters such as Gibb's free energy, enthalpy and entropy of the on-going adsorption process have also been evaluated. The thermodynamic analyses of the dye adsorption on Al-Hussainiyat clay indicated that the system was endothermic in nature.

* Corresponding Authors

E-Mail: sadiataher@yahoo.com

[a] Chemistry Department – College of Science for Women – Baghdad University

INTRODUCTION

Wastewater pollution gives adverse effects on public water supplies which may cause health problems such as diarrhea.^{1,2} It may also cause property damage such as the discharge of sewage that affects industrial water supplies by changing the character of the water. Apart from that, it may affect the buildings, monuments and boats by fading paints and colours.³ Dyes have long been used in dyeing, paper and pulp, textiles, plastics, leather, cosmetics and food industries. Effluents discharged from these industries poses certain hazards and environmental problems. Wastewater from these industries may present an eco-toxic hazard and introduce the potential danger of bioaccumulation, which may eventually affect human beings.⁴ There are various conventional methods of removing dyes from wastewaters. Among these methods, adsorption is the most versatile and widely used method because of its low cost and ease of operation.⁵⁻⁶ A number of agricultural waste and by-products of cellulose origin have been studied for their abilities to remove dyes from aqueous solutions,⁷ such as peanut hulls,⁸ maize bran,⁹ sawdust,¹⁰ clay sugar beet pulp,¹¹ crab peel,¹² granular kohlrabi peel,¹³ raw barley straw,¹⁴ eggshell,¹⁵ aquaculture shell powders etc.¹⁶ Activated carbon is regarded as one of the most effective materials for the removal of dyes,¹⁷ but due to its high cost and 10–15 % loss during regeneration, unconventional adsorbents like wood,¹⁸ silica,¹⁹ clay and activated clay,^{20,21} agricultural residues,²² etc. have attracted the attention of several investigations for the removal of dyes. In the present work, the ability of Al-Hussainiyat clay to remove cationic dye, by adsorption, has been considered. The effects of contact time, initial dye concentration and pH on the amount of colour removal were investigated. The equilibrium

experimental data were fitted into Langmuir and Freundlich equations to determine the best isotherm correlation.

MATERIALS AND METHODS

The adsorbate

The cationic dye (MG), in commercial purity, was used without further purification, $\lambda_{\max} = 617 \text{ nm}$.²³ The MG stock solution was prepared by dissolving accurately weighted dye in distilled water to the concentration of 20 mg L^{-1} . The experimental solutions were prepared by diluting the dye stock solution in accurate proportions to different initial concentrations from 2 to 16 ppm. The chemical name and their properties of this dye listed in Table 1

Table 1. The physical and chemical properties of MG

| Specification | | Structure of dye |
|-------------------|--|---|
| Empirical formula | $\text{C}_{23}\text{H}_{23}\text{ClN}_2$ | |
| Molar mass | 364.9179 | |
| Melting point | 210 °C | |
| Class | T.A.M | |
| Solubility | Water | * 4-[[4-(Dimethylamino)phenyl]methylene]phenyl-1-iminium chloride |

The adsorbent

Al-Hussainiyat clay was used as adsorbent throughout this study, it was obtained from the general company of Geological Survey and Mining, Ministry of Industry and Minerals Baghdad, Iraq. It was sieved to the required particle size between 150 and 212 μm . This clay was used in all experiments.²⁴ Surface information and analytical data for the clay under study were also supplied by the same company and are given below in Table 2.

Table 2. Chemical specifications of Al-Hussainiyat clay.

| Constituent | SO ₃ | Al ₂ O ₃ | Fe ₂ O ₃ | TiO ₂ | CaO | MgO | SiO ₂ | L.O.I |
|-------------|-----------------|--------------------------------|--------------------------------|------------------|--------|-------|------------------|--------|
| Wt % | <0.7 | 11.22 % | 29.48% | 0.80% | <2.0 % | 0.2 % | 20-28 | 10-14% |

Batch mode adsorption studies

Batch experiments were carried out to determine the effects of pH, adsorbent dose, initial dye concentration and contact time by varying the parameter under study and keeping other parameters constant. The stock solution was prepared by dissolving an accurately weighed quantity 0.25 g of solid dye in 1 L of deionized water to give 25 mg L⁻¹. The experimental solution of desired concentration was obtained by successive dilution of stock solution. The pH of all these solutions was maintained by adding 0.1 M HCl or 0.1 M NaOH. The experiments were carried out by taking 100 mL of MG solution and required amount of adsorbent into 250 mL conical flasks and stirred on water bath shaker at the speed of 200 rpm. The adsorption was monitored by determining the concentration of MG in solution using double beam UV-Visible spectrophotometer, at λ max 617 nm. Percentage of dye removal (ϕ , in %) and quantity of MG adsorbed on adsorbent at the time of equilibrium (Q_e) was calculated using Eq. 1 and 2 respectively.²⁵

$$\phi = 100 \times \frac{C_0 - C_e}{C_0} \quad (1)$$

$$q_e = \frac{(C_0 - C_e)V}{W} \quad (2)$$

where C_0 and C_e are the initial and the equilibrium concentrations (mg L⁻¹) of MG in solution, respectively. Q_e is quantity of MG adsorbed on the adsorbent at the time of equilibrium (mg g⁻¹), V is volume (in L) of solution and W is the mass of adsorbent (g) taken for experiment.

Effect of variable parameters

Dosage of adsorbent

The various doses of the adsorbents are mixed with the dye solutions and the mixture was agitated in a mechanical shaker. The adsorption capacities for different doses were determined at definite time intervals by keeping all other factors constant.

Initial concentration of dye

In order to determine the rate of adsorption, experiments were conducted with different initial concentrations of dyes ranging from 2 to 16 mg L⁻¹. All other factors are kept constant.

Contact time

The effect of period of contact on the removal of the dye on adsorbent in a single cycle was determined by keeping particle size, initial concentration, dosage, pH and concentration of other ions constant.

pH

Adsorption experiments were carried out at pH 2, 3, 4, 5, 6, 7, 8, and 9. The acidic and alkaline pH of the media was maintained by adding the required amounts of dilute HCl and NaOH solutions. The parameters like particle size of the adsorbents, dye concentration, dosage of the adsorbent and concentration of other ions were kept constant while carrying out the experiments.

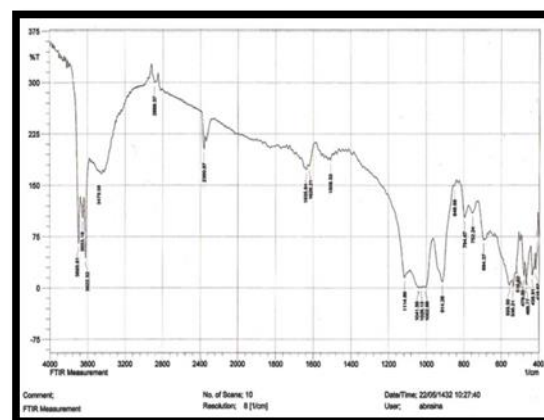
Temperature

The adsorption experiments were performed at four different temperatures viz., 20, 25, 30, 35 and 40 °C in a thermostat attached with a shaker. The temperature made constant and was maintained with an accuracy of ± 0.5 °C.

RESULTS AND DISCUSSION

FT-IR study

Fourier Transform Infrared spectroscopy (FTIR) studies of Al-Hussiniyat clay the adsorbent were carried out and the spectra taken before and after adsorption were shown in Figs. 1 and 2. It is evident from the figures that there is no appreciable change in the spectra. This may be due to the fact that adsorption did not alter the chemical nature of the surface of the adsorbent, i.e the adsorption physical in nature.

**Figure 1.** FTIR spectrum of al-hussiniyat clay before adsorption.

Effect of agitation time

Equilibrium Time

The effect of contact time on the amount of MG adsorbed per unit of adsorbent was investigated at 20 °C and constant pH and concentration. Figure 3 and Table 3 show the variation of Q_e and C_e with MG for 10 ppm at 20 °C and pH =7 .

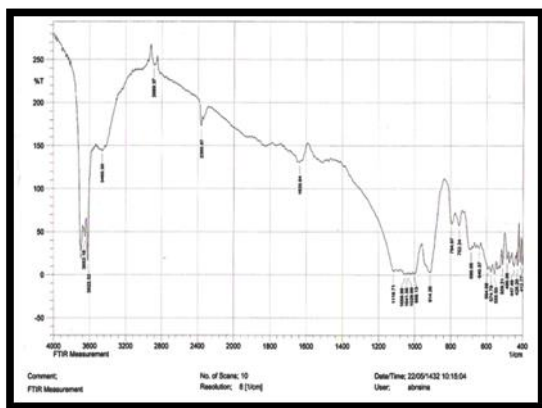


Figure 2. FTIR spectrum of al-hussiniyat clay after adsorption .

Table 3. The variation of values of Q_e and C_e with time the adsorption of MG

| Time, min | C_e , mg L ⁻¹ | Q_e , mg g ⁻¹ |
|-----------|----------------------------|----------------------------|
| 5 | 3.88 | 9.228 |
| 10 | 3.023 | 9.359 |
| 15 | 2.965 | 9.407 |
| 20 | 2.269 | 9.540 |
| 25 | 2.027 | 9.594 |
| 30 | 1.512 | 9.697 |
| 35 | 1.270 | 9.746 |
| 40 | 1.059 | 9.788 |
| 45 | 1.059 | 9.788 |
| 50 | 1.058 | 9.782 |

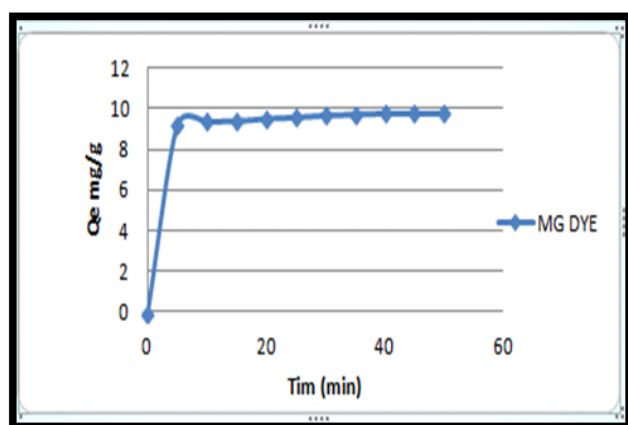


Figure 3. The effect of contact time on the adsorption of malachite green

A sharp change in adsorption is observed at 5 minutes and thereafter a gradual increase was observed in adsorption with increasing contact time up to 40 minutes, after which a maximum value of adsorption is attained. After this time, the amount of dye adsorbed was not significant, very small decreases in the amount of the dye adsorbed were observed, indicating to desorption process. Therefore, the time of 40 minutes may be treated as the optimum contact time. Similar results have been reported for the adsorption.²⁵

Adsorbent Dosage

The effect of adsorbent weight on the adsorption of MG dye was studied by changing the amount of adsorbent (0.1, 0.2, 0.3, 0.4, 0.5, 0.6 and 0.7g per 100 ml) in the test solution while keeping the initial dye concentration (10 ppm) and contact times (40 minutes) constant. The results are shown in Table 4 and Fig. 4.

Table 4. The values of Q_e (in %) and quantity of adsorbent for the MG concentration (10 ppm).

| Quantity of adsorbent, W, g | C_{eq} , mg L ⁻¹ | Q_e , % |
|-----------------------------|-------------------------------|-----------|
| 0.1 | 3.01 | 69 |
| 0.2 | 2.26 | 77 |
| 0.3 | 1.42 | 84 |
| 0.4 | 1.51 | 85 |
| 0.5 | 1.05 | 89 |
| 0.6 | 1.11 | 88 |
| 0.7 | 1.18 | 88 |

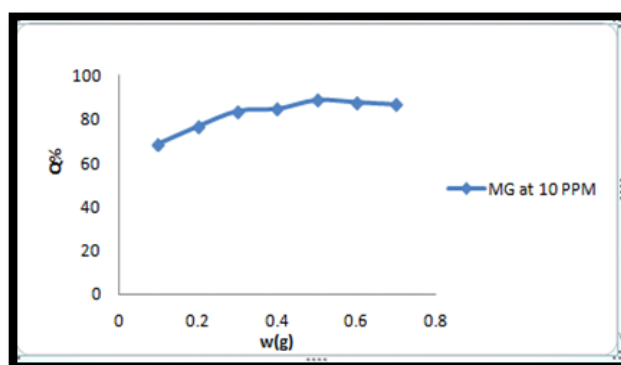


Figure 4. Effect of adsorbent dosage

It is apparent that the percentage removal (Q_e , %) of the dye increases with the increase in adsorbent dose but beyond a value of 0.5 g the percentage removal reaches almost to a maximum value. This is probably due to the greater availability of the exchangeable sites or the increased surface area where the adsorption takes place. As seen in Figure 4 optimum clay dosage that can be used in MG removal is 0.5 gm per 100 mL. Thus, all experiments were carried out by using 0.5 g of adsorbent.

Effect of pH

In the present work, the effect of pH on the MG adsorption onto Al-Hussainiyat clay was studied while the initial dye concentration, shaking time, amount of Al Hussainiyat clay and temperature were fixed at 10 mg L⁻¹, 45 min, 0.5 g and 20 °C, respectively. The effect of pH on the adsorption of MG by the Al-Hussainiyat is presented in Figure 5. The effect of pH on adsorption of dye was studied within pH range 3–10, the maximum adsorption takes place onto neutral medium (pH=7,^{23,26,27} Fig. 5) due the high

affinity of dye to connection with SiO₂ and Al₂O₃. The decrease in the removal of dye at pH 3, due to the similar electrostatic repulsion between the dye and Al-Hussaniyat surface only. Table 5 show the result obtained in the effect of pH on Malachite green removal.

Table 5. The values of Q_e % and C_e for 10 ppm MG at different pH.

| pH | C_{eq} , mg/l | Q_e , % |
|----|-----------------|-----------|
| 3 | 5.45 | 45% |
| 4 | 5.55 | 44% |
| 5 | 5.53 | 44.7% |
| 6 | 5.56 | 45.4% |
| 7 | 1.05 | 89% |
| 8 | 2.77 | 72% |
| 9 | 2.50 | 75% |

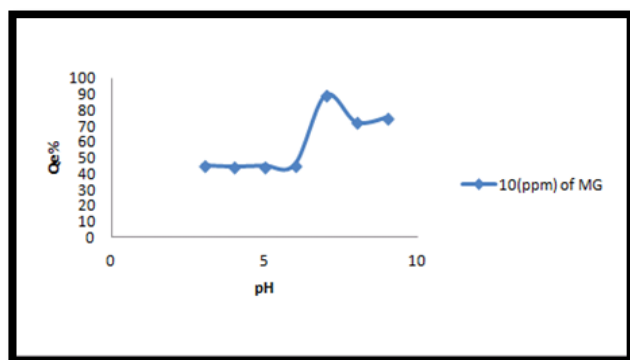


Figure 5. Effect of pH on removal of MG at 10 ppm

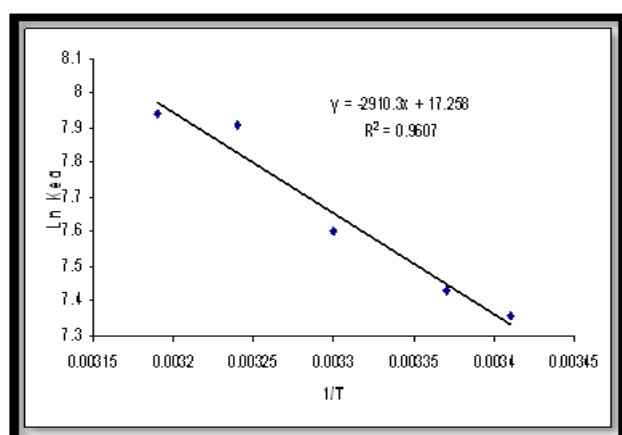


Figure 6. Van't Hoff plot of MG adsorption

Thermodynamic parameters

The thermodynamic studies play an important role in understanding the nature of adsorption. The thermodynamics parameters related to the adsorption of dye, such as, enthalpy change, ΔH° entropy change ΔS° and Gibbs free energy change ΔG° . ΔH° has been calculated for all adsorption processes, according to Van't Hoff equation

(Eqn. 3) via plotting logarithmic value of the adsorption equilibrium constant (K_{eq}) as $\ln Q_e/C_e$ against the temperature as $(1/T)^{(28)}$ The results are listed in Table 6 and Figure 6.

$$\ln K_{eq} = \frac{-\Delta H}{RT} + \frac{\Delta S}{R} \quad (3)$$

$$\Delta G = -RT \ln K_{eq} \quad (4)$$

where R is the gas constant, K_{eq} is adsorption equilibrium constant. The plot of $\ln K_{eq}$ against $1/T$ (in Kelvin) should be linear. The slope of the Van't Hoff plot is equal to $-\Delta H^\circ/R$, and its intercept is equal to $\Delta S^\circ/R$. ΔH° and ΔS° obtained are given in Table 7. The positive values of ΔH° indicate that the adsorption is involved with weak forces of attraction. It was observed that the ΔH° values increased with decrease of particle size. The adsorption was found to be endothermic in nature. The positive values of ΔS° suggest the increased randomness. The negative ΔG° value indicated the spontaneous nature of the adsorption model.²⁹

Table 6. Values of $1/T$ and $\ln K_{eq}$ for the MG

| C_0 , 10 ppm | T , K | $1/T$ | C_e , mg.L ⁻¹ | Q_e , mg.g ⁻¹ | $\ln K_{eq}$ |
|----------------|---------|---------|----------------------------|----------------------------|--------------|
| 10 | 293 | 0.00341 | 1.134 | 1.778 | 7.357 |
| | 298 | 0.00337 | 1.059 | 1.791 | 7.43 |
| | 303 | 0.00330 | 0.907 | 1.818 | 7.603 |
| | 308 | 0.00324 | 0.763 | 1.847 | 7.791 |
| | 313 | 0.00319 | 0.665 | 1.867 | 7.940 |

Physisorption and chemisorptions can be classified, to a certain extent, by the magnitude of enthalpy change. Bonding strengths of 84 kJ mole⁻¹ are typically considered as those of physisorption bonds. Chemisorption bond strengths can be 84–420 kJ mole⁻¹.³⁰ Generally, ΔG° for physisorption is less than that for chemisorption.

The former is between -20 and 0 kJ mol⁻¹ and the later is between -80 and -400 kJ mol⁻¹.³¹ Therefore, the values of ΔH° and ΔG° suggest that adsorption of MG onto Al-hussiyat deposit was driven by a physisorption.

Adsorption Isotherms

Adsorption properties and equilibrium parameters, commonly known as adsorption isotherms, describe how the adsorbate interacts with adsorbents, and comprehensive understanding of the nature of interaction. Isotherms help to provide information about the optimum use of adsorbents.

Therefore, in order to optimize the design of an adsorption system to remove dye from solutions, it is necessary to establish the most appropriate correlation for the equilibrium curve. Out of several isotherm equation available for analyzing experimental sorption equilibrium parameters, the most common isotherms are the Langmuir and Freundlich models.

Table 7. Thermodynamic parameters of MG adsorption on AL-hussinyat clay at 10 ppm, 0.5g, and pH 7

| C_0 , ppm | ΔH° , kJ mol ⁻¹ | ΔS , J mol ⁻¹ K ⁻¹ | ΔG° , kJ mol ⁻¹ | | | | |
|-------------|--|---|---|--------|--------|-------|--------|
| | | | 20 °C | 25 °C | 30 °C | 35 °C | 40 °C |
| | 15.17 | 35 | -14.6 | -18.40 | -19.15 | -19.6 | -20.02 |

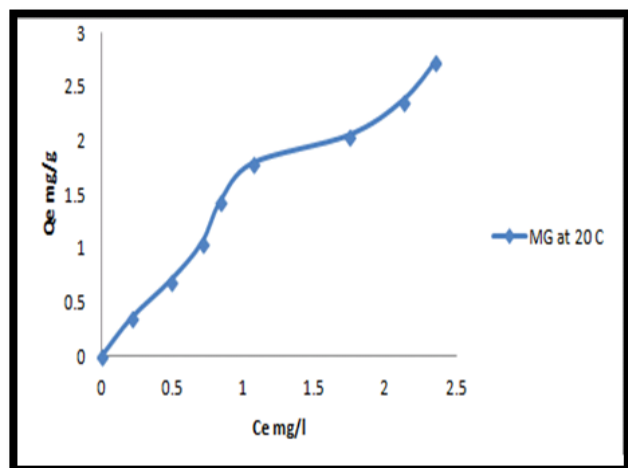
**Figure 7.** Adsorption isotherms of MG on Al-Hussiniyat clay at 20 °C.

Table 8 and Figure 7 shown the adsorption isotherm was of S-type, indicating that the adsorbent is possibly mesoporous or is not porous and has a high energy of adsorption.³² Also, this indicating a vertical or flat orientation of adsorbate, and the adsorbate is mono functional.³³

Table 8. The values of C_{eq} mg L⁻¹ and Q_e mg g⁻¹ for adsorption of Malachite green

| C_0 , ppm | C_{eq} , mg/L | Q_e , mg g ⁻¹ |
|-------------|-----------------|----------------------------|
| 2 | 0.211 | 0.357 |
| 4 | 0.484 | 0.703 |
| 6 | 0.748 | 1.050 |
| 8 | 0.832 | 1.433 |
| 10 | 1.059 | 1.791 |
| 12 | 1.739 | 2.052 |
| 14 | 2.118 | 2.375 |
| 16 | 2.344 | 2.731 |

The Freundlich equation was employed for the adsorption of MG dye on the adsorbent, which is represented by Eqn. 5.³⁴

$$\log Q_e = \log K_f + \frac{1}{n} \log C_e \quad (5)$$

where Q_e is the amount of MG dye adsorbed (mg g⁻¹), C_e is the equilibrium concentration of dye in solution (mg L⁻¹), and K_f and $1/n$ are constants incorporating the factors affecting the adsorption capacity and intensity of adsorption, respectively.

Linear plots of $\log Q_e$ versus $\log C_e$ shows that the adsorption of malachite green dye obeys the Freundlich adsorption isotherm (Figure 8). The values of K_f and $1/n$ are given in Table 5. These data are analyzed according to the linear form of Langmuir equation (Eqn. 6).

$$\frac{C_e}{Q_e} = \frac{1}{Q_m} k_L + \frac{C_e}{Q_m} \quad (6)$$

where C_e is the equilibrium concentration (mg L⁻¹), Q_e is the amount adsorbed at equilibrium (mg g⁻¹), and Q_m and k_L are Langmuir constants related to adsorption efficiency and energy of adsorption, respectively.³⁵ The linear plots of C_e/Q_e versus C_e suggest the applicability of the Langmuir isotherms (Fig. 9). The values of Q_m and k_L were determined from slope and intercepts and are presented in Table 10. To confirm the favourability of the adsorption process, the separation factor (R_L) is calculated by using the (Eqn. 7) and presented in Table 10.

$$R_L = \frac{1}{1 + K_L C_0} \quad (7)$$

Table 9. The experimental data C_e/Q_e , C_e , $\log C_e$, and $\log Q_e$ for the adsorption of MG

| C_0 | C_e , mg L ⁻¹ | C_e/Q_e | $\log Q_e$ | $\log C_e$ |
|-------|----------------------------|-----------|------------|------------|
| 2 | 0.211 | 0.591 | -0.447 | -0.675 |
| 4 | 0.484 | 0.688 | -0.153 | -0.315 |
| 6 | 0.748 | 0.712 | -0.021 | -0.126 |
| 8 | 0.832 | 0.65 | 0.156 | -0.079 |
| 10 | 1.059 | | | |
| | | 0.666 | 0.253 | 0.024 |
| 12 | 1.739 | 0.841 | 0.312 | 0.24 |
| 14 | 2.118 | 0.891 | 0.375 | 0.325 |
| 16 | 2.344 | 0.898 | 0.436 | 0.369 |

The values of R_L are found to be between 0 and 1 and confirm that the ongoing adsorption process is favourable. R_L values indicate that the type of isotherm is irreversible ($R_L=0$), favorable ($0 < R_L < 1$), linear ($R_L=1$) or unfavourable ($R_L > 1$).²⁸

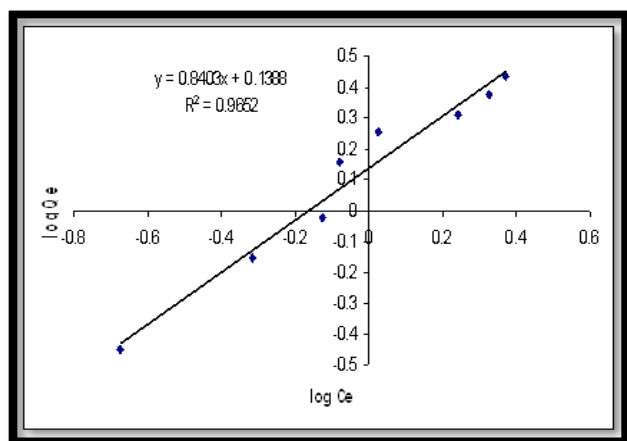


Figure 8. The linear plot of Freundlich isotherm

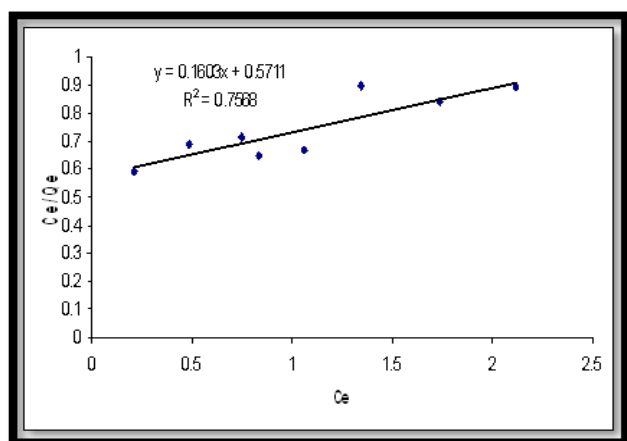


Figure 9. The linear plot of Langmuir isotherms

The values of $n > 1$ indicate favourable adsorption conditions.²⁵ The values of linear R^2 coefficient were high (> 0.9) for Freundlich isotherm indicating the useful values of its constants. The adsorption isotherm for the present system is explained better by Freundlich isotherm model.³²

Table 10. The parameters of Freundlich and Langmuir equation for the adsorption of MG dye.

| Freundlich parameter | | | | |
|----------------------|-------|-------|--------|-------|
| $T, ^\circ\text{C}$ | $1/n$ | K_F | R^2 | |
| 20 | 0.816 | 0.717 | 0.9652 | |
| Langmuir parameter | | | | |
| $T, ^\circ\text{C}$ | q_L | K_L | R_L | R^2 |
| 20 | 0.816 | 0.717 | 0.260 | 0.765 |

CONCLUSIONS

The main conclusions that can be drawn from the above mentioned results and discussion are given below. The optimum pH for favourable adsorption were 7 for MG.

1) The adsorption system could be explained by the electrostatic attraction (physical adsorption). This confirmed by the values obtained of ΔH° and ΔG° .

2) The amount of dye adsorbed onto the adsorbent increases with an increase in the adsorption temperature of the dye solution from 20-40 $^\circ\text{C}$. This trend is indication of the fact that the adsorption process is endothermic in nature.

3) Thermodynamic analysis indicated that the adsorption of the dye onto clay was endothermic and spontaneous.

4) For equilibrium adsorption, MG dye was best fitted to the Freundlich isotherm.

REFERENCES

- Gupta, V. K., Mittal, A., Krishnan, L., Gajbe, V., *Sep. Purif. Technol.*, **2004**, *40*, 87-96.
- Kareem, S. H., and Ennas, A. B., *J. Baghdad Sci.*, **2013**, *9(4)*, 680-688
- Rahmatollah, R., Mahboube, R., and Marziye, J. K., *ECSOC-14: The 14th Int. Electronic Conf. Synth. Org. Chem.*, **2010**, 213.
- Low cost biosorbents for dye removal*, CES Technical Report 113, **2004**.
- Min-Yu, T., Su-Hsia, L., *Desalination*, **2006**, *201*, 71-81.
- Malik, P. K., *Dyes Pigments*, **2003**, *56*, 239-249.
- Nafeesa, J. K., *J. Baghdad Sci.*, **2012**, *9(1)*, 153-159.
- Brown, P., Jefcoat, I. A., Parrish, D., Gill, S. and Graham, E., *Adv. Environment. Res.*, **2000**, Ed. 4, 19-29.
- Singh, K. K., Talat, M. and Hasan, S. H., *Bioresour. Technol.*, **2006**, *97*, 2124-2130.
- Taty-Costodes, V. C., Fauduet, H., Porte, C. and Delacroix, A., *J. Hazard. Mater.*, **2003**, *B105*, 121-142.
- Reddad, Z., Gerente, C., Andres Y. and Cloirec, P. L., *J. Environmental Sci. Technol.*, **2002**, *36*, 2067-2073.
- Vasanth, K. K., *Dyes Pigments*, **2007**, *74*, 595-597
- Gong, R. M., Zhang, X. P., Liu, H. J., Sun, Y. Z. and Liu, B. R., *Bioresour. Technol.*, **2007**, *98*, 1319-1323.
- Husseien, M. A., Amer A., El-Maghraby, A. and Nahla, A., *J. Appl. Sci. Res.*, **2007**, *3(11)*, 1352-1358.
- Nuttawan, P. and Nuttakan N., Kasetsart, J., *Natural Sci.*, **2006**, *40*, 192-197.
- Tsai, W. T., Chen, H. R., Kuo, K. C., Lai, C. Y., Su, T. C., Chang, Y. M., Yang, J. M., *J. Environmental. Eng. Manag.*, **2009**, *19(3)*, 165-172.
- Zollinger H., *Colour Chemistry-Synthesis, Properties and Application of Organic Dyes and Pigments*, VCH Publishers, New York, **1987**.
- Muqing, Q., Qian, C., Xu, J., Wu, J., Wang, G., *Desalination*, **2009**, *243*, 286-292.
- Lorenc, G. E., and Graz, G., *Dyes Pigments*, **2007**, *74*, 34-40.
- Mas, R., Mas, H., and Kathiresan, S., *Am. J. Appl. Sci.*, **2009**, 1690-1700.
- Lian, L., Guan, L., and Wang, A., *Desalination*, **2009**, *249*, 797-801.
- Belter, P. A. and Cussler, E. L., *Bioseparation Downstream Processing for Biotechnology*, New York, **1988**, 145-179.
- Dash, B., *Competitive Adsorption of dyes (congo red, methylene blue, malachite green) on Activated Carbon* Roll No. 10600008, ROURKELA -769 008, INDIA **2010**

- ²⁴Ministry of Industry and Minerals State Company of Geological Survey Mining: "Physical and Chemical specifications of Geological Raw Materials and Processed products", **2000**.
- ²⁵Venkatraman, B. R., Hema, K., Nandhakumar, V. and Arivoli, S. *J. Chem. Pharm. Res.*, **2011**, 3(2), 637-649.
- ²⁶LeKaa, H. K., "Adsorption of Some Dyes on Surface of White Iraqi Kaolin Clay", University of Kufa, **2005**.
- ²⁷Goswami, B. K., Purkait, M. K., *J. Hazard. Mater.*, **2009**, 161, 378-395.
- ²⁸Keller, J. U., Staudt, R., *Gas adsorption equilibria experimental method and Adsorptive Isotherms*, Universität Siegen, Germany, ISBN 0-287-23597-3, **2005**.
- ²⁹Atul, K. K., Gupta, N., Chattopadhyaya, M. C., *J. Chem. Pharm. Res.*, **2010**, 2(6), 34-45.
- ³⁰Kipling, J. J., *Adsorption from Solution of Non-Electrolytes*, Academic Press, London, **1965**, 101-257.
- ³¹Fasut, S. D. and Aly, D M., *Adsorption processes for water treatment*, Butterworth, **1987**.
- ³²Janes, C. B., *Surface area and porosity determinations by physisorption: measurements and theory*, Elsevier, New York, 1st ed., **2006**.
- ³³Giles C. H., *J. Chem. Soc.*, **1960**, 3973-3993.
- ³⁴Freundlich, H., "Adsorption in Solutions", *Z. Phys Chemie*, **1906**, 57, 384.
- ³⁵Langmuir, I., *J. Am. Chem. Soc.*, **1918**, 40, 1361.

Received: 05.05.2013.

Accepted: 30.06.2013.



HETEROGENEOUS ELECTRON TRANSFER KINETICS OF DIBENZOYLFERROCENE IN APROTIC SOLVENTS

Adnan Ahmed Khan,^[a] Rashida Parveen^{[a]*} and Maria Ashfaq^[a]

Keywords: Dibenzoyl ferrocene, Cyclic voltammetry, Mass transport

The electrochemical behavior of dibenzoyl ferrocene was investigated by cyclic voltammetry in the temperature range 303–333K in the DMSO, DMF and DMA. The experimental results indicated that the redox reaction was quasi-reversible. Mass transport towards the electrode is a simple diffusion process and the diffusion coefficient (D) for redox couple has been also calculated for all the solvents. The diffusion coefficient is sensitive to the viscosity, dipolarizability and temperature of the system. These results indicated that the k^0 and D increase in the following order of solvent DMSO < DMA < DMF.

Corresponding Authors*

E-Mail: rashidap@uok.edu.pk

[a] Department of Chemistry, University of Karachi, Pakistan.

Introduction

Ferrocene and its derivatives belong to a class of compounds called organo-metallic compounds. These compounds attracted a great deal of interest of researchers due to their unusual stability and electrochemical behavior. Some Ferrocene derivatives have fairly high stability under visible irradiations therefore, they are good quenchers of excited states. De Santis et al.¹ studied fluorescence quenching of the excited anthracene unit, after binding of the Ferrocene carboxylate anion by the Zn^{+2} center.² Some ferrocene and ferrocenyl derivatives may undergo chemical modifications in the presence of light, or may be used as photosensitizers, that is as catalysts of photochemical reactions (Fery-Forgues and Delavaux-Nicot, 2000). Electron transfer is so viable for Ferrocene in its more complex molecules that many ferrocene derivatives and ferrocene labeled proteins are used as electrochemical enzyme biosensor.³ The electrochemical reactivity and catalytic activity of Fc-HRP (ferrocenyl horseradish peroxidase) is much higher than HRP (horseradish peroxidase).⁴ In electrochemical glucose sensors ferrocene derivatives mediate the electron transfer between the catalytic centre of the enzyme and the electrode surfaces.⁵⁻⁸

Ferrocene and its derivatives, being stable, non-toxic⁹ and electro active, have large applications in medicines and very promising activity *in vitro* and *in vivo* against several diseases. 1,1'-disubstituted ferrocene unit with easily rotating Cp-rings seems to be highly beneficial to the desired activity allowing the molecule to adopt a conformation in which the two cooperating groups are situated in optimal distance from each other. Ferrocenyl moiety may increase the biological activity and spectrum of a drug. Ferrocenyl moiety increases cytotoxicity of tamoxifen and hydroxytamoxifen¹⁰ and with estradiol in breast cancer treatment.¹¹ Derivatives of polyphenolic compounds containing Ferrocene moiety has good antiproliferative effect on the standard breast cancer cell lines.¹²⁻¹³

Some water soluble ferrocene derivatives appear more effective against cancer cell than water insoluble ferrocene derivatives. Ferrocene-based *bis*-amide exhibits very important *in vitro* anticancer activity.¹⁴ Other very important examples of water soluble ferrocene derivatives with anticancer activity are ferrocenium tetrafluoroborate salt¹⁵ and ferrocenium triiodide in Rauscher leukaemia.¹⁶ Ferroquine appears more effective against malaria causing parasites than Chloroquine.¹⁷

Electroactive labeling of non-electroactive biomolecule with ferrocene enables the electrochemical detection of these biomolecules like cysteine- containing biomolecules¹⁸. Ferrocene and its derivatives show reversible oxidation behaviour. Since last three decades, several studies have been made pertaining to the effects of the substituents on the properties of ferrocene.¹⁹⁻²⁴

Early ferrocene couple ($Fc^{+/0}$) was considered as internal redox standard for reporting electrode potentials,²⁵ due to independent behavior of standard electrode potential of $Fc^{+/0}$ against nature of different solvents (Strehlow assumption). The potential variations by liquid junction potentials, was then reduced by usage of $Fc^{+/0}$.²⁶ But in some cases Ferrocenium ion interact with nucleophile which affect the chemical reversibility of $Fc^{+/0}$ couple.²⁶⁻²⁸ The interaction of solute and solvent molecules like hydrogen bonding, Lewis acid-base and π -stacking of ring system play important role in redox electrode potentials. Kamlet, Abboud and Taft correlate physicochemical quantity with solvent properties for numbers of solvent-solute systems.²⁸

Experimental

Reagents

Chemicals Tetrabutylammonium perchlorate (99% TBAP) from Tokyo KASEI was used as the supporting electrolyte. Dimethylformamide (DMF) from Sigma Aldrich USA, dimethyl sulfoxide (DMSO) from BDH chemicals UK(99.5%), Dimethylacetamide (DMA) from Fischer Scientific UK (99.97%) and Dichloromethane (DCM) from Merck Germany were used. For the synthesis of 1,1'-dibenzoyl ferrocene, ferrocene, Sodium sulfate and

anhydrous aluminum chloride from Merck Germany, Benzoyl Chloride and Ethanol from Sigma Aldrich USA (99.5%) were used in synthesis. Deionized water was used throughout the synthesis.

Synthesis of 1,1'-dibenzoyl ferrocene

4.32 g (3.5 mL) of benzoyl chloride was added drop wise into solution of 3.61g of anhydrous Aluminum chloride in 12 mL of dichloromethane in 40 minutes with constant stirring. Subsequently, slow addition of 2.5g ferrocene in 12 mL dichloromethane made into the mixture. It took 80 minutes for complete addition with constant stirring. This mixture was then further stirred for 2 hours at room temperature. The reaction mixture was then poured in 80 mL crushed ice. The two aqueous and non-aqueous layers were separated. The aqueous layer was washed twice with 3 mL dichloromethane, separated and collected with non-aqueous layer. The non-aqueous layer was washed twice with 10 mL of 10% NaOH and once with 10 mL of water then dried over sodium sulphate. The red syrup was concentrated in vacuum and recrystallized by ethanol.²⁹

Electrochemical Analysis

All electrochemical measurements were performed with 3 electrode assembly consisting of a platinum electrode as the working electrode, a Ag/AgCl reference electrode and a platinum wire as the counter electrode. A double walled electrochemical cell was used to maintain the temperature during electrochemical observation. Pure N₂ was purged for at least 15 minutes before each electrochemical observation. A CHI660 electrochemical workstation was used for electrochemical analysis and scan rates ranging from 25 to 500 mVs⁻¹.

Results and discussions

Reversibility

The reversibility of electron transfer of DBF is analyzed by different parameters of cyclic voltammetry. The voltammograms were recorded at platinum versus Ag/AgCl reference electrode. Tetrabutylammonium perchlorate (0.1 mol dm⁻³) was used as a supporting electrolyte. The peak potentials and peak current density at different scan rates (0.025 V s⁻¹ to 0.5 V s⁻¹) and temperatures (303 K to 333 K) are reported in Table 1.

The ratios of I_{pa}/I_{pc} were evaluated by varying scan rates range (0.025 V s⁻¹ to 0.5 V s⁻¹) different temperatures (303 K to 333 K), and the solvents (DMF, DMA and DMSO) employed for study. As it is apparent from Fig. 1, CVs are symmetrical with equal cathodic (I_{pc}) and anodic (I_{pa}) peak currents and therefore, the I_{pa}/I_{pc} ratio approach the unit value during all the course of reactions in DMF, DMA and DMSO. It is indicative of the stability reduced and oxidized species of DBF in the time frame of the reaction and indicative of reversibility of charge-transfer process. In addition, there is no side reaction coupled with electron transfer process. Therefore, corroborate the reversible or quasi reversible nature of electron transfer reaction

The number of electron is calculated by the Eqn. (1).

$$E_{p/2} - E_p = 2.2 \left(\frac{RT}{nF} \right) \quad (1)$$

By using the above equation, the number of electron transfer “ n ” for electrochemical reaction were calculated (Table 2). It is evaluated nearly one for various sweep rates at different temperatures and solvents. Therefore heterogeneous reaction is following one electron transfer mechanism.

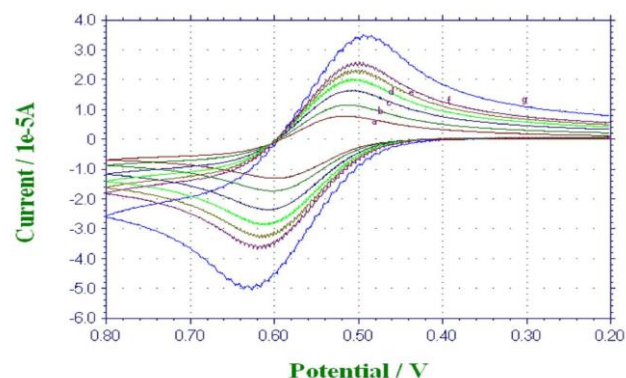


Figure 1. Cyclic voltammogram of 3 mM DBF at 303 K and scan rates of (a) 0.025 V s⁻¹, (b) 0.05 V s⁻¹, (c) 0.1 V s⁻¹, (d) 0.15 V s⁻¹, (e) 0.2 V s⁻¹, (f) 0.25 V s⁻¹, (g) 0.5 V s⁻¹.

The donor-acceptor Lewis-type interactions shift the $E_{1/2}$ values. The $E_{1/2}$ values show the dependence of redox reaction at electrode over a particular solvent.³⁰ The positive charge of oxidized form of DBF has more Lewis electron pair acceptor and donor interaction with electron pair donor atom of solvents than reduced form. The strength of this attraction depends on the electron pair donor tendency of solvent (donor number of solvent) and the redox pair. Strong electron pair donor tendency will reduce the half wave potential of DBF cation. Therefore DMSO having a higher donor number (124.7 kJ mol⁻¹), has smallest half wave potential $E_{1/2}=0.503$, DMA with donor number (116.2 kJ mol⁻¹) has $E_{1/2}=0.559$ and DMF with donor number (111.2 kJ mol⁻¹) has $E_{1/2}=0.539$. $E_{1/2}$ values for DBF redox pair were found to be almost independent of the scan rate for a given temperature but increases with temperature. The $E_{1/2}$ values change considerably with solvents polarity. It is evident that $E_{1/2}$ shifts toward more positive potentials and following the order DMSO < DMA < DMF

The large value of peak to peak separation in the less polar solvent may be attributed to incomplete i_R compensation, since the heterogeneous rate are known to be large.³¹ The diffusion controlled reversible electron transfer reaction of DBF was established by Randle Sevcik equation.³²

$$I_p = 0.4463 (nF)^{3/2} (RT)^{-1/2} A D^{1/2} C_0 \nu^{1/2} \quad (2)$$

where I_p is peak current density, “ n ” is number of electron transfer, A is surface area of working electrode, D is diffusion coefficient of electroactive substance, ν is the sweep rate and C_0 is concentration of electroactive substance.

Table 1a. Voltammetric data for 3 mM 1,1'-dibenzoyl ferrocene in DMSO at different temperatures.

| T, K | Scan rate, V s ⁻¹ | E _{pa} , V | E _{pc} , V | ΔE | E _{1/2} | I _{pa} , μA.cm ⁻² | I _{pc} , μA cm ⁻² | I _{pa} /I _{pc} |
|------|------------------------------|---------------------|---------------------|-------|------------------|---------------------------------------|---------------------------------------|----------------------------------|
| 303 | 0.025 | 0.552 | 0.462 | 0.09 | 0.507 | 9.46 | 9.23 | 1.02 |
| | 0.050 | 0.546 | 0.458 | 0.088 | 0.502 | 13.90 | 12.0 | 1.15 |
| | 0.100 | 0.546 | 0.454 | 0.092 | 0.500 | 19.30 | 16.3 | 1.18 |
| | 0.150 | 0.552 | 0.449 | 0.103 | 0.501 | 22.90 | 19.9 | 1.14 |
| | 0.200 | 0.557 | 0.449 | 0.108 | 0.503 | 26.00 | 22.7 | 1.14 |
| | 0.250 | 0.562 | 0.446 | 0.116 | 0.504 | 28.60 | 25.1 | 1.14 |
| | 0.500 | 0.569 | 0.437 | 0.132 | 0.503 | 37.20 | 33.8 | 1.09 |
| 313 | 0.025 | 0.544 | 0.459 | 0.085 | 0.502 | 10.5 | 10.6 | 0.98 |
| | 0.050 | 0.543 | 0.458 | 0.085 | 0.501 | 14.5 | 13.6 | 1.06 |
| | 0.100 | 0.547 | 0.454 | 0.093 | 0.501 | 19.8 | 18.5 | 1.06 |
| | 0.150 | 0.553 | 0.451 | 0.102 | 0.502 | 23.9 | 22.3 | 1.07 |
| | 0.200 | 0.557 | 0.447 | 0.110 | 0.502 | 27.8 | 25.4 | 1.09 |
| | 0.250 | 0.558 | 0.455 | 0.103 | 0.506 | 30.0 | 27.8 | 1.07 |
| | 0.500 | 0.561 | 0.436 | 0.125 | 0.498 | 40.8 | 37.7 | 1.08 |
| 323 | 0.025 | 0.546 | 0.459 | 0.087 | 0.502 | 11.4 | 11.1 | 1.02 |
| | 0.050 | 0.546 | 0.456 | 0.090 | 0.501 | 15.3 | 14.6 | 1.04 |
| | 0.100 | 0.550 | 0.453 | 0.097 | 0.502 | 21.1 | 19.4 | 1.08 |
| | 0.150 | 0.555 | 0.449 | 0.106 | 0.502 | 25.4 | 23.3 | 1.08 |
| | 0.200 | 0.555 | 0.448 | 0.107 | 0.502 | 29.0 | 26.7 | 1.08 |
| | 0.250 | 0.555 | 0.448 | 0.107 | 0.502 | 32.4 | 29.2 | 1.10 |
| | 0.500 | 0.575 | 0.439 | 0.136 | 0.507 | 43.4 | 39.7 | 1.09 |
| 333 | 0.025 | 0.551 | 0.446 | 0.105 | 0.498 | 13.0 | 13.4 | 0.97 |
| | 0.050 | 0.552 | 0.455 | 0.097 | 0.504 | 16.7 | 15.9 | 1.05 |
| | 0.100 | 0.550 | 0.453 | 0.097 | 0.502 | 22.4 | 20.4 | 1.09 |
| | 0.150 | 0.551 | 0.451 | 0.100 | 0.501 | 27.0 | 24.6 | 1.10 |
| | 0.200 | 0.552 | 0.446 | 0.106 | 0.499 | 30.8 | 27.8 | 1.10 |
| | 0.250 | 0.558 | 0.446 | 0.112 | 0.502 | 33.9 | 30.8 | 1.10 |
| | 0.500 | 0.559 | 0.446 | 0.113 | 0.502 | 35.0 | 34.5 | 1.01 |

Table 1b. Voltammetric data for 3 mM 1,1'-dibenzoyl ferrocene in DMF at different temperatures.

| T, K | Scan rate, V s ⁻¹ | E _{pa} , V | E _{pc} , V | ΔE | E _{1/2} | I _{pa} , μA.cm ⁻² | I _{pc} , μA cm ⁻² | I _{pa} /I _{pc} |
|------|------------------------------|---------------------|---------------------|-------|------------------|---------------------------------------|---------------------------------------|----------------------------------|
| 303 | 0.025 | 0.581 | 0.494 | 0.087 | 0.538 | 16.1 | 15.1 | 1.06 |
| | 0.050 | 0.583 | 0.491 | 0.092 | 0.537 | 21.8 | 20.5 | 1.06 |
| | 0.100 | 0.589 | 0.488 | 0.101 | 0.539 | 29.9 | 28.0 | 1.06 |
| | 0.150 | 0.591 | 0.487 | 0.104 | 0.539 | 35.8 | 33.6 | 1.06 |
| | 0.200 | 0.596 | 0.483 | 0.113 | 0.540 | 40.7 | 37.9 | 1.07 |
| | 0.250 | 0.600 | 0.48 | 0.120 | 0.540 | 44.9 | 41.7 | 1.07 |
| | 0.500 | 0.609 | 0.468 | 0.141 | 0.539 | 60.2 | 55.1 | 1.09 |
| 313 | 0.025 | 0.581 | 0.497 | 0.084 | 0.539 | 17.1 | 14.9 | 1.14 |
| | 0.050 | 0.584 | 0.493 | 0.091 | 0.539 | 22.9 | 21.9 | 1.04 |
| | 0.100 | 0.588 | 0.487 | 0.101 | 0.538 | 31.1 | 29.0 | 1.07 |
| | 0.150 | 0.590 | 0.486 | 0.104 | 0.538 | 37.2 | 34.3 | 1.08 |
| | 0.200 | 0.595 | 0.482 | 0.113 | 0.539 | 42.3 | 38.5 | 1.09 |
| | 0.250 | 0.599 | 0.479 | 0.120 | 0.539 | 46.5 | 42.3 | 1.09 |
| | 0.500 | 0.610 | 0.471 | 0.139 | 0.541 | 62.3 | 56.4 | 1.10 |

| | | | | | | | | |
|-----|-------|-------|-------|-------|-------|------|------|------|
| 323 | 0.025 | 0.591 | 0.490 | 0.101 | 0.541 | 18.9 | 17.8 | 1.06 |
| | 0.050 | 0.588 | 0.494 | 0.094 | 0.541 | 24.8 | 23.5 | 1.05 |
| | 0.100 | 0.588 | 0.491 | 0.097 | 0.540 | 33.0 | 30.9 | 1.06 |
| | 0.150 | 0.593 | 0.487 | 0.106 | 0.540 | 39.8 | 36.4 | 1.09 |
| | 0.200 | 0.597 | 0.486 | 0.111 | 0.542 | 45.0 | 40.8 | 1.10 |
| | 0.250 | 0.597 | 0.481 | 0.116 | 0.539 | 49.5 | 45.0 | 1.10 |
| | 0.500 | 0.597 | 0.469 | 0.138 | 0.538 | 66.4 | 59.4 | 1.11 |
| 333 | 0.025 | 0.594 | 0.494 | 0.100 | 0.544 | 22.5 | 21.1 | 1.02 |
| | 0.050 | 0.594 | 0.493 | 0.101 | 0.544 | 27.5 | 26.9 | 1.06 |
| | 0.100 | 0.597 | 0.491 | 0.106 | 0.544 | 36.6 | 33.5 | 1.09 |
| | 0.150 | 0.601 | 0.490 | 0.111 | 0.546 | 43.2 | 38.1 | 1.13 |
| | 0.200 | 0.601 | 0.488 | 0.113 | 0.545 | 48.7 | 43.8 | 1.11 |
| | 0.250 | 0.607 | 0.483 | 0.124 | 0.545 | 53.7 | 46.6 | 1.15 |
| | 0.500 | 0.610 | 0.481 | 0.129 | 0.546 | 71.3 | 63.2 | 1.12 |

Table 1c. Voltammetric data for 3 mM 1,1'-dibenzoyl ferrocene in DMA at different temperatures.

| T, K | Scan rate, V s ⁻¹ | E _{pa} , V | E _{pc} , V | ΔE | E _{1/2} | I _{pa} , μA.cm ⁻² | I _{pc} , μA cm ⁻² | I _{pa} /I _{pc} |
|------|------------------------------|---------------------|---------------------|-------|------------------|---------------------------------------|---------------------------------------|----------------------------------|
| 303 | 0.025 | 0.600 | 0.516 | 0.084 | 0.549 | 12.8 | 11.2 | 1.13 |
| | 0.050 | 0.604 | 0.511 | 0.093 | 0.548 | 17.0 | 15.6 | 1.09 |
| | 0.100 | 0.608 | 0.507 | 0.101 | 0.557 | 23.4 | 21.4 | 1.09 |
| | 0.150 | 0.612 | 0.506 | 0.106 | 0.559 | 28.4 | 25.9 | 1.09 |
| | 0.200 | 0.614 | 0.504 | 0.110 | 0.559 | 32.4 | 29.6 | 1.09 |
| | 0.250 | 0.620 | 0.499 | 0.121 | 0.562 | 36.0 | 32.5 | 1.10 |
| | 0.500 | 0.627 | 0.494 | 0.133 | 0.568 | 48.6 | 43.5 | 1.11 |
| 313 | 0.025 | 0.617 | 0.516 | 0.101 | 0.567 | 14.8 | 15.4 | 0.96 |
| | 0.050 | 0.614 | 0.526 | 0.088 | 0.565 | 18.5 | 16.2 | 1.14 |
| | 0.100 | 0.618 | 0.520 | 0.098 | 0.569 | 25.1 | 22.5 | 1.11 |
| | 0.150 | 0.622 | 0.516 | 0.106 | 0.569 | 30.2 | 27.4 | 1.10 |
| | 0.200 | 0.623 | 0.516 | 0.107 | 0.570 | 34.5 | 30.7 | 1.12 |
| | 0.250 | 0.630 | 0.511 | 0.119 | 0.571 | 37.9 | 33.7 | 1.12 |
| | 0.500 | 0.635 | 0.504 | 0.131 | 0.570 | 51.5 | 44.6 | 1.15 |
| 323 | 0.025 | 0.619 | 0.529 | 0.090 | 0.572 | 15.0 | 14.7 | 1.02 |
| | 0.050 | 0.623 | 0.528 | 0.095 | 0.576 | 20.4 | 20.3 | 1.00 |
| | 0.100 | 0.621 | 0.522 | 0.099 | 0.572 | 26.5 | 26.8 | 0.98 |
| | 0.150 | 0.626 | 0.521 | 0.105 | 0.574 | 31.8 | 27.6 | 1.15 |
| | 0.200 | 0.627 | 0.519 | 0.108 | 0.573 | 36.1 | 32.6 | 1.10 |
| | 0.250 | 0.632 | 0.514 | 0.118 | 0.573 | 40.0 | 34.4 | 1.16 |
| | 0.500 | 0.642 | 0.507 | 0.135 | 0.575 | 54.0 | 46.3 | 1.16 |
| 333 | 0.025 | 0.627 | 0.547 | 0.080 | 0.581 | 17.2 | 17.9 | 0.95 |
| | 0.050 | 0.639 | 0.529 | 0.110 | 0.584 | 22.8 | 22.1 | 1.03 |
| | 0.100 | 0.632 | 0.534 | 0.098 | 0.583 | 28.2 | 27.3 | 1.03 |
| | 0.150 | 0.635 | 0.529 | 0.106 | 0.582 | 33.5 | 26.9 | 1.24 |
| | 0.200 | 0.640 | 0.529 | 0.111 | 0.585 | 38.0 | 32.4 | 1.17 |
| | 0.250 | 0.638 | 0.526 | 0.112 | 0.582 | 42.1 | 35.2 | 1.19 |
| | 0.500 | 0.644 | 0.519 | 0.125 | 0.582 | 56.4 | 46.9 | 1.20 |

The linear variation of I_{pa} versus square root of scan rate (ν) was observed for 3 mM concentration of 1,1'-dibenzoyl ferrocene at different temperatures (303 K to 333 K) and

solvents (DMSO, DMA, DMF) shown in Figure 2. No evidence for adsorption process at the surface of electrode was found.

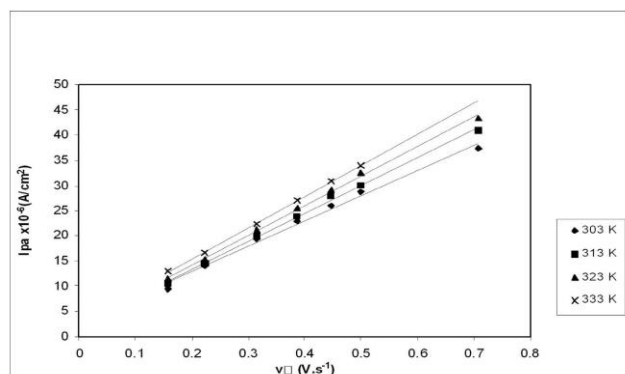


Figure 2a. Peak current density versus square root of scan rate for 3 mM DBF at 303 K, 313 K, 323 K, 333 K in DMSO

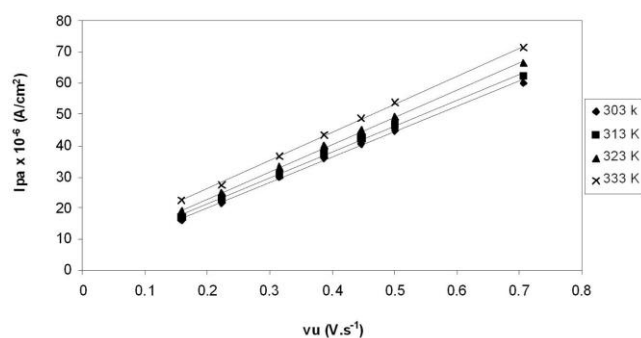


Figure 2b. Peak current density versus square root of scan rate for 3 mM DBF at 303 K, 313 K, 323 K, 333 K in DMF

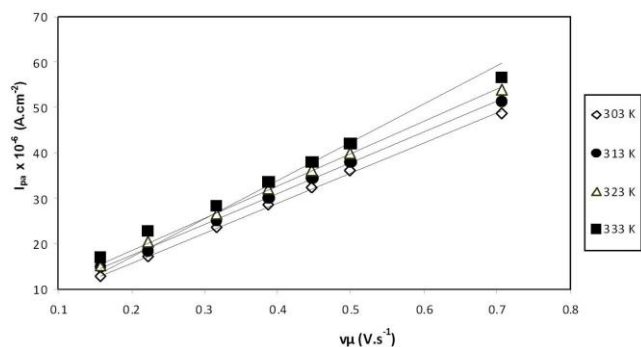


Figure 2c. Peak current density versus square root of scan rate for 3 mM DBF at 303 K, 313 K, 323 K, 333 K in DMA.

The effect of concentration (1.2 mmol dm⁻³ to 6.5 mmol dm⁻³) of DBF at scan rate of 0.2 V s⁻¹ and 313 K in different solvents (DMSO, DMA, DMF) are reported in Table 3. It shows the linear trend over the above mentioned concentration range (Fig. 3).

Kinetic parameters

The heterogeneous electron transfer rate constant k^0 was calculated by plotting graph $\ln I_{pa}$ vs $E_p - E_{p/2}$, according to the equation:³³

$$\ln I_p = \frac{\alpha n_a F}{RT} (E_p - E_{p/2}) + \ln (0.227 n_a F A C_0 k^0) \quad (3)$$

where E_p is anodic peak potential α is transfer coefficient and k^0 is a heterogeneous electron transfer rate constant.

Table 2. Cathodic peak potentials, half peak potential and number of electron transferred for 3mM DBF at 303 K and scan rate of 0.2 V s⁻¹.

| Solvents | E_p | $E_{p/2}$ | $E_p - E_{p/2}$ | N |
|----------|-------|-----------|-----------------|-------|
| DMSO | 0.557 | 0.503 | 0.054 | 0.940 |
| DMF | 0.596 | 0.539 | 0.057 | 0.992 |
| DMA | 0.614 | 0.559 | 0.055 | 0.957 |

The plot of logarithmic peak current would not linearly relate with $E_p - E_{1/2}$ that would be the result of ignorance of temperature dependence nature of charge transfer coefficient. At 303 K temperature slope: $\alpha n_a F / RT$ of the linear relation αn_a equals to be 0.94, 0.99 and 0.957 for DMSO, DMF and DMA respectively (Table 2). As the charge-transfer rate constant evaluated from the intercept of plot so it is not greatly influenced by the curved slope.

| [DBF], mM | I_{pa} , A | | |
|-----------|----------------------|---------------------|---------------------|
| | 10 ⁵ DMSO | 10 ⁵ DMF | 10 ⁵ DMA |
| 1.20 | 0.933 | 1.71 | 1.57 |
| 2.18 | 1.94 | 3.10 | 2.52 |
| 3.00 | 2.78 | 4.23 | 3.45 |
| 4.50 | 3.72 | 6.04 | 4.73 |
| 5.53 | 4.24 | 7.16 | 5.63 |
| 6.50 | 5.83 | 7.95 | 6.60 |

Table 3. Effect of concentration change over peak current potential of DBF at 0.2V/s and 313K in DMSO, DMF, DMA.

The k^0 was measured at different temperatures ranging from 303 K to 333 K for DMF, DMSO and DMA [Table 4]. The value of k^0 increases with increasing the operating temperature in all the solvents. It is attributed to viscosity of the medium, hence, decreases with increasing the operating temperature, resulting in k^0 increasing. The value of k^0 following the order in different solvents.

DMSO < DMA < DMF

The diffusion coefficients for different solvents were measured in 3mM concentration of DBF at 0.2 V s⁻¹ scan rate and 303 K to 333 K (Table 4). The diffusion coefficients increase with increase in temperature in all cases. An increase in rate constant k^0 with increase in diffusion coefficient is seen because in a diffusion control reaction, its kinetics will definitely depends upon diffusion coefficient. The similar trend for diffusion coefficient was observed as k^0 in different solvents.

DMSO < DMA < DMF

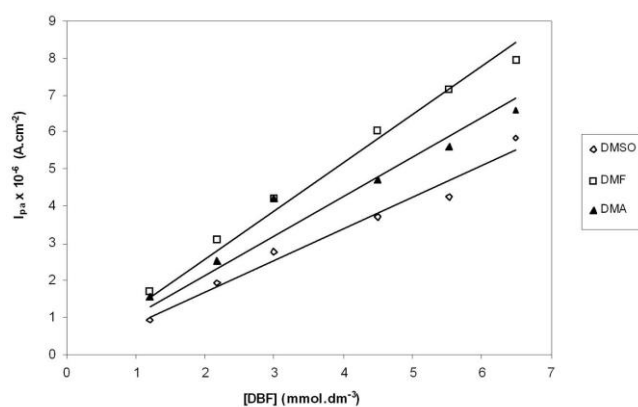
The kinetics of heterogeneous electron transfer reaction is influenced by the dynamics of solvent medium. The diffusive characteristic of solute in a particular solvent system is affected by the solvent dipolar relaxation.³⁴ Solvent dipolar relaxation depends upon solute-solvent shell formation which results in concentration change and change in macroscopic viscosity of the system. The dipolar interaction or polarizability of a solvent influence the solvent effects on kinetics of electron transfer.³⁵

Table 4. Kinetic parameter (k^0) and diffusion coefficient (D) for 3mM DBF at 0.2 V s⁻¹ in DMSO, DMF and DMA.

| T, K | $k^0, 10^{-6} \text{ cm s}^{-1}$ | $D, 10^{-6} \text{ cm}^2 \cdot \text{s}^{-1}$ | $k^0, 10^{-6} \text{ cm s}^{-1}$ | $D, 10^{-6} \text{ cm}^2 \cdot \text{s}^{-1}$ | $k^0, 10^{-6} \text{ cm s}^{-1}$ | $D, 10^{-6} \text{ cm}^2 \cdot \text{s}^{-1}$ |
|------|----------------------------------|---|----------------------------------|---|----------------------------------|---|
| | DMSO | | DMF | | DMA | |
| 303 | 0.353 | 5.41 | 1.30 | 13.3 | 0.550 | 8.47 |
| 313 | 0.781 | 6.42 | 1.41 | 14.8 | 0.711 | 9.88 |
| 323 | 0.942 | 7.19 | 2.10 | 17.3 | 0.810 | 11.2 |
| 333 | 1.331 | 8.35 | 1.76 | 20.9 | 0.986 | 12.8 |

Table 5. Activation energy (E_a) for diffusion of 3 mM DBF at 0.2 V s⁻¹ temperature ranging 303 K to 333 K in DMSO, DMA and DMF.

| T, K | 1/T | $\ln D$ | $E_a, \text{ kJ mol}^{-1}$ | $\ln D$ | $E_a, \text{ kJ mol}^{-1}$ | $\ln D$ | $E_a, \text{ kJ mol}^{-1}$ |
|------|---------|----------|----------------------------|----------|----------------------------|----------|----------------------------|
| | | DMSO | | DMF | | DMA | |
| 303 | 0.00330 | -12.1273 | | -11.2323 | | -11.6789 | |
| 313 | 0.00319 | -11.9561 | 14.86 | -11.0966 | 13.56 | -11.5250 | 11.47 |
| 323 | 0.00309 | -11.8428 | | -10.7559 | | -11.3996 | |
| 333 | 0.00300 | -11.6932 | | -10.8124 | | -11.2660 | |

**Figure 3.** Peak current density versus concentration for 3mM DBF at 0.2 V/s in DMSO, DMF and DMA.

The nonspecific electrostatic interactions of the solvent system or empirical π^* parameters describe the relative stability of the oxidation state of an analyte.³⁶ The change in the electronic state density by solvent molecules changes solvation of solute. The solvation involving Fe(II) of ferrocene moiety is affected by proton donor tendency (Brønsted acid) of solvent molecule to the non-bonding filled orbital to produce Fe (IV) hydride.³⁷⁻³⁸ Solvent may strongly behave like Lewis base with Fc^+ than Fc. Solvent molecule equatorial to the Fe(III) of Fc^+ may form weak bond.³⁹

According to Arrhenius equation:⁴⁰

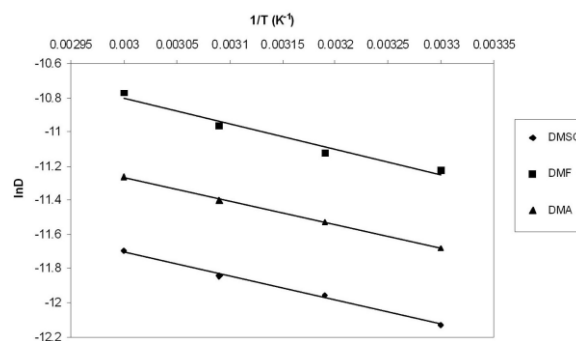
$$D = D_0 e^{-E/RT}$$

or

$$\ln D = \ln D_0 - \frac{E}{RT}$$

here “ E ” is the activation energy for diffusion of the ferrocene derivative. The slope of the curve plotted between $\ln D$ and $1/T$ gives activation energy for diffusion (Table 5).

The activation energy of 3mM DBF at 0.2 V s⁻¹ in temperature range from 303 K to 333 K for DMF, DMA and DMSO were found to be 12.63 kJ mol⁻¹, 11.33 kJ mol⁻¹ and 11.76 kJ mol⁻¹ respectively.

**Figure 4.** Diffusion coefficient versus temperature for 3 mM DBF at 0.2 V s⁻¹ in DMSO, DMF and DMA .

Acknowledgment

We are thankful to Dean Faculty of Science , University of Karachi for providing funds.

References

- Santis, G. De., Fabbrizzi, Licchelli, L., Poggi, M., A., Taglietti, A., *Angew. Chem. Int. Ed. Engl.*, **1996**, 35, 202.
- Fery-Forgues, S., Delavaux-Nicotc, B., *J. Photochem. Photobiol. A: Chemistry* **2000**, 132, 137.
- Seiwert, B., Karst, U., *Anal. Bioanal. Chem.*, **2008**, 390, 181.
- Ryabov, A. D., Goral V. N., L. Gorton, Csöregi, E., *Chem. Eur. J.*, **1999**, 5(3), 961.
- Matthews, D. R., Bown, E., Warson, A., Holman, R. R., Steemmson, J., Hughes, S., Scott, D., *Lancet*, **1987**, 778.

- ⁶Degani, Y., Heller, A., *J. Am. Chem. Soc.*, **1988**, *110*, 2615.
- ⁷Lawrence, N. S., Deo, R. P., Wang, J., *Anal. Chem.*, **2004**, *76*, 3735.
- ⁸Hoche, T., Cinquantini, A., Zanello, P., Hey-Hawkins, E., *Polyhedron*, **2005**, *24*, 1340.
- ⁹Ikeda, T., *Bull. Electrochem.*, **1992**, *8*, 145.
- ¹⁰Top, S., Vessieres, A., Leclercq, G., Quivy, J., Tang, J., Vaissermann, J., Huche, M., Jaouen, G. *Chem. Eur. J.*, **2003**, *9*, 5223.
- ¹¹Osella, D., Mahboobi, H., Colangelo, D., Cavigiolio, G., Vessie'res, A., Jaouen, G. *Inorg. Chim. Acta*, **2005**, *358*, 1993.
- ¹²Vessieres, A., Top, S., Pigeon, P., Hillard, E., Boubeker, L., Spera, D., Jaouen, G., *J. Med. Chem.* **2005**, *48*, 3937.
- ¹³Hillard E, Vessieres A, Le Bideau F, Plazuk D, Spera D, Huch M, Jaouen G. *Chem. Med. Chem.* **2006**, *1*, 551.
- ¹⁴Károlyi, I., Bösze, S., Orbán, E., Sohár, P., Drahos, L., Gál, E., Csámpai, A., *Molecules* **2012**, *17*, 2316.
- ¹⁵Koepf-Maier, P., Koepf, H., *Chem. Rev.*, **1987**, *87*, 1137.
- ¹⁶Popova, L. V., Babin, V. N., Belousov, Y. A., Nekrasov, Y. S., Snegireva, A. E., Borodina, N. P., Shaposhnikova, G. M., Bychenko, O. B., Raevskii, P. M., *Appl. Organomet. Chem.*, **1993**, *7*, 85.
- ¹⁷Seiwert, B., Karst, U., *Anal. Bioanal. Chem.*, **2007**, *388*, 1633.
- ¹⁸Gorton, J. E., Lentzner, H. L., Watta, W. E. *Tetrahedron*, **1971**, *27*, 4353.
- ¹⁹Britton W. E., Kashyap, R., El-Hashash, M., El-Kady, M., Herberhold, M. *J. Organomet. Chem.*, **1986**, *5(5)*, 1029.
- ²⁰Hillman, M., Gordon, B., Weiss, A. J., Guzikowska, A. P., *J. Organomet. Chem.*, **1978**, *155*, 77.
- ²¹Silva M. E. N. P. R. A., Pombeiro A. J. L., da Silva J. J. R. F., Herrmann R., Deus N., Bozak R. E., *J. Organomet. Chem.* **1991**, *421*, 775.
- ²²Silva M. E. N. P. R. A., Pombeiro A. J. L., da Silva J. J. R. F., Herrmann R., Deus N., Bozak R. E., *J. Organomet. Chem.*, **1994**, *480*, 1281.
- ²³Asahara, M., Natsume, S., Kurihara, H., Yamaguchi, T., Erabi, T., Wada, M., *J. Organomet. Chem.*, **2000**, *601*, 2246.
- ²⁴Kamlet, M. J., Abboud, J. M., Abraham, M. H., Taft, R.W., *J. Org. Chem.* **1983**, *48*, 2877.
- ²⁵Gritzner, G.; Kuta, J. *Pure Appl. Chem.* **1982**, *54*, 1527-1532.
- ²⁶Prins, R.; Korswagen, A. R.; Kortbeek, A. G. T. G. *J. Organomet. Chem.* **1972**, *39*, 335-344.
- ²⁷Karpinski, Z. J.; Nanjundiah, C.; Osteryoung, R. A. *Inorg. Chem.* **1984**, *23*, 3358-3364.
- ²⁸Zara, A. J.; Machado, S. S.; Bulhoes, L. O. S.; Benedetti, A. V.; Rabockai, T. *J. Electroanal. Chem.* **1987**, *221*, 165-174
- ²⁹Suh, J. T., **US 3,382,267**.
- ³⁰Ranchet, D., Tommasino, J. B., Vittori, O., Fabre, P. L. *J. Solution Chem.*, **1998**, *27(II)*, 979.
- ³¹Wipf, D. O., Kristensen, E. W., Deakin, M. R., Wightman, R. M., *Anal. Chem.* **1988**, *60*, 306.
- ³² Bard, A. J. Faulkner, L. R., *Electrochemical Methods, Fundamentals and Applications*, John Wiley and Sons, New York, 1980, pp. 218.
- ³³Bard, A. J., Faulkner, L. R., *Electrochemical Methods, Fundamentals and Applications*, John Wiley and Sons, New York, 1980, pp. 223.
- ³⁴Pyati, R. and Murray, R. W., *J. Am. Chem. Soc.* 1996, *118*, 1743-1749
- ³⁵Reichardt, C. *Solvents and solvent effects in Organic Chemistry*, 2nd ed.; VCH: Weinheim, Germany, **1988**
- ³⁶Churg, A. K.; Warshel A. *Biochemistry* **1986**, *25*, 1675-1681; Moore, G. R.; Pettigrew, G. W.; Rogers, N. K., *Proc. Natl. Acad. Sci. U.S.A.* **1985**, *82*, 3082-3085
- ³⁷Curphey, T. J.; Santer, J. O.; Rosenblum, M.; Richards, J. H. J. *Am. Chem. Soc.*, **1960**, *82*, 5249-5250.
- ³⁸Lauher, J. W.; Hoffmann, R., *J. Am. Chem. Soc.*, **1976**, *98*, 1729-1742
- ³⁹Lay, P. A.; Sasse, W. H. F., *Inorg. Chem.*, **1985**, *24*, 4707-4710
- ⁴⁰Matsumiya, M., Terazono, M., Tokuraku, K., *Electrochim. Acta* **2006**, *51*, 1178-1183

Received: 16.05.2013.

Accepted: 30.06.2013.



HEAVY METAL REMEDIATION OF WASTEWATER BY AGROWASTES

Choudhari Deepika^[a], Sharma Dipak^[a] and Phadnis Anjani^[a]

Keywords: wastewater treatment, low cost adsorbent, non biodegradable heavy metals.

Advanced wastewater treatment techniques such as adsorption are economically and environmentally essential in the removal of non biodegradable heavy metals from wastewater. Adsorption by activated carbon is being widely used but activated carbon remain an expensive material. In recent years, the need for safe and economical methods for the elimination of heavy metals from contaminated waters has necessitated research interest towards the production of low cost alternatives to commercially available activated carbon. Therefore there is an urgent need that all possible sources of agro-based inexpensive adsorbents should be explored and their feasibility for the removal of heavy metals should be studied in detail. This review focuses on the use of low cost adsorbent prepared from rice husk, cajanus cajan, maize cob, sago waste, mosambi fruit peel, watermelon shells, almond shells, apricot shells etc.

Keywords: wastewater treatment, low cost adsorbent, non biodegradable heavy metal.

Corresponding Authors

E-Mail: deepinkey811@gmail.com

[a] Department of Chemical Sciences, Maharaja Ranjit Singh College, Indore, M. P., India

Introduction

Water pollution due to toxic heavy metals has been a major cause of concern for environmental engineers. The industrial and domestic wastewater is responsible for causing several damages to the environment and adversely affecting the health of the people. Several episodes due to heavy metal contamination in aquatic environment increased the awareness about the heavy metal toxicity. Metals can be distinguished from other toxic pollutants, since they are non-biodegradable and can accumulate in living tissues, thus becoming concentrated throughout the food chain. A variety of industries for the release of heavy metals into the environment through their wastewater as suggested by Braukmann et al.¹

However years of increased industrial, agricultural and domestic activities have resulted in the generation of large amount of wastewater containing a number of toxic pollutants, which are polluting the available fresh water continuously. With the realization that pollutants present in water adversely effect human and animal life domestic and industrial activities, pollution control and management is now a high priority area. The availability of clean water for various activities is becoming the most challenging task for researcher and practitioners worldwide.

Heavy metals have been excessively released into the environment due to rapid industrialization and have created a major global concern. Cadmium, zinc, copper, nickel, lead, mercury and chromium are often detected in industrial wastewaters, which originate from metal plating, mining activities, smelting, battery manufacture, tanneries, petroleum refining, paint manufacture, pesticides, pigment manufacture, printing and photographic industries, etc.^{2,3} Unlike organic wastes, heavy metals are non-biodegradable and they can be accumulated in living tissues, causing various diseases and disorders; therefore they must be

removed before discharge. Namasivayam C.J. et al.⁴ interest into the production of cheaper adsorbents to replace costly wastewater treatment methods such as chemical precipitation, ion-exchange, electroflotation, membrane separation, reverse osmosis, electrodialysis solvent extraction, etc. are attracting attention of scientists. Adsorption is one the physico-chemical treatment processes found to be effective in removing heavy metals from aqueous solutions. Most of the adsorption studies have been focused on untreated plant wastes such as *Eucalyptus* Bark,⁵ almond and apricot shell,⁶ bael fruit,⁷ *Moringa oleifera* pods,⁸ *Opuntia*,⁹ *Thespesia Populnea* Bark,¹⁰ *Adathoda vasica*,¹¹ Jaswand Leaf Powder.¹²

In general, an adsorbent can be termed as a low cost adsorbent if it requires little processing, is abundant in nature, or is a by-product or waste material from another industry. Of course improved sorption capacity may compensate the cost of additional processing as suggested by Bailey et al.¹³ Therefore there is an urgent need that all possible sources of agro-based inexpensive adsorbents should be explored and their feasibility for the removal of heavy metals should be studied in detail. The objective of this study is to contribute in the search for less expensive adsorbents and their utilization possibilities for various agricultural waste by-products, which are in many cases also pollution sources.

Relevant Literature

Reviews of some agricultural adsorbents for the removal of heavy metals from wastewater are presented as follows:

Rice husk: Rice husk is an agricultural waste material generated in rice producing countries, especially in Asia. The annual world rice production is approximately 500 million metric tons, of which 10 – 20 % is rice husk. Dry rice husk contains 70– 85 % of organic matter (lignin, cellulose, sugars, etc) and the remainder consists of silica, which is present in the cellular membrane carried out by Vempati et al.¹⁴ Srinivasan et al.³⁶ studied on chromium removal by rice husk carbon. The activated carbon prepared

by carbonization of rice husk with sulphuric acid followed by CO₂ activation showed 88 % removal of total chromium and greater than 99 % removal of hexavalent chromium. Column studies showed capacity of 8.9 mg g⁻¹ and 6.3 mg g⁻¹ for rice husk and commercial carbons respectively, for Cr(VI) removal. Ayub S. et al.¹⁶ studied on chromium removal by rice husk carbon. The activated carbon prepared by carbonization of rice husk with sulphuric acid followed by CO₂ activation showed 88 % removal of total chromium and greater than 99 % removal of hexavalent chromium. Column studies showed capacity of 8.9 mg g⁻¹ and 6.3 mg g⁻¹ for rice husk and commercial carbons respectively, for Cr(VI) removal. Guo Y. et al.¹⁷ studied on adsorption of Cr(VI) on micro- and mesoporous rice husk-based activated carbon. They have concluded that the rice husk carbon is a good sorbent for the removal of Cr(VI) from aqueous solution range from 5 to 60 mg L⁻¹ with adsorbent dose of 0.8 g L⁻¹ at pH < 5 under the minimum equilibration time of 2 hours. There is a sharp decrease in adsorption above pH 5.0 and the adsorption in the higher pH range would be negligible. Maximum reported adsorption is >95 % removal of Cr(VI). A study on utilization of agro-residues (rice husk) in small wastewater treatment plants was done by Daifullah et al.¹⁸ They have characterized and evaluated two types of sorbents made from rice husk. The efficiency of both sorbents in the removal of the complex matrix containing six heavy metal was nearly 100 %. These metals are Fe, Mn, Zn, Cu, Cd, and Pb, which are found in the drain containing the agricultural and sewage wastewater. Wong et al.¹⁹ using tartaric acid modified rice husk as adsorbent have carried out batch studies for the removal of lead and copper and reported the effects of various parameters such as pH, initial concentration of adsorbent, particle size, temperature etc. It was reported that modified rice husk is a potentially useful material for the removal of Cu and Pb from aqueous solutions. The rapid uptake and high adsorption capacity makes it a very attractive alternative adsorption material. It was also shown that the uptake of Cu and Pb was maximum when pH was increased from 2 to 3, thereafter remained relatively constant. Adsorption behaviour of Ni(II), Zn(II), Cd(II), and Cr(VI) on untreated and phosphate treated rice husk (PRH) by Ajmal M. et al.²⁰ showed that adsorption of Ni(II) and Cd(II) was greater when PRH was used as adsorbent. Adsorption of Cd(II) was dependent on contact time, concentration, temperature, adsorbent doses and pH of the solution. It was also reported that the maximum adsorption (>90%) was obtained at a pH value of 12. Subramaniam P.²¹ studied on raw rice on the removal of Cr(VI). The overall result indicated that the maximum removal (66 %) of Cr(VI) for raw rice husk was obtained at pH 2, when it is given adsorbent dose of 70 g L⁻¹ for 2 hours. It has also showed good fit to Freundlich isotherm with 1/n value of 2.863. The adsorption behavior of Zn²⁺ and Pb²⁺ ions on rice husk was investigated by Asrari et al.²² using rice husk to remove the metals ions in dairy wastewater. The removal of heavy metal ions from aqueous solutions was studied by batch method. The main parameters that influencing Zn²⁺ and Pb²⁺ sorption on rice husk were: amount of adsorbent, contact time and pH value of wastewater. The influences of pH (2–9), contact time (5–70 min) and adsorbent amount (0.5–3 g) have been studied. The percent adsorption of Zn²⁺ and Pb²⁺ ions increased with an increase in contact time and dosage of rice husk. The binding process was strongly affected by pH and the optimum pH for Zn²⁺ and Pb²⁺ ions were 7.0 and 9.0, respectively. The experimental data were analyzed by

Langmuir isotherm. The maximum adsorption capacity of the adsorbent for Zn²⁺ and Pb²⁺ ions was calculated from the Langmuir isotherm and found to be 19.617 and 0.6216 mg g⁻¹, respectively. The percent of removing Zn²⁺ and Pb²⁺ ions reached maximum to 70 % and 96.8 %, respectively. Nhapi I et al.²³ reported that, adsorbents, carbonized rice husk (CRH) and activated rice husk (ARH) made out of rice husks, available as agriculture waste, are investigated as viable materials for treatment of Pb, Cd, Cu, and Zn containing industrial wastewater at controlled pH. The results obtained from the batch experiments revealed a relative ability of the rice husk in removing some heavy metals at pH 7. One hand one, the CRH adsorption capacity decreases in the order of Cu>Pb>Zn>Cd in batch adsorption whereas during rapid small scale column tests the adsorption capacity decrease as follow Cu>Zn>Pb>Cd. On the other hand, ARH adsorption capacity performance is similar to CRH. However, during rapid small scale column tests the adsorption capacity decreases in the order Zn>Cu>Pb>Cd. The kinetic removal in batch experiment shows that the net uptake of Pb, Cd, Cu, Zn was 54.3 %, 8.24 %, 51.4 % and 56.7 %, respectively whereas using CRH, while it varied as 74.04 %, 43.4 %, 70.08 % and 77.2 % for the same dosages of ARH. Therefore, it is concluded that as regards to CRH, ARH demonstrated higher potential to remove relatively all selected heavy metals. Biosorption of cadmium ions from simulated wastewater using rice husk was studied by Ebrahim et al.²⁴ with initial concentration of 25 mg L⁻¹. Equilibrium isotherm was studied using Langmuir, Freundlich, BET and Timken models. The results show that the Freundlich isotherm is the best fit model to describe this process with high determination coefficient equals to 0.983. There was a good compliance between the experimental and theoretical results. Highest removal efficiency 97 % was obtained at 2.5g of adsorbent, pH 6 and contact time 100 min. Singh²⁵ reported that, adsorbent is prepared from rice husk, a low cost by product from a rice mill. The rice husk carbon is activated using H₃PO₄ (40 %). The stock solution of Cr(VI) is prepared by dissolving 2.828 g of potassium dichromate (Central Drug House (CDH), India) in 1 litre of demineralized water. Batch mode experiments are done. The effect of various parameters like adsorbent dose, pH and contact time are studied. The studies demonstrate that the rice husk carbon (RHC) has a significant capacity for adsorption of Cr(VI) from aqueous solution. The RHC characteristics are reported as FTIR. The break through capacity for Cr(VI) (100 mg L⁻¹, pH 2) is on average 38.1 mg g⁻¹. The adsorption of chromium(VI) was found to be maximum (93–94 %) at low values of pH (around 2) for the carbon dosage of 1000 mg L⁻¹ and nearly 100 % for carbon dosage of 1200 mg L⁻¹. RHC exhibits high degree of selectivity for Cr(VI) adsorption. Table 1 summarizes the usage of types of rice husk as an adsorbent:

Maize/Corn Cob: The study on oxidation of corncob by citric acid and nitric acid was carried out by Leyva-Ramos et al.²⁶ Upon oxidation of corncob, a significant increase in the surface area of the adsorbent was observed. An increase in the amount of oxygen found in corncob was due to more oxygenated groups being introduced on the adsorbent surface after oxidation. After oxidation, a higher proportion of acidic sites (carboxylic, phenolic and lactonic) was detected, which results in a reduction in the pHzpc (pH at zero point charge) value. It was also reported that the adsorption capacities for citric acid and nitric acid oxidized corncob were much higher than unmodified corncob.

Table 1. Types of rice husk as adsorbent for heavy metal

| Adsorbent | Heavy metal removal efficiency, % | | | | | | | References |
|--|-----------------------------------|--------|--------|--------|--------|--------|--------|------------|
| | Cr(VI) | Ni(II) | Cu(II) | Zn(II) | Cd(II) | Hg(II) | Pb(II) | |
| Rice husk carbon | >99 | - | - | - | - | - | - | 16 |
| Phosphate treated rice husk | - | - | - | - | >90 | - | - | 20 |
| Tartaric acid modified rice husk | - | - | >80 | - | - | - | >95 | 19 |
| Rice husk carbon | - | - | ≈ 100 | ≈ 100 | ≈ 100 | - | ≈ 100 | 18 |
| Raw rice husk | 66 | - | - | - | - | - | - | 21 |
| Rice husk | - | - | - | 70 | - | - | 96.8 | 22 |
| Carbonised rice husk | - | - | 51.4 | 56.7 | 8.24 | - | 54.3 | 23 |
| Activated rice husk | - | - | 70.08 | 77.2 | 43.4 | - | 74.04 | 23 |
| Rice husk | - | - | - | - | 97 | - | - | 24 |
| Rice husk carbon using H ₃ PO ₄ (40 %) | 93-94 | - | - | - | - | - | - | 25 |

Table 2. Types of Maize/Corn Cob as adsorbent for heavy metal

| Adsorbent | Heavy metal removal efficiency, % | | | | | | | References |
|--------------------------------|-----------------------------------|--------|--------|--------|--------|--------|--------|------------|
| | Cu(II) | Cr(VI) | Ni(II) | Fe(II) | Co(II) | Zn(II) | Cd(II) | |
| Sulfuric acid treated corncobs | 90 | - | - | - | - | - | - | 27 |
| Maize cob | - | - | 99 | - | - | - | - | 32 |
| Corn cob | - | >90 | - | - | - | - | - | 31 |

Besides carbonization at high temperature, an adsorbent can be activated by chemical treatment using a concentrated acid. Khan and Wahab et al.²⁷ in the study of adsorption of copper by concentrated sulfuric acid treated corncobs. It was reported that upon treatment of corncobs with sulfuric acid and heated at 150 °C, the pHzpc of the adsorbent reduced from 5.2 (untreated) to 2.7 (treated) and the functional groups present in the adsorbent are mainly oxygen containing groups such as –OH, –COOH and –COO⁻. The maximum adsorption capacity obtained from Langmuir isotherm was 31.45 mg L⁻¹. Adsorption was more favored at higher pH value (4.5) due to low competing effect of protons for the adsorption sites. Effect of interfering ions such as Zn(II), Pb(II) and Ca(II) was also studied. It was noticed that copper removal efficiency was reduced by 53 %, 27 % and 19 % in the presence of Pb(II), Ca(II) and Zn(II), respectively. Regeneration study indicates that sulfuric acid treated corncobs can be regenerated by acidified hydrogen peroxide solution and as much as 90 % copper could be recovered. Daniela et al.²⁸ describe chemical modeling of metal biosorption requires the characterization of biomass used as sorbent. The (local) structural environment of Cu(II) and Zn(II) sorbed on corn cobs biomass has been investigated by secondary electron microscopy (SEM) and energy-dispersive X-ray analysis (EDX). The IR spectrum obtained for the above said biomass render a complex nature of the corn cobs biomass. Despite this complexity some characteristic peaks may be identified and assigned, revealing the presence of hydroxyl, carboxyl, carbonyl and amino functional groups in the structure of investigated biomass. The paper also deals with studies of physical and biochemical properties of the

sorbent: bulk density, apparent density, surface area, iodine number, CEC. From biomass characterization a possible mechanism of biosorption is suggested. The sorption experiments were carried out at a pH of 5.5 and low and high ionic strength in a 0.01 M Na₂SO₄ solution. The results showed a high capacity of corn cobs with respect to the removal of the investigated metals cations. Akporhonor et al.²⁹ prepared maize cob carbon was prepared by pyrolysis at 300 °C and 400 °C for 35 min. This was followed by steeping in saturated ammonium chloride. The activated carbon which was characterized for bulk density, surface area, surface area charge, abrasion resistance and pH was used in the removal of Cd²⁺, Ni²⁺, Cu²⁺ and Zn²⁺. The surface areas of the maize cob carbon at 300 °C and 400 °C were 0.010 and 0.021 g sample per mg iodine, respectively. The effectiveness of the modified maize cobs in removing the metal ions from solution was found to be Zn>Ni>Cd. The removal efficiency of the metal ions is depended on the metal ion concentration and temperature of carbonization. Igwe³⁰ reported that the use of EDTA modified and unmodified maize Cob for the removal of Co(II), Fe(II) and Cu(II) ions from aqueous solutions is feasible. It was found that modification enhanced the adsorption predominantly due to chelates formation. Co(II) ion was adsorbed more for both unmodified and modified maize cob, than the other two metal ions. The trend of the uptake is Co(II)>Fe(II)>Cu(II) for the unmodified and Co(II)>Cu(II)>Fe(II) for the modified maize cob. It was found that the pseudo second order equation gave a better fit to the sorption process than the pseudo first order equation. It was also possible to use Elovich equation to model the sorption process. The intraparticle diffusion

plot confirmed that the sorption process was particle diffusion controlled. The regression models that were generated for these equations could be used as predictive models for these heavy metals sorption on maize cob at any other contact time. Also, the results of this study could serve as parameters for designs of treatment plants for the treatment of heavy metal bearing effluents using maize cob or even any other agricultural by-products as adsorbents. Therefore, maize cob which is a waste has been employed in treating another waste, which is heavy metal wastewater, thereby achieving environmental friendliness. Study of Abdullahi Balarabe Sallau³¹ explores the potential of corn cob powder for adsorption of Cr(VI) in aqueous solution. Effects of adsorbent dosage, pH, temperature, contact time and Cr(VI) concentration were investigated. Maximum adsorption was observed at 80 °C under acidic condition of pH 4 with a contact time of 120 min. The percentage removal efficiency was more than 90 % at lower initial Cr(VI) concentrations. Both Langmuir and Freundlich adsorption isotherms fitted reasonably well with the data and showed high correlation coefficient (R^2) values of 0.999 and 0.991, respectively. Based on this, the adsorbent can be used as a low cost alternative in biosorption of wastewaters containing lower concentrations of Cr(VI). The adsorption of Ni(II) on maize cob has been studied by Muthusamy et al.³² using atomic absorption spectroscopy for metal estimation. Parameters like heavy metal concentration, adsorbent dose, contact time and agitation speed were studied. Langmuir and Freundlich isotherms were employed to describe adsorption equilibrium. Maximum amount of nickel adsorbed as evaluated by Freundlich isotherm is up to 99 %. Study concluded that maize cob, a waste material, have good potential as an adsorbent to remove toxic heavy metal like nickel from industrial wastewater. Table 2 summarizes the usage of types of rice maize/corn cob as an adsorbent.

Cajanus Cajan: Husk of tur dal (*Cajanus cajan*) was investigated by Ahalya et al.³³ as a new biosorbent for the removal of Fe(III) and Cr(VI) ions from aqueous solutions. Parameters like agitation time, adsorbent dosage and pH were studied at different initial Fe(III) and Cr(VI) concentrations. The biosorptive capacity of the tur dal husk was dependent on the pH of the chromium and iron solution, with pH 2 and 2.5 respectively being optimal. The adsorption data fit well with Langmuir and Freundlich isotherm models. The practical limiting adsorption capacity (q_{max}) calculated from the Langmuir isotherm was 96.05 mg of Cr(VI)/g of the biosorbent at an initial pH of 2.0 and 66.65 mg g⁻¹ at pH 2.5. The infrared spectra of the biomass revealed that hydroxyl, carboxyl and amide bonds are involved in the uptake of Cr(VI) and Fe(III) ions. Characterisation of tur dal husk has revealed that it is an excellent material for treating wastewaters containing low concentration of metal ions. Karunakaran et al.³⁴ *Cajanus Cajan* (L) milsp seed shell activated carbons (CCC), an agricultural waste, abundance, cheapness and environmentally friendly nature could be used as potential adsorbent for the removal of Fe(III) from aqueous solution contains heavy metals and polluted water. The Freundlich adsorption isotherm model describes the adsorption behaviour with good correlation coefficient. The adsorption of Fe(III) was depended on the pH of the solution. Based on the results, the optimum contact time is 30 minutes and

adsorbent dosage is 50 mg L⁻¹. Polypyrrole conducting polymer is the most important conducting polymer that can be synthesized by chemical polymerization as coated form on the surface of CCC from aqueous solution. It was found that polypyrrole based conducting polymer was better adsorbent for removal Fe(III) compared to CCC from aqueous solution. The metal ion adsorption obeyed the pseudo- second order model based on the experimental and calculated q_e values. The removal of Fe(III) is simultaneously increased with increase in the temperature from 30 °C to 50 °C. The adsorptive removal of Ni(II) from aqueous solution using *Cajanus Cajan* (L) Milsp seed shells activated carbon and polypyrrole coated *Cajanus cajan* (L) milsp seed shells activated carbon (PPy/CCC) has been carried out by Thamilarasu et al.³⁵ under various experimental conditions. Quality of Ni(II) uptake at 50 mg of activated carbon is 25.75 mg g⁻¹ for CCC and 29.60 mg g⁻¹ for PPy/CCC. Adsorption data are modeled with Freundlich, Langmuir and Temkin adsorption isotherm. Thermodynamic parameters such as ΔH^0 , ΔS^0 and ΔG^0 have been calculated and the findings indicate that the adsorption is spontaneous and endothermic. Enthalpy change values range from 8.90 kJ mol⁻¹ to 23.04 kJ mol⁻¹, and based on these values the adsorption of Ni(II) by CCC could be a physisorption. A mechanism involving intra particle diffusion and surface adsorption has been proposed for adsorption of Ni(II) onto adsorbent. Adsorbent used in this study is also characterized by FT-IR and SEM before and after the adsorption of metal ions. Table 3 summarizes the usage of types of *Cajanus cajan* as an adsorbent.

Other agricultural waste product: Quek et al.³⁶ in their study on the use of sago waste for the sorption of lead and copper. Sago processing waste, which is both a waste and a pollutant, was used to adsorb lead and copper ions from solution. The sorption process was examined in terms of its equilibria and kinetics. The most effective pH range was found to be 4 to 5.5 for both metals. The equilibria data for both metals fitted both the Langmuir and the Freundlich models and based on the Langmuir constants, the sago waste had a greater sorption capacity for lead (46.6 mg g⁻¹) than copper (12.4 mg g⁻¹). The kinetic studies showed that the sorption rates could be described well by a second-order expression than by the more commonly applied Lagergren equation. Kadirvelu et al.³⁷ studied on utilization of various agricultural wastes for activated carbon preparation and application for the removal of dyes and metal ions from aqueous solution. Mercury(II) and nickel(II) were used in the study for various adsorbents. Activated carbon was prepared from agricultural solid wastes such as, silk cotton hulls, coconut tree sawdust, sago waste, maize cob and banana pitch. Erhan Demirbas et al.³⁸ reported that the batch removal of Cr(VI) from aqueous solution using low-cost adsorbents such as cornelian cherry, apricot stone and almond shell under different experimental conditions was investigated in this study. The influences of initial Cr(VI) ion concentration (20 to 300 mg·L⁻¹), pH (1 to 4) and particle size (0.63 to 1.60 mm) have been reported. Adsorption of Cr(VI) is highly pH-dependent and the results indicate that the optimum pH for the removal was found to be 1 for all types of carbon. A comparison of kinetic models applied to the adsorption of Cr(VI) ions on the adsorbents was evaluated for the pseudo first-order, the pseudo second-order, Elovich and intraparticle

diffusion kinetic models, respectively. Results show that the pseudo second-order kinetic model was found to correlate the experimental data well. In the investigation of Hema Krishna et al.³⁹ the powder of mosambi fruit

peelings (PMFP) was used as an inexpensive and efficient adsorbent for Ni(II) removal from aqueous solutions. The influence of physico-chemical key parameters such as the initial metal ion concentration, pH, agitation time, particle

Table 3. Types of *Cajanus Cajan* as adsorbent for heavy metal

| Adsorbent | Heavy metal removal efficiency, % | | | References |
|---|-----------------------------------|---------|--------|------------|
| | Cr(VI) | Fe(III) | Ni(II) | |
| Tur dal husk | 96.05 | 66.63 | - | 33 |
| CCC (50 mg L ⁻¹) at 50 °C | - | 86.39 | - | 34 |
| PPy/CCC (50 mg L ⁻¹) at 50 °C | - | 90.47 | - | |
| CCC (50 mg L ⁻¹) at 50 °C | - | - | 88.60 | 35 |
| PPy/CCC (50 mg L ⁻¹) at 50 °C | - | - | 93.7 | |

Table 4. Other types of agricultural wastes as adsorbent for heavy metal

| Adsorbent | Heavy metal removal efficiency, % | | | | | | | References |
|-----------------------------|-----------------------------------|--------|--------|--------|--------|--------|---------|------------|
| | Ni(II) | Hg(II) | Cu(II) | Pb(II) | Cr(VI) | Cd(II) | Fe(III) | |
| Silk cotton carbon | 64 | 100 | - | - | - | - | - | |
| Coconut tree sawdust carbon | 84.3 | 100 | - | - | - | - | - | 36 |
| Sago waste carbon | 100 | 100 | - | - | - | - | - | |
| Banan pitch carbon | 96.40 | 100 | - | - | - | - | - | |
| Sago waste | - | - | >75 | >95 | - | - | - | 35 |
| Cornelian cherry | - | - | - | - | >99 | - | - | |
| Apricot stone | - | - | - | - | >98 | - | - | 37 |
| Almond shells | - | - | - | - | >99 | - | - | |
| Mosambi fruit peeling | >90 | - | - | - | - | - | - | 38 |
| Watermelon shell | - | - | >90 | - | - | - | - | 39 |
| Almond shell | - | - | - | - | - | - | >90 | 40 |
| Spent grain | - | - | - | >90 | - | >90 | - | 42 |
| Coconut husk | - | - | - | - | >80 | - | - | |
| Palm pressed fibre | - | - | - | - | >80 | - | - | 44 |
| Eucalyptus bark | - | - | - | - | 99 | - | - | 5 |

size and adsorbent dosage has been considered in batch tests. Sorbent ability to adsorb Ni(II) ions was examined and the mechanism involved in the process investigated. The optimum results were determined at an initial metal ion concentration of 50 (mg L⁻¹), pH=4, agitation time – 90 min, an adsorbent dose (125 mg/50 ml) and the particle size (0.6 mm). The % adsorption, Langmuir constants [$Q_0=29.41 \text{ mg g}^{-1}$ and $b=0.4789 \text{ L mg}^{-1}$], Freundlich constant $K_f=23.92 \text{ mg g}^{-1}$ and $n=2.24 \text{ L mg}^{-1}$, Lagergren rate constants [$K_{ad}=4.37 \times 10^{-2} \text{ min}^{-1}$] for [Ni(II)] 50 mg L⁻¹, were determined for the adsorption system as a function of sorbate concentration. The equilibrium data obtained were tested using Langmuir, Freundlich adsorption isotherm models, and the kinetic data obtained were fitted to pseudo first order model. The study of Koel Banerjee et al.⁴⁰ deals with the application of watermelon shell, an agricultural waste, for the adsorptive removal of Cu(II) from its aqueous solutions. This paper incorporates the effects of time, dose, temperature, concentration, particle size, agitation speed

and pH. Analytical techniques have been employed to find pore properties and characteristics of adsorbent materials. Batch kinetic and isotherm studies have also been performed to understand the ability of the adsorbents. The adsorption behavior of the Cu(II) has been studied using Freundlich, Langmuir and Tempkin adsorption isotherm models. The monolayer adsorption capacity determined from the Langmuir adsorption equation has been found as 111.1 mg g⁻¹. Kinetic measurements suggest the involvement of pseudo-second-order kinetics in adsorptions and is controlled by a particle diffusion process. Adsorption of Cu(II) on adsorbents was found to increase on decreasing initial concentration, increasing pH up to 8, increasing temperature, increasing agitation speed and decreasing particle size. Overall, the present findings suggest that watermelon outer shell is environmentally friendly, efficient and low-cost biosorbent which is useful for the removal of Cu(II) from aqueous media. G. Anusha et al.⁴¹ discuss the ability of the almond shell based activated

carbon in removing iron from the synthetic solution. The results clearly indicate that the carbon was effective in removing iron from the synthetic solution. For synthetic solution it was observed that the percentage removal of iron with increase in time of contact up to 20 minutes and after that there was no appreciable increase in the percentage removal. Hence the optimum contact time for synthetic solution was taken as 20 minutes. For synthetic solution, it was found that the percentage Iron removal increases from pH 1-9. Optimum pH is 5.0 which is the original pH of the solution. Spent grain obtained from brewery can be used to treat Pb(II) and Cd(II) ions as demonstrated by Low et al.⁴¹ Treatment of spent grain with NaOH greatly enhanced adsorption of Cd(II) and Pb(II) ions, whereas HCl treated spent grain showed lower adsorption than the untreated spent grain. The increase in adsorption of heavy metal ions after base treatment could be explained by the increase in the amount of galacturonic acid groups after hydrolysis of O-methyl ester groups. The best pH range for metal adsorption was 4–6. Kinetic study reveals that the equilibrium time of adsorption was 120 min for both metal ions and adsorption followed pseudo-second-order model. The maximum adsorption capacity for lead was two times higher than cadmium. The effect of organic ligands (EDTA, nitrilotriacetic acid and salicylic acid) on adsorption efficiency was assessed and adsorption was greatly reduced by EDTA and nitrilotriacetic acid at molar ratio of 1:1 (metal:ligand). EDTA and nitrilotriacetic acid could chelate the heavy metal ions, therefore more metal ions would remain in the solutions rather than being adsorbed as suggested by Jeon and Park et al.⁴² Salicylic acid on the other hand slightly reduced the percentage of cadmium adsorption but did not affect adsorption of lead. Halim et al.⁴³ studied on removal of lead ions from industrial wastewater by different types of natural materials. From the research done it was reported that at lead concentration of 4 mg L⁻¹ and pH 6 the adsorption capacity is maximum for Nile rose plant powder at 80 % removal and at the same concentration and pH it was also reported that bone powder removed 98.8 % of lead. Tan et al.⁴⁴ Studied on removal of chromium (VI) from solution by coconut husk and palm pressed fibres and it was investigated using batch and column techniques. For both substrates, the optimum pH for maximum removal is at 2.0 which corresponds to > 80 % removal. Sarin et al.⁵ reported that removal of poisonous hexavalent form of chromium from solutions was possible using selected adsorbents. Eucalyptus bark (EB) was the most effective for which the removal reached more than 99 % for Cr(VI) at concentration of 200 ppm and at pH 2. Increase in the dose of adsorbent, initial concentration of Cr(VI) and increase in contact time upto 2 h are favorable for all increase the adsorption of Cr(VI). The kinetic of the Cr(VI) adsorption on EB was found to follow first order mechanism. The Gibbs free energy was obtained for each system. It was found to be -1.884 kJ mol⁻¹ for Cr(VI) and -3.872 kJ mol⁻¹ for Cr(III) for removal from industrial effluent. The adsorption data can be satisfactorily explained by Freundlich isotherm. Higher sorption capacity of this sorbent indicates that eucalyptus bark can be used for the treatment of chromium effluent. Table 4 summarizes the usage of some of agricultural waste as an adsorbent:

Conclusion

According to literature data adsorption is very popular method for the removal of heavy metals from wastewater. In this paper, the removal performance of low cost adsorbent derived from agricultural waste such as rice husk, maize cob, *Cajanus cajan*, sago waste, apricot shell, almond shell, mosambi fruit peel, watermelon shell etc. has been reviewed. It is evident from Table 1 to table 4 that low cost adsorbent have outstanding removal capabilities for heavy metals like Cu(II), Fe(III), Ni(II), Cd(II), Hg(II), Cr(VI), Pb(II) etc. Adsorption capacity of an adsorbent depends on several parameters like dosage of adsorbent, initial concentration of heavy metals in solution, pH value and temperature. It is important to note, adsorption capacities of the adsorbents presented in this article vary, depending on the characteristics of the individual adsorbents. Low-cost, effectiveness and availability of described materials suggest that they can be used in place of expensive activated carbon for the removal of heavy metal ions from solutions.

Reference

- ¹Braukmann, B. M., *Industrial solution amenable to biosorption*, In *Biosorption* (Edited by Volusky B), CRC Press, Boca Raton, FL, **1990**.
- ²Kadirvelu, K., Thamaraiselvi, K., and Namasivayam, C., *Bioresour. Technol.*, **2001**, 76, 63–65.
- ³Williams, C. J., Aderhold, D. and Edyvean, G. J., *Water Res.*, **1998**, 32, 216–224.
- ⁴Namasivayam, C. and Ranganathan, K., *Environ. Technol.* **1995**, 16, 851–860.
- ⁵Sarin, V. and Pant K. K., *Bioresource Technology*, **2006**, 97, 15–20.
- ⁶Khazaei, I., Aliabadi, M. and Hamed Mosavian, H. T., *Iranian J. Chem. Eng.*, **2011**, 8(4), 11-23.
- ⁷Anusha, G., 2nd Int. Conf. Environ. Sci. Technol., IPCBEE vol. 6, IACSIT Press, Singapore, **2011**.
- ⁸Adelaja, O. A., Amoo, I. A and Aderibigbe, A. D., *Archiv. Appl. Sci. Res.*, **2011**, 3(6), 50-60.
- ⁹Mane, P. C, Bhosle, A. B., Jangam, C. M. and Mukate, S. V., *J. Nat. Prod. Plant Resour.*, **2011**, 1(1), 75-80.
- ¹⁰Prabakaran, R. and Arivoli, S., *Arch. Appl. Sci. Res.*, **2011**, 3(6), 218-232.
- ¹¹Ahamed, A. J. and Begum, A. S., *Arch. Appl. Sci. Res.*, **2012**, 4(3), 1532-1539.
- ¹²Shelke, R. S., Bharad, J. V., Madje, B. R. and Ubale, M. B., *Arch. Appl. Sci. Res.*, **2010**, 2(3), 260-266.
- ¹³Bailey, S. E., Olin, T. J., Bricka, R. M. and Adrian, D. D., *Water Res.*, **1999**, 33, 2469–2479.
- ¹⁴Vempati, R. K., Musthyala, S. C., Molle, Y. A., and Cocke, D. L., *Fuel*, **1995**, 74(11), 1722-1725.
- ¹⁵Srinivasan, K., Balasubramaniam, N. and Ramakrishna, T. V., *Indian J. Environ. Health*, **1998**, 30(4), 376-387.
- ¹⁶Ayub, S., Ali, S. I., and Khan, N. A., *Environ. Pollut. Control J.*, **2001**, 4(4), 34 – 38.
- ¹⁷Guo Y., Qi, S., Yang, S., Yu, K., Wang, Z., and Xu, H., *Mater. Chem. Phys.*, **2002**, 78, 132–137.
- ¹⁸Daifullah A. A. M., Girgis, B. S., and Gad, H. M. H, *Mater. Lett.*, **2003**, 57, 1723–1731.

- ¹⁹Wong, K. K., Lee, C. K., Low, K. S. and Haron, M. J., *Chemosphere*, **2003**, *50*, 23-28.
- ²⁰Ajmal, M., Rao, R. A. K., Anwar, S., Ahmad, J. and Ahmad, R., *Bioresour. Tech.*, 2003, *86*, 147-149.
- ²¹Subramaniam P., Khan N.A., and Ibrahim S., *Rice husk as an adsorbent for heavy metal*. Proc. Int. Conf. Water Wastewater (ASIAWATER), Kuala Lumpur, Malaysia **2004**.
- ²²Elham, A., Hossein, T., Mahnoosh, H., *J. Appl. Sci. Environ. Manage. JASEM* **2010**, 1119-8362 .
- ²³Nhapi, I., Banadda, N., Murenzi R., Sekomo, C. B. and Wali, U. G., *The Open Environ. Eng. J.*, **2011**, *4*, 170-180.
- ²⁴Ebrahim, S. E. and Mohammed, S. Y., *J. Eng.*, **2012**, *7(18)*, 868-875.
- ²⁵Singh, S. R. and Singh, A. P., *Int. J. Environ. Res.*, **2012**, *6(4)*, 917-924.
- ²⁶Leyva-Ramos, R., Bernal-Jacome, L. A. and Acosta-Rodriguez, I., *Sep. Purif. Technol.*, **2005**, *45*, 41-49.
- ²⁷Khan, M. N. and Wahab, M. F., *J. Hazard. Mater. B*, **2006**, *141*, 237-244 .
- ²⁸Stefan, D. S., Stefan, M. and Vaireanu, D. I., *Rev. Roum. Chim.*, **2006**, *51(6)*, 541-546.
- ²⁹Akporhonor, E. E. and Egwaikhide, P. A., *Sci. Res. Essay*, **2007**, *2(4)*, 132-134.
- ³⁰Igwe, J. C. and Abia, A. A., *Int. J. Phys. Sci.*, **2007**, *2(5)*, 119-127.
- ³¹Sallau, A. B., Aliyu, S., Ukuwa, S., *Int. J. Env. Bioener.*, **2012**, *4(3)*, 131-140.
- ³²Muthusamy, P., Murugan, S. and Smitha, M., *ISCA J. Biol. Sci.*, **2012**, *1(2)*, 7-11.
- ³³Ahalya1, N. Kanamadi R. D. and Ramachandra, T. V., *J. Environ. Biol.*, **2007**, *28(4)*, 765-769.
- ³⁴Karunakaran, K., Thamilarasu, P., *Arch. Appl. Sci. Res.*, **2010**, *2(1)*, 176-186.
- ³⁵Thamilarasu, P. Sivakumar P. and Karunakar, K., *Indian J. Chem. Technol.*, **2011**, *18*, 414-420.
- ³⁶Quek, S. Y., Wase, D. A. J. and Forster, C. F., *Water S.A.*, **1998**, *24(3)*, 251-256.
- ³⁷Kadirvelu, K., Kavipriya, M., Karthika, C., Radhika, M., Vennilamani N. and Pattabhi, S., *Bioresour. Tech.*, **2003**, *87*, 129-132.
- ³⁸Demirbas, E., Kobya, M., Senturk, E., Ozkan, T., *Water SA*, **2004**, *30(4)*, 533-540.
- ³⁹Hema Krishna, R., Swamy, A. V. V. S., *Chem. Sci. J.*, **2011**, 1-13.
- ⁴⁰Banerjee, K., Ramesh, S. T., Gandhimathi, R., Nidheesh, P. V., and Bharathi, K. S., *Iran. J. Energy Environ.*, **2012**, *3(2)*, 143-156.
- ⁴¹Low, K. S., Lee, C. K., Liew, S. C., *Process Biochem.*, **2000**, *36*, 59-64.
- ⁴²Jeon, C., Park, K. H., *Water Res.*, 2005, *36*, 3938-3944.
- ⁴³Halim S. H. A., Shehata, A. M. A. and El-Shahat, M. F., *Water Res.*, **2003**, *37*, 1678-1683.
- ⁴⁴Tan, W. T., Ooi, S. T., and Lee, C. K., *Environ. Technol.*, **1993**, *14*, 277-282.
- ⁴⁵Nasim, A. K., Shaliza, I. and Piarapakaran, S., *Malaysian J. Sci.*, **2004**, *23*, 43-51.
- ⁴⁶Kumar, U., *Sci. Res. Essay*, **2006**, *1(2)*, 33-37.
- ⁴⁷Wan Ngah W. S., Hanafiah, M. A. K. M., *Bioresour. Technol.*, **2008**, *99*, 3935-3948.

Received: 29.04.2013.

Accepted: 03.07.2013.



CORRELATIONS OF SOLUTE PARTITIONING AND ENTHALPIES OF SOLVATION FOR ORGANIC SOLUTES IN IONIC LIQUIDS USING A TEMPERATURE INDEPENDENT FREE ENERGY RELATIONSHIP

Timothy W. Stephens^a, Bria Willis^a, Nishu Dabadge^a, Amy Tian^a, William E. Acree, Jr.^a,

Michael H. Abraham^b

Keywords: partition coefficient, 1-hexyl-3-methylimidazolium tetracyanoborate, 1-(2-methoxyethyl)-1-methylpiperidinium bis(trifluoromethylsulfonyl)imide and 1-(2-methoxyethyl)-1-methylpyrrolidinium bis(trifluoromethylsulfonyl)imide, ionic liquids, temperature independence, linear free energy relationships, enthalpies of solvation.

Experimental data have been collected from the published literature for the gas-to-ionic liquid partition coefficients and molar enthalpies of solvation for over 60 solutes in the ionic liquids 1-hexyl-3-methylimidazolium tetracyanoborate ([MHIm]⁺[B(CN)₄]⁻), 1-(2-methoxyethyl)-1-methylpiperidinium bis(trifluoromethylsulfonyl)imide ([MeoMPip]⁺[Tf₂N]⁻), and 1-(2-methoxyethyl)-1-methylpyrrolidinium bis(trifluoromethylsulfonyl)imide ([MeoMPyr]⁺[Tf₂N]⁻) over the temperature range 318.15 K to 368.15 K. The logarithm of the gas-to-ionic liquid partition coefficient, $\log K_L$, have been correlated to a temperature independent free energy relationship utilizing known Abraham solvation parameters. The resulting mathematical expressions describe the experimental $\log K_L$ values to within a standard deviation of 0.077 log units or less and ΔH_{solv} to within a standard deviation of 1.344 kJ mol⁻¹ or less.

* Corresponding Authors

Fax: 940-565-4318

E-Mail: acree@unt.edu

[a] Department of Chemistry, 1155 Union Circle Drive #305070, University of North Texas, Denton, TX 76203-5017 (USA)

[b] Department of Chemistry, University College London, 20 Gordon Street, London, WC1H 0AJ (UK)

Introduction

For over twenty years, room-temperature ionic liquids (RTILs) have been used in an ever growing area of study with regards to chemical separations. One of the most prominent features of ionic liquids is the ability to fine-tune and target specific solubilizing effects based on the choice of cation or anion, or even the side chains on the cation. The RTILs 1-(2-methoxyethyl)-1-methylpiperidinium bis(trifluoromethylsulfonyl)imide ([MeoMPip]⁺[Tf₂N]⁻), and 1-(2-methoxyethyl)-1-methylpyrrolidinium bis(trifluoromethylsulfonyl)imide ([MeoMPyr]⁺[Tf₂N]⁻), specifically the 2-methoxyethyl side chain, have both been shown to be particularly good at separations involving polar/non-polar azeotropic mixtures,^{1,2} while the RTIL 1-hexyl-3-methylimidazolium tetracyanoborate ([MHIm]⁺[B(CN)₄]⁻) has been shown to be very selective for aromatic and aliphatic hydrocarbons.³ RTILs that contain the anion [Tf₂N]⁻ have been shown to be completely immiscible with water while RTILs containing the cation [MHIm]⁺ have been shown to be partly soluble in water. These solubilizing characteristics allow for RTILs of this type to be used in liquid-liquid extractions between the RTIL and aqueous solution.

To date, the Abraham Solvation Parameter Model has been used to predict various solvation processes in a variety of types of solvent systems, including: the partitioning of solutes in polar organic solvents,⁴⁻⁹ the partitioning of solutes in non-polar organic solvents,¹⁰⁻¹² the partitioning

within micelles,^{13,14} solute partitioning within important biological systems,¹⁵⁻¹⁷ toxicity in aquatic organisms,¹⁸⁻²¹ solute partitioning in RTILs,²²⁻²⁷ and solute partitioning in binary solvent systems.²⁸ The Abraham Model can be written to predict the logarithm of the gas-to-solvent partition coefficient ($\log K_L$) and the logarithm of the water-to-solvent partition coefficient $\log P$, as shown in Eqns. 1 and 2 respectively. The Abraham Model has also been applied in the prediction of enthalpies of solvation,²⁹⁻³⁴ as shown in Eqn. 3.

$$\log K_L = c_K + e_K E + s_K S + a_K A + b_K B + l_K L \quad (1)$$

$$\log P = c_P + e_P E + s_P S + a_P A + b_P B + v_P V \quad (2)$$

$$\Delta H_{\text{solv}} = c_{H,\text{solv}} + e_{H,\text{solv}} E + s_{H,\text{solv}} S + a_{H,\text{solv}} A + b_{H,\text{solv}} B + l_{H,\text{solv}} L \quad (3)$$

Within the Abraham Model, the independent values are defined as solute-specific descriptor terms. These terms are defined as: E is the solute's excess molar refraction in units of 0.1 cm² mol⁻¹,³⁵ S is a measure of the solute's combined polarizability and dipolarity,³⁶ A is a measure of the solute's overall hydrogen-bond acidity,³⁷ B is a measure of the solute's overall hydrogen-bond basicity,³⁸ V is the solute's characteristic McGowan's molecular volume in units of 0.01 cm³ mol⁻¹,³⁹ and L is the logarithm of the solute's gas-to-hexadecane partition coefficient at 298 K.⁴⁰ The calculated coefficients c_K , e_K , s_K , a_K , b_K , l_K , c_P , e_P , s_P , a_P , b_P , v_P , $c_{H,\text{solv}}$, $e_{H,\text{solv}}$, $s_{H,\text{solv}}$, $a_{H,\text{solv}}$, $b_{H,\text{solv}}$, $l_{H,\text{solv}}$ have the following defined physico-chemical properties: e is a

measure of the solvent system's interactions with the solute's π - and non-bonding electrons, s is a measure of the solvent system's combined polarizability and dipolarity, a is a measure of the solvent system's hydrogen-bond basicity and is complimentary to the solute's hydrogen-bond acidity, b is a measure of the solvent system's hydrogen-bond acidity and is complimentary to the solute's hydrogen-bond basicity, and l and v are measures of general dispersion forces necessary to create a cavity in the solvent system for solubilizing the solute. When the solvent coefficients are combined with their complimentary descriptors, the resulting product can be used to characterize that particular solute-solvent interaction. For the partitioning between two condensed phases, the coefficient values can be used to indicate the differences between the two phases of that particular property.

Sprunger, et al.⁴¹⁻⁴³ have expanded the Abraham Model so that the gas-to-RTIL partition coefficient can be predicted based on ion-specific coefficients for individual cations and anions, as shown in Eqn. 4. Utilizing the ion-specific coefficients, RTILs can be synthesized that take advantage of specific properties that may be attractive for specific separations.

$$\log K_L = (c_{K,\text{cation}} + c_{K,\text{anion}}) + (e_{K,\text{cation}} + e_{K,\text{anion}}) E + (s_{K,\text{cation}} + s_{K,\text{anion}}) S + (a_{K,\text{cation}} + a_{K,\text{anion}}) A + (b_{K,\text{cation}} + b_{K,\text{anion}}) B + (l_{K,\text{cation}} + l_{K,\text{anion}}) L \quad (4)$$

Mintz, et al.⁴⁴ and Sprunger, et al.⁴⁵ describe a basis for incorporating temperature dependent terms into the Abraham Model that comes from the Gibbs' Free Energy Relationship, Eqn. 5, and the relation between ΔG_{solv} and K_L , Eqn. 6, where R is the universal gas constant in units of $\text{J mol}^{-1} \text{K}^{-1}$, T is the temperature of the system in Kelvin, and K_L is the gas-to-solvent partition coefficient.

$$\Delta G_{\text{solv}} = \Delta H_{\text{solv}} - T \Delta S_{\text{solv}} \quad (5)$$

$$\Delta G_{\text{solv}} = -RT \ln K_L \quad (6)$$

Converting Eqn. 6 from base e to base 10 so that the results correspond to previous Abraham Model correlations, yields Eqn. 7.

$$\Delta G_{\text{solv}} = -2.303 RT \log K_L \quad (7)$$

Using Eqns. 1, 3, 5 and 7, the Abraham Model can be applied to the prediction of ΔS_{solv} , expressed as Eqn. 8.

$$\Delta S_{\text{solv}} = c_{S,\text{solv}} + e_{S,\text{solv}} E + s_{S,\text{solv}} S + a_{S,\text{solv}} A + b_{S,\text{solv}} B + l_{S,\text{solv}} L \quad (8)$$

Eqns. 3, 5, 7, and 8 can now be combined and rewritten as Eqn. 9, and simplified into Eqn. 10.

$$-2.303 RT \log K_L = c_{H,\text{solv}} + e_{H,\text{solv}} E + s_{H,\text{solv}} S + a_{H,\text{solv}} A + b_{H,\text{solv}} B + l_{H,\text{solv}} L - T (c_{S,\text{solv}} + e_{S,\text{solv}} E + s_{S,\text{solv}} S + a_{S,\text{solv}} A + b_{S,\text{solv}} B + l_{S,\text{solv}} L) \quad (9)$$

$$\log K = \left(c_S - \frac{c_H}{T} \right) \frac{1}{2.303R} + \left(e_S - \frac{e_H}{T} \right) \frac{E}{2.303R} + \left(s_S - \frac{s_H}{T} \right) \frac{S}{2.303R} + \left(a_S - \frac{a_H}{T} \right) \frac{A}{2.303R} + \left(b_S - \frac{b_H}{T} \right) \frac{B}{2.303R} + \left(l_S - \frac{l_H}{T} \right) \frac{L}{2.303R} \quad (10)$$

Because of the relationship between $\log K_L$ and ΔH_{solv} , the c_H , e_H , s_H , a_H , b_H , and l_H coefficients from Eqn. 10 should yield the same coefficients as for Eqn. 3.

Data sets and computation methodology

Gas-to-solvent partition coefficients K_L were found for the RTILs 1-hexyl-3-methylimidazolium tetracyanoborate ($[\text{MHIIm}]^+[\text{B}(\text{CN})_4]^-$),³ 1-(2-methoxyethyl)-1-methylpiperidinium bis(trifluoromethylsulfonyl)imide ($[\text{MeoeMPip}]^+[\text{Tf}_2\text{N}]^-$),² and 1-(2-methoxyethyl)-1-methylpyrrolidinium bis(trifluoromethylsulfonyl)imide ($[\text{MeoeMPyrr}]^+[\text{Tf}_2\text{N}]^-$)¹ by performing a search of the chemical literature. All of the partition coefficients were converted to $\log K_L$ and tabulated with the necessary solute descriptors in a 12 column matrix. Enthalpies of solvation were calculated using the relationship given in Eqn. 11 and tabulated with the necessary solute descriptors into a 5 column matrix. A linear regression was performed on each matrix using the statistical software program SPSS 20.0. For the $\log K_L$ correlation, the linear regression was forced through the origin. For the ΔH_{solv} correlation, the linear regression was not forced through the origin.

$$\Delta H_{\text{solv}} = -2.303 R [\text{d} \log K_L / \text{d}(1/T)] \quad (11)$$

Table 1 lists all solute descriptors used for the analysis of the three RTILs. The solute descriptors used came from a database that the authors have compiled and were initially obtained using experimental data such as water-to-solvent partition coefficients, gas-to-solvent partition coefficients, solubility, and chromatographic data. Numerical values for the descriptors used in the analysis of the three ionic liquids cover the same area of predictive space, with values for each descriptor ranging from: $E = -0.063$ to $E = 0.851$, $S = 0.000$ to $S = 0.950$, $A = 0.000$ to $A = 0.820$, $B = 0.000$ to $B = 0.640$, and $L = 0.260$ to $L = 4.686$. The solutes used in each correlation show a wide range of functionality as well as non-polar and polar characteristics. For all correlations, the authors report the N (number of data points), R^2 (square of the correlation coefficient), F (Fisher's F-Statistic), and SD (standard deviation).

Table 1. Solute descriptors used in the analyses

| Solute | <i>E</i> | <i>S</i> | <i>A</i> | <i>B</i> | <i>L</i> |
|---------------------------------|----------|----------|----------|----------|----------|
| Pentane | 0.000 | 0.000 | 0.000 | 0.000 | 2.162 |
| Hexane | 0.000 | 0.000 | 0.000 | 0.000 | 2.668 |
| 3-Methylpentane | 0.000 | 0.000 | 0.000 | 0.000 | 2.581 |
| 2,2-Dimethylbutane | 0.000 | 0.000 | 0.000 | 0.000 | 2.352 |
| Heptane | 0.000 | 0.000 | 0.000 | 0.000 | 3.173 |
| Octane | 0.000 | 0.000 | 0.000 | 0.000 | 3.677 |
| 2,2,4-trimethylpentane | 0.000 | 0.000 | 0.000 | 0.000 | 3.106 |
| Nonane | 0.000 | 0.000 | 0.000 | 0.000 | 4.182 |
| Decane | 0.000 | 0.000 | 0.000 | 0.000 | 4.686 |
| Cyclopentane | 0.263 | 0.100 | 0.000 | 0.000 | 2.477 |
| Cyclohexane | 0.310 | 0.100 | 0.000 | 0.000 | 2.964 |
| Methylcyclohexane | 0.244 | 0.060 | 0.000 | 0.000 | 3.319 |
| Cycloheptane | 0.350 | 0.100 | 0.000 | 0.000 | 3.704 |
| Cyclooctane | 0.413 | 0.100 | 0.000 | 0.000 | 4.329 |
| Pent-1-ene | 0.093 | 0.080 | 0.000 | 0.070 | 2.047 |
| Hex-1-ene | 0.080 | 0.080 | 0.000 | 0.070 | 2.572 |
| Cyclohexene | 0.395 | 0.280 | 0.000 | 0.090 | 2.952 |
| Hept-1-ene | 0.092 | 0.080 | 0.000 | 0.070 | 3.063 |
| Oct-1-ene | 0.090 | 0.080 | 0.000 | 0.070 | 3.568 |
| Dec-1-ene | 0.093 | 0.080 | 0.000 | 0.070 | 4.554 |
| Hex-1-yne | 0.166 | 0.220 | 0.100 | 0.120 | 2.510 |
| Hept-1-yne | 0.160 | 0.230 | 0.090 | 0.100 | 3.000 |
| Oct-1-yne | 0.155 | 0.220 | 0.090 | 0.100 | 3.521 |
| Benzene | 0.610 | 0.520 | 0.000 | 0.140 | 2.786 |
| Toluene | 0.601 | 0.520 | 0.000 | 0.140 | 3.325 |
| Ethylbenzene | 0.613 | 0.510 | 0.000 | 0.150 | 3.778 |
| <i>o</i> -Xylene | 0.663 | 0.560 | 0.000 | 0.160 | 3.939 |
| <i>m</i> -Xylene | 0.623 | 0.520 | 0.000 | 0.160 | 3.839 |
| <i>p</i> -Xylene | 0.613 | 0.520 | 0.000 | 0.160 | 3.839 |
| Styrene | 0.849 | 0.650 | 0.000 | 0.160 | 3.856 |
| α -Methylstyrene | 0.851 | 0.640 | 0.000 | 0.190 | 4.290 |
| Thiophene | 0.687 | 0.570 | 0.000 | 0.150 | 2.819 |
| Methanol | 0.278 | 0.440 | 0.430 | 0.470 | 0.970 |
| Ethanol | 0.246 | 0.420 | 0.370 | 0.480 | 1.485 |
| Propan-1-ol | 0.236 | 0.420 | 0.370 | 0.480 | 2.031 |
| Propan-2-ol | 0.212 | 0.360 | 0.330 | 0.560 | 1.764 |
| Butan-1-ol | 0.224 | 0.420 | 0.370 | 0.480 | 2.601 |
| Butan-2-ol | 0.217 | 0.360 | 0.330 | 0.560 | 2.338 |
| 2-Methyl-1-propanol | 0.217 | 0.390 | 0.370 | 0.480 | 2.413 |
| <i>tert</i> -Butanol | 0.180 | 0.300 | 0.310 | 0.600 | 1.963 |
| Water | 0.000 | 0.600 | 0.590 | 0.460 | 0.245 |
| Acetic acid | 0.265 | 0.640 | 0.620 | 0.440 | 1.816 |
| Tetrahydrofuran | 0.289 | 0.520 | 0.000 | 0.480 | 2.636 |
| 1,4-Dioxane | 0.329 | 0.750 | 0.000 | 0.640 | 2.892 |
| <i>tert</i> -Butyl methyl ether | 0.024 | 0.220 | 0.000 | 0.550 | 2.372 |
| <i>tert</i> -Butyl ethyl ether | -0.020 | 0.160 | 0.000 | 0.600 | 2.720 |
| <i>tert</i> -Amyl methyl ether | 0.050 | 0.210 | 0.000 | 0.600 | 2.916 |
| Diethyl ether | 0.041 | 0.250 | 0.000 | 0.450 | 2.015 |
| Dipropyl ether | 0.008 | 0.250 | 0.000 | 0.450 | 2.954 |
| Diisopropyl ether | -0.063 | 0.170 | 0.000 | 0.570 | 2.501 |
| Dibutyl ether | 0.000 | 0.250 | 0.000 | 0.450 | 3.924 |
| Acetone | 0.179 | 0.700 | 0.040 | 0.490 | 1.696 |
| Pentan-2-one | 0.143 | 0.680 | 0.000 | 0.510 | 2.755 |
| Pentan-3-one | 0.154 | 0.660 | 0.000 | 0.510 | 2.811 |
| Methyl acetate | 0.142 | 0.640 | 0.000 | 0.450 | 1.911 |
| Ethyl acetate | 0.106 | 0.620 | 0.000 | 0.450 | 2.314 |

| | | | | | |
|-------------------|-------|-------|-------|-------|-------|
| Methyl propanoate | 0.128 | 0.600 | 0.000 | 0.450 | 2.431 |
| Methyl butanoate | 0.106 | 0.600 | 0.000 | 0.450 | 2.893 |
| Butanal | 0.187 | 0.650 | 0.000 | 0.450 | 2.270 |
| Acetonitrile | 0.237 | 0.900 | 0.070 | 0.320 | 1.739 |
| Pyridine | 0.631 | 0.840 | 0.000 | 0.520 | 3.022 |
| 1-Nitropropane | 0.242 | 0.950 | 0.000 | 0.310 | 2.894 |

RESULTS AND DISCUSSION

Values for $\log K_L$ and ΔH_{solv} have been assembled and tabulated in Table 2 for the partitioning of 61 solutes in ([MHIm]⁺[B(CN)₄]⁻) over the temperature range of 318.15 K to 368.15 K. A regression analysis of the entire data set listed in Table 2 yielded Eqns. 12 and 13. Figure 1 is presented as a comparison of the experimental $\log K_L$ values from Table 2 and the calculated $\log K_L$ from Eqn. 12.

$$\log K_L = -7.641(0.471)/(2.303R) + [16.206(10.807) - (5233(3708)/T)][E/(2.303R)] + [-15.729(10.624) - (-19911(3644)/T)][S/(2.303R)] + [-37.872(10.466) - (25751(3587)/T)][A/(2.303R)] + [-8.254(10.711) - (-4842(3668)/T)][B/(2.303R)] + [-14.280(0.935) - (-8336(316)/T)][L/(2.303R)] \quad (12)$$

$$N = 361, R^2 = 0.999, F = 25965, SD = 0.077 \text{ log units}$$

$$\Delta H_{\text{solv}} = 4098(1159) E - 17444(1147) S - 24979(1142) A - 6532(1181) B - 8313(104) L \quad (13)$$

$$N = 61, R^2 = 0.998, F = 6880, SD = 1344 \text{ J mol}^{-1}$$

For these correlations, the ΔH_{solv} data was converted from kJ mol⁻¹ to J mol⁻¹ so that a comparison of the c_H , e_H , s_H , a_H , b_H and l_H coefficients from Eqn. 12 could be made to the $c_{H,\text{solv}}$, $e_{H,\text{solv}}$, $s_{H,\text{solv}}$, $a_{H,\text{solv}}$, $b_{H,\text{solv}}$ and $l_{H,\text{solv}}$ coefficients from Eqn. 13. During the analysis of the $\log K_L$ data, it was found that the c_S coefficient had a linear covariance and was thus excluded from the regression. When the c_H term from the original $\log K_L$ correlation was compared to the original $c_{H,\text{solv}}$ term from the original ΔH_{solv} correlation, the two terms were not in agreement with each other. Therefore, a new regression was calculated for $\log K_L$ which excluded the c_H term, presented as Eqn. 12, and a new regression was calculated for ΔH_{solv} which excluded the $c_{H,\text{solv}}$ term, presented as Eqn. 13.

Eqn. 14 was derived by writing the e_H , s_H , a_H , b_H and l_H coefficients from Eqn. 12 to predict ΔH_{solv} .

$$\Delta H_{\text{solv}} = 5233(3708) E - 19911(3644) S - 25751(3587) A -$$

$$4842(3688) B - 8336(316) L \quad (14)$$

$$SD = 1424 \text{ J mol}^{-1}, AAE = 1064 \text{ J mol}^{-1}, AE = 192 \text{ J mol}^{-1}$$

Reported are the SD , AAE (absolute average error), and AE (average error) for the prediction of ΔH_{solv} based on Eqn. 14. As shown, Eqn. 14 predicts ΔH_{solv} to within a similar standard deviation as Eqn. 13. The very low AE and AAE values show very little bias between using Eqn. 13 or Eqn. 14 to predict ΔH_{solv} . Eqn. 14 also illustrates that the e_{H} , s_{H} , a_{H} , b_{H} and l_{H} coefficients from Eqn. 12 and the $e_{\text{H,solv}}$, $s_{\text{H,solv}}$, $a_{\text{H,solv}}$, $b_{\text{H,solv}}$ and $l_{\text{H,solv}}$ coefficients from Eqn. 13 are individually within the statistical error of their respective counterparts.

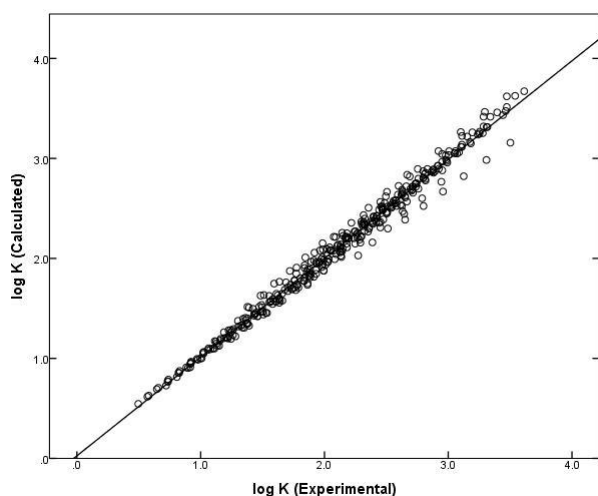


Figure 1. Graph of experimental logarithm of gas-to- $[\text{MHIm}]^+[\text{B}(\text{CN})_4]^-$ partition coefficient ($\log K_L$) versus calculated $\log K_L$ based on Eq. 12.

As an informational note one could develop Abraham model correlations for each individual temperature. As noted by Mintz et al.⁴⁴ and Sprunger et al.⁴⁵ offers over such temperature-specific correlations is that one can develop correlations for more partitioning process and for more ionic liquid solvents. For example, let's assume that one was able to find $\log K_L$ data 20 solutes in $([\text{MHIm}]^+[\text{B}(\text{CN})_4]^-)$ at 298 K, $\log K_L$ data for a different set of 20 solutes in $([\text{MHIm}]^+[\text{B}(\text{CN})_4]^-)$ at 318.15 K, and $\log K_L$ data for a third set of 20 different solutes in $([\text{MHIm}]^+[\text{B}(\text{CN})_4]^-)$ at 368 K. There would be insufficient experimental data to develop a meaningful Abraham model correlation at any of the three temperatures mentioned. However, by pooling the 60 $\log K_L$ values for $([\text{MHIm}]^+[\text{B}(\text{CN})_4]^-)$ into a single dataset, one could develop a predictive correlation based on Eqn. 10. Such predictions would not be possible with Eqn. 1 which requires that all of the experimental data be at the same temperature.

To determine the predictability of Eqn. 12, the data in Table 2 was analyzed using a training set and test analysis. In this method of analysis, the complete data set is randomly split in half and divided into a training set and a test set. In the event that the complete data set has an odd number of data points, the extra data point is included in the training set. A linear regression is then performed on the training set and a new training correlation is calculated. This training

correlation is then used to predict the values in the test set, and the SD , AAE , and AE are reported. Eqn. 15 is the resultant correlation from randomly splitting half of the $\log K_L$ data reported in Table 2. Using Eqn. 15 to predict the values in the test set yielded a $SD = 0.083$ log units, $AAE = 0.055$, and $AE = -0.004$. The very small difference in the coefficient values calculated between the training set and parent set show that the training set compounds and temperatures are representative of the parent compounds and temperatures. The low AE value shows very little bias between using Eqns. 12 and 15.

$$\begin{aligned} \log K_L = & -7.699(0.653)/(2,303 R) + \\ & [15.446(14.979) - (4914(5133)/T)] [E/(2.303 R)] + \\ & [-14.226(15.704) - (-19294(5388)/T)] [S/(2.303 R)] + \\ & [-58.028(17.935) - (-33067(6232)/T)] [A/(2.303 R)] + \\ & [-9.661(15.007) - (-5405(5189)/T)] [B/(2.303 R)] + \\ & [-14.012(1.297) - (-8245(445)/T)] [L/(2.303 R)] \quad (15) \end{aligned}$$

$$N = 181, R^2 = 0.999, F = 13690, SD = 0.074 \text{ log units}$$

Values for $\log K_L$ and ΔH_{solv} have been assembled and tabulated in Table 3 for the partitioning of 61 solutes in $([\text{MeoeMPip}]^+[\text{Tf}_2\text{N}]^-)$ over the temperature range of 318.15 K to 368.15 K. A regression analysis of the entire data set listed in Table 3 yielded Eqns. 16 and 17. Figure 2 is presented as a comparison of the experimental $\log K_L$ values from Table 3 and the calculated $\log K_L$ from Eqn. 16.

$$\begin{aligned} \log K_L = & -10.878(0.387)/(2.303 R) + \\ & [0.536(6.437) - (-14440(2202)/T)] [S/(2.303 R)] + \\ & [-29.947(9.729) - (-23020(3325)/T)] [A/(2.303 R)] + \\ & [-17.927(7.920) - (-7332(2707)/T)] [B/(2.303 R)] + \\ & [-12.721(0.706) - (-7802(239)/T)] [L/(2.303 R)] \quad (16) \end{aligned}$$

$$N = 365, R^2 = 0.999, F = 31686, SD = 0.069 \text{ log units}$$

$$\begin{aligned} \Delta H_{\text{solv}} = & -14486(805) S - 22955(1223) A - \\ & 7248(991) B - 7791(88) L \quad (17) \end{aligned}$$

$$N = 61, R^2 = 0.998, F = 7868, SD = 1335 \text{ J/mol}$$

For these correlations, the ΔH_{solv} data was converted from kJ mol^{-1} to J mol^{-1} so that a comparison of the c_{H} , e_{H} , s_{H} , a_{H} , b_{H} and l_{H} coefficients from Eqn. 16 could be made to the $c_{\text{H,solv}}$, $e_{\text{H,solv}}$, $s_{\text{H,solv}}$, $a_{\text{H,solv}}$, $b_{\text{H,solv}}$ and $l_{\text{H,solv}}$ coefficients from Eqn. 17. Coincidentally, during the analysis of the $\log K_L$ data for $([\text{MeoeMPip}]^+[\text{Tf}_2\text{N}]^-)$, it was found that the c_{S} coefficient was found to have a linear covariance and was thus excluded from the regression. When the c_{H} term from

the original $\log K_L$ correlation was compared to the original $c_{H,solv}$ term from the original ΔH_{solv} correlation, the two terms were also not in agreement with each other, as occurred for $([MHIm]^+[B(CN)_4]^-)$. Further analysis of the correlation for $\log K_L$ showed that the e_S and e_H terms were very small, 9.267(8.538) and 1986(2921) respectively. These terms were subsequently set equal to zero and the regression was performed once again. Eqn. 16 is the resultant correlation obtained by removing the c_H , e_S and e_H terms and Eqn. 17 is the resultant correlation obtained when the $c_{H,solv}$ and $e_{H,solv}$ terms are removed.

Eqn. 18 was derived by writing the s_H , a_H , b_H and l_H coefficients from Eqn. 16 to predict ΔH_{solv} .

$$\Delta H_{solv} = -14440(2202) S - 23020(3325) A - 7332(2707) B - 7802(239) L \quad (18)$$

$$SD = 1335 \text{ J mol}^{-1}, AAE = 1011 \text{ J mol}^{-1}, AE = -93 \text{ J mol}^{-1}.$$

Reported are the SD , AAE , and AE for the prediction of ΔH_{solv} based on Eqn. 18. As shown, Eqn. 18 predicts ΔH_{solv} to within the same standard deviation as Eqn. 17. The very low AE and AAE values show very little bias between using Eqn. 17 or Eqn. 18 to predict ΔH_{solv} . Eqn. 18 also illustrates that the s_H , a_H , b_H and l_H coefficients from Eqn. 16 and the $s_{H,solv}$, $a_{H,solv}$, $b_{H,solv}$ and $l_{H,solv}$ coefficients from Eqn. 17 are individually within the statistical error of their respective counterparts.

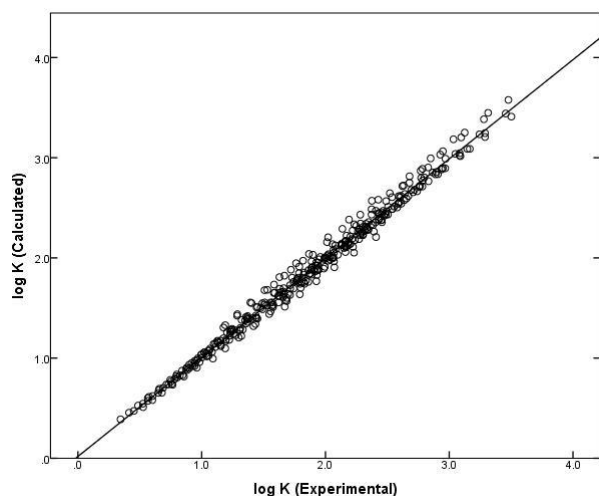


Figure 2. Graph of experimental logarithm of gas-to- $([MeoeMPip]^+[Tf_2N]^-)$ partition coefficient ($\log K_L$) versus calculated $\log K_L$ based on Eqn. 16.

To determine the predictability of Eqn. 16, the data in Table 3 was also analyzed using a training set and test analysis. Eqn. 19 is the resultant correlation from randomly splitting half of the $\log K_L$ data reported in Table 3. Using Eqn. 19 to predict the values in the test set yielded a $SD = 0.071$ log units, $AAE = 0.053$, and $AE = 0.002$.

The very small difference in the coefficient values calculated between the training set and parent set show that the training set compounds and temperatures are representative of the parent compounds and temperatures. The low AE value shows very little bias between using Eqns. 16 and 19.

$$\begin{aligned} \log K_L = & -10.992(0.562)/(2.303 R) + \\ & [5.061(9.173) - (-12834(3131)/T)] [S/(2.303 R)] + \\ & [-16.206(14.399) - (-18341(4871)/T)] [A/(2.303 R)] + \\ & [-27.181(12.155) - (-10547(4150)/T)] [B/(2.303 R)] + \\ & [-12.610(0.926) - (-7777(307)/T)] [L/(2.303 R)] \end{aligned} \quad (19)$$

$$N = 183, R^2 = 0.999, F = 17102, SD = 0.068 \text{ log units}$$

It should be noted that Marciniak and Wlazło² also correlated the $\log K_L$ data for $([MeoeMPip]^+[Tf_2N]^-)$ in terms of the Abraham model. The authors developed temperature-specific correlations in the form of Eqn. 1 for each of the six temperatures studied. A total of 36 curve-fit equation coefficients were needed to describe the 365 experimental data points to an average standard deviation of $SD = 0.059$ log units. Our method, Eqn. 16, has only nine curve-fit equation coefficients and describes the 365 $\log K_L$ values to within $SD = 0.069$ log units. Very little loss in predictive ability resulted from our method of combining all 365 experimental values into a single regression analysis.

Values for $\log K_L$ and ΔH_{solv} have been assembled and tabulated in Table 4 for the partitioning of 61 solutes in $([MeoeMPyr]^+[Tf_2N]^-)$ over the temperature range of 318.15 K to 368.15 K. A regression analysis of the entire data set listed in Table 4 yielded Eqns. 20 and 21. Figure 3 is presented as a comparison of the experimental $\log K_L$ values from Table 4 and the calculated $\log K_L$ from Eqn. 20.

$$\begin{aligned} \log K_L = & -10.033(0.375)/(2.303 R) + \\ & [10.075(8.499) - (2557(2905)/T)] [E/(2.303 R)] + \\ & [-7.117(8.475) - (-16471(2897)/T)] [S/(2.303 R)] + \\ & [-33.881(9.165) - (-24144(3132)/T)] [A/(2.303 R)] + \\ & [-12.474(8.752) - (-6027(2992)/T)] [B/(2.303 R)] + \\ & [-13.508(0.763) - (-7875(258)/T)] [L/(2.303 R)] \end{aligned} \quad (20)$$

$$N = 366, R^2 = 0.999, F = 30869, SD = 0.064 \text{ log units}$$

$$\begin{aligned} \Delta H_{solv} = & -2534(1090) E - 16481(1086) S - \\ & 24066(1175) A - 5998(1123) B - 7856(97) L \end{aligned} \quad (21)$$

$$N = 61, R^2 = 0.998, F = 6976, SD = 1260 \text{ J/mol}$$

For these correlations, the ΔH_{solv} data was converted from kJ mol^{-1} to J mol^{-1} so that a comparison of the c_H , e_H , s_H , a_H , b_H and l_H coefficients from Eqn. 20 could be made to the $c_{H,solv}$, $e_{H,solv}$, $s_{H,solv}$, $a_{H,solv}$, $b_{H,solv}$ and $l_{H,solv}$ coefficients from Eqn. 21. Coincidentally, during the analysis of the $\log K_L$ data for $([MeoeMPyr]^+[Tf_2N]^-)$, it was found that the c_S coefficient was found to have a linear covariance and was

thus excluded from the regression. When the c_H term from the original $\log K_L$ correlation was compared to the original $c_{H,solv}$ term from the original ΔH_{solv} correlation, the two terms were also not in agreement with each other, as occurred for $([MHIm]^+[B(CN)_4]^-)$ and $([MeoEMPIP]^+[Tf_2N]^-)$. Once again, Eqn. 20 is the resultant correlation obtained by removing the c_H term and Eqn. 21 is the resultant correlation obtained when the $c_{H,solv}$ term is removed.

Eqn. 22 was derived by writing the e_H , s_H , a_H , b_H , and l_H coefficients from Eqn. 20 to predict ΔH_{solv} .

$$\Delta H_{solv} = 2557(2905) E - 16471(2897) S -$$

$$24144(3132) A - 6027(2992) B - 7875(258) L \quad (22)$$

$$SD = 1263 \text{ J mol}^{-1}, AAE = 1005 \text{ J mol}^{-1}, AE = -7 \text{ J mol}^{-1}$$

Reported are the SD , AAE , and AE for the prediction of ΔH_{solv} based on Eqn. 22. As shown, Eqn. 22 predicts ΔH_{solv} to within a similar standard deviation as Eqn. 21. The very low AE and AAE values show very little bias between using Eqn. 21 or Eqn. 22 to predict ΔH_{solv} . Eqn. 22 also illustrates that the e_H , s_H , a_H , b_H and l_H coefficients from Eqn. 20 and the $c_{H,solv}$, $e_{H,solv}$, $s_{H,solv}$, $a_{H,solv}$, $b_{H,solv}$ and $l_{H,solv}$ coefficients from Eqn. 21 are individually within the statistical error of their respective counterparts.

Table 2. Logarithm of gas-to- $([MHIm]^+[B(CN)_4]^-)$ partition coefficients at various temperatures and enthalpies of solvation (in kJ mol^{-1})^a

| Solute Temperature, K | $\log K_L$ | | | | | | ΔH_{solv} kJ mol ⁻¹ |
|--------------------------|------------------------------|--------|--------|--------|--------|--------|---|
| | 318.15 | 328.15 | 338.15 | 348.15 | 358.15 | 368.15 | |
| Pentane | 0.917 | 0.820 | 0.732 | 0.645 | 0.569 | 0.496 | -18.887 |
| Hexane | 1.246 | 1.130 | 1.021 | 0.919 | 0.827 | 0.736 | -22.814 |
| 3-Methylpentane | 1.215 | 1.100 | 0.997 | 0.898 | 0.808 | 0.720 | -22.131 |
| 2,2-Dimethylbutane | 1.025 | 0.923 | 0.830 | 0.739 | 0.658 | 0.580 | -19.965 |
| Heptane | 1.567 | 1.431 | 1.305 | 1.188 | 1.079 | 0.977 | -26.423 |
| Octane | 1.884 | 1.728 | 1.583 | 1.446 | 1.322 | 1.204 | -30.448 |
| 2,2,4-Trimethylpentane | 1.491 | 1.362 | 1.241 | 1.124 | 1.021 | 0.922 | -25.547 |
| Nonane | 2.196 | 2.021 | 1.857 | 1.703 | 1.565 | 1.431 | -34.262 |
| Decane | 2.508 | 2.310 | 2.130 | 1.959 | 1.805 | 1.658 | -38.033 |
| Cyclopentane | 1.365 | 1.255 | 1.155 | 1.057 | 0.970 | 0.885 | -21.531 |
| Cyclohexane | 1.679 | 1.555 | 1.439 | 1.332 | 1.228 | 1.134 | -24.481 |
| Methylcyclohexane | 1.840 | 1.704 | 1.581 | 1.459 | 1.350 | 1.246 | -26.650 |
| Cycloheptane | 2.179 | 2.033 | 1.892 | 1.760 | 1.640 | 1.526 | -29.312 |
| Cyclooctane | 2.615 | 2.442 | 2.283 | 2.134 | 1.994 | 1.863 | -33.670 |
| Hex-1-ene | 1.459 | 1.336 | 1.220 | 1.111 | 1.009 | 0.915 | -24.433 |
| Cyclohexene | 1.985 | 1.846 | 1.720 | 1.593 | 1.484 | 1.378 | -27.185 |
| Hept-1-ene | 1.779 | 1.634 | 1.501 | 1.375 | 1.260 | 1.149 | -28.194 |
| Oct-1-ene | 2.093 | 1.930 | 1.777 | 1.633 | 1.504 | 1.380 | -31.974 |
| Dec-1-ene | 2.714 | 2.508 | 2.324 | 2.146 | 1.985 | 1.832 | -39.487 |
| Hex-1-yne | 2.029 | 1.879 | 1.740 | 1.606 | 1.486 | 1.371 | -29.510 |
| Hept-1-yne | 2.352 | 2.182 | 2.025 | 1.873 | 1.736 | 1.607 | -33.403 |
| Oct-1-yne | 2.666 | 2.476 | 2.299 | 2.130 | 1.980 | 1.836 | -37.206 |
| Benzene | 2.629 | 2.471 | 2.320 | 2.182 | 2.053 | 1.931 | -31.295 |
| Toluene | 2.982 | 2.801 | 2.629 | 2.473 | 2.326 | 2.188 | -35.599 |
| Ethylbenzene | 3.252 | 3.053 | 2.866 | 2.695 | 2.534 | 2.384 | -38.901 |
| o-Xylene | 3.464 | 3.254 | 3.058 | 2.879 | 2.710 | 2.553 | -40.820 |
| m-Xylene | 3.316 | 3.110 | 2.919 | 2.744 | 2.579 | 2.425 | -39.887 |
| p-Xylene | 3.310 | 3.103 | 2.915 | 2.737 | 2.574 | 2.420 | -39.850 |
| Styrene | | 3.441 | 3.239 | 3.052 | 2.878 | 2.715 | -41.945 |
| α -Methylstyrene | | 3.614 | 3.395 | 3.195 | 3.007 | 2.831 | -45.191 |
| Methanol | 2.400 | 2.250 | 2.111 | 1.984 | 1.865 | 1.757 | -28.807 |
| Ethanol | 2.582 | 2.418 | 2.267 | 2.127 | 1.994 | 1.874 | -31.737 |
| Propan-1-ol | 2.925 | 2.739 | 2.569 | 2.408 | 2.260 | 2.127 | -35.771 |
| Propan-2-ol | 2.625 | 2.452 | 2.292 | 2.143 | 2.009 | 1.884 | -33.194 |
| Butan-1-ol | 3.279 | 3.072 | 2.880 | 2.703 | 2.542 | 2.391 | -39.749 |
| Butan-2-ol | 2.952 | 2.759 | 2.582 | 2.417 | 2.267 | 2.127 | -36.920 |
| 2-Methyl-1-propanol | 3.087 | 2.891 | 2.708 | 2.539 | 2.384 | 2.238 | -38.043 |
| tert-Butanol | 2.631 | 2.452 | 2.290 | 2.137 | 1.993 | 1.864 | -34.386 |
| Water | 2.668 | 2.505 | 2.356 | 2.217 | 2.090 | 1.964 | -31.458 |
| Acetic acid | | 3.540 | 3.340 | 3.153 | 2.979 | 2.816 | -41.860 |
| Solute | $\log K_L$ | | | | | | ΔH_{solv} |

| Temperature, K | 318.15 | kJ mol ⁻¹ | | 338.15 | 348.15 | 358.15 | 368.15 | kJ mol ⁻¹ |
|-------------------------|--------|----------------------|-------|--------|--------|--------|--------|----------------------|
| Thiophene | 2.759 | 2.593 | 2.441 | 2.301 | 2.167 | 2.045 | | -31.953 |
| Tetrahydrofuran | 2.626 | 2.465 | 2.318 | 2.179 | 2.053 | 1.935 | | -30.959 |
| 1,4-Dioxane | 3.295 | 3.101 | 2.921 | 2.754 | 2.599 | 2.452 | | -37.775 |
| tert-Butyl methyl ether | 1.914 | 1.768 | 1.634 | 1.507 | 1.391 | 1.281 | | -28.346 |
| tert-Butyl ethyl ether | 1.839 | 1.689 | 1.553 | 1.422 | 1.301 | 1.188 | | -29.186 |
| tert-Amyl methyl ether | 2.248 | 2.083 | 1.933 | 1.790 | 1.660 | 1.535 | | -31.894 |
| Diethyl ether | 1.623 | 1.496 | 1.378 | 1.265 | 1.161 | 1.064 | | -25.063 |
| Dipropyl ether | 2.076 | 1.920 | 1.775 | 1.636 | 1.511 | 1.391 | | -30.694 |
| Diisopropyl ether | 1.759 | 1.612 | 1.473 | 1.342 | 1.225 | 1.114 | | -28.922 |
| Dibutyl ether | 2.689 | 2.496 | 2.316 | 2.143 | 1.987 | 1.839 | | -38.115 |
| Acetone | 2.621 | 2.468 | 2.326 | 2.196 | 2.072 | 1.958 | | -29.707 |
| Pentan-2-one | 3.176 | 2.987 | 2.813 | 2.650 | 2.501 | 2.360 | | -36.526 |
| Pentan-3-one | 3.182 | 2.993 | 2.816 | 2.652 | 2.502 | 2.360 | | -36.822 |
| Methyl acetate | 2.456 | 2.299 | 2.152 | 2.021 | 1.893 | 1.773 | | -30.557 |
| Ethyl acetate | 2.661 | 2.486 | 2.326 | 2.182 | 2.041 | 1.915 | | -33.372 |
| Methyl propanoate | 2.735 | 2.559 | 2.394 | 2.243 | 2.104 | 1.975 | | -34.044 |
| Methyl butanoate | 3.002 | 2.810 | 2.630 | 2.467 | 2.316 | 2.173 | | -37.080 |
| Butanal | 2.944 | 2.789 | 2.644 | 2.512 | 2.387 | 2.272 | | -30.120 |
| Acetonitrile | 3.502 | 3.309 | 3.125 | 2.958 | 2.800 | 2.651 | | -38.133 |
| Pyridine | | 3.473 | 3.285 | 3.111 | 2.950 | 2.797 | | -39.012 |
| 1-Nitropropane | | 3.473 | 3.285 | 3.111 | 2.950 | 2.797 | | -39.012 |

^a Experimental gas-to-liquid partition coefficient data taken from Domańska et al.³

Table 3. Logarithm of gas-to-([MeoMPip]⁺[Tf₂N]⁻) partition coefficients at various temperatures and enthalpies of solvation (in kJ mol⁻¹)^a

| Solute Temperature, K | logK _L | | | | | | ΔH _{solv} |
|--------------------------|-------------------------|----------|----------|----------|----------|----------|--------------------------|
| | 318.15 K | 328.15 K | 338.15 K | 348.15 K | 358.15 K | 368.15 K | kJ mol ⁻¹ |
| Pentane | 0.751 | 0.653 | 0.565 | 0.486 | 0.413 | 0.344 | -18.120 |
| Hexane | 1.061 | 0.944 | 0.841 | 0.746 | 0.658 | 0.574 | -21.706 |
| 3-Methylpentane | 1.041 | 0.926 | 0.824 | 0.732 | 0.648 | 0.566 | -21.169 |
| 2,2-Dimethylbutane | 0.884 | 0.780 | 0.688 | 0.604 | 0.525 | 0.452 | -19.293 |
| Heptane | 1.365 | 1.230 | 1.111 | 0.999 | 0.899 | 0.798 | -25.292 |
| Octane | 1.662 | 1.509 | 1.371 | 1.246 | 1.127 | 1.021 | -28.653 |
| 2,2,4-Trimethylpentane | 1.360 | 1.228 | 1.111 | 1.000 | 0.901 | 0.804 | -24.804 |
| Nonane | 1.958 | 1.785 | 1.630 | 1.490 | 1.358 | 1.236 | -32.259 |
| Decane | 2.248 | 2.057 | 1.888 | 1.730 | 1.583 | 1.444 | -35.887 |
| Cyclopentane | 1.176 | 1.068 | 0.969 | 0.879 | 0.794 | 0.714 | -20.638 |
| Cyclohexane | 1.476 | 1.350 | 1.238 | 1.134 | 1.037 | 0.947 | -23.604 |
| Methylcyclohexane | 1.627 | 1.491 | 1.369 | 1.260 | 1.155 | 1.057 | -25.445 |
| Cycloheptane | 1.926 | 1.780 | 1.645 | 1.524 | 1.413 | 1.307 | -27.621 |
| Cyclooctane | 2.326 | 2.161 | 2.009 | 1.870 | 1.742 | 1.621 | -31.537 |
| Pent-1-ene | 0.961 | 0.857 | 0.765 | 0.679 | 0.601 | 0.526 | -19.393 |
| Hex-1-ene | 1.274 | 1.155 | 1.041 | 0.943 | 0.846 | 0.758 | -23.104 |
| Cyclohexene | 1.763 | 1.628 | 1.508 | 1.393 | 1.288 | 1.190 | -25.619 |
| Hept-1-ene | 1.579 | 1.438 | 1.307 | 1.193 | 1.083 | 0.983 | -26.638 |
| Oct-1-ene | 1.876 | 1.716 | 1.569 | 1.438 | 1.312 | 1.196 | -30.392 |
| Dec-1-ene | 2.458 | 2.262 | 2.083 | 1.919 | 1.765 | 1.618 | -37.540 |
| Hex-1-yne | 1.862 | 1.713 | 1.576 | 1.450 | 1.332 | 1.223 | -28.601 |
| Hept-1-yne | 2.161 | 1.995 | 1.841 | 1.699 | 1.566 | 1.442 | -32.200 |
| Oct-1-yne | 2.456 | 2.272 | 2.100 | 1.943 | 1.795 | 1.658 | -35.754 |
| Benzene | 2.505 | 2.348 | 2.201 | 2.064 | 1.941 | 1.825 | -30.493 |
| Toluene | 2.833 | 2.654 | 2.489 | 2.336 | 2.193 | 2.061 | -34.568 |
| Ethylbenzene | 3.084 | 2.889 | 2.708 | 2.539 | 2.384 | 2.238 | -37.904 |
| <i>o</i> -Xylene | 3.289 | 3.085 | 2.895 | 2.719 | 2.556 | 2.403 | -39.667 |
| <i>m</i> -Xylene | 3.166 | 2.967 | 2.783 | 2.612 | 2.452 | 2.303 | -38.658 |
| <i>p</i> -Xylene | 3.146 | 2.945 | 2.760 | 2.589 | 2.430 | 2.279 | -38.806 |
| Styrene | 3.502 | 3.289 | 3.090 | 2.908 | 2.740 | 2.580 | -41.258 |
| α-Methylstyrene | | 3.457 | 3.244 | 3.050 | 2.866 | 2.693 | -44.091 |
| Thiophene | 2.636 | 2.473 | 2.322 | 2.182 | 2.053 | 1.932 | -31.538 |
| Solute | logK_L | | | | | | ΔH_{solv} |

| Temperature, K | 318.15 K | 318.15 K | 318.15 K | 318.15 K | 318.15 K | 318.15 K | kJ mol ⁻¹ |
|-------------------------|----------|----------|----------|----------|----------|----------|----------------------|
| Pyridine | 3.314 | 3.125 | 2.948 | 2.784 | 2.631 | 2.490 | -36.943 |
| Methanol | 2.158 | 2.017 | 1.887 | 1.770 | 1.660 | 1.556 | -26.906 |
| Ethanol | 2.336 | 2.182 | 2.037 | 1.906 | 1.781 | 1.665 | -30.082 |
| Propan-1-ol | 2.640 | 2.465 | 2.303 | 2.158 | 2.017 | 1.889 | -33.637 |
| Propan-2-ol | 2.391 | 2.223 | 2.068 | 1.930 | 1.800 | 1.679 | -31.795 |
| Butan-1-ol | 2.970 | 2.773 | 2.592 | 2.428 | 2.274 | 2.134 | -37.420 |
| Butan-2-ol | 2.669 | 2.481 | 2.316 | 2.161 | 2.021 | 1.889 | -34.815 |
| 2-Methyl-propan-1-ol | 2.799 | 2.607 | 2.431 | 2.274 | 2.127 | 1.992 | -36.095 |
| tert-Butanol | 2.408 | 2.230 | 2.072 | 1.926 | 1.792 | 1.671 | -32.935 |
| Water | 2.427 | 2.281 | 2.137 | 2.013 | 1.898 | 1.788 | -28.590 |
| Methyl acetate | 2.288 | 2.134 | 1.993 | 1.862 | 1.742 | 1.630 | -29.419 |
| Methyl propanoate | 2.542 | 2.371 | 2.215 | 2.068 | 1.936 | 1.811 | -32.713 |
| Methyl butanoate | 2.786 | 2.602 | 2.433 | 2.274 | 2.130 | 1.994 | -35.447 |
| Ethyl acetate | 2.493 | 2.324 | 2.167 | 2.025 | 1.893 | 1.770 | -32.340 |
| Tetrahydrofuran | 2.373 | 2.220 | 2.079 | 1.948 | 1.827 | 1.714 | -29.489 |
| 1,4-Dioxane | 3.034 | 2.850 | 2.679 | 2.520 | 2.373 | 2.233 | -35.879 |
| tert-Butyl methyl ether | 1.686 | 1.545 | 1.418 | 1.299 | 1.190 | 1.090 | -26.666 |
| tert-Butyl ethyl ether | 1.590 | 1.450 | 1.322 | 1.204 | 1.097 | 0.994 | -26.629 |
| tert-Amyl methyl ether | 1.986 | 1.831 | 1.688 | 1.556 | 1.435 | 1.320 | -29.814 |
| Diethyl ether | 1.380 | 1.262 | 1.152 | 1.053 | 0.959 | 0.872 | -22.752 |
| Dipropyl ether | 1.819 | 1.668 | 1.530 | 1.403 | 1.286 | 1.176 | -28.761 |
| Diisopropyl ether | 1.508 | 1.371 | 1.243 | 1.127 | 1.021 | 0.919 | -26.331 |
| Dibutyl ether | 2.375 | 2.190 | 2.021 | 1.866 | 1.721 | 1.584 | -35.348 |
| Acetone | 2.452 | 2.303 | 2.164 | 2.037 | 1.917 | 1.806 | -28.926 |
| Pentan-2-one | 2.947 | 2.765 | 2.598 | 2.441 | 2.297 | 2.161 | -35.193 |
| Pentan-3-one | 2.938 | 2.757 | 2.588 | 2.430 | 2.286 | 2.149 | -35.338 |
| Butanal | 2.507 | 2.348 | 2.201 | 2.064 | 1.941 | 1.824 | -30.568 |
| Acetonitrile | 2.830 | 2.679 | 2.538 | 2.407 | 2.283 | 2.170 | -29.577 |
| 1-Nitropropane | 3.478 | 3.280 | 3.097 | 2.927 | 2.769 | 2.621 | -38.370 |

^a Experimental gas-to-liquid partition coefficient data taken from Marciniak and Wlazło.²

Table 4. Logarithm of gas-to-([MeoeMPyrr]⁺[Tf₂N]⁻) partition coefficients at various temperatures and enthalpies of solvation (in kJ mol⁻¹)^a

| Solute Temperature, K | logK _L | | | | | | ΔH _{solv} |
|--------------------------|-------------------|----------|----------|----------|----------|----------|----------------------|
| | 318.15 K | 328.15 K | 338.15 K | 348.15 K | 358.15 K | 368.15 K | kJ mol ⁻¹ |
| Pentane | 0.717 | 0.623 | 0.537 | 0.458 | 0.386 | 0.322 | -17.685 |
| Hexane | 1.029 | 0.919 | 0.817 | 0.719 | 0.633 | 0.551 | -21.422 |
| 3-Methylpentane | 1.009 | 0.897 | 0.794 | 0.702 | 0.614 | 0.538 | -21.093 |
| 2,2-Dimethylbutane | 0.855 | 0.754 | 0.662 | 0.577 | 0.500 | 0.430 | -19.036 |
| Heptane | 1.328 | 1.196 | 1.072 | 0.960 | 0.859 | 0.766 | -25.159 |
| Octane | 1.623 | 1.476 | 1.336 | 1.210 | 1.093 | 0.984 | -28.630 |
| 2,2,4-Trimethylpentane | 1.326 | 1.196 | 1.076 | 0.965 | 0.860 | 0.768 | -25.033 |
| Nonane | 1.920 | 1.747 | 1.589 | 1.444 | 1.310 | 1.188 | -32.791 |
| Decane | 2.217 | 2.021 | 1.849 | 1.688 | 1.543 | 1.407 | -36.186 |
| Cyclopentane | 1.146 | 1.037 | 0.941 | 0.851 | 0.769 | 0.694 | -20.221 |
| Cyclohexane | 1.436 | 1.318 | 1.210 | 1.104 | 1.013 | 0.925 | -22.900 |
| Methylcyclohexane | 1.591 | 1.459 | 1.336 | 1.225 | 1.124 | 1.033 | -24.988 |
| Cycloheptane | 1.887 | 1.745 | 1.616 | 1.493 | 1.382 | 1.276 | -27.333 |
| Cyclooctane | 2.288 | 2.124 | 1.975 | 1.833 | 1.707 | 1.587 | -31.386 |
| Pent-1-ene | 0.938 | 0.834 | 0.740 | 0.656 | 0.574 | 0.504 | -19.433 |
| Hex-1-ene | 1.248 | 1.127 | 1.017 | 0.913 | 0.822 | 0.735 | -22.965 |
| Cyclohexene | 1.735 | 1.600 | 1.474 | 1.362 | 1.255 | 1.158 | -25.801 |
| Hept-1-ene | 1.544 | 1.403 | 1.272 | 1.155 | 1.045 | 0.946 | -26.747 |
| Oct-1-ene | 1.834 | 1.678 | 1.535 | 1.398 | 1.279 | 1.164 | -30.000 |
| Dec-1-ene | 2.417 | 2.217 | 2.037 | 1.875 | 1.722 | 1.579 | -37.417 |
| Hex-1-yne | 1.838 | 1.691 | 1.558 | 1.431 | 1.316 | 1.210 | -28.134 |
| Hept-1-yne | 2.130 | 1.966 | 1.815 | 1.673 | 1.543 | 1.422 | -31.742 |
| Oct-1-yne | 2.420 | 2.236 | 2.068 | 1.912 | 1.766 | 1.630 | -35.323 |
| Solute Temperature, K | logK _L | | | | | | ΔH _{solv} |
| | 318.15 K | 328.15 K | 338.15 K | 348.15 K | 358.15 K | 368.15 K | kJ mol ⁻¹ |

| | | | | | | | |
|---------------------------------|-------|-------|-------|-------|-------|-------|---------|
| Benzene | 2.473 | 2.314 | 2.167 | 2.033 | 1.906 | 1.790 | -30.556 |
| Toluene | 2.792 | 2.613 | 2.447 | 2.294 | 2.152 | 2.017 | -34.664 |
| Ethylbenzene | 3.039 | 2.843 | 2.663 | 2.494 | 2.338 | 2.193 | -37.874 |
| <i>o</i> -Xylene | 3.241 | 3.037 | 2.848 | 2.673 | 2.511 | 2.358 | -39.558 |
| <i>m</i> -Xylene | 3.111 | 2.911 | 2.726 | 2.554 | 2.394 | 2.246 | -38.744 |
| <i>p</i> -Xylene | 3.091 | 2.892 | 2.708 | 2.538 | 2.378 | 2.230 | -38.554 |
| Styrene | 3.444 | 3.231 | 3.037 | 2.855 | 2.687 | 2.530 | -40.911 |
| α -Methylstyrene | 3.625 | 3.398 | 3.188 | 2.992 | 2.808 | 2.637 | -44.261 |
| Thiophene | 2.605 | 2.442 | 2.290 | 2.152 | 2.021 | 1.903 | -31.487 |
| Pyridine | 3.293 | 3.103 | 2.927 | 2.763 | 2.611 | 2.470 | -36.885 |
| Methanol | 2.176 | 2.033 | 1.903 | 1.780 | 1.668 | 1.562 | -27.475 |
| Ethanol | 2.346 | 2.188 | 2.045 | 1.909 | 1.785 | 1.669 | -30.297 |
| Propan-1-ol | 2.647 | 2.465 | 2.301 | 2.152 | 2.013 | 1.885 | -34.069 |
| Propan-2-ol | 2.393 | 2.225 | 2.072 | 1.930 | 1.800 | 1.678 | -31.990 |
| Butan-1-ol | 2.967 | 2.766 | 2.588 | 2.417 | 2.265 | 2.121 | -37.832 |
| Butan-2-ol | 2.665 | 2.479 | 2.310 | 2.155 | 2.013 | 1.882 | -34.994 |
| 2-Methyl-propan-1-ol | 2.796 | 2.605 | 2.435 | 2.272 | 2.124 | 1.991 | -36.062 |
| <i>tert</i> -Butanol | 2.415 | 2.236 | 2.076 | 1.928 | 1.792 | 1.671 | -33.264 |
| Water | 2.473 | 2.318 | 2.176 | 2.045 | 1.922 | 1.813 | -29.568 |
| Methyl acetate | 2.299 | 2.143 | 2.004 | 1.872 | 1.751 | 1.638 | -29.535 |
| Methyl propanoate | 2.545 | 2.373 | 2.215 | 2.068 | 1.936 | 1.812 | -32.829 |
| Methyl butanoate | 2.780 | 2.594 | 2.423 | 2.262 | 2.114 | 1.979 | -35.938 |
| Ethyl acetate | 2.497 | 2.328 | 2.173 | 2.029 | 1.895 | 1.770 | -32.544 |
| Tetrahydrofuran | 2.364 | 2.210 | 2.068 | 1.938 | 1.816 | 1.704 | -29.528 |
| 1,4-Dioxane | 3.027 | 2.841 | 2.670 | 2.511 | 2.362 | 2.223 | -36.006 |
| <i>tert</i> -Butyl methyl ether | 1.672 | 1.534 | 1.408 | 1.290 | 1.182 | 1.083 | -26.395 |
| <i>tert</i> -Butyl ethyl ether | 1.574 | 1.435 | 1.305 | 1.185 | 1.076 | 0.977 | -26.763 |
| <i>tert</i> -Amyl methyl ether | 1.969 | 1.815 | 1.673 | 1.542 | 1.422 | 1.310 | -29.515 |
| Diethyl ether | 1.369 | 1.250 | 1.140 | 1.037 | 0.943 | 0.856 | -22.996 |
| Dipropyl ether | 1.790 | 1.639 | 1.504 | 1.377 | 1.260 | 1.152 | -28.517 |
| Diisopropyl ether | 1.493 | 1.356 | 1.228 | 1.107 | 1.000 | 0.899 | -26.642 |
| Dibutyl ether | 2.340 | 2.155 | 1.987 | 1.831 | 1.688 | 1.551 | -35.271 |
| Acetone | 2.465 | 2.316 | 2.176 | 2.049 | 1.928 | 1.818 | -29.028 |
| Pentan-2-one | 2.945 | 2.762 | 2.593 | 2.436 | 2.290 | 2.155 | -35.390 |
| Pentan-3-one | 2.932 | 2.751 | 2.582 | 2.425 | 2.279 | 2.143 | -35.373 |
| Butanal | 2.511 | 2.350 | 2.204 | 2.068 | 1.942 | 1.825 | -30.665 |
| Acetonitrile | 2.853 | 2.700 | 2.558 | 2.425 | 2.301 | 2.185 | -29.943 |
| 1-Nitropropane | 3.488 | 3.290 | 3.107 | 2.936 | 2.777 | 2.630 | -38.435 |

^a Experimental gas-to-liquid partition coefficient data taken from Marciniak and Wlazlo¹.

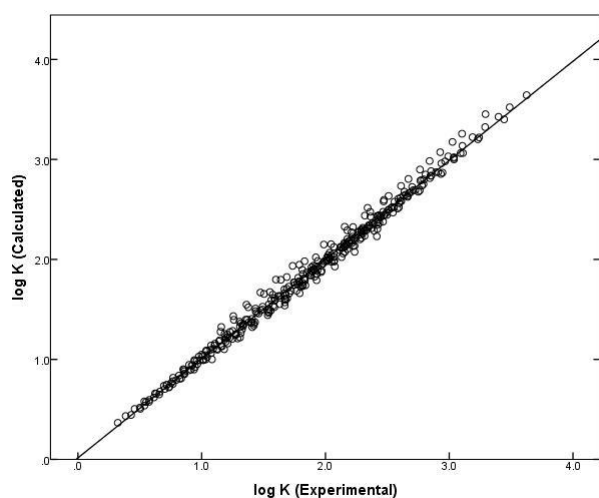


Figure 3. Graph of experimental logarithm of gas-to- $([\text{MeoeMPyrr}]^+[\text{Tf}_2\text{N}]^-)$ partition coefficient ($\log K_L$) versus calculated $\log K_L$ based on Eqn. 20.

To determine the predictability of Eqn. 20, the data in Table 4 was also analyzed using a training set and test

analysis. Eqn. 23 is the resultant correlation from randomly splitting half of the $\log K_L$ data reported in Table 4. Using Eqn. 23 to predict the values in the test set yielded a $SD = 0.068$ log units, $AAE = 0.051$, and $AE = 0.007$. The very small difference in the coefficient values calculated between the training set and parent set show that the training set compounds and temperatures are representative of the parent compounds and temperatures. The low AE value shows very little bias between using Eqns. 20 and 23.

For comparison, the six temperature-specific Abraham model correlations developed by Marciniak and Wlazlo¹ for solutes dissolved in $([\text{MeoeMPyrr}]^+[\text{Tf}_2\text{N}]^-)$ had an average standard deviation of $SD=0.058$ log units. Each temperature specific correlation used six curve-fit equation coefficients. Equations 20 and 23 require far fewer equation coefficients and are able to describe the experimental data to within a standard deviation of less than 0.064 log units.

$$\log K_L = -10.280(0.514)/(2.303 R) + [2.246(12.310) - (48.518(4167)/T)] [E/(2.303 R)] +$$

$$\begin{aligned}
& [3.492(14.742) - (-13094(4958)/T)] [S/(2.303 R)] + \\
& [-30.517(16.211) - (23364(5530)/T)] [A/(2.303 R)] + \\
& [-29.979(16.360) - (-11689(5524)/T)] [B/(2.303 R)] + \\
& [-13.310(1.037) - (-7834(340)/T)] [L/(2.303 R)] \quad (23)
\end{aligned}$$

$$N = 183, R^2 = 0.999, F = 15882, SD = 0.062 \text{ log units}$$

The removal of the c_H term from each of the three $\log K_L$ expressions and subsequent removal of $c_{H,solv}$ from the three ΔH_{solv} expressions is purely coincidental. Mintz, et al.⁴³ and Sprunger, et al.⁴⁴ have shown that temperature independent $\log K_L$ correlations for humic acid and polyurethane ether foam, respectively, produce twelve unique terms for all of the coefficients in Eqn. 11. The covariance encountered by the authors of this paper will most likely not occur with a data set that covers a much larger area of predictive space. In order to widen the area of predictive space, new partition coefficients will need to be determined for more acidic and more basic solutes.

CONCLUSIONS

Mathematical correlations are determined for predicting the gas-to-IL partition coefficients based on the Abraham solvation parameter model with temperature independent equation coefficients. The derived mathematical correlations (Eqns. 12, 16, and 20) are shown to provide reasonably accurate predictions the logarithm of the gas-to-IL partition coefficient for a wide variety of nonpolar and polar organic solutes dissolved in ([MHIm]⁺[B(CN)₄]⁻), ([MeoeMPip]⁺[Tf₂N]⁻), and ([MeoeMPyrr]⁺[Tf₂N]⁻) at temperatures from 318.15 K to 368.15 K to within a standard deviation of 0.077 log units or less. The success of the derived equations in predicting gas-to-ionic liquid partition coefficients suggests that the model can be used for other gas-to-condensed phase partitioning and for correlating gas chromatographic retention factor data measured at temperatures. As part of the present study, mathematical expressions (Eqns. 13, 17, and 21) were also derived for predicting the enthalpy of solvation for the dissolution of solutes in ([MHIm]⁺[B(CN)₄]⁻), ([MeoeMPip]⁺[Tf₂N]⁻), and ([MeoeMPyrr]⁺[Tf₂N]⁻) to within a standard deviation of 1.344 kJ/mol.

The method of regression analysis used in developing the log K_L correlations involved determining each of the equation coefficients solely from the measured gas-to-IL partition coefficient data. An alternative computational method could be to first regress the experimental ΔH_{solv} data, and then to insert the computed ΔH_{solv} equation coefficients into Eqn. 10. This would ensure identical values of $c_{H,solv}$, $e_{H,solv}$, $s_{H,solv}$, $a_{H,solv}$, $b_{H,solv}$ and $l_{H,solv}$ for both the log K_L and ΔH_{solv} correlations. This latter method was not pursued in the current study because our primary focus was in documenting the ability of Eqn. 10 to correlate gas-to-IL partition coefficient determined at different temperatures.

ACKNOWLEDGMENTS

Nishu Dabadge and Amy Tian thank the University of North Texas's Texas Academy of Math and Science (TAMS) program for a summer research fellowship. Bria Willis thanks the National Science Foundation for support received under NSF-REU grant (CHE-1004878).

REFERENCES

- Marciniak, A., Wlazło, M. *J. Chem. Thermodyn.*, **2012**, *54*, 90.
- Marciniak, A., Wlazło, M. *J. Chem. Thermodyn.*, **2012**, *49*, 137.
- Domańska, U., Lukoshko, E. V., Wlazło, M. *J. Chem. Thermodyn.*, **2012**, *47*, 389.
- Sprunger, L. M., Achi, S. S., Acree, W. E. Jr., Abraham, M. H. *Fluid Phase Equilib.*, **2010**, *288*, 139.
- Sprunger, L. M., Achi, S. S., Pointer, R., Acree, W. E. Jr., Abraham, M. H. *Fluid Phase Equilib.*, **2010**, *288*, 121.
- Abraham, M. H., Acree, W. E. Jr., Leo, A. J., Hoekman, D. *New J. Chem.*, **2009**, *33*, 568.
- Grubbs, L. M., Saifullah, M., De La Rosa, N. E., ye, S., Achi, S. S., Acree, W. E. Jr., Abraham, M. H. *Fluid Phase Equilib.*, **2010**, *298*, 48.
- Sprunger, L. M., Achi, S. S., Acree, W. E. Jr., Abraham, M. H., Leo, A. J., Hoekman, D., *Fluid Phase Equilib.*, **2009**, *281*, 144.
- Sprunger, L. M., Proctor, A., Acree, W. E. Jr., Abraham, M. H., Benjelloun-Dakhama, N. *Fluid Phase Equilib.*, **2000**, *270*, 30.
- Stephens, T. W., De La Rosa, N. E., Saifullah, M., Ye, S., Chou, V., Quay, A. N., Acree, W. E. Jr., Abraham, M. H. *Fluid Phase Equilib.*, **2011**, *308*, 64.
- Stephens, T. W., Quay, A. N., Chou, V., Loera, M., Shen, C., Wilson, A., Acree, W. E. Jr., Abraham, M. H. *Glob. J. Phys. Chem.*, **2012**, *1/1*.
- Stephens, T. W., Wilson, A., Dabadge, N., Tian, A., Hensley, H. J., Zimmerman, M., Acree, W. E. Jr., Abraham, M. H. *Glob. J. Phys. Chem.*, **2012**, *3*, 9/1.
- Sprunger, L. M., Gibbs, J., Acree, W. E. Jr., Abraham, M. H. *QSAR Comb. Sci.*, **2009**, *28*, 72.
- Sprunger, L., Acree, W. E. Jr., Abraham, M. H. *J. Chem. Inf. Model.*, **1997**, *47*, 1808.
- Abraham, M. H., Ibrahim, A., Acree, W. E. Jr. *Eur. J. Med. Chem.*, **2008**, *43*, 478.
- Abraham, M. H., Ibrahim, A., Acree, W. E. Jr. *Eur. J. Med. Chem.*, **2007**, *42*, 743.
- Sprunger, L. M., Gibbs, J., Acree, W. E. Jr., Abraham, M. H. *QSAR Comb. Sci.*, **2008**, *27*, 1130.
- Bowen, K. R., Flanagan, K. B., Acree, W. E. Jr., Abraham, M. H., Rafols, C. *Sci. Total Environ.*, **2006**, *371*, 99.
- Bowen, K. R., Flanagan, K. B., Acree, W. E. Jr., Abraham, M. H. *Sci. Total Environ.*, **2006**, *369*, 109.
- Hoover, K. R., Flanagan, K. B., Acree, W. E. Jr., Abraham, M. H. *J. Environ. Eng. Sci.*, **2007**, *6*, 165.
- Hoover, K. R., Acree, W. E. Jr., Abraham, M. H. *Chem. Res. Toxicol.*, **2005**, *18*, 1497.
- Anderson, J. L., Ding, J., Welton, T., Armstrong, D. W. *J. Am. Chem. Soc.*, **2002**, *124*, 14247.
- Domańska, U., Krolikowska, M., Acree, W. E. Jr., Baker, G. A., *J. Chem. Thermodyn.*, **2011**, *43*, 1050.
- Mutelet, F., Revelli, A.-L., Jaubert, J.-N., Sprunger, L. M., Acree, W. E. Jr., Baker, G. A. *J. Chem. Eng. Data*, **2010**, *55*, 234.

- ²⁵Stephens, T. W., Acree, W. E. Jr., Twu, P., Anderson, J. L., Baker, G. A., Abraham, M. H. *J. Solution Chem.*, **2012**, *41*, 1165.
- ²⁶Twu, P., Anderson, J. L., Stephens, T. W., Acree, W. E. Jr., Abraham, M. H. *Eur. Chem. Bull.*, **2012**, *1*, 212.
- ²⁷Jiang, R., Anderson, J. L., Stephens, T. W., Acree, W. E., Abraham, M. H. *Eur. Chem. Bull.*, **2013**, *2*, 741.
- ²⁸Abraham, M. H., Acree, W. E. Jr., *J. Solution Chem.*, **2011**, *40*, 1279.
- ²⁹Mintz, C., Gibbs, J., Acree, W. E. Jr., Abraham, M. H. *Thermochim. Acta*, **2009**, *484*, 65.
- ³⁰Mintz, C., Burton, K., Ladlie, T., Clark, M., Acree, W. E. Jr., Abraham, M. H. *J. Mol. Liq.*, **2009**, *144*, 23.
- ³¹Mintz, C., Ladlie, T., Burton, K., Clark, M., Acree, W. E. Jr., Abraham, M. H. *QSAR Comb. Sci.*, **2008**, *27*, 627.
- ³²Mintz, C., Burton, W. E. Jr., Abraham, M. H., *QSAR Comb. Sci.*, **2008**, *27*, 179.
- ³³Stephens, T. W., Chou, V., Quay, A. N., Acree, W. E. Jr., Abraham, M. H., *Thermochim. Acta*, **2011**, *519*, 103.
- ³⁴Stephens, T. W., De La Rosa, N. E., Saifullah, M., Ye, S., Chou, V., Quay, A. N., Acree, W. E. Jr., Abraham, M. H. *Thermochim. Acta*, **2011**, *523*, 214.
- ³⁵Abraham, M. H., Whiting, G. S., Doherty, R. M., Shuely, W. J. *J. Chem. Soc., Perkin Trans. 2*, **1990**, 1451.
- ³⁷Abraham, M. H., Grellier, P. L., Prior, D. V., Duce, P. P., Morris, J. J., Taylor, P. J. *J. Chem. Soc., Perkin Trans. 2*, **1989**, 699.
- ³⁸Abraham, M. H., Grellier, P. L., Prior, D. V., Morris, J. J., Taylor, P. J., *J. Chem. Soc., Perkin Trans. 2*, **1990**, 521.
- ³⁹Abraham, M. H., McGowan, J. C. *Chromatographia*, **1987**, *23*, 243.
- ⁴⁰Abraham, M. H., Grellier, P. L., McGill, R. A., *J. Chem. Soc., Perkin Trans 2*, **1987**, 797.
- ⁴¹Sprunger, L. M., Gibbs, J., Proctor, A., Acree, W. E. Jr., Abraham, M. H., Meng, Y., Yao, C., Anderson, J. L. *Ind. Eng. Chem. Res.*, **2009**, *48*, 4145.
- ⁴²Grubbs, L. M., Saifullah, M., De La Rosa, N. E., Acree, W. E. Jr., Abraham, M. H., Zhao, Q., Anderson, J. L., *Glob. J. Phys. Chem.*, **2010**, *1*, 1.
- ⁴³Grubbs, L. M., Ye, S., Saifullah, M., McMillan-Wiggins, M. C., Acree, W. E. Jr., Abraham, M. H. *Fluid Phase Equilibr.*, **2011**, *301*, 257.
- ⁴⁴Mintz, C., Ladlie, T., Burton, K., Clark, M., Acree, W. E. Jr., Abraham, M. H., *QSAR Comb. Sci.*, **2008**, *27*, 483.
- ⁴⁵Sprunger, L., Acree, W. E. Jr., Abraham, M. H. *Anal. Chem.*, **2007**, *79*, 6891.

Received: 01.06.2013.

Accepted: 03.07.2013.

³⁶Abraham, M. H., Whiting, G. S., Doherty, R. M., Shuely, W. J. *J. Chromatogr.*, **1991**, *587*, 213.



SYNTHESIS OF RING FUSED CYCLIC KETONES VIA DOMINO FRIEDEL-CRAFTS REACTIONS OF FUNCTIONALIZED 5-MEMBERED HETEROCYCLIC PERCHLORATES

Mahmoud R. Mahmoud^[a], Hamed A. Derbala^[a], Hassan M. F. Madkour^[a] and Naglaa F. El-Said^[b]

Keywords: Oxazolonium perchlorates, Indanones, Domino Friedel-Crafts

Z-4-(Naphth-2-ylmethylene)-2-phenyloxazol-5(4H)-one and 3-(phenylcarbamoyl)but-3-enoic acid **2** and **5**, respectively, are readily transformed into the corresponding perchlorate salts **3** and **6** with acetic anhydride-perchloric acid mixture. Conduct the latter salts with arenes in the presence of anhydrous AlCl₃ provided novel derivatives of benzo[g]indanones **7** and 1-tetralones **8**, respectively, via two consecutive Friedel-Crafts reaction *in situ*. The structure of all the synthesized products was characterized using IR, ¹H NMR, ¹³C NMR and mass spectra.

Corresponding Authors*

E-Mail: mrefaee2000@yahoo.com

[a] Chemistry Department, Faculty of Science, Ain Shams University, Abbassia 11566, Cairo, Egypt

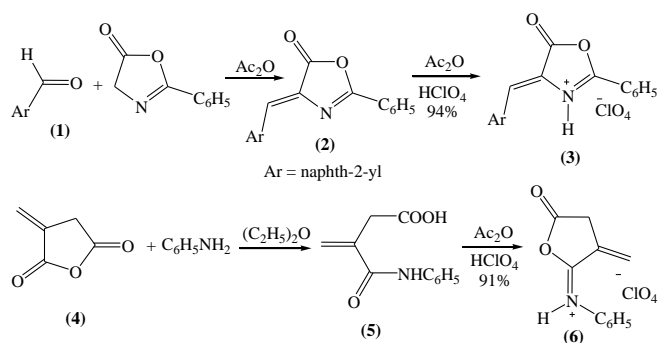
[b] National Research Center, Dokki, Giza, Egypt

Introduction

Ring fused cyclic ketones, particularly, indanones and tetralones have been frequently encountered in the synthesis of pharmaceuticals, natural products and industrially relevant compounds.¹⁻⁵ For examples, the E-2-benzylidene, 1-tetralones and 1-indanones exhibited highly cytotoxic effects, and their Mannich ketones revealed antibacterial activity, besides the 2-benzyl-1-indanone showed AChE inhibitor activity superior to rivatigmine, however, the thiosemicarbazones of the latter ketone were determined as antiviral agents against BVDV and for the treatment of infections caused by hepatitis C virus.⁶⁻⁹ Further, the gallic acid based indanones showed potent anticancer activity against MCF-7, that is, hormone dependent breast cancer cell line, besides indanones and indenones analogues of combretastain A4 a potent anticancer agent known for its antimetabolic and antiangiogenic properties, were assessed as inhibitors of tubulin polymerization, as well as the indanone extracted from the marine cyanobacterium *Lyngbya majuscula*, demonstrated inhibition of hypoxia induced activation of the VEGF promoter in Hep3B cells.¹⁰⁻¹³ Among recent developed synthetic methods of these ketones, an immense number of publications have adopted Friedel-Crafts protocol, nevertheless, few number of them involved domino process.¹⁴⁻²⁶ To the best of our knowledge, the utility of heterocyclic perchlorates has never been involved so far. Accordingly, in this work the first application of the latter reaction type on the salts, (Z)-4-(Naphth-2-ylmethylene)-2-phenyloxazol-5(4H)-onium and 4-methylenedihydrofuran-2-(3H)-one-5-(phenyliminium) perchlorates **3** and **6**, respectively, to synthesize the corresponding benzo[g]indanones **7** and 1-tetralones **8**, is reported which represents a new type of domino process.

Results and Discussion

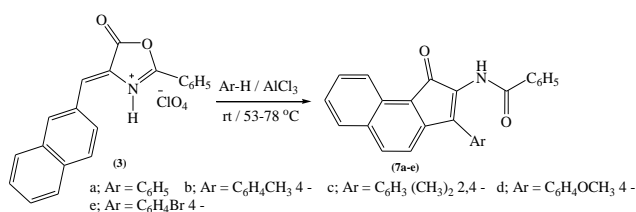
The novel functionalized salt, (Z)-4-(Naphth-2-ylmethylene)-2-phenyloxazol-5(4H)-onium perchlorate salt **3** was easily obtained by attempting of the recently prepared (Z)-4-(Naphth-2-ylmethylene)-2-phenyloxazol-5(4H)-one **2** using acetic anhydride-perchloric acid dehydrating mixture according to the procedure previously described in refs.²⁷⁻²⁹ The (Z) configuration of **2** was inferred by analogy with the literature.³⁰⁻³¹ Alternatively, the formation of salt **6** commenced by carrying out ring opening reaction of 3-methylene-tetrahydro furan-2,5-dione **4** with aniline to give 3-(phenylcarbamoyl)but-3-enoic acid **5**, which subsequently, underwent exo-trig cyclization to yield the salt 4-methylene dihydrofuran-2-(3H)-one-5-phenyliminium perchlorate **6** (Scheme 1).



Scheme 1

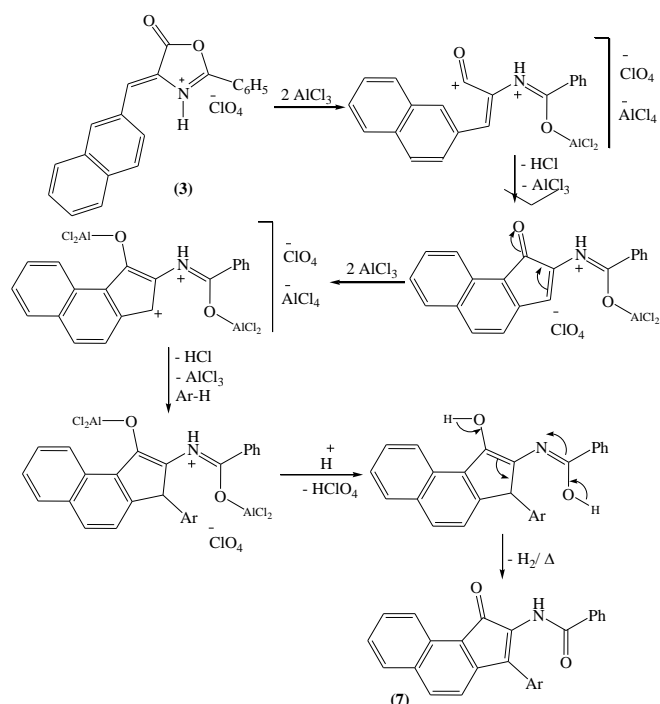
The IR spectra of the salts **3** and **6** exhibited the characteristic higher frequency absorption at 1847 and 1858 cm⁻¹, respectively. However, the EI-MS fragmentation pattern of the perchlorate salts **3** and **6** displayed peaks at m/z (%) 299 (100) and 187 (100) corresponding to the base peak [M-HClO₄]. (c.f. Exp.)

Traditionally, the aluminium chloride mediated Friedel-Crafts acylation of oxazolones with arenes proceeds via intermolecular ring opening to afford 2-acylamino ketones.^{32,33} In conjunction to these reports, we aimed in this context to construct annelated indenones by application of the forementioned reaction type on salt **3**. Thus, salt **3** was reacted with benzene, toluene, m-xylene, anisole and bromobenzene in the presence of catalytic amount of anhydrous aluminium chloride and the reaction mixture was stirred at room temperature for 4-8 h (reaction was monitored by TLC). Careful examination of physical and spectral data indicated that the novel products were benz[*g*]indenones (**7a-e**), respectively, having aryl moieties contained at C-3 (Scheme 2).



Scheme 2

Presumably, this suggested that the reaction successfully proceeded via two consecutive Friedel-Crafts types in situ, a domino process involving annelation of the fused cyclic ketone and a non-conventional intermolecular alkylation incorporating aryl moiety at position **3** of indenone nucleus.²⁵

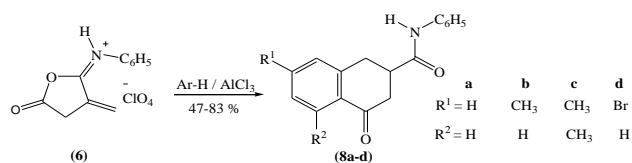


Scheme 3

Infrared spectra of **7a-e** exhibited absorption bands at 1671-1662 cm^{-1} assigned for the amide carbonyl and sharp absorption at 1704-1690 cm^{-1} referred to the existence of the unsaturated cyclic 5-membered ring ketones. Besides, the 1H -NMR spectra ($CDCl_3/DMSO$, δ ppm), exhibited broad singlets at δ 10.06-9.83 (1H, Ph-CONH, exch. D_2O), however, the signal attributable to the naphthylidene =CH

proton disappeared. Moreover, the mass spectra of these products were in consistency with the proposed structure. For instances, the EI-MS fragmentation of **7a** showed m/z (%): 375 (12.9), and 105 (100) due to the molecular ion and the base peaks, respectively.

When the perchlorate **6** was subjected to react with benzene, toluene, m-xylene and bromobenzene under the forementioned reaction conditions afforded 3-(*N*-phenyl carboxamido)benzocyclohexanones (**8a-d**) in yields 47-83 % (Scheme 4).



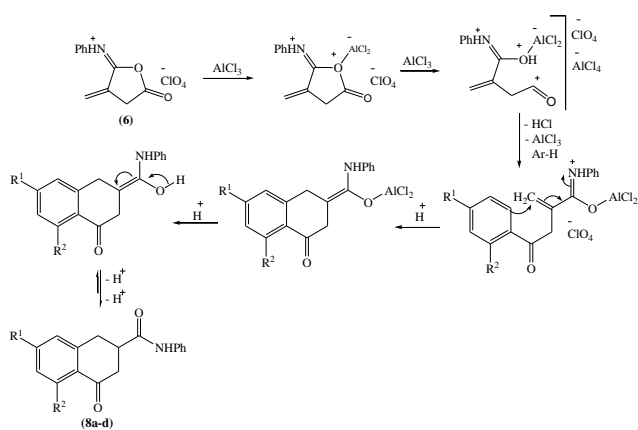
Scheme 4

The structure of these products was inferred on the basis of the IR (KBr) absorption band revealed at the 3 μm region at ν 3353-3274 cm^{-1} characteristic to the secondary amide NH functionality, besides the bands displayed at 1683-1664 cm^{-1} due to the open amide carbonyl group frequency. However, the bands appeared at ν 1710-1692 cm^{-1} referred to the absorption of the ketonic group of fused cyclohexanone ring moiety. Compelling evidences for the confirmation of the assigned structure were gained from careful examination of 1H -NMR spectra. For example, the structure of **8a** was based on its 1H -NMR spectrum ($CDCl_3$) which revealed a singlet at δ 8.4 ppm (1H, NH, exch. D_2O), two doublets of doublets (4H, 2 CH_2) due to the absorption protons centered at C2 and C4 of 6-membered ring ketone at δ 3.37 and δ 3.01 ppm, besides multiplet peaks exhibited at δ 2.66 ppm stand to the proton located at C3. However, the 1H -NMR ($DMSO-d_6$) spectra of compound **8b** and **8c**, displayed in the up-field region the singlet signals at δ 2.38 ppm characteristic to the aromatic CH_3 protons located at 6-position, δ 2.31 and δ 2.26 ppm stand to the two aromatic CH_3 protons centered at 6- and 8-positions. Further support for the assigned structure was gained from the fragmentation pattern of the concerned compounds. Thus, the EI-MS of **8a** showed the molecular ion peak at m/z (%): 265 (16.4) and the base peak at m/z (%): 115 (100, indenium ion), however, the EI-MS of **8d** exhibited m/z (%): 346 (40.63) and 344 (41.92) due to $M^+ + 2$ and the molecular ion (base peak), respectively.

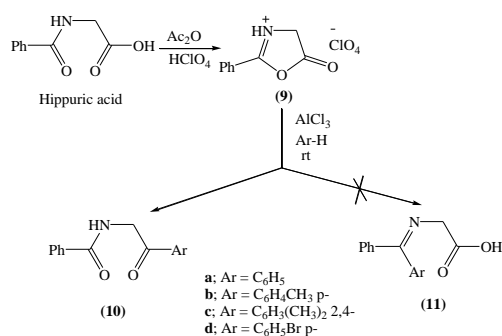
The conversion of **6** to **8** could be visualized as shown in Scheme 5.

Hippuric acid (*N*-benzoylglycine) gave the perchlorate salt **9** (86%) upon treatment with acetic anhydride-perchloric acid whose IR spectrum exhibited characteristic high absorption frequency at 1874 cm^{-1} .

When compound **9** was treated with aromatic hydrocarbon, namely, benzene, toluene, m-xylene and bromobenzene in the presence of anhydrous aluminium chloride with stirring, and no heat was provided, the reaction proceeded readily to give α -benzoylaminoacetophenone derivatives **10** in moderate yields. There were no evidences for the formation of the acidic product **11** which might be formed if attack of the carbon nucleophile, were on the alternative iminium - $C=N^+H$ functionality (Scheme 6).

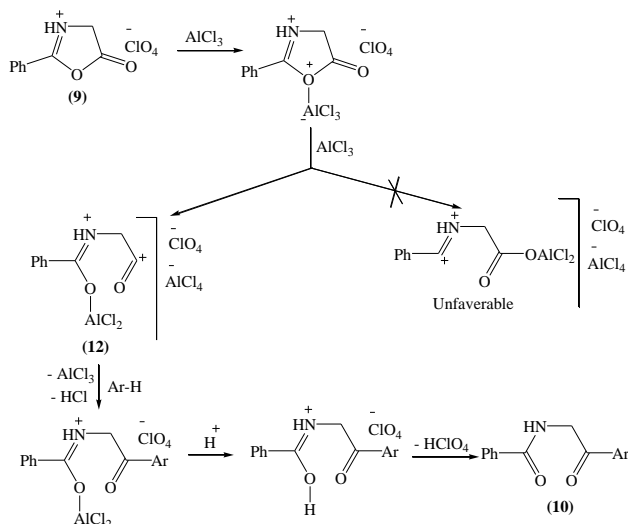


Scheme 5



Scheme 6

The reaction goes through ring opening of the heterocyclic cation that arises in the formation of the intermediate acylium ion **12** which consequently undergoes electrophilic attack on the aromatic hydrocarbon. (Scheme 7)



Scheme 7

The structure **7** was deduced from the correct analytical and spectral data (c.f. Exp.)

Experimental

All melting points are uncorrected. IR spectra were recorded on FTIR Mattson (Infinity Series) spectrometer as KBr disc. The ^1H NMR spectra were measured on a Varian Gemini 200 MHz instrument with chemical shift (δ) expressed in ppm downfield from TMS as internal standard. Mass spectra were recorded on a Shimadzu GC-MS-QP 1000 Ex instrument operating at 70 eV. Satisfactory elemental analyses were measured using a Perkin Elmer 2400 CHN Elemental Analyzer. TLC was run using TLC aluminium sheets silica gel F₂₅₄ (Merck).

Z-4-(Naphth-2-ylmethylene)-2-phenyloxazol-5(4H)-one **2** and 3-(phenylcarbamoyl)but-3-enoic acid **5**, were prepared by the following reported procedures.²¹⁻²³

Z-4-(Naphth-2-ylmethylene)-2-phenyloxazol-5(4H)-one (2)

Yellow crystals, (78 %), mp. 143-144 °C, (Lit²⁴ 142-143 °C), IR: (CO oxaz. ring) 1784, C=N 1631 cm^{-1} . ^1H NMR (DMSO- d_6) δ 8.14-7.96 (m, 3H_{arom.}), 7.71-7.43 (m, 5H_{arom.}), 7.18-6.8 (m, 4H_{arom.}), 7.03 (s, 1H, $\text{CH}=\text{}$).

Z-4-(Naphth-2-ylmethylene)-2-phenyloxazol-5(4H)-onium perchlorate (3)

Perchloric acid (3 ml) was slowly added to a stirred solution of oxazolone **2** (2.9 g, 10 mmol) in acetic anhydride (40 ml), the temperature being kept below 30 °C by external cooling, during the addition the product separated out was filtered off and washed with dry ether (2x5 ml) to give **3** as yellow crystals, (94%), mp 182-183 °C, IR: NH 3310, C=O 1847, C=N 1651 cm^{-1} . ^1H NMR (DMSO- d_6) δ 10.1 (br.s, 1H, C=NH⁺, exch. with D₂O), 8.8-7.51 (m, 12H_{arom.}), 6.2 (s, 1H, $\text{CH}=\text{}$). ms: m/z: 299 (M-HClO₄, 100), 255 (22.1), 196 (42.6), 141 (36.17), 77 (50.1). Anal.: Calcd. for C₂₀H₁₄ClNO₆ (399.7): C, 60.09; H, 3.50; N, 3.50; Cl, 8.87. Found; C, 60.21; H, 3.37; N, 3.62; Cl, 9.13.

4-(Anilino)-4-oxo-3-methylenebutanoic acid (5)

Colourless crystals, (88 %), mp 161-2°C, IR: br. OH_{acid} 3228, C=O 1704, C=O 1651 cm^{-1} . ^1H NMR (DMSO- d_6) δ 12.52 (br.s, 1H, acidic OH, exch. with D₂O), 10.0 (br.s, 1H, amide NH, exch. with D₂O), 7.63-7.58 (d, J = 10 Hz, 2H_{arom.}), 7.34-7.26 (t, J = 7.6 Hz, 2H_{arom.}), 7.07-7.0 (d,d, J = 6.8 Hz, 1H_{arom.}), 6.20 (s, 1H, CH₂=), 5.76 (s, 1H, CH₂=), 3.37 (s, 2H, CH₂-CO).

4-Methylene-2-oxo-tetrahydrofuran-5-N-phenyliminium perchlorate (6)

4-(Anilino)-4-oxo-3-methylenebutanoic acid **5** (2.05 g, 10 mmol) was stirred in freshly distilled acetic anhydride (40 ml). The perchloric acid (3 ml) was slowly added to the suspension and temperature being kept below 30 °C by external cooling.²¹⁻²³ The product deposited during the addition, washed with dry ether and dried to give **6** as colourless crystals, (91 %), mp 122-3 °C, IR: br. ⁺NH 3314, C=O 1858, C=O 1669 cm^{-1} . ^1H NMR (DMSO- d_6) δ 10.15 (br.s, 1H, ⁺NH, exch. with D₂O), 7.57 (d, J = 7.8 Hz, 2H_{arom.}), 7.33-7.25 (d,d, J = 2.2 Hz, J = 5.4 Hz, 2H_{arom.}), 7.03 (t, J =

7.2 Hz, 1H_{arom.}), 6.13 (d,d, 1H, CH₂=), 5.72 (d, 1H, CH₂=), 3.29 (s, 2H, CH₂). ms: m/z: 187 (M⁺ -HClO₄, 100), 91 (70.1), 77 (63.4). Anal.: Calcd. for C₁₁H₁₀ClNO₆ (287.591): C, 45.94; H, 3.50; N, 4.87; Cl, 12.33. Found; C, 45.64; H, 3.53; N, 5.14; Cl, 12.66.

3-Aryl-2-benzoylamino benzo[g]indenones (7a-e)

Anhydrous aluminum chloride (1 g, 7.5 mmol) was added portionwise to a solution of perchlorate **3** (1.2 g, 3 mmol) in the aromatic hydrocarbon (30 ml). The reaction mixture was stirred for one hour at room temperature, heated on water bath with continuous stirring for 3 h, and left overnight. The reaction mixture was hydrolyzed by the addition of ice and concentrated 1 N hydrochloric acid. The residual organic product was filtered off and washed with 0.01 N aqueous sodium bicarbonate solution (3 x 40 ml) then with water (3 x 50 ml). The precipitate was filtered off, dried and crystallized from the suitable solvent to give **7a-e**, yields 53-78 %.

2-Benzoylamino-3-phenylbenzo[g]indenone (7a)

Pale yellow crystals (benzene), (63 %), mp 212-213 °C, IR: NH 3259, C=O 1690, C=O 1662 cm⁻¹. ¹H NMR (DMSO-d₆) δ 10.06 (br.s, 1H, NH, exch. with D₂O), 8.2-7.5 (m, 16H_{arom.}). ¹³C NMR (DMSO-d₆) δ 184.6 (C=O₅-memb.), 161 (C=O_{amide}), 142.1, 134.4, 133.3, 131.2, 130.6, 127.3, 126.6. ms: m/z: 375 (M⁺, 12.9), 332 (64.51), 215 (22.58), 139 (32.25), 105 (100), 77 (45.5). Anal.: Calcd. for C₂₆H₁₇NO₂ (375.3): C, 83.19; H, 4.56; N, 3.73. Found; C, 83.44; H, 4.76; N, 3.65.

2-Benzoylamino-3-p-tolylbenzo[g]indenone (7b)

Pale yellow crystals (benzene – light pet. b.p. 60-80 °C), (69 %), mp 189-9 °C, IR: NH 3341, C=O 1704, C=O 1667 cm⁻¹. ¹H NMR (DMSO-d₆) δ 9.83 (br.s, 1H, NH, exch. with D₂O), 7.88-7.07 (m, 15H_{arom.}), 2.36 (s, 3H, CH₃). ¹³C NMR (DMSO-d₆) δ 188.1 (C=O₅ memb.), 161 (C=O_{amide}), 139.3, 136.2, 132.4, 131.7, 130.2, 128.4, 126.9, 124.2, 24.7 (CH₃). ms: m/z: 389 (M⁺, 17.26), 270 (29.17), 105 (34.74), 91 (100), 77 (52.16). Anal.: Calcd. for C₂₇H₁₉NO₂ (389.417): C, 83.28; H, 4.91; N, 3.59. Found; C, 82.93; H, 5.11; N, 3.32.

2-Benzoylamino-3(2,4-dimethylphenyl)benzo[g]indenone (7c)

Yellow powder (benzene – light pet. b.p. 60-80 °C), (78 %), mp 204-6 °C, IR: NH 3338, C=O 1687, C=O 1658 cm⁻¹. ¹H NMR (DMSO-d₆) δ 8.72 (br.s, 1H, NH, exch. with D₂O), 7.94 (m, 11H_{arom.}), 7.23 (d,d, 1H_{arom.}), 6.93-6.79 (m, 2H_{arom.}), 2.37 (s, 3H, CH₃), 2.26 (s, 3H, CH₃). ms: m/z: 404 (M⁺ +1, 9.42), 403 (M⁺, 10.12), 133 (37.13), 105 (100), 91, (43.62), 77 (31.1). Anal.: Calcd. for C₂₈H₂₁NO₂ (403.442): C, 83.36; H, 5.24; N, 3.47. Found; C, 83.61; H, 5.47; N, 3.66.

2-Benzoylamino-3-p-methoxyphenylbenzo[g]indenone (7d)

Brownish yellow powder (ethanol), (59 %), mp 261-2 °C, IR: NH 3284, C=O 1694, C=O 1661 cm⁻¹. ¹H NMR (DMSO-d₆) δ 10.24 (br.s, 1H, NH, exch. with D₂O), 8.12-7.67 (m, 8H_{arom.}), 7.53-7.48 (m, 5H_{arom.}), 7.33 (d,d, 2H_{arom.}),

3.82 (s, 3H, OCH₃). ¹³C NMR (DMSO-d₆) δ 194.3 (C=O₅-memb.), 165.2 (C=O_{amide}), 141.4, 133.5, 131.7, 130.1, 128.6, 126.4, 123.6, 121.5, 54.8 (OCH₃). ms: m/z: 374 (M⁺ -OCH₃, 63.28), 285 (42.54), 105 (100), 77 (52.16). Anal.: Calcd. for C₂₇H₁₉NO₃ (405.407): C, 79.99; H, 4.72; N, 3.45. Found; C, 80.14; H, 4.93; N, 3.54.

2-Benzoylamino-3-(p-bromophenyl)benzo[g]indenone (7e)

Yellow crystals (ethanol), (53 %), mp 230-2 °C, IR: NH 3228, C=O 1693, C=O 1663 cm⁻¹. ¹H NMR (DMSO-d₆) δ 9.91 (br.s, 1H, NH, exch. with D₂O), 8.72-7.23 (m, 11H_{arom.}), 7.44 (d,d, 2H_{arom.}), 6.85 (d,d, 2H_{arom.}). ¹³C NMR (DMSO-d₆) δ 187.8 (C=O₅-memb.), 165.3 (C=O_{amide}), 138.2, 134.2, 130.4, 129.8, 128.3, 126.7, 124.6. ms: m/z: 456 (M⁺ +2, 44.71), 454 (M⁺, 45.68), 322 (23.68), 154 (100), 105 (40.08), 77 (28.74). Anal.: Calcd. for C₂₆H₁₆BrNO₂ (454.289): C, 68.74; H, 3.55; N, 3.08; Br, 17.59. Found; C, 69.02; H, 3.46; N, 3.24; Br, 17.84.

3-N-Phenylcarboxamido-6-substituted- and 6,8-disubstituted-1-tetralones (8a-d)

Anhydrous aluminum chloride (1g, 7.5 mmol) was added portionwise to a stirred cold solution of N-phenylmethylenesuccinisoimidium perchlorates **6** (0.86 g, 3 mmol) in dry aromatic hydrocarbon as a reagent and a cosolvent (50 ml). The reaction was carried out similarly as in the previous experiment on **3**. The excess solvent was removed by steam distillation. The residual organic product was filtered off, washed with 0.01N sodium bicarbonate solution (3 x 40 ml) and crystallized from a suitable solvent to give **8a-d**, yields 47-83 %

3-N-Phenylcarboxamido-1-tetralone (8a)

Light brown crystals (light pet. bp 100-120 °C), (64 %), mp 138-140 °C, IR: NH 3353, C=O 1703, C=O 1683 cm⁻¹. ¹H NMR (CDCl₃) δ 8.4 (s, 1H, NH, exch. with D₂O), 8.2-7.03 (m, 9H_{arom.}), 3.59-3.15 (d,d, 2H, C₂-H₂), 3.07-2.96 (d,d, 2H, C₄-H₂), 2.95(m, 1H, C₃H). ¹³C NMR δ 197.1 (C=O₆-memb.), 173.2 (C=O_{amide}), 140.1, 139.2, 138.5, 131.0, 128.7, 128.5, 126.7, 125.8, 123.4, 40.9(CH₂), 37.4(CH), 34.4(CH₂). ms: m/z: 265 (16.4), 173 (12.12), 145 (30.2), 117 (51.04), 115 (100), 93 (31.4), 91 (41.26), 77 (39.54). Anal.: Calcd. for C₁₇H₁₅NO₂ (265.279): C, 76.97; H, 5.69; N, 5.28. Found; C, 77.08; H, 5.42; N, 5.07.

6-Methyl-3-N-phenylcarboxamido-1-tetralone (8b)

Beige crystals (light pet. Bp. 100-120 °C), (62 %), mp. 160-161 °C, IR: NH 3347, C=O 1710, C=O 1680 cm⁻¹. ¹H NMR (CDCl₃) δ 9.34 (s, 1H, NH, exch. with D₂O), 7.59-7.03 (m, 8H_{arom.}), 3.3-2.97 (d,d, 2H, C₂-H₂), 2.94-2.84 (d,d, 2H, C₄-H₂), 2.7-2.6 (m, 1H, C₃H), 2.38 (s, 3H, Ar-CH₃). ¹³C NMR δ 196.3 (C=O₆-memb.), 171.6 (C=O_{amide}), 140.7, 138.8, 138.3, 132.1, 129.4, 128.2, 127.1, 125.6, 122.6, 42.1 (CH₂), 38.3 (CH), 33.7 (CH₂), 23.8 (CH₃). ms: m/z: 279 (100, M⁺), 187 (70.2), 159 (30.1), 92 (17.9), 91 (41.26), 77 (42.4). Anal.: Calcd. for C₁₈H₁₇NO₂ (279.304): C, 77.40; H, 6.13; N, 5.01. Found; C, 77.51; H, 5.86; N, 4.93.

6,8-Dimethyl-3-N-phenylcarboxamido-1-tetralone (8c)

Beige crystals (EtOH), (83 %), mp 193-194 °C, IR: NH 3329, C=O 1692, C=O 1664 cm⁻¹. ¹H NMR (DMSO-d₆) δ 9.94 (s, 1H, NH, exch. with D₂O), 7.72-6.76 (m, 7H_{arom.}), 3.02-2.93 (d,d, 2H, C₂-H₂), 2.74-2.65 (d,d, 2H, C₄-H₂), 2.63 (m, 1H, C₃-H), 2.31 (s, 3H, Ar-CH₃), 2.26 (s, 3H, Ar-CH₃). ¹³C NMR δ 198.2(C=O_{6-memb.}), 173.3 (C=O_{amide}), 141.1, 138.3, 137.7, 132.6, 128.8, 128.4, 126.4, 124.3, 121.6, 41.4 (CH₂), 37.7 (CH), 32.4 (CH₂), 24.2 (CH₃), 23.6 (CH₃). ms: m/z: 279 (M⁺- C₆H₅N, 100), 187 (16.37), 154 (67.89), 91 (46.3), 77 (24.8). Anal.: Calcd. for C₁₉H₁₉NO₂ (293.329): C, 77.79; H, 6.52; N, 4.77. Found: C, 78.03; H, 6.74; N, 4.64.

6-Bromo-3-N-phenylcarboxamido-1-tetralone (8d)

Pale yellow powder (EtOH), (47 %), mp 183-4 °C, IR: NH 3274, C=O 1701, C=O 1668 cm⁻¹. ¹H NMR (CDCl₃) δ 8.76 (s, 1H, NH, exch. with D₂O), 8.14-7.05 (m, 8H_{arom.}), 3.22-3.04 (d,d, 2H, C₂-H₂), 2.73-2.54 (d,d, 2H, C₄-H₂), 2.31 (m, 1H, C₃-H). ms: m/z: 346 (M⁺+2, 40.63), 344 (M⁺, 41.92), 252 (21.72), 92 (100, C₆H₇N⁺). Anal.: Calcd. for C₁₇H₁₄BrNO₂ (344.176): C, 59.33; H, 4.09; N, 4.07; Br, 23.22. Found: C, 59.18; H, 3.87; N, 4.24; Br, 22.85.

Reaction of 2-phenyl-5(4H)-oxazolium perchlorate 9 with aromatic hydrocarbons: Formation of α-benzoylaminoacetophenone derivatives 10a-d

To a suspension of the perchlorate salt **9** (2 g, 0.007 mol) in aromatic hydrocarbon (50 ml), anhydrous aluminum chloride (3.34 g, 0.025 mol) was added portionwise with stirring in cold ice-bath for one hour, then on water-bath for 2 h. The reaction mixture left overnight and then hydrolysed by addition of ice cold HCl. The organic product was filtered off, washed with aqueous sodium bicarbonate solution, then water, dried and recrystallized from the suitable solvent to give **10a-d**.

α-Benzoylaminoacetophenone (10a)

Pale yellow crystals (benzene-light pet. bp 80-100 °C), (75 %), mp 125-6 °C (lit.⁸ 124 °C), IR: NH, OH 3356, C=O 1692, C=O 1665 cm⁻¹. ¹H NMR (CDCl₃) δ 8.88 (t, 1H, NH, exch. with D₂O), 8.09-7.51 (m, 10H_{arom.}), 4.83-4.82 (d,d, 2H, CH₂, J = 5.6 Hz). ms: m/z: 239 (M⁺, 22.9), 105 (100), 77 (56.5). Anal.: Calcd. for C₁₅H₁₃NO₂ (239): C, 75.31; H, 5.43; N, 5.85. Found: C, 75.56; H, 5.34; N, 5.66.

α-Benzoylamino-4-methylacetophenone (10b)

Light yellow crystals (light pet. bp 60-80 °C), (67 %), mp 117-118 °C (lit.⁸ 118-9 °C), IR: br. NH, OH 3375, C=O 1686, C=O 1660 cm⁻¹. ¹H NMR (CDCl₃) δ 8.79 (t, 1H, NH, exch. with D₂O), 8.44-7.3 (m, 9H_{arom.}), 4.76-4.74 (d,d, 2H, CH₂, J = 6.3 Hz), 2.39 (s, 3H, Ar-Me). ms: m/z: 253 (M⁺, 19.7), 225 (18.2), 206 (25.3), 119 (100), 105 (38.6), 77 (40.1). Anal.: Calcd. for C₁₆H₁₅NO₂ (253): C, 75.88; H, 5.92; N, 5.53. Found: C, 76.0; H, 5.81; N, 5.22.

α-Benzoylamino-2,4-dimethylacetophenone (10c)

Pale yellow crystals (light pet. bp 60-80 °C), (70 %), mp 128-9 °C (lit.⁸ 130 °C), IR: NH, OH 3396, C=O 1680, C=O 1649 cm⁻¹. ¹H NMR (CDCl₃) δ 7.36 (br.s, 1H, NH, exch. with D₂O), 7.91-7.11 (m, 8H_{arom.}), 4.86-4.84 (d,d, 2H, CH₂, J = 5.8 Hz), 2.57 (s, 3H, Me), 2.37 (s, 3H, Me). ms: m/z: 267 (M⁺, 11.7), 239 (8.4), 139 (100), 105 (77.3), 77 (75.4). Anal.: Calcd. for C₁₇H₁₇NO₂ (267): C, 76.4; H, 6.36; N, 5.24. Found: C, 76.32; H, 6.18; N, 5.28.

α-Benzoylamino-4-bromoacetophenone (10d)

Pale yellow crystals (benzene-light pet. bp 60-80 °C), (80 %), mp 100-102 °C, IR: br. NH, OH 3371, C=O 1693, C=O 1666 cm⁻¹. ¹H NMR (CDCl₃) δ 7.84 (t, 1H, NH, exch. with D₂O), 8-7.46 (m, 9H_{arom.}), 4.89-4.87 (d, 2H, CH₂, J = 5.3 Hz). ms: m/z: 320 (M⁺+2, 26.9), 318 (M, 30.8), 238 (50.3), 105 (100), 77 (90.3). Anal.: Calcd. for C₁₅H₁₂BrNO₂ (318): C, 56.6; H, 3.77; N, 4.4. Found: C, 56.91; H, 3.58; N, 4.11.

References

- Welch, W. M.; Kraska, A. R.; Sarges, R.; Kow, B. K.; *J. Med. Chem.*, **1984**, *27*, 1508.
- Stalker, R. A.; Munsch, T. E.; Tran, J. D.; Nie, X.; Warmuth, R.; Beatty, A.; Aakeroy, C.B.; *Tetrahedron*, **2002**, *58*, 4837.
- Koehler, K.; Gillner, M.; Liu, Y.; Cheng, A.; Heck, J. V.; Hammond, M. L.; Mosley, R. T.; Rahimi, G. M.; *Pct Int Appl* **2002**, WO 0246134.
- Woudenberg, R. H.; *PCT Int Appl* **2002**, WO 0236537, *Chem. Abstr.*, **2002**, *136*, 369521.
- Mori, H.; Hachiya, T.; *Jpn. Kokai Tokkyo Koho JP*, **2001**, 2001247505, *Chem. Abstr.*, **2001**, *135*, 242011.
- Shin, H.; Deng, L.; Carrera, C. J.; Adachi, S.; Cottam, H. B.; Carson, D. A.; *Bioorg. Med. Chem.*, **2000**, *10*, 487.
- Sheng, R.; Xu, Y.; Hu, C.; Zhang, J.; Lin, X.; Li, J.; Yang, B.; He, Q.; Hu, Y.; *Eur. J. Med. Chem.*, **2009**, *44*, 7.
- Saxena, H.O.; Faridi, U.; Srivastava, S.; Kumar, J.K.; Darokar, M.P.; Luqman, S.; Krishna, C.S.; Negi, A.S.; Khanuja, S.P.; *Bioorg. Med. Chem. Lett.*, **2008**, *18*, 3914.
- Finkielstein, L. M.; Castro, E. F.; Fabian, L. E.; Moltrasio, G. Y.; Campos, R. H.; Cavallero, L. V.; Moglioni, A. G.; *Eur. J. Med. Chem.*, **2008**, *43*, 1767.
- Kerr, D. J.; Hamel, E.; Jung, M. K.; Flynn, B. L.; *Bioorg. Med. Chem.*, **2007**, *15*, 3290.
- Singh, R.; Kaur, H.; *Synthesis* **2009**, *15*, 2471.
- Ngel, D. G.; Zahu, Y. D.; Park, P. U.; Paul, V. J.; Ragbhandari, L.; Duncan, C.; Pasco, D. S.; *J. Nat. Prod.*, **2000**, *63*, 1431.
- Lorand, T.; Kocsis, B.; Nagy, G.; Jozser, P.; Kispal, G.; Laszlo, R.; Proai, L.; *Eur. J. Med. Chem.*, **2002**, *37*, 803.
- Yin, W.; Ma, Y.; Xu, J.; Zhao, Y.; *J. Org. Chem.*, **2006**, *71*, 4312.
- Parakash, G. S.; Pakina, F.; Vaghoo, .; Rasul, G.; Mathew, T.; Olah, G.; *J. Org. Chem.*, **2010**, *75*, 2219.
- Fillion, F.; Dumas, A. M.; *J. Org. Chem.*, **2008**, *73*, 2920.
- Fillion, F.; Fishlock, D.; Wilsily, A.; Goll, J. M.; *J. Org. Chem.*, **2005**, *70*, 1316.
- Fillion, F.; Fishlock, D.; *Org. Lett.*, **2003**, *5*, 4653.

- ¹⁹Vasilyev, A. V.; Walspurger, S.; Pale, P.; Sommer, J.; *Tetrahedron Lett.*, **2004**, *45*, 3379.
- ²⁰Kangani, O.; Day, B.W.; *Org. Lett.*, **2008**, *10*, 2645.
- ²¹Coyanis, E.M.; Panayides, J.L.; Fernandes, M.A.; Koning, C.B.; Van-Otterlo, A.L.; *J. Organomet. Chem.*, **2006**, *691*, 5222.
- ²²Womack, G.B.; Angeles, J.G.; Fanetti, V.E.; Indradas, B.; Snowden, R.L.; Sonnay, P.; *J. Org. Chem.*, **2009**, *74*, 5738.
- ²³Womack, G.B.; Angeles, J.G.; Fanetti, V.E.; Heyer, C.A.; *J. Org. Chem.*, **2007**, *72*, 7046.
- ²⁴Holden, M.S.; Crouch, D.; Barker, K.A.; *J. Chem. Educ.*, **2005**, *82*, 934.
- ²⁵Nguyen, P.; Corpuz, E.; Heidelbaugh, M.; Chow, K.; Garst, E., *J. Org. Chem.*, **2003**, *68*, 10195.
- ²⁶Prakash, K.S.; Yan, P.; Torok, b.; Olah, G.A.; *Cata Lett.*, **2003**, *87*, 109.
- ²⁷Ismail, F.; El-Khamry, F.; Said, F.; Younes, H.; Mansour, M.; *Synth. Commun.*, **1996**, *26*, 1223.
- ²⁸Azab, M.; Madkour, H.; Mahmoud, M.R.; *Synth. Commun.*, **2002**, *32*, 393.
- ²⁹Mahmoud, M.R.; El-Shawi, M.; Farahat, S.; *J. Chem. Res.*, **2008**, 59.
- ³⁰Maekawa, K.; Shinozuka, A.; Naito, M.; Igarashi, T.; Sakurai, T.; *Tetrahedron*, **2004**, *60*, 10293.
- ³¹Gelmi, M.L.; Clerici, F.; Beccalli, E.M.; *Tetrahedron*, **1999**, *55*, 781.
- ³²Keni, M.; Tepe, J.J.; *J. Org. Chem.*, **2005**, *70*, 4211.
- ³³Madkour, H.M.; *Chem. Pap.*, **2002**, *56*, 313.
- ³⁴El-Zohry, M.F.; El-Khawaga, A.M.; *J. Org. Chem.*, **1990**, *55*, 4036.
- ³⁵Kumamoto, T.; Etomi, N, Nakanishi, W.; Ishikawa, T.; *Bielst. J. Org. Chem.*, **2008**, *4*, 15.

Received: 29.05.2013.

Accepted: 06.07.2013.



OXIDATION OF SOME ALIPHATIC ALDEHYDES BY QUINOLINIUM CHLOROCHROMATE: A KINETIC AND MECHANISTIC STUDY

Seema Panwar^[a], Shilpa Pohani^[a], Preeti Swami^[b], Shweta Vyas^[c] and Pradeep K. Sharma^{*[a]}

Keywords: aliphatic aldehydes, correlation analysis, quinolinium chlorochromate, kinetics, mechanism, oxidation

The oxidation of six aliphatic aldehydes by quinolinium chlorochromate (QCC) in dimethyl sulfoxide (DMSO) leads to the formation of corresponding carboxylic acids. The reaction is first order in QCC. A Michaelis-Menten type of kinetics is observed with respect to the aldehydes. The reaction is catalysed by hydrogen ions, the hydrogen-ion dependence has the form: $k_{\text{obs}}=a + b[\text{H}^+]$. The oxidation of deuteriated acetaldehyde, MeCDO, exhibited a substantial primary kinetic isotope effect ($k_{\text{H}}/k_{\text{D}}=5.78$ at 298 K). The oxidation of acetaldehyde has been studied in nineteen different organic solvents. The solvent effect has been analysed using Taft's and Swain's multiparametric equations. The rate constants correlate well with Taft's σ^* values; reaction constants being negative. A mechanism involving transfer of hydride ion has been suggested.

Corresponding Authors

E-Mail: drpkvs27@yahoo.com

- [a] Department of Chemistry, J.N.V. University, Jodhpur 342 005, India
[b] Department of Applied Sciences, Global College of Technology, EPIP, Sitapura, Jaipur - India
[c] Department of Chemistry, University of Kota, Kota – India

and passing its vapours in DMSO. The amount of HCHO in DMSO was determined by chromotropic acid method⁸. Other aldehydes were commercial products and were used as such. p-Toluenesulphonic acid (TsOH) was used as a source of hydrogen ions. Deuteriated acetaldehyde (MeCDO) was obtained from Sigma Chemicals. Solvents were purified by their usual methods.⁹

Introduction

Various halochromates have been used as mild and selective oxidizing reagents in synthetic organic chemistry.¹ Quinolinium chlorochromate (QCC) is one such compound used for the oxidation of compounds of industrial importance.² Oxidation of substituted benzaldehydes with various oxidants is an intensively studied area as well.³ We have been interested in the kinetic and mechanistic aspects of the oxidation by complexed Cr(VI) species and several reports on halochromates have already been reported from our laboratory.^{4,6} There seems to be only a few reports on the oxidation aspects of QCC are available in literature.⁷ In continuation of our earlier work, we report here the kinetics and mechanism of oxidation of six aliphatic aldehydes by QCC in dimethylsulphoxide (DMSO) as solvent. The mechanistic aspects are discussed.

The main aims of the present investigation are to (i) determine kinetic parameters and to evaluate the rate laws, (ii) to study the correlation analysis of effect of structure on rate and (iii) to postulate a suitable mechanism for the oxidation process.

Experimental Section

Materials

QCC was prepared by the reported method² and its purity checked by an iodometric determinations. Solutions of formaldehyde were prepared by heating para-formaldehyde

Product analysis

The product analysis was carried out under kinetic conditions. In a typical experiment, acetaldehyde (4.4 g, 0.1mol) and QCC (1.88 g, 0.01mol) were dissolved in DMSO (100 ml) and the reaction mixture was allowed to stand for *ca.* ≈ 24 h to ensure completion of the reaction. It was then rendered alkaline with NaOH, filtered and the filtrate was reduced to dryness under pressure. The residue was acidified with perchloric acid and extracted with diethyl ether (5 %, 50 ml). The ether extract was dried (MgSO_4) and treated with 10 ml of thionyl chloride. The solvent was allowed to evaporate. Dry methanol (7 ml) was added and the HCl formed was removed in a current of dry air. The residue was dissolved in diethyl ether (200 ml) and the ester content was determined colorimetrically as Fe(III) hydroxymate by the procedure of Hall and Schaefer.¹⁰ Several determinations indicated a 1:1 stoichiometry. The oxidation state of chromium in a completely reduced reaction mixture, determined by iodometric titrations was 3.95 ± 0.1 .

Kinetic Measurements

Pseudo-first-order conditions were attained by keeping an excess ($\times 15$ or greater) of the [aldehyde] over [QCC]. The solvent was DMSO, unless mentioned otherwise. All reactions were carried out in flasks blackened from the outside to prevent any photochemical reactions. The reactions were carried out at constant temperature (± 0.1 K) and were followed up to 80% of the extent of reaction, by

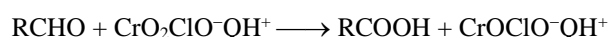
monitoring the decrease in [QCC] at 352 nm. The pseudo-first-order rate constant, k_{obs} , was computed from the linear least-squares plot of $\log [\text{QCC}]$ versus time. Duplicate runs showed that the rate constants were reproducible to within $\pm 3\%$. The second order rate constant, k_2 , was calculated from the relation: $k_2 = k_{\text{obs}}/[\text{aldehyde}]$.

Results

The rate and other experimental data were obtained for all the aldehydes. Since the results are similar, only representative data are reproduced here.

Stoichiometry

The oxidation of aliphatic aldehydes by QCC leads to the formation of corresponding carboxylic acids. The overall reaction may therefore, be written as:



QCC undergoes two-electron change. This is in accordance with the earlier observations with structurally similar other halochromates also. It has already been shown that both pyridinium chlorochromate (PCC)¹¹ and pyridinium fluorochromate (PFC)¹² act as two electron oxidants and are reduced to chromium (IV) species, determining the oxidation state of chromium by magnetic susceptibility, ESR and IR studies.

Rate-laws

The reactions are of first order with respect to QCC. Further, the pseudo-first order rate constant, k_{obs} is independent of the initial concentration of QCC. The reaction rate increases with increase in the concentration of the aldehydes but not linearly (Table 1).

Table 1. Rate constants for the oxidation of acetaldehyde by QCC at 288 K

| $10^3 [\text{QCC}]$ mol dm^{-3} | $[\text{MeCHO}]$ mol dm^{-3} | $[\text{TsOH}]$ mol dm^{-3} | $10^4 k_{\text{obs}}$ s^{-1} |
|---|--|---|--|
| 1.00 | 0.10 | 0.00 | 7.79 |
| 1.00 | 0.20 | 0.00 | 11.3 |
| 1.00 | 0.40 | 0.00 | 14.3 |
| 1.00 | 0.60 | 0.00 | 16.2 |
| 1.00 | 0.80 | 0.00 | 17.1 |
| 1.00 | 1.00 | 0.00 | 17.8 |
| 1.00 | 1.50 | 0.00 | 18.6 |
| 1.00 | 3.00 | 0.00 | 19.6 |
| 2.00 | 0.40 | 0.00 | 15.5 |
| 4.00 | 0.40 | 0.00 | 14.6 |
| 6.00 | 0.40 | 0.00 | 15.0 |
| 8.00 | 0.40 | 0.00 | 14.4 |
| 1.00 | 0.20 | 0.00 | 12.6 |

* contained $0.001 \text{ mol dm}^{-3}$ acrylonitrile

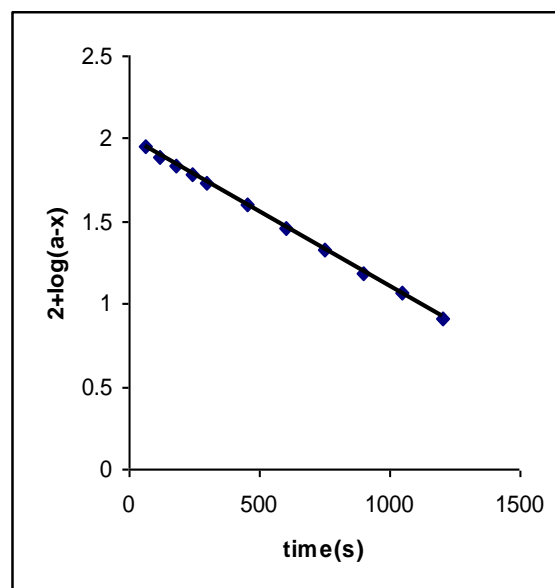
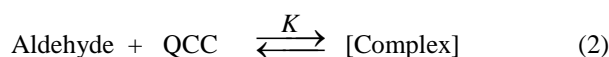


Figure 1. Oxidation of Acetaldehyde by QCC: A typical Kinetic Run

The Fig 1 depicts a typical kinetic run. A plot of $1/k_{\text{obs}}$ against $1/[\text{aldehyde}]$ is linear ($r > 0.995$) with an intercept on the rate-ordinate (Fig. 2). Thus, Michaelis-Menten type kinetics is observed with respect to the aldehydes. This leads to the postulation of following overall mechanism (2) and (3) and rate law (4).



The dependence of reaction rate on the reductant concentration was studied at different temperatures and the values of K and k_2 were evaluated from the double reciprocal plots. The thermodynamic parameters of the complex formation and activation parameters of the decomposition of the complexes were calculated from the values of K and k_2 respectively at different temperatures (Tables 3 and 4).

$$\text{Rate} = \frac{k_2 K [\text{Aldehyde}] [\text{QCC}]}{1 + K [\text{Aldehyde}]} \quad (4)$$

Induced polymerization of acrylonitrile/test for free radicals

The oxidation of aldehydes, in an atmosphere of nitrogen, failed to induce polymerisation of acrylonitrile. Further, the addition of acrylonitrile did not affect the rate. This indicates that a one-electron oxidation, giving rise to free radicals, is unlikely in the present reaction (Table 1). To further confirm the absence of free radicals in the reaction pathway, the reaction was carried out in the presence of 0.05 mol dm^{-3} of 2,6-di-*t*-butyl-4-methylphenol (butylated hydroxytoluene or BHT). It was observed that BHT was recovered unchanged, almost quantitatively.

Table 2. Dependence of the reaction rate on hydrogen-ion concentration

| [Aldehyde]: 0.10 mol dm ⁻³ | [QCC]: 0.001 mol dm ⁻³ | | | | Temperature: 298 K | |
|---|-----------------------------------|------|------|------|--------------------|------|
| [TsOH]/ mol dm ⁻³ | 0.10 | 0.20 | 0.40 | 0.60 | 0.80 | 1.00 |
| 10 ⁴ k _{obs} /s ⁻¹ | 9.18 | 10.8 | 13.5 | 16.2 | 18.9 | 22.5 |

Table 3. Rate constants and activation parameters of the oxidation of aliphatic aldehydes – QCC complexes.

| R | 10 ⁴ k ₂ (dm ³ mol ⁻¹ s ⁻¹) | | | | ΔH*, kJ mol ⁻¹ | -ΔS*, J mol ⁻¹ K ⁻¹ | ΔG*, kJ mol ⁻¹ |
|--------------------------------|---|------|------|------|------------------------------|--|------------------------------|
| | 288 | 298 | 308 | 318 | | | |
| H | 1.48 | 3.60 | 7.92 | 18.0 | 60.5±0.6 | 108±2 | 92.7±0.4 |
| Me | 20.7 | 45.9 | 90.9 | 189 | 53.2±0.6 | 112±2 | 86.4±0.5 |
| Et | 35.1 | 77.4 | 144 | 297 | 50.9±0.9 | 115±3 | 85.2±0.8 |
| Pr | 38.7 | 80.1 | 153 | 315 | 50.3±0.9 | 117±3 | 85.0±0.7 |
| Pr ⁱ | 57.8 | 117 | 234 | 459 | 50.3±0.9 | 117±3 | 85.0±0.7 |
| ClCH ₂ | 0.072 | 0.20 | 0.49 | 1.26 | 69.7±0.7 | 102±2 | 99.8±0.6 |
| MeCDO | 3.42 | 7.29 | 15.3 | 32.4 | 54.4±0.7 | 123±2 | 90.9±0.6 |
| k _H /k _D | 6.01 | 5.78 | 5.63 | 5.38 | | | |

Kinetic isotope effect

To ascertain the importance of the cleavage of the aldehydic C–H bond in the rate-determining step, the oxidation of deuteriated acetaldehyde (MeCDO) was studied. The oxidation of deuteriated acetaldehyde exhibited a substantial primary kinetic isotope effect (Table 3).

Effect of acidity

The reaction is catalysed by hydrogen ions (Table 2). The hydrogen-ion dependence has the following form $k_{\text{obs}} = a + b[\text{H}^+]$. The values of a and b , for acetaldehyde, are $1.81 \pm 0.46 \times 10^{-4} \text{ s}^{-1}$ and $3.23 \pm 0.76 \times 10^{-4} \text{ mol}^{-1} \text{ dm}^3 \text{ s}^{-1}$ respectively ($r^2 = 0.9978$).

$$\text{Rate} = k_2[\text{QCC}][\text{Aldehyde}] + k_3[\text{QCC}][\text{Aldehyde}][\text{TsOH}]$$

(5)

Effect of solvents

The oxidation of acetaldehyde was studied in 19 different organic solvents. The choice of solvents was limited due to the solubility of QCC and its reaction with primary and secondary alcohols. There was no reaction with the solvents chosen. The kinetics was similar in all the solvents. The values of formation constants K and of decomposition constants of the complex, k_2 are recorded in Table 5.

Discussion

There is a fair correlation between the activation enthalpies and entropies of the oxidation of aldehydes ($r^2 = 0.9782$), indicating the operation of a compensation effect¹³. A correlation between the calculated values of enthalpies and entropies is often vitiated by the experimental errors associated with them. The reaction, however, exhibited an

excellent isokinetic relationship, as determined by Exner's method¹⁴. An Exner's plot between $\log k_2$ at 288 K and at 318 K was linear ($r^2 = 0.9992$) (Figure 3). The value of isokinetic temperature evaluated from the Exner's plot is $882 \pm 25 \text{ K}$. The linear isokinetic correlation implies that all the aldehydes are oxidized by the same mechanism and the change in the rate of oxidation is governed by changes in both the enthalpy and entropy of the activation.

Solvent effect

The rate constants, k_2 , in eighteen solvents (CS₂ was not considered, as the complete range of solvent parameters was not available) were correlated in terms of the linear solvation energy relationship (6) of Kamlet et al.¹⁵

$$\log k_2 = A_0 + p\pi^* + b\beta + \alpha a \quad (6)$$

In this equation, π^* represents the solvent polarity, β the hydrogen bond acceptor basicities and α is the hydrogen bond donor acidity. A_0 is the intercept term. It may be mentioned here that out of the 18 solvents, 12 have a value of zero for α . The results of correlation analyses in terms of (6), a biparametric equation involving π^* and β , and separately with π^* and β are given below as Eqns. 7-10.

$$\log k_2 = -3.97 + 1.41(\pm 0.17)\pi^* + 0.20(\pm 0.14)\beta +$$

$$0.15(\pm 0.13)\alpha \quad (7)$$

$$R^2 = 0.8681; \text{sd} = 0.16; n = 18; \psi = 0.39.$$

$$\log k_2 = -4.01 + 1.47(\pm 0.17)\pi^* + 0.15(\pm 0.11)\beta \quad (8)$$

$$R^2 = 0.8559; \text{sd} = 0.16; n = 18; \psi = 0.40$$

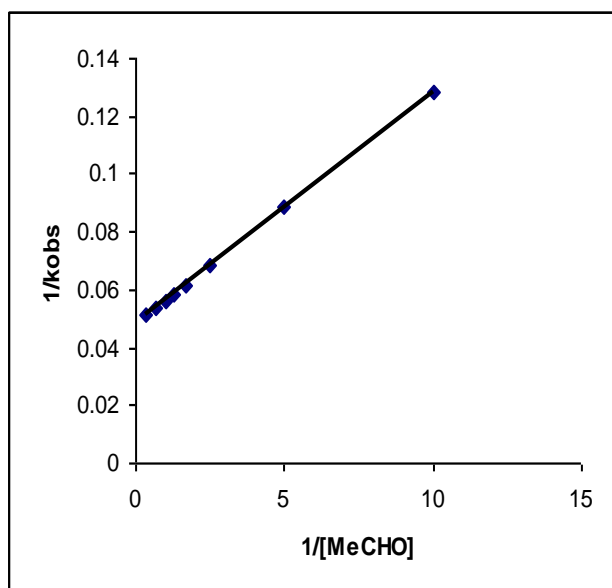


Figure 2. – Oxidation of Aldehyde by QCC: A double reciprocal plot

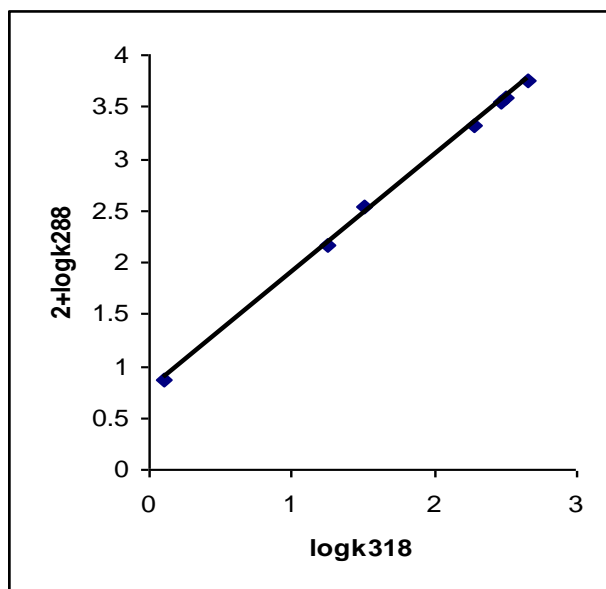


Figure 3. Exner's Isokinetic Relationship in the oxidation of Aldehydes by QCC

$$\log k_2 = -3.98 + 1.51(\pm 0.16)\pi^* \quad (9)$$

$$r^2 = 0.8437; \text{sd}=0.16; n=18; \psi=0.41$$

$$\log k_2 = -3.15 + 0.42(\pm 0.33)\beta \quad (10)$$

$$r^2=0.0806; \text{sd}=0.39; n=18; \psi=0.98$$

Here n is the number of data points and ψ is the Exner's statistical parameter.¹⁶

Kamlet's¹⁵ triparametric equation explains *ca.* 87% of the effect of solvent on the oxidation. However, by Exner's criterion¹⁶ the correlation is not even satisfactory (cf. 7). The major contribution is of solvent polarity. It alone accounted for *ca.* 84% of the data. Both β and α play relatively minor roles.

The data on the solvent effect were analysed in terms of Swain's equation¹⁷ of cation- and anion-solvating concept of the solvents also as equation (11).

$$\log k_2 = aA + bB + C \quad (11)$$

Here A represents the anion-solvating power of the solvent and B the cation-solvating power. C is the intercept term. $(A+B)$ is postulated to represent the solvent polarity. The rates in different solvents were analysed in terms of equation (8), separately with A and B and with $(A+B)$.

$$\log k_2 = 0.61(\pm 0.09)A + 1.60(\pm 0.06)B - 4.24 \quad (12)$$

$$R^2 = 0.9765; \text{sd} = 0.07; n = 19; \psi = 0.07$$

$$\log k_2 = 0.39(\pm 0.53)A - 3.14 \quad (13)$$

$$r^2 = 0.0298; \text{sd} = 0.43; n = 19; \psi = 0.86$$

$$\log k_2 = 1.55(\pm 0.12)B - 4.04 \quad (14)$$

$$r^2 = 0.9091; \text{sd} = 0.18; n = 19; \psi = 0.32$$

$$\log k_2 = 1.27 \pm 0.14(A+B) - 4.21 \quad (15)$$

$$r^2 = 0.8369; \text{sd} = 0.18; n = 19; \psi = 0.41$$

The rates of oxidation of acetaldehyde in different solvents showed an excellent correlation in Swain's equation [cf. (12)] with the cation-solvating power playing the major role. In fact, the cation-solvating alone accounts for *ca.* 97% of the data. The correlation with the anion-solvating power was very poor. The solvent polarity, represented by $(A+B)$, also accounted for *ca.* 83% of the data. In view of the fact that solvent polarity is able to account for *ca.* 80% of the data, an attempt was made to correlate the rate with the relative permittivity of the solvent. However, a plot of $\log k_2$ against the inverse of the relative permittivity is not linear ($r^2 = 0.5253$; $\text{sd} = 0.30$; $\psi = 0.66$).

Correlation analysis of reactivity

The rates of the oxidation of six aldehydes show an excellent correlation with Taft's σ^* substituent constants,¹⁸ the reaction constant being negative (Table 6). The negative polar reaction constant indicates an electron-deficient carbon centre in the transition state of the rate-determining step.

Table 4. Formation constants and thermodynamic parameters of the oxidation of aliphatic aldehydes – QCC complexes.

| R | $10^4 k_2 \text{ dm}^3 \text{ mol}^{-1} \text{ s}^{-1}$ | | | | | ΔH^* , kJ mol ⁻¹ | $-\Delta S^*$, J mol ⁻¹ K ⁻¹ | ΔG^* , kJ mol ⁻¹ | |
|-------------------|---|-----|-----|------|------|--|--|--|---------|
| | 288 | 298 | 308 | 3 | 1 | | | | |
| H | 5.85 | | | 5.23 | 4.57 | 3.96 | 12.40.4 | 201 | 6.560.3 |
| Me | 6.03 | | | 5.45 | 4.79 | 4.15 | 12.00.5 | 180 | 6.570.4 |
| Et | 5.56 | | | 4.92 | 4.33 | 3.70 | 12.70.4 | 221 | 6.420.3 |
| Pr | 5.32 | | | 4.72 | 4.05 | 3.42 | 13.70.6 | 252 | 6.290.4 |
| Pr ⁱ | 5.94 | | | 5.30 | 4.65 | 4.05 | 12.20.3 | 191 | 6.600.3 |
| ClCH ₂ | 6.12 | | | 5.50 | 4.85 | 4.32 | 11.40.2 | 161 | 6.690.2 |
| MeCDO | 5.67 | | | 5.15 | 4.52 | 3.85 | 12.70.5 | 212 | 6.520.4 |

Table 5. Effect of solvents on the oxidation of acetaldehyde-QCC complex at 298 K

| Solvents | $K, \text{ dm}^{-3} \text{ mol}^{-1}$ | $k_{\text{obs}}, \text{ s}^{-1}$ |
|---------------------|---------------------------------------|----------------------------------|
| Chloroform | 6.03 | 14.8 |
| Toluene | 5.84 | 5.25 |
| 1,2-Dichloroethane | 5.85 | 18.2 |
| Acetophenone | 5.45 | 20.0 |
| Dichloromethane | 5.90 | 15.8 |
| THF | 5.26 | 9.77 |
| DMSO | 5.45 | 45.9 |
| t-Butylalcohol | 5.15 | 7.24 |
| Acetone | 6.12 | 17.0 |
| 1,4-Dioxane | 5.34 | 8.51 |
| DMF | 5.38 | 27.5 |
| 1,2-Dimethoxyethane | 5.67 | 5.62 |
| Butanone | 5.90 | 12.0 |
| CS ₂ | 5.89 | 1.57 |
| Nitrobenzene | 5.88 | 22.4 |
| Acetic acid | 5.50 | 3.34 |
| Benzene | 6.15 | 5.25 |
| Ethyl Acetate | 5.19 | 7.76 |
| Cyclohexane | 5.18 | 0.85 |

Table 6. Temperature dependence of the reaction constant

| Temp. | 288 K | 298 K | 308 K | 318 K |
|----------|------------|------------|------------|------------|
| ρ^* | -2.34±0.01 | -2.24±0.02 | -2.15±0.01 | -2.06±0.05 |
| r^2 | 0.9999 | 0.9998 | 0.9999 | 0.9989 |
| SD | 0.003 | 0.009 | 0.009 | 0.006 |
| ψ | 0.01 | 0.02 | 0.01 | 0.04 |

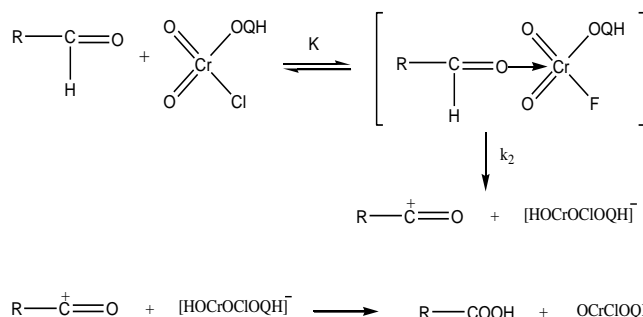
Mechanism

The observed hydrogen-ion dependence suggests that the reaction follows the two mechanistic pathways, one is acid-independent and the other is acid dependent. The acid-catalysis may well be attributed to a protonation of QCC to give a stronger oxidant and electrophile (16). Both QCC and QCCH⁺ are reactive species with the protonated form being more reactive.



Formation of a protonated Cr(VI) species has earlier been reported in the reactions of structurally similar halochromates.⁷⁻¹⁰

In aqueous solutions most aliphatic aldehydes exist predominantly in the hydrate form¹⁹ and in many oxidations, in aqueous solutions, it has been postulated that the hydrate is the reactive species. However, owing to the non-aqueous nature of the solvent in the present reaction, only the free carbonyl form can be the reactive species. The presence of a substantial primary kinetic isotope effect ($k_{\text{H}}/k_{\text{D}} = 5.78$ at 298 K), confirms that the aldehydic C-H bond is cleaved in the rate-determining step. The large negative value of the polar reaction constant together with the substantial deuterium isotope effect indicates that the transition state approaches a carbocation in character. Hence, transfer of a hydride ion from the aldehyde to the oxidant is suggested. The hydride ion transfer mechanism is also supported by major role of cation-solvating power of the solvents.



Scheme - 1

High values of activation indicate that in the rate determining step bond breaking is more important in transition state. Large negative entropy of activation supports a transition state formed from two independent molecules.

Conclusion

The reaction is proposed to proceed through a hydride-ion transfer from aldehyde to the oxidant. The hydride ion

transfer mechanism is also supported by major role of cation-solvating power of the solvents. Both deprotonated and protonated forms of QCC are the reactive oxidising species. An aldehydic C–H bond is cleaved in the rate-determining step.

References

- ¹Corey, E. J., Suggs, W. J. *Tetrahedron Lett.*, **1975**, 2647; Guziec, F. S., Luzio, F. A. *Synthesis*, **1980**, 691; Bhattacharjee, M. N., Choudhuri, M. K., Dasgupta, H. S., Roy, N., Khathing, D. T. *Synthesis*, **1982**, 588; Balasubramanian, K., Prathiba, V. *Indian J. Chem.*, **1986**, 25B, 326; Pandurangan, A., Murugesan, V., Palamichamy, P. *J. Indian Chem. Soc.*, **1995**, 72, 479; Sharma, P. D., Panchariya, P., Purohit, P., Sharma, P. K., *Eur. Chem. Bull.*, **2013**, 2(10), 816-824; Panchariya, P., Purohit, T., Sharma, D., Malani, N., Kotai, L., Sharma, P. K., *J. Ind. Chem. Soc.*, **2012**, 89(9), 1203-1207; Daiya, A., Purohit, P., Kumbhat, R., Kotai, L., Sharma, V., *Int. J. Chem.*, **2012**, 1(2), 230-240; Gilla, M., Meena, A., Choudhary, A., Baghmar, M., Sharma, I. K., Kotai, L., Sharma, V., *J. Chem. Biol. Phys. Sci.*, **2011**, 1(1), 30-38; Barthora, S., Baghmar, D., Gilla, M., Choudhary, A., Kotai, L., V. Sharma, *J. Chem. Biol. Phys. Sci.*, **2011**, 1(1), 7-20; Panchariya, P., Vadera, K., Malani, N., Prasadrao, P., Kotai, L., Sharma, P. K., *J. Chem. Asia*, **2011**, 2(4), 225-229.
- ²Singh, J., Kalsi, P. S., Jawanda, J. S., Chhabra, B. R., *Chem. Ind.*, **1986**, 751.
- ³Banerji, J., Kotai, L., Sharma, P. K., Banerji, K. K., *Eur. Chem. Bull.*, **2012**, 1(5), 135-140; Ashgar, B. H., Mansoor, S. S., Malik, V. S., *Eur. Chem. Bull.*, **2013**, 2(8), 538-544; Purohit, T., Banerji, J., Kotai, L., Sajo, I., Banerji, K. K., Sharma, P. K., *J. Ind. Chem. Soc.*, **2012**, 89, 1045-1052.
- ⁴Vadera, K., Yajurvedi, D., Purohit, P., Mishra, P., Sharma, P. K., *Prog. React. Kinet. Mech.*, **2010**, 35, 265; Sharma, D., Panchariya, P., Vadera, K., Sharma, P. K. *J. Sulfur Chem.*, **2011**, 32(4) 315–326; Khatri, J., Choudhary, A., Purohit, P., Kumbhat, R., Sharma, V., *Eur. Chem. Bull.*, **2012**, 1, 49-57;
- ⁵Sharma, D., Panchariya, P., Vyas, S., Kotai, L., Sharma, P.K. *Int. J. Chem.*, **2012**, 1(1), 29;
- ⁶Sharma, D., Panchariya, P., Purohit, P., Sharma, P.K. *Oxid. Commun.*, **2012**, 35(4) 821; Panchariya, P.; Purohit, T.; Swami, P.; Malani, N.; Kotai, L.; Prakash, O; Sharma, P. K. *Int. J. Chem. Sci.*, **2012**, 10, 557-567.
- ⁷Khatri, J., Sharma, D., Vyas, S., Prakash, O., Sharma, V., *Int. J. Chem.*, **2012**, 1(3), 353; Vyas, N., Sharma, A., Daiya, A., Choudhary, A., Sharma, M., Sharma, V., *Eur. Chem. Bull.*, **2013**, 2(11), 859-865.
- ⁸Mitchell J. Jr., *Organic analysis*, Vol. II, Interscience, New York, , **1954**, 273.
- ⁹Perrin, D. D., Armarego, W. L., Perrin, D. R., *Purification of organic compounds*, Oxford, Pergamon Press, **1966**.
- ¹⁰Hall, R. T., Schaefer, W. E., *Organic Analysis*, Vol II, Interscience, New York, **1954**, 55.
- ¹¹Bhattacharjee, M. N., Choudhuri, M. K., Purakayastha S. *Tetrahedron*, **1987**, 43, 5389.
- ¹² Brown, H. C., Rao, G. C., Kulkarni, S. U., *J. Org. Chem.*, **1979**, 44, 2809.
- ¹³Liu, L., Guo, W. E. , *Chem Rev.*, **2001**, 101, 673.
- ¹⁴Exner, O. *Coll. Chem. Czech. Commun.*, **1977**, 38, 411.
- ¹⁵Kamlet, M. J., Abboud, J. L. M., Abraham, M. H., Taft, R. W., *J. Org. Chem.*, **1983**, 48, 2877.
- ¹⁶Exner, O. *Coll. Chem. Czech. Commun.*, **1966**, 31, 3222.
- ¹⁷Swain, C. G., Swain, M. S., Powel, A. L., Alunni, S., *J. Am. Chem. Soc.*, **1983**, 105, 502.
- ¹⁸Taft, R. W., *Steric effects in organic chemistry*, Ed. M. S. Newman, Wiley, New York, **1956**, 13.
- ¹⁹Bell, R. P., *Adv. Phys. Org. Chem.*, **1966**, 4, 1.

Received: 03.06.2013.

Accepted: 06.07.2013.



PYRIDAZINE AND ITS RELATED COMPOUNDS, PART 27.¹⁾

SYNTHESIS AND INSECTICIDAL ACTIVITY OF SOME PYRIDAZINE DERIVATIVES

Ali Deeb^{[a],*}, Elsayed Mourad^[b] and Diaa Elenany^[b]

Keywords: Pyridazine derivatives, synthesis, insecticide activity, *Mucsa domestica*, *Macrosiphum pisi*

An effective methods has been developed for the preparation under mild conditions of novel pyridazine derivatives from the easily accessible starting materials benzilmonohydrazone, p,p'-dichlorobenzilmono-hydrazone, diethyl malonate and ethyl phenylacetate. All the synthesized compounds were fully characterized and some of them displayed good insecticide activities against *Mucsa domestica* and *Macrosiphum pisi* in preliminary insecticide activity tests.

Corresponding Authors

E-Mail: dralideeb@hotmail.com

[a] Department of Chemistry, Faculty of Science, Zagazig University, Egypt

[b] Central Agricultural Pesticides Laboratory, Agricultural Research Center, El-Mansoura, Egypt 2

Introduction

Many pyridazine are well known to possess a wide range of bioactivities and are often employed as plant virucides,² antitumor agents,³ fungicides,⁴ insecticides,⁵ herbicides⁶ and anti-inflammatory agents.⁷ They have immense potential in agricultural science as plant growth regulators and crop protection agents. Several derivatives of these compounds incorporating 1,3,4-thiadiazole, 1,3,4-oxadiazole and oxazolidin-2-one rings have been shown to display moderate to good insecticide activities.⁸ The present investigation, which is a continuation of our previous work⁹ on pyridazine derivatives and related compounds, deals with the synthesis of different substituted pyridazines and studies their insecticidal activities.

Materials and Methods

Instruments and reagents

Melting points were determined in open-glass capillaries using Buchi 510 apparatus and were reported uncorrected. Infrared spectra were recorded as potassium bromide disks on a Bruker Vector 22 Germany spectrometer. ¹H-NMR spectra were obtained on a Varian Gemini 200 MHz spectrometer, and chemical shifts are expressed in δ ppm using TMS as an internal standard. Electron impact mass spectra were obtained at 70 eV using a GCMS-1000 Ex Shimadzu spectrometer, elemental analysis was performed on an Elemental Vario-

III CHN analyzer. The course of the reactions was monitored by TLC; analytical TLC was performed on silica gel GF₂₅₄; column chromatographic purification was carried out using silica gel.

Preparation of ethyl 3-chloro-5,6-diarylpyridazine-4-carboxylates (3a,b)

A mixture of pyridazinone derivatives **1a,b** (10 mmol) and phosphoryl chloride (10 mL) was refluxed for 4 hours. The cooled reaction mixture was poured onto ice-H₂O (50 mL), the precipitate was filtered off, dried and recrystallized from ethanol to give **3a,b**.

Ethyl 3-chloro-5,6-diphenylpyridazine-4-carboxylate (3a): Yield as 95%; Mp. 118-120 °C; IR (KBr) cm⁻¹: 3050, 2983, 1735, 761. ¹H NMR, δ ppm (DMSO-*d*₆): 7.43-7.30 (m, 10H, 2Ph-H), 4.31 (q, 2H, CH₂), 1.20 (t, 3H, CH₃). Anal. Calcd for C₁₉H₁₅ClN₂O₂: C, 67.36; H, 4.46; N, 8.27. Found: C, 67.20; H, 4.30; N, 8.10.

Ethyl 3-chloro-5,6-bis(4-chlorophenyl)pyridazine-4-carboxylate (3b): Yield 96%; Mp. 80-82 °C; IR (KBr) cm⁻¹: 3088, 2932, 1734, 782. ¹H NMR, δ ppm (DMSO-*d*₆): 7.79-7.41 (m, 8H, 2Ar-H), 4.30 (q, 2H, CH₂), 1.29 (t, 3H, CH₃). Anal. Calcd for C₁₉H₁₃Cl₃N₂O₂: C, 55.97; H, 3.21; N, 6.87. Found: C, 55.90; H, 3.00; N, 6.70.

Preparation of ethyl 6,7-diaryltetrazolo[1,5-b]pyridazine-8-carboxylates (4a,b)

Sodium azide (0.65g, 10.0 mmol) was added to a solution of ethyl 3-chloro-5,6-diarylpyridazine-4-carboxylates **3a,b** (4.0 mmol) in ethanol (20 mL). The stirred reaction mixture was heated under reflux for 6 hours. The solvent was evaporated under reduced pressure, then the solid residue was diluted with H₂O (100 mL) and the precipitated product was isolated by suction, dried and recrystallized from ethanol to give title compounds **4a,b**.

Ethyl 6,7-diphenyltetrazolo[1,5-b]pyridazine-8-carboxylate (**4a**): Yield 76%, Mp. 147-148 °C (as reported).¹¹⁾

Ethyl 6,7-bis(4-chlorophenyl)tetrazolo[1,5-b]pyridazine-8-carboxylate (**4b**): Yield 72%, Mp. 145-147 °C; IR (KBr) cm^{-1} : 3061, 2981, 1741, 730. ^1H NMR, δ ppm (DMSO- d_6): 7.78-7.42 (m, 8H, 2Ar-H), 4.30 (q, 2H, CH_2), 1.29 (t, 3H, CH_3). MS (m/z): 414 (M^+ , 5.1%), 343 [M^+ - CO_2Et , 1.1% (ion A)], 330 [(ion A) - N, 17.8% (ion B)], 303 [(ion B) - N_2 , 2%]. Anal. Calcd for $\text{C}_{19}\text{H}_{13}\text{Cl}_2\text{N}_5\text{O}_2$: C, 55.09; H, 3.16; N, 16.91. Found: C, 55.00; H, 3.00; N, 16.80.

Preparation of 4,5-diaryl-3-hydroxy-1H-pyrazolo[3,4-c]pyridazine (5a,b)

To solution of 3-chloro derivatives **3a,b** (7.0 mmol) in 1-butanol (15 mL) hydrazine hydrate (2 mL, 80%) was added. The reaction mixture was refluxed for 4 hours, upon cooling the solid product formed was filtered, dried and recrystallized from methanol to give title compounds **5a,b**

3-Hydroxy-4,5-diphenyl-1H-pyrazolo[3,4-c]pyridazine (**5a**): Yield 90%, Mp. 285-287 °C (dec.). IR (KBr) cm^{-1} : 3274, 3059, 1439. ^1H NMR, δ ppm (DMSO- d_6): 13.26 (s, 1H, NH), 11.53 (s, 1H, OH), 7.41-7.79 (m, 10H, 2 Ph-H). MS (m/z): 288 (M^+ , 56.8%), 287 (M^+ - H, 100%), 286 (M^+ - 2H, 1.3%). Anal. Calcd for $\text{C}_{17}\text{H}_{12}\text{N}_4\text{O}$: C, 70.82; H, 4.19; N, 19.43. Found: C, 70.70; H, 4.00; N, 19.30.

4,5-Bis(4-chlorophenyl)-3-hydroxy-1H-pyrazolo[3,4-c]pyridazine (**5b**): Yield 85%, Mp. 290-292 °C (dec.). IR (KBr) cm^{-1} : 3094, 1619, 748. ^1H NMR, δ ppm (DMSO- d_6): 13.26 (s, 1H, NH), 11.53 (s, 1H, OH), 7.55-7.79 (m, 8H, 2 Ar-H). MS (m/z): 359 (M^+ + 2, 23.85%), 358 (M^+ + 1, 66.72%), 357 (M^+ , 86.01%), 355 (M^+ - 2H, 100%). Anal. Calcd for $\text{C}_{17}\text{H}_{10}\text{Cl}_2\text{N}_4\text{O}$: C, 57.16; H, 2.82; N, 15.69. Found: C, 57.10; H, 2.70; N, 15.00.

Preparation of 2-carbethoxy-4,5-diphenyl-3-oxo-1H-pyrazolo[3,4-c]pyridazine (6)

A mixture of 3-hydroxy derivative **5a** (1.2 g, 4.0 mmol) and ethyl chloroformate (5 mL) was heated under reflux for 3 hr, upon cooling the solid product formed was filtered off, dried and recrystallized from ethanol to give title compound **6**, yield 98.9%, Mp. 110-112 °C; IR (KBr) cm^{-1} : 3057, 2980, 1760. ^1H NMR, δ ppm (DMSO- d_6): 1.29 (t, 3H, CH_3), 4.0 (s, 1H, NH), 4.13 (q, 2H, CH_2), 7.41-7.79 (m, 10H, 2Ph-H). MS (m/z): 360 (M^+ , 59%), 287 (M^+ - CO_2Et , 100%), 231 (M^+ - HNCO_2Et , 9.1%). Anal. Calcd for $\text{C}_{20}\text{H}_{16}\text{N}_4\text{O}_3$: C, 66.56; H, 4.47; N, 15.55. Found: C, 66.50; H, 4.30; N, 15.30.

Preparation of N-ethylthio-4,5-diphenyl-3-oxo-1,2-dihydro-pyrazolo [3,4-c]pyridazine-2-carboxamide (7)

To a solution of 3-hydroxy derivative **5a** (1.8 g, 6.0 mmol) in dry acetone (50 mL), ethyl isothiocyanate (0.87 g, 10.0 mmol) and potassium hydroxide (0.6 g, 10.0 mmol) were added. The reaction mixture was refluxed for 5 hours. The cooled reaction mixture was poured onto water (50 mL) and upon neutralization with hydrochloric

acid, a precipitate which obtained was filtered, washed several times with water, dried and recrystallized from ethanol, to afford compound **7**, yield 91%; Mp. 230-232 °C. IR (KBr) cm^{-1} : 3169, 3085, 2818, 1656, 1164. ^1H NMR, δ ppm (DMSO- d_6): 0.86 (t, 3H, CH_3), 1.57 (q, 2H, CH_2), 2.0 (s, 1H, NH), 4.0 (s, 1H, pyrazolo NH), 7.42-7.79 (m, 10H, 2-Ph-H). MS (m/z): 375 (M^+ , 1.1%). Anal. Calcd for $\text{C}_{20}\text{H}_{17}\text{N}_5\text{OS}$: C, 63.97; H, 4.57; N, 18.66. Found: C, 63.90; H, 4.50; N, 18.50.

Preparation of 5,6-diaryl-3-oxo-2,3-dihydropyridazine-4-carbohydrazides (8a,b)

To a solution of 4-carbethoxy derivatives **1a,b** (5.0 mmol) in 1-butanol (20 mL), hydrazine hydrate (1 mL, 80%) was added. The reaction mixture was heated under reflux for 5 hours. After cooling the solid product formed was filtered, dried and recrystallized from ethanol to give title compounds **8a,b**.

5,6-Diphenyl-3-oxo-2,3-dihydropyridazine-4-carbohydrazide (**8a**): Yield 73%; mp 123-125 °C, (as reported)¹¹⁾.

5,6-Bis(4-chlorophenyl)-3-oxo-2,3-dihydropyridazine-4-carbohydrazide (**8b**): Yield 72%; Mp. 193-195 °C. IR: (KBr) cm^{-1} : 3422, 3189, 1651. ^1H NMR, δ ppm (DMSO- d_6): 2.0 (s, 2H NH₂), 7.0 (s, 1H, ring NH), 7.52-7.77 (m, 8H, Ar-H), 8.0 (s, 1H, NH). Anal. Calcd. for $\text{C}_{17}\text{H}_{12}\text{Cl}_2\text{N}_4\text{O}_2$: C, 54.42; H, 3.22; N, 14.93. Found: C, 54.30; H, 3.10; N, 14.80.

Preparation of 5,6-diaryl-3-oxo-2,3-dihydropyridazine-4-yl-carboxylic acids (9a,b)

A slurry of carbohydrazide derivatives **8a,b** (3.0 mmol), water (15 mL), and conc. HCl (30 mL) was cooled to 5 °C. To this slurry was added a solution of sodium nitrite (1.1 g) in water (5 mL) dropwise, after the addition, the cooling bath was removed, the mixture was allowed to warm slowly to room temperature, transferred to a large beaker, and heated on a steam bath until dissolution occurred. Continued heating was accompanied by gas evolution followed by precipitation. After cooling, the solid was filtered, washed several times with water, dried and recrystallized from ethanol to give title compound **9a,b**.

5,6-diphenyl-3-oxo-2,3-dihydropyridazine-4-yl-carboxylic acid (**9a**): Yield 82 %, Mp. 222-224 °C. IR (KBr) cm^{-1} : 3594, 3107, 1708. ^1H NMR, δ ppm (DMSO- d_6): 7.0 (s, 1H, NH), 7.17-7.98 (m, 10H, 2Ph-H), 13.50 (s, 1H, COOH). MS (m/z): 292 (M^+ , 0.9%), 264 (M^+ - CO, 17%). Anal. Calcd For $\text{C}_{17}\text{H}_{12}\text{N}_2\text{O}_3$: C, 69.85; H, 4.14; N, 9.29. Found: C, 69.70; H, 4.00; N, 9.40.

5,6-Bis(4-chlorophenyl)-3-oxo-2,3-dihydropyridazine-4-yl-carboxylic acid (**9b**): Yield 84%; Mp. 280 - 281 °C. IR (KBr) cm^{-1} : 3456, 3131, 1725. MS (m/z): 361. ^1H NMR, δ ppm (DMSO- d_6): 7.14 - 7.73 (m, 8H, 2 Ar-H), 13.73 (s, 1H, COOH). MS (m/z): 361 (M^+ , 7.2%), 360 (M^+ - H, 24.5%), 315 (M^+ - H, COOH, 100%). Anal. Calcd. For $\text{C}_{17}\text{H}_{10}\text{Cl}_2\text{N}_2\text{O}_3$: C, 56.53; H, 2.79; N, 7.76. Found: C, 56.40; H, 2.60; N, 7.60.

Hydrolysis of 4-carboethoxy-5,6-diarylpyridazin-3(2H)-ones (1a,b)

6-Carboethoxy derivatives **1a,b** (1.1 mmol) were separately dissolved in ethanol (15 mL). Following addition of sodium hydroxide (0.5 g), the reaction mixture were placed on a steam bath, when the solvent had evaporated, the residues were dissolved in warm water (10 mL) and filtered. The filtrates were acidified with hydrochloric acid, and the resulting precipitates were separated by filtration, dried and recrystallized from ethanol, to give 78 and 79% yield respectively that were identical with compounds **9a,b**.

Preparation of 3-chloro-5,6-diaryl-4-phenylpyridazines (10a,b)

A mixture of pyridazinone derivatives **2a,b** (9.0 mmol) and phosphoryl chloride (6 mL) was refluxed for 5 hrs. The cooled reaction mixture was poured into ice-H₂O (50 mL), the precipitate was filtered, dried and recrystallized from ethanol to give the title compounds **10a,b**.

3-Chloro-4,5,6-triphenylpyridazine (10a): Yield 94%; Mp. 170-172 °C as reported.^{10c)}

3-Chloro-5,6-bis(4-chlorophenyl)-4-phenylpyridazine (10b): Yield 91%, Mp. 149-151 °C. IR (KBr) cm⁻¹: 3056, 1594, 731. Anal. Calcd. for C₂₂H₁₃Cl₃N₂: C, 64.18; H, 3.18; N, 6.81. Found: C, 64.10; H, 3.00; N, 6.70.

Preparation of 6,7-diaryl-8-phenyltetrazolo[1,5-b]pyridazines (11a,b)

Sodium azide (0.06 g, 0.9 mmol) was added to a solution of compounds 10a,b (1.0 mmol) in ethanol (20 mL). The reaction mixture was heated under reflux for 10 hours. The solvent was evaporated under reduced pressure, then the solid residue was diluted with water (100 mL) and the precipitated product was isolated by suction dried and recrystallized from ethanol.

6,7,8-Triphenyltetrazolo[1,5-b]pyridazine (11a): Yield 73%, Mp. 225-227 °C as reported.^{10c)}

6,7-Bis(4-chlorophenyl)-8-phenyltetrazolo[1,5-b]pyridazine (11b): Yield 79 %, Mp. 194-196 °C. IR (KBr) cm⁻¹: 3064, 1660, 754. MS (m/z): 418 (M⁺, 0.1%), 326 (M⁺ - 4N, Cl, 100%), 300 (M⁺ - 4N, Cl, CN, 5.5%), 214 (M⁺ - 4N, Cl, CN, CPh, 29.1%). Anal. Calcd for C₂₂H₁₃Cl₂N₅: C, 63.17; H, 3.13; N, 16.74. Found: C, 63.10; H, 3.00; N, 16.60.

Preparation of 4,5,6-triphenyl-3-(triphenylphosphoranylideneamino)pyridazine (12)

To a solution of compound **11a** (1.7 g, 4.8 mmol) in 1,2-dichlorobenzene (10 mL), triphenylphosphine (1.57 g, 5.9 mmol) was added, the reaction mixture was refluxed for 6 hours, the solvent was evaporated and the residue was washed with petroleum ether 40/60 °C, the precipitate was filtered, dried and recrystallized from ethanol. Yield 88 %; Mp. 212-214 °C. IR (KBr) cm⁻¹:

3055, 1597, 1537. ¹H NMR, δ ppm (DMSO-*d*₆): 6.81-7.93 (m, 30H, 6Ph-H). Anal. Calcd for C₄₀H₃₀N₃P: C, 82.31; H, 5.18; N, 7.19. Found: C, 82.20; H, 5.10; N, 7.10.

Preparation of 5,6-diaryl-3-β-hydroxyethylamino-4-phenylpyridazine (13a,b)

A mixture of compound **10a,b** (0.9 mmol) and ethanolamine (5 mL) was refluxed for 2 hours. The cooled reaction mixture was poured onto water (100 mL). A precipitate which obtained was filtered, washed several times with water, dried and recrystallized from benzene to give the title compounds **13a,b**.

4,5,6-Triphenylpyridazine-3-β-hydroxyaminopyridazine (13a): Yield 84%; Mp. 185-187 °C as reported.^{10c)}

5,6-Bis(4-chlorophenyl)-3-β-hydroxyethylamino-4-phenylpyridazine (13b): Yield 91.7 %; Mp. 85-87 °C. IR (KBr) cm⁻¹: 3259, 3081, 2909, 767. ¹H NMR, δ ppm (DMSO-*d*₆): 3.48-3.65 (m, 5H, CH₂CH₂OH), 4.0 (s, 1H, NH), 7.41-7.98 (m, 13H, aromatic-H). MS (m/z): 435 (M⁺ + 1, 2.7%), 416 (M⁺ - H₂O, 14%), 404 (M⁺ - CH₂OH, 19%), 390 (M⁺ - CH₂CH₂OH, 100%). Anal. Calcd. for C₂₄H₁₉Cl₂N₃O: C, 66.06; H, 4.39; N, 9.63. Found: C, 66.00; H, 4.30; N, 9.50.

Preparation of 5,6-diaryl-3-morpholino-4-phenylpyridazines (13c,d)

A mixture of 3-chloro derivatives **10a,b** (1.0 mmol) and morpholine (4 mL) was refluxed for 3 hours. The cooled mixture was poured onto water (100 mL). A precipitate which obtained was filtered, washed several times with water, dried and recrystallized from ethanol.

4,5,6-Triphenyl-3-morpholinopyridazine (13c): Yield 91 %; Mp. 190-191 °C. IR (KBr) cm⁻¹: 3390, 3060, 2912, 1115. ¹H NMR, δ ppm (DMSO-*d*₆): 3.57 (m, 4H, CH₂NCH₂), 3.65 (m, 4H, CH₂OCH₂), 7.41-7.98 (m, 15H, 3Ph-H). Anal. Calcd for C₂₆H₂₄N₃O: C, 79.16; H, 6.13; N, 10.65. Found: C, 79.00; H, 6.00; N, 10.40.

5,6-Bis(4-chlorophenyl)-3-morpholino-4-phenylpyridazine (13d): Yield 87 %; Mp. 219-221 °C. IR (KBr) cm⁻¹: 3409, 3058, 2912, 1115. ¹H NMR, δ ppm (DMSO-*d*₆): 3.56 (m, 4H, CH₂NCH₂), 3.69 (m, 4H, CH₂OCH₂), 7.41-7.98 (m, 13H, aromatic-H). MS (m/z): 462 (M⁺ + 1, 66.9%), 460 (M⁺ - H₂, 61%), 376 (M⁺-morpholino, 8.27%). Anal. Calcd for C₂₆H₂₂N₃O: C, 67.39; H, 4.79; N, 9.07. Found: C, 67.20; H, 4.40; N, 9.00.

Preparation of 5,6-aryl-4-phenyl-3-piperidinopyridazine (13e,f)

To a solution of 3-chloro derivative **10a,b** (1.0 mmol) in ethanol (25 mL), piperidine (1 mL, 12.0 mmol) was added, the reaction mixture was refluxed for 15 hours. The solvent was evaporated under reduced pressure. To the residue, water (100 mL) was added followed by few drops of hydrochloric acid. The precipitate was filtered, dried and recrystallized from ethanol to give **13e,f**.

4,5,6-Triphenyl-3-piperidinopyridazine (13e): yield 68.1 %, Mp. 235-237 °C; as reported.^{10c)}

5,6-Bis(4-chlorophenyl)-3-piperidino-4-phenylpyridazine (13f): yield 85%, Mp. 208-210 °C. IR (KBr) cm^{-1} : 3052, 2844, 760. $^1\text{H NMR}$, δ ppm (DMSO- d_6): 1.53-1.59 (m, 6H, $\text{CH}_2\text{CH}_2\text{CH}_2$), 3.71 (t, 4H, CH_2NCH_2), 7.41-7.79 (m, 13H, aromatic-H). Anal. Calcd for $\text{C}_{27}\text{H}_{23}\text{Cl}_2\text{N}_3$: C, 70.44; H, 5.03; N, 9.13. Found: C, 70.30; H, 5.00; N, 9.10.

Preparation of 5,6-diaryl-3-hydrazino-4-phenylpyridazines (13g,h)

To a solution of 3-chloro derivatives **10a,b** (10.0 mmol) in 1-butanol (20 mL), hydrazine hydrate (6 mL, 80%) was added. The reaction mixture was refluxed for 8 hours, after cooling the solid product formed was filtered, dried and recrystallized from ethanol.

3-Hydrazino-4,5,6-triphenylpyridazine (13g): Yield 88 %, Mp. 229-231 °C. IR (KBr) cm^{-1} : 3470, 3355, 3200, 1620, 1560. $^1\text{H NMR}$, δ ppm (DMSO- d_6): 7.50-7.70 (m, 15H, 3 Ph-H), 5.80-6.10 (m, 3H, NHNH_2). Anal. Calcd for $\text{C}_{22}\text{H}_{18}\text{N}_4$: C, 78.08; H, 5.36; N, 16.56. Found: C, 78.00; H, 5.10; N, 16.40.

5,6-Bis(4-chlorophenyl)-3-hydrazino-4-phenylpyridazine (13h): Yield 65%; Mp. 220-222 °C; IR (KBr) cm^{-1} : 3427, 3262, 3063, 1491, 730. $^1\text{H NMR}$, δ ppm (DMSO- d_6): 2.0 (s, 2H, NH_2), 4.0 (s, 1H, NH), 7.41-7.79 (m, 13H, aromatic-H). Anal. Calcd for $\text{C}_{22}\text{H}_{16}\text{Cl}_2\text{N}_4$: C, 64.87; H, 3.96; N, 13.76. Found: C, 64.70; H, 3.80; N, 13.60.

Preparation of N-(4,5,6-triphenylpyridazine-3-yl)-N'-[alkylthio(carbamoyl)]hydrazine (14a,b)

A solution of 3-hydrazino derivative **13g** (1.7 g, 5.0 mmol) and equimolar amount of alkyl isothiocyanate (5.0 mmol) in acetone (30 mL) was heated under reflux for 6 hours, the solvent was evaporated under reduced pressure, the residue was collected and recrystallized from benzene to give the title compounds **14a,b**.

N-(4,5,6-Triphenylpyridazin-3-yl)-N'-[methylthio(carbamoyl)]hydrazine (14a): Yield 95 %; Mp. 215-217 °C. IR (KBr) cm^{-1} : 3446, 3055, 2975, 1130. $^1\text{H NMR}$, δ ppm (DMSO- d_6): 2.0 (s, 2H, NHCNH), 2.80 (s, 3H, CH_3), 4.0 (s, 1H, NH), 7.40-7.78 (m, 15H, Ph-H). Anal. Calcd for $\text{C}_{24}\text{H}_{21}\text{N}_5\text{S}$: C, 70.04; H, 5.14; N, 17.02. Found: C, 70.00; H, 5.00; N, 16.90.

N-(4,5,6-Triphenylpyridazin-3-yl)-N'-[ethylthio(carbamoyl)]hydrazine (14b): Yield 92%; Mp. 220-222 °C. IR (KBr) cm^{-1} : 3375, 3049, 2979, 1155. $^1\text{H NMR}$, δ ppm (DMSO- d_6): 1.29 (t, 3H, CH_3), 2.0 (s, 2H, NHCNH), 4.0 (s, 1H, NH), 4.43 (m, 2H, CH_2). Anal. Calcd for $\text{C}_{25}\text{H}_{23}\text{N}_5\text{S}$: C, 70.56; H, 5.44; N, 16.46. Found: C, 70.40; H, 5.30; N, 16.40.

Preparation of 3-alkylamino-6,7,8-triphenyl-1,2,4-triazolo[4,3-b]pyridazines (15a,b)

Method A: To a solution of 3-hydrazino derivative **13g** (1.7g, 5.0 mmol) and equimolar amount of alkyl isothiocyanate (5.0 mmol) in acetone (30 mL), potassium hydroxide (0.6 mL, 2N) was added. The reaction mixture

was heated under reflux for 6 hrs; the solvent was evaporated under reduced pressure. The residue was dissolved in water (100 mL) and neutralized with hydrochloric acid. The solid product obtained was filtered, dried and recrystallized from ethanol to give the title compounds **15a,b**

3-Methylamino-6,7,8-triphenyl-1,2,4-triazolo[4,3-b]pyridazine (15a): Yield 56.5%; Mp. 215-217 °C. IR (KBr) cm^{-1} : 3375, 3049, 2979. $^1\text{H NMR}$, δ ppm (DMSO- d_6): 2.91 (s, 3H, CH_3), 4.0 (s, 1H, NH), 7.41-7.79 (m, 15H, 3Ph-H). MS (m/z): 377 (M^+ , 3%), 362 ($\text{M}^+ - \text{CH}_3$, 1.4%). Anal. Calcd for $\text{C}_{24}\text{H}_{19}\text{N}_5$: C, 76.37; H, 5.07; N, 18.56. Found: C, 76.10; H, 4.80; N, 18.20.

3-Ethylamino-6,7,8-triphenyl-1,2,4-triazolo[4,3-b]pyridazine (15b): Yield 51 %; Mp. 220-221 °C. IR (KBr) cm^{-1} : 3365, 3020, 2969. $^1\text{H NMR}$, δ ppm (DMSO- d_6): 1.14 (t, 3H, CH_3), 3.47 (q, 2H, CH_2), 7.41-7.79 (m, 15H, 3Ph-H). MS (m/z): 391 (M^+ , 0.6%), 363 ($\text{M}^+ - \text{C}_2\text{H}_5$, 100%). Anal. Calcd for $\text{C}_{25}\text{H}_{21}\text{N}_5$: C, 76.70; H, 5.41; N, 17.89. Found: C, 76.40; H, 5.10; N, 17.60.

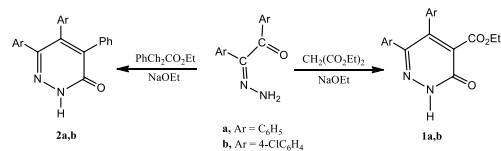
Method B: To a solution of compound **14a,b** (5.0 mmol) in acetone (30 mL), potassium hydroxide (0.6 mL, 2N) was added. The reaction mixture was refluxed for 6 hours, the same work-up as in method A, gave 70% yield of **15a** and 66% yield of **15b**. It was identical with that prepared by method A.

Insecticidal activity

Out of the synthesized compounds, only compounds **3a**, **5a**, **10b**, **12**, **13a** and **15b** were examined for their insecticidal activity against two insects viz. *Mucsa domestica* and Aphid. *Macrosiphum pisi* by dipping method¹²⁾ at 500 ppm concentration.

Results and Discussion

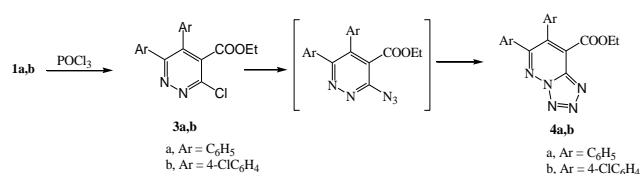
The parents 4-carboethoxy-5,6-diarylpyridazin-3(2H)-ones **1a,b** and 5,6-diaryl-4-phenyl-pyridazin-3(2H)-ones **2a,b** required in the present work were prepared more conveniently and in higher yields starting from benzil (*p,p'*-dichlorobenzilmonohydrazone with diethyl malonate and with ethyl phenylacetate in presence of sodium ethoxide as described earlier¹⁰ (Scheme 1).



Scheme 1

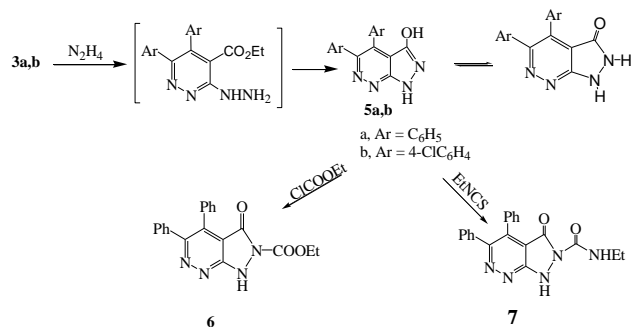
Ethyl 3-chloro-5,6-diarylpyridazine-4-carboxylates **3a,b** were conveniently prepared in good yields by treatment of 4-carboethoxy-5,6-diarylpyridazin-3(2H)-ones **1a,b** with phosphoryl chloride at refluxing temperature. The structures of compounds **3a,b** were established on the basis of their spectroscopic data. The IR spectra showed an absorption bands at 1735 and at 1734 cm^{-1} referred to ester carbonyl groups and no absorption bands referred to amide carbonyl groups.

On reacting compounds **3a,b** with one equivalent of sodium azide in boiling ethanol gave the corresponding tetrazolopyridazine derivatives **4a,b**.¹¹ Wherein 3-azido derivatives was formed at the first step in these reactions and intramolecular cyclization to the tetrazole derivatives **4a,b** occurred immediately. The predominant existence of tetrazole derivatives were supported by the IR spectral data, which exhibited no absorption bands around 2200 cm^{-1} . The mass spectrum of ethyl 6,7-bis(4-chlorophenyl)tetrazolo-[1,5-*b*]pyridazine-8-carboxylate **4b** could be accounted as follows: the molecular ion at m/z 414 underwent the following fragmentation. It could be lose COOEt to give the ion at m/z 343, which in turn gives rise to the ion at m/z 330 by lose of (N, COOEt), this ion lose 2N to give the ion at m/z 303.



Scheme 2.

The starting **3a,b** required for the synthesis of pyrazolopyridazines **5a,b** is important synthesis for annellations of pyrazole such compounds **3a,b** on reaction with hydrazine hydrate in boiling 1-butanol gave 3-hydroxy-4,5-diaryl-1*H*-pyrazolo[3,4-*c*]pyridazine **5a,b** in a good yields. Mechanistically the formation of **5a,b** involve the nucleophilic substitution of hydrazine at carbon-3, which undergoes immediate intramolecular nucleophilic cyclization of the hydrazine primary amino group to the carboxy group with elimination of ethanol molecule (Scheme 3).

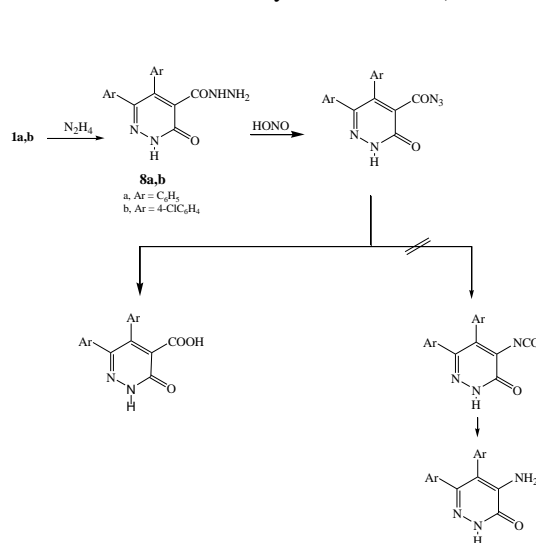


Scheme 3.

With a view of studying some of the reaction of **5a**, it was allowed to react with excess of ethyl chloroformate at reflux temperature, a crystals deposited during the refluxing time, as a single product. The isolated product was proven to be 2-carboxy-4,5-diphenyl-3-oxo-1*H*-pyrazolo[3,4-*c*]pyridazine **6**. As the progress of the reaction was monitored by TLC, the possibility of a side reaction through the oxygen substituted could not obtain. The assignment of structure **6** was based on an analytical and spectral data.

Also, the reaction of compound **5a** with ethyl isothiocyanate in presence of potassium hydroxide in boiling acetone furnished 2-substituted product **7** as the only product.

Heating a mixture of 4-carbethoxy-5,6-diarylpyridazin-3(2*H*)-ones **1a,b** with hydrazine hydrate in 1-butanol gave the corresponding 4,6-diaryl-2,3-dihydro-3-oxopyridazine-4-carbohydrazide **8a,b** (Scheme 4). The reaction of this carbohydrazide with one equivalent of sodium nitrite in hydrochloric acid at 5°C, afforded the acid azide intermediate, the latter when heated gave the carboxylic acid derivatives **9a,b** rather than the corresponding 4-amino derivatives, *via* Curtius rearrangement on the basis of spectral data and elemental analysis. The formation of 4-carboxy derivatives involves a nucleophilic substitution of water to the 4-carbonylazide group with elimination of hydrazoic acid. Also, the structures were assigned by comparison with authentic samples prepared from the basic hydrolysis followed by neutralization of 4-carbethoxy derivatives **1a,b**.



Scheme 4.

Compounds **2a,b** were also separately reacted (Scheme 5) with phosphoryl chloride at refluxing temperature gave the corresponding 3-chloro derivatives **10a,b**. Since the reactivity of the chlorine atoms were expected, the compounds were subjected to nucleophilic substitution reactions to obtained the next derivatives of the ring systems.

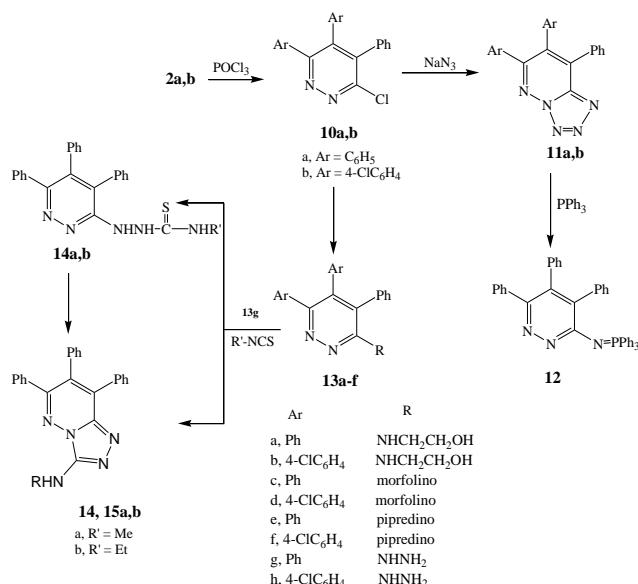
On reacting compounds **10a,b** with sodium azide afforded tetrazolo derivatives **11a,b** in a single step in^{10c} 73% and 79% respectively.

The pyridazine derivatives **12** was easily obtained in 88% yield by the reaction of 6,7,8-triphenyltetrazolo[1,5-*a*]pyridazine **11a** with triphenylphosphine in refluxing 1,2-dichlorobenzene (b.p. 179°C).

Compounds **10a,b** were also separately reacted with ethanolamine, morpholine, piperidine and/or hydrazine to afforded 3-substituted pyridazines **13a-f**.

Reacting equimolecular quantities of the 3-hydrazino derivatives **13e** and alkyl isothiocyanate in boiling acetone yielded the corresponding *N*-(4,5,6-triphenylpyridazin-3-yl)-*N'*-[alkylthio(carbonyl)]hydrazines **14a,b** in 95% and 92% yield respectively. On the other hand, reaction of compound **13a** with alkyl isothiocyanate in boiling 2*N* acetone potassium hydroxide afforded, unexpectedly a single product. The isolated product was proved to be

identical in every respect with 3-alkylamino-6,7,8-triphenyl-1,2,4-triazolo[3,4-*b*]pyridazines **15a,b**. Mechanistically, the formation of tricyclic derivatives **15a,b** from **13e** involves the initial formation of **14a,b** which undergo immediate intramolecular nucleophilic attack of ring-2 nitrogen on thione group with elimination of hydrogen sulfide molecule. This mechanism was proved by converting **14a,b** to **15a,b** upon boiling in acetone potassium hydroxide indicates that **14a,b** are thermostable at the boiling point of acetone.



Scheme 5.

Evaluation of insecticidal activity

The result of insecticidal activity studies are recorded in table 1. After 24 hr, % mortality was calculated using the following formula:

$$\phi = 100 \times \frac{N_1}{N_2} \quad (1)$$

where

- ϕ - mortality in %
 N_1 - no. of dead insects
 N_2 - no. of insects released

The compounds **5b** and **13a** showed good activities (Table 1). The other tested compounds showed lower activity as compared to the standard insecticides Diazinon and Carbosulfan. From the insecticidal data, it is clear that the combination of chloro atom at position 4 of the phenyl ring with hydroxypyrazolopyridazine works better, the maximum (+++) against *Mucsa domestica* was observed with compound **5b**. Ethanolamino derivative in compound **13a** has the maximum (+++) against *Macrosiphum pisi*.

Table 1. Insecticidal activity (mortality %) of compounds **3a**, **5a**, **6**, **10b**, **12**, **13a** and **15b**

| Compounds | <i>Mucsa domestica</i> | <i>Macrosiphum pisi</i> |
|-------------|------------------------|-------------------------|
| 3a | ++ | +++ |
| 5a | ++ | + |
| 5b | +++ | + |
| 6 | + | ++ |
| 10b | ++ | + |
| 12 | ++ | ++ |
| 13a | ++ | +++ |
| 16b | + | ++ |
| Diazinon | ++++ | - |
| Carbosulfan | - | ++++ |

Mortality is indicated by symbols (-) \approx 0-20%, (+) \approx 21- 40%, (++) \approx 41- 60%, (+++) \approx 61- 80%, (++++) \approx > 80%.

References

- For part 26: Deeb, A., Aouf, N., Yassine, F., Shehata, W., *Coloration Technolgy* (in press).
- Zou, X. J., Jin, G. Y., Yang, Z., *Chin. J. Appl. Chem.*, **2001**, *18*, 599.
- Dumas, J. P., Boyer, S. J., Dixon, J. A., Joe, T. K., H. Kluender, C. E., Lee, W., Nagarathnam, D., Sibley, R. N., Su. N., *US 6689883*, **2004**; [*Chem. Abstr.* **140**, 163891 (2004)].
- Shinichiro, S. Shinichiro, M. A. Akio, M., *JP 2007182430*, **2007**; [*Chem. Abstr.* **147**, 166329, 2007].
- Hoshino, K., Koike, Y., *JP 2005263694*, **2005**; [*Chem. Abstr.* **143**, 320612, 2005].
- Yang, H. Z., Zou, X. M., Hu, F. Z., Liu, B., Yang, X. F., *CN 1676518*, **2005**; [*Chem. Abstr.* **144**, 412521,2005].
- Sacchi, S., Laneri, F., Arena, E., Abignente, M., Gallitelli, M., D'amico, M., Filippelli, W., Rossi, F., *Eur. J. Med. Chem.* **1999**, *34*, 1003.
- Ishimukai, M. Matsusaka, M., *JP 2007077140*, **2007**; [*Chem. Abstr.* **146**, 332508, 2007].
- Deeb, A. Mourad, E. Elenany, D. *Phosphorus, Sulfur, and Silicon*, **2010**, *185*, 222.
- (a)Dirnow, A. Abele; W., *Chem. Ber.*, **1964**, *97*, 3349; (b) Deeb, A. Bayoumy, B. Essawy, A. Fikry, R., *Heterocycles*, **1991**, *32*, 901; (c) Deeb, A. Said, A., *Collect. Czech. Chem. Commun*, **1990**, *55*, 2795.
- Deeb, A., Saad, H. *Heterocycles*, **2003**, *60*, 1873.
- Abbott, W. S., *J. Econ. Entemol.*, **1925**, *18*, 265.

Received:04.06.2013.

Accepted:21.07.2013.



L-PROLINE-CATALYZED SYNTHESIS OF FUSED DIHYDROPYRIDINES THROUGH HANTZSCH REACTION

Farahnaz K. Behbahani^[a] and Mahsa Mohammadloo^[a]

Keywords: Synthesis; Polyhydroquinoline; L-proline; Catalyst; Four components

An efficient Hantzsch four-component condensation reaction for the synthesis of polyhydroquinolines was found to proceed in the presence of *L*-proline in ethanol at room temperature. The method is really simple and environmentally benign. The keys features of this protocol are the use of a bio, organic and reusable catalyst, high yields of products, using nontoxic solvent and short reaction times from the principles of green chemistry point of view.

Corresponding Authors

Tel: +98 026 3448145

Fax: +98 026 34418156

Email: Farahnazkargar@yahoo.com

[a] Department of Chemistry, Karaj Branch, Islamic Azad University, Karaj, Iran

Introduction

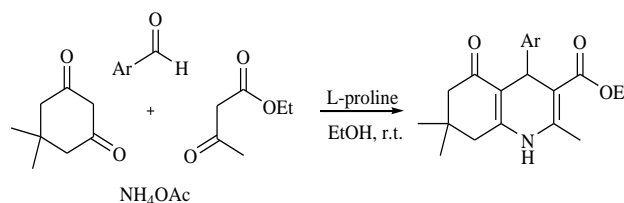
Among various biologically active heterocyclic scaffolds, Hantzsch 1,4-dihydropyridines (1,4-DHPs) are an important class of biologically active heterocycles. 1,4-Dihydropyridines are analogues of NADH coenzymes and an important class of drugs.¹ These compounds possess a variety of biological activities such as curing the disordered heart ratio as the chain-cutting agent of factor IV channel and having the calcium channel agonist-antagonist modulation activities.²⁻⁶

Classical method for the synthesis of 1,4-dihydropyridines is one-pot condensation of aldehydes with ethyl acetoacetate, and ammonia either in acetic acid or by refluxing in alcohol.⁷ This method, however, involves long reaction time, harsh reaction conditions or generally gives low yields. Therefore, it is necessary to develop an efficient and versatile method for the preparation of 1,4-DHPs and the progress in this field is remarkable including recently the promotion of microwave,⁸ TMSCl,^[10] ionic liquid,⁹ polymer,^{10,11} Yb(OTf)₃,¹² silica sulfuric acid,¹³ Sc(OTf)₃,¹⁴ MCM-41,¹⁵ sulfamic acid,¹⁶ hafnium(IV) bis(perfluorooctanesulfonyl)imide,¹⁷ guanidine hydrochloride (GuHCl),¹⁸ grinding till,¹⁹ fluoro alcohols,²⁰ cerium(IV) ammonium nitrate,²¹ and Cs_{2.5}H_{0.5}PW₁₂O₄₀.²² However, the use of high temperatures, expensive metal precursors and catalysts those are harmful to environment, and longer reaction times limit the use of these methods. Therefore, the search for a better method for the synthesis of polyhydroquinolines is still the need of the day.

In recent years, *L*-proline has gained importance as versatile catalyst for effecting various organic transformations such as the synthesis of coumarins in ionic

liquid²³ and density functional study of the *L*-proline-catalyzed α -aminoxylation of aldehydes.²⁴ Moreover, *L*-proline and *L*-proline derivatives were successfully used as organo catalysts in asymmetric aldol and Michael addition reactions.²⁵

On the other hand, a part of our program aiming at developing selective and environmental friendly methodologies for the preparation of fine chemicals,^[26] therefore in this paper, we wish to disclose our finding about the *L*-proline catalyzed four-component Hantzsch reaction of aldehydes, dimedone, ethylacetoacetate and ammonium acetate in the presence of *L*-proline as an inexpensive, eco-friendly and recyclable catalyst in ethanol at room temperature (Scheme 1).

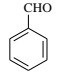
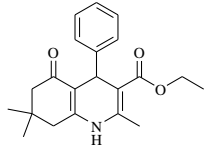
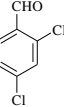
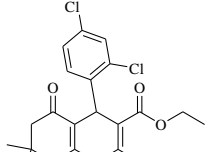
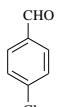
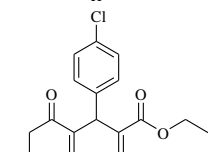
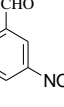
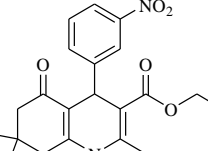
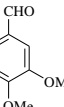
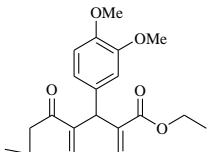
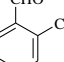
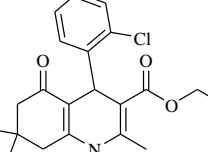
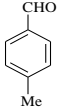
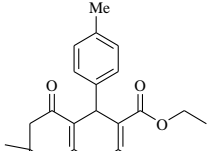


Scheme 1

Results and discussion

Firstly, the mixture of benzaldehyde, dimedone, ethyl acetoacetate and ammonium acetate was chosen as the model reaction to detect whether the use of *L*-proline was efficient and investigate the optimized conditions. Thus, we selected the optimized reaction condition to exam the universality of this catalyst's application. Various aromatic aldehydes were selected to undergo the Hantzsch reaction in the presence of catalytic amount of *L*-proline in ethanol at room temperature. The results of this study are summarized in Table 1. It was indicated that both electron-rich and electron-deficient aldehydes giving high yields of products with little difference.

Table 1 Synthesis of polyhydroquinolines using L-proline

| Entry | Aldehyde | Product | Time, h | Yield, % | MP., °C | MP., °C (Lit.) |
|-------|---|---|---------|----------|---------|-----------------------|
| 1 |  |  | 3.5 | 96 | 196-198 | 202-204 ²⁷ |
| 2 |  |  | 3.0 | 90 | 210-212 | 214-216 ²⁷ |
| 3 |  |  | 2.5 | 91 | 238-241 | 244-246 ²⁷ |
| 4 |  |  | 3.0 | 93 | 178-180 | 178-180 ²⁷ |
| 5 |  |  | 3.5 | 90 | 190-195 | 197-199 ²⁷ |
| 6 |  |  | 2.0 | 85 | 204-206 | 208-209 ²⁷ |
| 7 |  |  | 3.0 | 88 | 254-256 | 265-268 ²⁷ |

Experimental

General procedure for the synthesis of polyhydroquinoline derivatives

To a mixture of benzaldehyde (1.0 mmol), dimedone (1.5 mmol), ethyl acetoacetate (1.0 mmol), and ammonium acetate (1.0 mmol) in ethanol (4.0 ml), L-proline (10 mol%) was added at room temperature. The progress of the reaction was monitored by TLC and the spot were detected either UV light. After completion of the reaction, ethanol was removed, ethyl acetate and water was added and the product was extracted. The crude product was obtained recrystallized from ethanol and water. Next, extracted

aqueous layer containing catalyst was washed with 10 ml of dichloromethane twice and was used for three times (Table 2).

Table 2 Reusability of the catalyst^a

| Entry | 1 | 2 | 3 | 4 |
|-----------------------|----|----|----|----|
| Yield, % ^b | 96 | 93 | 93 | 90 |

^aReaction condition: benzaldehyde (1.0 mmol), dimedone (1.5 mmol), ethylacetoacetate (1.0 mmol) and ammonium acetate (1.0 mmol) at r.t.; ^bIsolated yield.

Spectral data for synthesized compound

R=C₆H₅, Ethyl 2,7,7-trimethyl-5-oxo-4-phenyl-1,4,5,6,7,8-hexahydroquinoline-3-carboxylate (1). IR (KBr, cm⁻¹): 3274, 3204, 3079, 2961, 1699, 1602. ¹H NMR (300 MHz, CDCl₃): δ 7.28–7.31 (m, 2H, Ar-H), 7.18–7.22 (m, 2H, Ar-H), 7.06–7.13 (m, 1H, Ar-H), 6.64 (s, 1H, NH), 5.04 (s, 1H, CH), 4.05 (q, J=7.1 Hz, 2H, CH₂), 2.35 (s, 3H, CH₃), 2.11–2.29 (m, 4H, 2CH₂), 1.19 (t, J=7.1 Hz, 3H, CH₃), 1.07 (s, 3H, CH₃), 0.96 (s, 3H, CH₃).

R=2,4-Cl₂C₆H₃, Ethyl 4-(2,4-dichlorophenyl)-2,7,7-trimethyl-5-oxo-1,4,5,6,7,8-hexahydroquinoline-3-carboxylate (2). IR (KBr, cm⁻¹): 3283, 3208, 3077, 2958, 1706, 1608. ¹H NMR (300 MHz, CDCl₃): δ 7.05–7.33 (m, 3H, Ar-H), 6.02 (s, 1H, NH), 5.32 (s, 1H, CH), 4.02 (q, J=7.0 Hz, 2H, CH₂), 2.30 (s, 3H, CH₃), 2.12–2.22 (m, 4H, 2CH₂), 1.20 (t, J=7.0 Hz, 3H, CH₃), 1.05 (s, 3H, CH₃), 0.92 (s, 3H, CH₃).

R=4-ClC₆H₄, Ethyl 4-(4-chlorophenyl)-2,7,7-trimethyl-5-oxo-1,4,5,6,7,8-hexahydroquinoline-3-carboxylate (3). IR (KBr, cm⁻¹): 3275, 3207, 3077, 2960, 1706, 1602. ¹H NMR (300 MHz, CDCl₃): δ 7.24–7.26 (m, 2H, Ar-H), 7.13–7.19 (m, 2H, Ar-H), 6.46 (s, 1H, NH), 5.04 (s, 1H, CH), 4.03 (q, J=7.1 Hz, 2H, CH₂), 2.37 (s, 3H, CH₃), 2.11–2.35 (m, 4H, 2CH₂), 1.18 (t, J=7.1 Hz, 3H, CH₃), 1.06 (s, 3H, CH₃), 0.92 (s, 3H, CH₃).

R=3-NO₂C₆H₄, Ethyl 2,7,7-trimethyl-4-(3-nitrophenyl)-5-oxo-1,4,5,6,7,8-hexahydroquinoline-3-carboxylate (4). IR (KBr, cm⁻¹): 3284, 3211, 3077, 2959, 1704, 1603. ¹H NMR (300 MHz, CDCl₃): δ 7.99 (m, 1H, Ar-H), 7.97 (m, 1H, Ar-H), 7.71 (d, J=7.9 Hz, 1H, Ar-H), 7.36 (t, J=7.9 Hz, 1H, Ar-H), 6.85 (s, 1H, NH), 5.16 (s, 1H, CH), 3.69 (q, J=7.1 Hz, 2H, CH₂), 2.12–2.42 (m, 7H, CH₃, 2CH₂), 1.22 (t, J=7.1 Hz, 3H, CH₃), 1.08 (s, 3H, CH₃), 0.93 (s, 3H, CH₃).

R=3,4-(OCH₃)₂C₆H₃, Ethyl 4-(3,4-dimethoxyphenyl)-2,7,7-trimethyl-5-oxo-1,4,5,6,7,8-hexahydroquinoline-3-carboxylate (5). IR (KBr, cm⁻¹): 3279, 3211, 3078, 2958, 1695, 1603. ¹H NMR (300 MHz, CDCl₃): δ 6.92 (d, J=1.96 Hz, 1H, Ar-H), 6.77 (dd, J=1.96, 8.31 Hz, 1H, Ar-H), 6.68 (d, J=8.30 Hz, 1H, Ar-H), 5.94 (s, 1H, NH), 5.03 (s, 1H, CH), 4.05 (q, J=7.3 Hz, 2H, CH₂), 3.85 (s, 3H, OCH₃), 3.81 (s, 3H, OCH₃), 2.38 (s, 3H, CH₃), 2.18–2.35 (m, 4H, 2CH₂), 1.20 (t, J=7.3 Hz, 3H, CH₃), 1.07 (s, 3H, CH₃), 0.95 (s, 3H, CH₃).

R=2-ClC₆H₄, Ethyl 4-(2-chlorophenyl)-2,7,7-trimethyl-5-oxo-1,4,5,6,7,8-hexahydroquinoline-3-carboxylate (6). IR (KBr, cm⁻¹): 3282, 3210, 3074, 2957, 1697, 1609. ¹H NMR (300 MHz, CDCl₃): δ 7.60 (s, 1H, NH), 7.11–7.29 (m, 4H, Ar-H), 4.60 (s, 1H, CH), 4.03 (q, J=7.2 Hz, 2H, CH₂), 2.40 (s, 3H, CH₃), 2.00–2.21 (m, 4H, 2CH₂), 1.18 (t, J=7.2 Hz, 3H, CH₃), 1.05 (s, 3H, CH₃), 0.95 (s, 3H, CH₃).

R=4-CH₃C₆H₄, Ethyl 2,7,7-trimethyl-5-oxo-4-p-tolyl-1,4,5,6,7,8-hexahydroquinoline-3-carboxylate (7). IR (KBr, cm⁻¹): 3281, 3208, 3077, 2961, 1700, 1607. ¹H NMR (300 MHz, CDCl₃): δ 7.19 (d, J=7.9 Hz, 2H, Ar-H), 7.03 (d, J=7.9 Hz, 2H, Ar-H), 6.66 (s, 1H, NH), 5.03 (s, 1H, CH), 4.03 (q, J=7.1 Hz, 2H, CH₂), 2.34 (s, 3H, CH₃), 2.11–2.28 (m, 7H, CH₃, 2CH₂), 1.19 (t, J=7.1 Hz, 3H, CH₃), 1.06 (s, 3H, CH₃), 0.93 (s, 3H, CH₃).

Conclusion

The use of inexpensive *L*-proline in a catalytic quantity is a general practical alternative to existing procedures for multicomponent Hantzsch synthesis of polyhydroquinolines. The procedure offers several advantages including increased variations of substituent in the product with high yields, operational simplicity, minimum environmental effects and above all, the ease in purification of products simply by crystallization.

References

- Mauzeral, D. and Westheimer, F. H., *J. Am. Chem. Soc.*, **1955**, *77*, 2261-2264.
- Kawase, M. Shah, A. Gaveriya, H. Motohashi, N. Sakagami, H. Varga, A. and Molnar, J., *Bioorg. Med. Chem.*, **2002**, *10*, 1051-1055.
- Suarez, M., Verdecia, Y., Illescas, B. Martinez-Alvarez, R., Avarez, A., Ochoa, E., Seoane, C., Kayali, N. and Martin, T. *Tetrahedron* **2003**, *59*, 9179-9186.
- Sabitha, G., Reddy, G. S. K. K., Reddy, C. S. and Yadav, J. S., *Tetrahedron Lett.* **44**: 4129-4131, 2003
- Sawada, Y., Kayakiri, H., Abe, Y., Mizutani, T., Inamura, N., Asano, M., Hatori, C., Aramori, I., Oku, T. and Tanaka H., *J. Med. Chem.*, **2004**, *47*, 2853-2863.
- Shan, R. Velazquez, C. and Knaus E. E., *J. Med. Chem.*, **2004**, *47*, 254-261.
- Love, B. and Snader, K. M., *J. Org. Chem.*, **1965**, *30*, 1914-1916.
- Tu, S.-J., Zhou, J.-F., Deng, X., Cai, P.-J., Wang, H. and Feng J.-C., *Chin. J. Org. Chem.*, **2001**, *21*, 313-316.
- Ji, S. J., Jiang, Z. Q., Lu, J. and Loh, T. P., *Synlett*, **2004**, 831-835.
- Breitenbucher, J. G. and Figliozzi, G., *Tetrahedron Lett.*, **2000**, *41*, 4311-4315.
- Dondoni, A., Massi, A., Minghini, E. and Bertolasi, V., *Tetrahedron*, **2004**, *60*, 2311-2326.
- Wang, L.-M. Sheng, J. Zhang, L. Han, J.-W. Fan, Z.-Y. Tian, H. and Qian, C.-T. *Tetrahedron*, **2005**, *61*, 1539-1543.
- Mobinikhaledi, A., Foroughifar, N., Bodaghi Fard, M. A., Moghanian, H., Ebrahimi, S. and Kalhor, M., *Synth. Commun.*, **2009**, *39*, 1166-1174.
- J. L. Donelson, R. A. Gibbs, and S. K. De *J. Mol. Catal. A: Chem.* **256**: 309-311, 2006
- Nagarapu, L., Kumari, M. D., Kumari, N. V. and Kantevari S., *Catal. Commun.*, **2007**, *8*, 1871-1875.
- Foroughifar, N., Mobinikhaledi, A., Bodaghi Fard, M. A., Moghanian, H. and Ebrahimi, S., *Synths React. Inorg., Metal-Org., Nano-Metal Chem.*, **2009**, *39*, 161-164.
- Hong, M. Cai, C. and Yi, W.-B., *J. Fluorine Chem.*, **2010**, *131*, 111-114.
- Baghbanian, S. M. Khaksar, S. Vahdat, S. M. Farhang, M. and Tajbakhsh, M., *Chin. Chem. Lett.*, **2010**, *21*, 563-567.
- Kumar, S. Sharma, P. Kapoor, K. K. and Hundal, M. S., *Tetrahedron*, **2008**, *64*, 536-542.
- Heydari, A. Khaksar, S. Tajbakhsh, M. and Reza Bijanzadeh H., *J. Fluorine Chem.* **2009**, *130*, 609-614.
- Reddy, C. S. and Raghu, M., *Chin. Chem. Lett.*, **2008**, *19*, 775-779.
- Khabazzadeh, H. Kermani, E. T. Afzali, D. Amiri, A. and Jalaladini, A., *Arabian J. Chem.* **2012**, *5*, 167.

- ²³Liu, X. H., Fan, J. C., Liu, Y., Shang, Z. C., *J. Zhejiang Univ. Sci. B*, **2008**, *12*, 990.
- ²⁴Wang, H. Yang, C. Han, K., *Struct. Chem.*, **2006**, *17*, 97.
- ²⁵Yuxia, L. Liu, Y. Zhiwei, M. Chuanchuan, W. Jingchao, T., *Chinese J. Catal.*, **2011**, *32*, 8.
- ²⁶Behbahani, F. K. Yektanezhad, T. and Khorrami, A. R. *Heterocycles*, **2010**, *81*, 2313-2321.
- ²⁷Cherkupally, S. R.; Mekala, R. *Chem. Pharm. Bull.* **2008**, *56*, 1002-1004.

Received: 30.06.2013.
Accepted: 21.07.2013.



CYCLODEXTRINS IN CHROMATOGRAPHY. PART 1. LIQUID CHROMATOGRAPHIC METHODS.

Gyula Oros^[a], Tibor Cserhádi^{[a]*} and Mária Szógyi^[a]

Keywords: cyclodextrins, high performance liquid chromatography, size exclusion chromatography, ultra performance chromatography, gel permeation chromatography

The objectives of the reviews are the collection, concise description, comparison and evaluation of the various chromatographic technologies using natural and modified cyclodextrins for the increase the separation capacity of various chromatographic separation systems.

* Corresponding Author

E-Mail: szogyim@t-online.hu

[a] Research Center for Natural Sciences, Hungarian Academy of Sciences, Budapest, Hungary

Introduction

Chromatographic procedures were developed and successfully employed for the separation of a high number of organic and inorganic compounds present at trace level in complicated accompanying matrices. The capacity of chromatographic separation technologies can be increased by the modification of both the stationary and the mobile phase of the system. Because of their specific adsorption character cyclodextrins (CD) and cyclodextrin derivatives (CDs) have been frequently applied for the improvement of the separation parameters (mainly chiral separation capacity) of various chromatographic methods. The chiral separation capacity of cyclodextrins has been frequently exploited for the separation of enantiomers with markedly different biological activity employing CDs. CDs and CD derivatives can be equally used as additives of stationary phase or modifier of the mobile phase. The number of studies dealing with the application of CDs and CD derivatives for the increase of the separation capacity of chromatographic systems increased considerably. Because of their versatility CDs have found application in many special branch of chromatography such as liquid chromatography (LC), gas chromatography (GC), size exclusion chromatography (SEC), gel permeation chromatography (GPC), and electrically driven separation methods (CE, CZE), and ultra performance liquid chromatography (UPLC).

Application of cyclodextrins in liquid chromatographic techniques

Because of their versatility, reproducibility and sensitivity various HPLC methods have been frequently employed for the separation of optical and positional isomers in HPLC systems employing CDs in the mobile and/or stationary phases. The applications and development of new CD chiral stationary phases (CD-CSPs) have been recently reviewed and their use in capillary electrochromatography (CEC),

open tubular CEC (OT-CEC, packed-bed CEC (P-CEC), pseudostationary CEC (PSP-CEC), monolithic CEC, and supercritical fluid chromatography (SFC), has been discussed more in detail.¹

Another review has been published on the application of sub- μm porous silica stationary phases in LC and CEC. The review established that these new materials are suitable for the rapid and efficacious separation of a wide variety of analytes.²

The application of new chiral selectors in the enantiomeric separation using HPLC and CE technologies has also been reviewed and the importance of chiral discrimination in biological samples is emphasized³. Chemically bonded cationic β -cyclodextrin derivatives were synthesized and employed for the enantioseparation of racemic pharmaceutical compounds. Vinylene-functionalized cationic β -CDs were co-polymerized with vinylized silica in the presence of AIBN and conjugated monomers. It was established that this new stationary phase can be successfully employed in packed column supercritical fluid chromatography.⁴

The characteristics of the quercetin/hydroxypropyl- β -CD were investigated in detail using various physicochemical analytical method such as differential scanning calorimetry, Fourier transform infrared spectroscopy, X-ray powder diffractometry, scanning electron microscopy and HPLC. The measurements indicated that the inclusion complex formation increases considerably the water solubility of the end product.⁵

Silica gel layers impregnated with β -CD were employed for the enantiomeric separation of (\pm)-propranolol and (\pm)-atenolol. Silicagel layers were bulk-impregnated with β -CD. Analytes were enantioseparated in solvent systems of DMF-ethyl acetate-butanol (3:2:5, v/v) and butanol-acetic acid-ethyl acetate-ammonia (5:2:2:0.5, v/v), respectively. Analytes were detected with iodine.⁶

Countercurrent chromatography was employed for the isolation of bitter acids from hops (*Humulus lupulus* L). Analytical procedure applied two separate countercurrent methods. The first step used hexane and aqueous buffer and

resulted in a mixture of cis/trans diastereomers. Cis and trans diastereomers were separated in the second step using mobile phase containing β -CD. The successful separation of individual bitter acids from commercially available hop extracts was reported.⁷

Affinity capillary electrophoresis and mass spectrometry (ACA-MS) has been used for label-free solution-based affinity analysis. Drugs included in the investigations were: ibuprofen, *s*-fluoribuprofen, phenylbutazone, naproxen, folic acid, resveratrol, 4,4'-propane-1,3-diy) dibenzoic acid. The results of ACE-MS were compared with those obtained with direct infusion mass spectrometry (DIMS) and ACE with UV detection. It was established that the application of ACE-MS facilitate the simultaneous affinity analysis of multiple interactive pairs resulting in high-throughput screening of drug candidates.⁸

Estrogens in pork and chicken samples were determined by stir bar sorptive extraction (SBSE). Poly(dimethylsiloxane) (PDMS)/ β -CD/divinylbenzene (DVB)-coated stir bar was prepared by the sol gel technique. Liquid desorption and HPLC followed by UV detection were employed for the separation and quantitative determination of the analytes. The limit of the detection was 0.21 – 1.6 $\mu\text{g L}^{-1}$, the dynamic range varied between 2 – 2000 $\mu\text{g L}^{-1}$. The relative standard deviation of the method was 6.0 – 9.7 %. It was stated that the method is simple, selective, sensitive, and can be successfully applied for the analysis of estrogens in pork and chicken samples.⁹

Thus, hydroxy- β -CD and gelatin were applied to increase the solubility of puerarin. The objectives of the measurements were to create puerarin nanoparticles which improves puerarin entrapment, efficacy, penetration and bioavailability. It was stated that puerarin nanoparticles are potentially applicable for the brain injury induced by ischemic-reperfusion.¹⁰

A new method combining in vivo microdialysis (MD) sampling, turbulent-flow chromatography (TFC) with LC/MS was developed and applied for the study of the pharmacokinetic of puqietinone. Separation was carried out on a fast LC column (4.6 mm x 50 mm x 1.8 μ). HP- β -CD was added to the system to increase the relative recovery of the analyte. The LOG value was 0.10 ng mL⁻¹. The method showed good linearity ($R^2 = 0.9993$) in the concentration range of 1.02 – 200.02 ng L⁻¹. It was established that the new method eliminates the influence of matrix effect. The efficacy of the technique was demonstrated by the application of the method for the pharmacokinetic study of the puqietinone in rats.¹¹

The bioactive polyphenol resveratrol shows marked beneficial biological effects such as antioxidant, anti-inflammatory, anti-carcinogenic, and anti-aging activity. A considerable number of drug delivery systems was developed to increase the poor bioavailability, the rapid metabolizing and excretion of resveratrol. The employments of various drug delivery systems such as nano and microformulations, liposomes, solid lipid nanoparticles, solid polymeric nanoparticles, solid lipid nanoparticles, liposomes, cyclodextrins. Polymeric microspheres, yeals cell carriers and calcium of zinc pectinate beads. The application of resveratrol in medicinal chemistry has been previously discussed.¹²

The inclusion complex of cefaclor with β -cyclodextrin was investigated by using thin-layer chromatography combined with densitometry and with proton nuclear magnetic resonance spectrometry.¹³

Cyclodextrins as mobile phase additives were successfully applied for the improvement of the separation of catechin components in tea. It was stated that the new method reduces the ratio of organic components in the mobile phase, improve resolution and retention factors. The best separation was obtained by employing a conventional C18 column and a mobile phase acetonitrile/water (12/88, v/v) containing 1.5 mM L⁻¹ β -cyclodextrin. The flow rate was 1.0 mL min⁻¹. It was stated that the method can be applied for the separation and determination of other active compounds from natural plants.¹⁴

The application of SBECD (sulfobutyl ether β -CD) in RP-HPLC was investigated in detail. The method make possible the enantiomeric separation of fenoterol, idazoxan and its hydrolyzate, orciprenaline, terbutaline, tranlycypromine, 1-aminoindane, nefopam, and imazalil. It was further established that SBECD modifies the impurity profiles for the fermentation-derived drugs A40926, ramoplanin, teicoplanin and vancomycin. The measurements suggested that SBECD can be used for the modification of the separation character of C18 column being a viable alternative for the commercial chiral columns.¹⁵

Nano-liquid chromatography (nano-LC) technology was developed for the enantioseparation of bioactive compounds. The monolithic column was synthesized using HP- β -CD as chiral selector and water-soluble comonomers. Analytes were separated employing aqueous mobile phases modified with methanol or acetonitrile and buffered with 0.1 % triethylamine-acetate. It was established that nomifensine and naproxen were baseline separate while praziquantel, metomidate and 5-methyl-5-phenyl-hydantoin was only partially resolved.¹⁶

A rapid and simple HPLC method was developed and successfully applied for the analysis of urocanic acid isomers extracted from human skin. Measurements were carried out on a β -CD column, the mobile phase was phosphate buffer-acetonitrile 15:85 v/v, the isocratic flow rate was 0.3 mL min⁻¹. Analytes were detected at 276 nm, the column temperature was 20°C. It was established that the method separates urocanic acid isomers, it is rapid and can be employed for the quantification of urocanic acid isomers extracted from skin.¹⁷

The enantioselective separation capacity of CDs and cyclofructans (CFs) was compared. The basic compounds were derivatized using either dimethylphenyl or *R*-naphthylphenyl and their separation characteristics were investigated using normal phase HPLC method. The measurements indicated that both the structure of the cyclic oligosaccharide and the character of the derivatizing agent influence markedly the enantioselectivity of the separation system.¹⁸

The beneficial characteristics of natural CDs and their derivatives have been discussed in detail. It was emphasized that CDs are successfully applied in foods and food products, pharmaceutical preparations, agricultural practice and in a

wide variety of analytical procedures. It was further established that CDs are produced from a renewable natural material (starch). Because of their encapsulation capacity they can be applied in the solution of many chemical problems, changing molecular solubility. Moreover, CDs and CD derivatives can enhance the stability of the included molecules. Because of their capacity to increase the solubility of environmental pollutants they can modify the departure of organic contaminants and heavy metal from soil, water and atmosphere.¹⁹

The influence of the drying method and drying carriers on the performance and physicochemical characteristics of spray-and spouted bed-dried phytopharmaceutical preparation of *Bidens pilosa* L. The efficacy of colloidal silicon dioxide, β -CD, maltodextrin dextrose equivalent (DE) 10, and microcrystalline cellulose on the drying process was investigated using the following parameters: particle size and morphology, total flavonoid content, solubility, flowability and water activity. Energetic efficiency, product recovery, elutriation and product accumulation were also determined.

The crystalline state of the powder was assessed by X-ray diffraction. The measurements indicated that the lowest flavonoid degradation (8.6 %) was achieved by using β -CD as drying carrier. The recoveries obtained by spray drying and spouted bed drying were 86.9 % and 72.9 %, respectively.²⁰

A pharmacokinetic study was carried out for the comparison of the characteristics of two docetaxel parenteral formulations (SID530) and β -CD. The concentration of the active agent in whole blood and plasma was followed by liquid chromatography-tandem mass spectrometry (LC-MS/MS). The measurements indicated that the behaviour of the two formulations were comparable. Maximum serum concentration, time to peak concentration, and area under the concentration-time curve were similar. It was concluded from the data that the drugs are bioequivalent in monkey. Experiments used cynomolgous monkey.²¹

The complex formation between CDs and the HIV inhibitor UC781 was studied in detail using RP-HPLC. CDs included in the experiments were: β -CD, HP- β -CD and methyl β -CD. Analytes were eluted isocratically with acetonitrile-water. It was established that the modification of β -CD also modified the complex formation.²²

A novel magnetic nanoadsorbent (CMCD-APTS-MNPs) containing the superparamagnetic and molecular recognition properties was synthesized by grafting CM- β -CD on-3-aminopropyl-triethoxysilane (APTS) modified FE304 nanoparticles. It was established that the new product can be employed for the rapid and selective separation of nucleosides and nucleotides in biological samples.²³

A molecularly imprinted polymer was prepared using ultrasonic irradiation, with attapulgitr as matrix, β -naphthol as template molecule, acryloyl- β -CD as functional monomer, and N,N-methylenebisacrylamide as cross-linking agent, respectively. The polymer was characterized by the traditional heat infrared spectroscopy and transmission electron microscopy. It was established that the new polymer has a better selectivity and the adsorption kinetic to

estrol, estradiol, estrone and diethylstilbestrol. The limit of detection for these analytes were between 100 and 1000 ng g⁻¹. RSDs (n = 6) were lower than 5.1 %.²⁴

A binary sorbent based on achiral liquid crystal 4-methoxy-4'-ethoxyazobenzene and macrocyclic heptakis(2,3,6-tri-O-acetyl)- β -CD (10.25 wt %) was prepared and the various physicochemical characteristics of the product was investigated (mesomorphous, sorption, selectivity), and the excess thermodynamic function of sorption by the binary sorbent from gaseous phase was determined using 29 organic compounds as model compounds (n-alkanes, cycloalkanes, arenes, monoatomic alcohols, heterocycles, optical isomers of camphene, limonene, and butanediol-2,3). It was established that the binary sorbent showed high structural selectivity over a wide temperature range.²⁵

Various physicochemical and thermodynamic methods were employed for the characterization of the bioactive hydroxy pentacyclic triterpenic acids (HPTAs). The inclusion complex formation of gamma-CD with ursolic, oleanolic, and betulinic acids was investigated by differential scanning calorimetry and H-1 NMR spectroscopy. The apparent formation constants (K-f) were determined by RP-HPLC. Thermodynamic parameters Delta GA(0), Delta HA(0), and Delta SA(0) were measured in the temperature range 25 – 45°C. The influence of gamma CD on the water solubility of HPTA was determined by phase-solubility measurements.²⁶

A new chiral stationary phase was synthesized using surface initiated atom-transfer radical polymerization (ATRP). Poly(2-methyl-3-butyn-2-yl methacrylate-co-divinylbenzene) was grafted on silica surface via ATRP technology. Azide-modified β -CD was immobilized on the alkyne of the polymer layer used as chiral separation stationary phase. HPLC measurements were carried out of an column of 150 mm x 4.6 mm i.d. filled with the new stationary phase. The retention behaviour of aromatic and chiral compounds was investigated. The measurements indicated that the retention characteristics of the new stationary phase differ markedly from that of the original stationary phase.²⁷

Two covalently bonded cationic β -CD chiral stationary phases (CSPs) were prepared and applied for the enantioselectivity of 12 racemic pharmaceuticals and 6 carboxylic acids. The new phases were prepared by graft polymerization of 6(A)-(3-vinylimidazolium)-6-deoxyperphenylcarbamate- β -cyclodextrin chloride or 6(A)-N,N-allylmethylammonium-6-deoxyperphenylcarbamoyl- β -cyclodextrin. The results indicated that the enantiomeric separation capacity of CSPs was different, the separation capacity of CS containing imidazolium was markedly higher.²⁸

A HPLC method was developed for the enantiomeric separation of flavanol enantiomers (+)- and (-)-epicatechin and (-)-catechin in cocoa-based products. Isocratic elution was carried out with methanol ammonium acetate buffer. Analytes were detected by fluorescence. The measurements indicated that concentration of monomeric flavanols was the highest in each sample (68-91 %). The interday and intraday precision of the method varied between 1.46 – 3.22 % in cocoa based products. Recoveries ranged 82.2-102.1 % at

50 % spiking level, 83.7-102.0 % at 100 % spiking level, at 80.4-101.1 % at 200 % spiking level. Because of the favorable separation characteristics the method was proposed for the routine analysis of cocoa-based products.²⁹

A silica adsorbent containing β -CD was developed for the preparative separation and purification of epicatechin gallate (EGCG) from green tea extracts. The measurements indicated that β -CD bonded silica sorbent possess excellent adsorption equilibrium capacity (over 55 %). Preparative separation of EGCG was achieved on a preparative column (220 mm x 15 mm i.d., particle size, 40 – 64). Analyte was eluted with methanol/acetonitrile/acetic acid. Sample was dissolved in acetonitrile and loaded at 0.8 mg g⁻¹ sorbent.³⁰

The enantioselectivity of nano-liquid chromatography and particulate capillary columns were compared using nonsteroidal anti-inflammatory drugs as model compounds (naproxen, ibuprofen, ketoprofen, fluorbiprofen, suprofen, indoprofen, cicloprofen, and carprofen). Measurements were carried out on achiral capillary columns and heptakis(2,3,6-tri-O-methyl)- β -cyclodextrin (TM- β -CD or hydroxypropyl- β -cyclodextrin (HP- β -CD) as chiral mobile phase additive (CMPA). Mobile phase consisted of water-ACN buffered with 50 mM sodium acetate at pH 3 containing 30 mM TM- β -CD (70:30, v/v). The column dimensions were 100 μ m i.d.. The analyses proved that the retention capacity of monolithic column was lower than that of traditional columns. It was further established that the enantioselectivity of the systems depended markedly on the type of stationary phase and on the composition of the mobile phase.³¹

A review was prepared for the elucidation of the role of click chemistry in the family of cyclic oligosaccharides, including chromatography, biological applications, elaboration of superstructures, and metal detection.³²

The separation and quantitative determination of resibufogenin and cinobufagin using RP-HPLC and gamma-cyclodextrin as mobile phase additive has been earlier reported. The factors influencing the retention have been studied in detail. The impact of the nature of cyclodextrin, the concentration of organic modifier in the mobile phase, the concentration of CD, the temperature of the separation was investigated. It was established that both resibufogenin and cinobufagin form inclusion complexes with CDs. The stability of the complex depends on the environmental conditions, and the stability of the inclusion complex decreases with increasing temperature. It was further determined that the complex formation spontaneous, exothermic and enthalpy driven. The method has been successfully applied for the separation and quantitative determination in Chansu (Bufonis venenum) samples.³³

Allyl- β -CD was prepared by treating β -CD with allylic bromine. A new type of molecularly imprinted polymers (MIPs) with selective adsorption for phtalate were synthesized using allyl- β -CD and methacrylic acid (MAA) as binary functional monomers. The product was characterized by scanning electron micrograph (SEM) and Fourier transform-infrared spectroscopy. Dipentyl phtalate (DPP) was employed as template. The allyl β -CD-MIPs was employed as selective sorbent for DPP and was employed

for solid phase extraction, and its application as molecularly imprinted solid-phase extraction was proposed.³⁴

A new polycarboxylate (MPC) superplasticizer was prepared by the copolymerization of acrylic acid, methallyl sulfonic acid, allyl poly(ethylene glycol)s and β -CD grafted maleic anhydride. The molecular characteristics of MPC was investigated by Fourier infrared spectroscopy and gel permeation chromatography. The impact of the concentration of β -CD on the application parameters of MPC was studied by the determination of cement paste fluidity, setting time, amount of adsorption of MPC on the cement particles. Differential scanning calorimetry and thermogravimetric measurements were also applied for the characterization of MPC. The measurements established that the initial fluidities and setting times of cement pastes increased with increasing number of β -CD side chains. It was assumed that the performance of MPC depended considerably on the solvation water film formed by the polyoxyethylene side chain and on the chelate formation between β -CD and the substructures of MPC.³⁵

A novel HPLC method was developed and applied for the analysis of alpha-tocopherol in inclusion complexes formed by natural β -CD and 2-hydroxy- β -CD. The validation parameters of the method were: specificity, selectivity, linearity, precision, range and recovery.³⁶

A novel RP-HPLC method was applied for the separation of five catechin compounds in tea. It was established that cyclodextrin additive in the mobile phase decreased considerably the use of toxic and inflammable organic solvents without reducing resolution and separation efficacy. Analytes were separated on a traditional C18 column using isocratic separation mode. Mobile phase consisted of acetonitrile/water (12/88, v/v) containing 1.5 mM L⁻¹ β -CD. The flow rate was 1.0 mL min⁻¹. It was stated that the method is eco-friendly, and can be applied for the separation and determination of other bioactive compounds from natural plants.³⁷

The 1:1 inclusion complex of quercetin with β -CD was prepared by rotational electromagnetic stirring and rotating evaporation. The inclusion complex was characterized by differential scanning calorimetry, and fourier-transform infrared spectroscopy. The water solubility of the inclusion complex was investigated by HPLC. It was concluded from the results that the formation of inclusion complex increased markedly the water solubility.³⁸

In vivo microdialysis sampling (MD) and turbulent-flow chromatography (TFC) followed by liquid chromatography-mass spectrometry was employed for the measurement of puqietinone after intravenous administration to rat. Separations were carried out on a column of 4.6 mm x 50 mm, particle size: 1.8 μ m. Puqietine, is a lipophilic alkaloid from *Fritillaria paqiensis*. It was found that the method employing MD combined with TFC-LC/MS is suitable for invivo monitoring experiments.³⁹

Chiral liquid chromatography was employed for the enantiomeric separation of ibuprofen in pharmaceutical formulations and the overlapping chromatographic profiles were evaluated by partial least squares regression (unfolded-partial least-squares regression, U-PLC). It was stated that

the method can be successfully applied for the analysis of ibuprofen. The analytes were partially separated on a permethyl- β -CD chiral column and the chromatograms were detected between 198 – 241 nm. U-PLC was employed for the evaluation of the chromatograms. It was found that the R(-)-enantiomer can be determined in tablet formulations at the level of 0.5 mg limits in the presence of 99.9 % of the S-(+)-enantiomer.⁴⁰

Hydroxypropyl- β -CD additive was employed in the HPLC analysis of isoflavone glycosides (calycosine-7-O- β -d-glucoside and formononetin-7-O- β -d-glucoside) and aglycones (calycosin and formononetin). The influence of validation parameters on the retention was investigated in detail. It was established that β -CD reduces considerably the retention of flavone aglycones. It was further assumed that the interaction between analytes and CD results in formation of 1:1 complexes influencing the retention of the analytes. It was further stated that the method can be successfully applied for the separation and quantitative determination of isoflavone glycosides and aglycones in *Radix Astragali* samples.⁴¹

The isomerization of perindopril was also determined by HPLC. The isomerization rate constants and Gibbs activation energies of isomerization were directly calculated from the chromatographic peak parameters. The relationships between peak shape and chromatographic conditions (flow-rate, temperature, pH, organic modifier, and the concentration of β -CD were investigated.⁴²

Three new β -CD-based chiral stationary phase were synthesized and their separation characteristics were determined and compared with each other. The derivatives included in the investigation were: β -cyclodextrin, (R,S)-2-hydroxypropyl- β -cyclodextrin and permethyl- β -CD based. The retention behavior of various analytes such as coumarins, dansyl amino acids and propionic acid derivatives was investigated. The measurements indicated that the CD derivatives showed considerably different retention behaviour, the differences in the retention markedly depended on the mode of preparation of the chiral stationary phase (CSP). The best enantiomeric separations were obtained on the stationary phase containing permethylated β -CD. The stationary phases consisted of 0.1 % aqueous triethylammonium phosphate (pH 3.5) and MeOH in different ratios.⁴³

Liquid chromatography-tandem mass spectrometry has been employed for the enantioselective separation of hexabromocyclododecane (HBCD) in fish. Analytes were microextracted with a supramolecular solvent (SUPRAS) made of reversed aggregates of decanoic acid. The enantiomers of α -, β -, and γ -HBCD were separated on a chiral stationary phase. Quantitative limit for the determination of individual HBCD enantiomers in hake, cod, sole, panga, whiting and sea bass were 0.5 - 3.4 ng g⁻¹; 0.9-2.5 ng g⁻¹; 0.6 - 1.4 ng g⁻¹; 1.0 - 5.6 ng g⁻¹; 0.8 - 1.03; 0.5 - 3.05 ng g⁻¹; respectively. Recoveries ranged 87 - 114 %, the relative standard deviation was between 1-10 %.⁴⁴

The chiral recognition and quantification of propranolol enantiomers was achieved by surface enhanced Raman scattering (SERS) combined with multivariate regression analysis. The factors influencing chiral recognition such as nature and concentration of chiral auxiliary, selector -

selectand ratio, pH, interaction time, etc. were investigated in detail. It was stated that the SERS method is simple, fast, and accurate and can be employed for the enantiomer analysis of propranolol without the use of tedious and expensive chiral separation technique. It was further established that the data obtained by SERS correlated well with the data obtained by chiral high-performance liquid chromatography.⁴⁴

A poly(dimethyl)siloxane (PDMS)/ β -cyclodextrin (β -CD)/divinylbenzene(DVB)-coated stir bar was prepared for the stir bar extraction of four estrogens from animal-derived foods. Stir bar was prepared by the sol gel technology for the stir-bar sorptive extraction (SBSE). Analytes were preconcentrated by liquid desorption (LD) followed with HPLC. Estrogens were detected by UV. LOD of the method was 0.21 - 1.6 μ g L⁻¹, the relative standard deviations varied between 6.0 % and 9.7 %. It was stated that the method was simple, sensitive and was successfully applied for the determination of estrogens in pork and chicken samples.⁴⁵

The current topics and trends in the chiral separation technologies were previously discussed in detail. The application of HPLC, micellar electrokinetic chromatography, counter-current chromatography, capillary-zone-electrophoresis, moving bed chromatography, tandem mass spectrometry, ultra-high pressure chromatography was mentioned. The advantages and disadvantages of the methods mentioned above has also been discussed thoroughly.⁴⁶

The retention behaviour of major isoflavonoids in *Radix Puerariae lobatae* and *Radix Puerariae thomsonii* was analysed by HPLC using CDs as mobile phase modifiers. The flavonoids included into the measurements were puerarin, daidzin, daidzein and genistein. Analytes were separated on a C18 column using isocratic elution. The influence of various chromatographic conditions on the retention such as the nature of the CD, the concentration of HP- β -CD, the amount of methanol in the mobile phase was studied in detail. The best separation was achieved with the mobile phase consisting methanol/water 25:75 containing 5 mM HP- β -cyclodextrin. It was established that the method can be successfully applied for the investigation of traditional Chinese herbs.⁴⁷

The pharmacokinetics of *Rhizoma Curcumae* oil-pure drug (RCO-PD) and its β -cyclodextrin inclusion complex (RCO- β -CD) were determined in pigs after oral administration. The concentration of the active ingredients in the plasma were measured by HPLC using UV detection.

The measurements indicated that the pharmacokinetics of the two preparations showed marked differences, the bioavailability of the RCO- β -CD being higher than that of RCO-PD.⁴⁸

The impact of temperature, ultrasonication, and chiral mobile phase composition on the separation of various analytes has been vigorously investigated. A new technology separated amino acids using CSP (chiral stationary phase) with CMPA (chiral mobile phase additive procedure). Mobile phase additive participating in the experiments were β -CD, γ -CD, and HP- β -CD. Separations were carried out at 25 and 50°C, with and without sonication.

It was found that the ultrasound decreased at each temperature the elution time and enantioselectivity.⁴⁹

HPLC has also been employed for the enantiomeric separation of nonproteinogenic amino acids. The methods applied up-till now have been recently listed and critically evaluated.⁵⁰

The inclusion of the antibacterial agent thymol on β -cyclodextrin-grafted organic cotton was obtained. It was established that the incorporation of monoterpene thymol into β -cyclodextrin-grafted organic cotton increased considerably the efficacy and durability of the end product. Grafting was carried out using citric acid as crosslinker in the presence of sodium hypophosphite by fixing at 150°C for 10 min. The efficacy of grafting procedure was verified by visible and FTIR spectroscopy of β -cyclodextrin, β -cyclodextrin-grafted fabric, ungrafted thymol and thymol-loaded fabric. Samples were extracted with ethanol and the concentration of thymol was determined by HPLC. It was established that the inclusion of antibacterial agent into grafted fabric showed marked enhanced antibacterial efficacy even after 10 cycles of washing. The investigations indicated that the grafting of CD on fabric, and inclusion of thymol into their cavity produced a durable antibacterial textile⁵¹.

Surface molecular imprinting technology was employed for the preparation of a highly selective sorbent. Solid-phase extraction followed by HPLC (SPE-HPLC) was employed for the determination of norfloxacin in complicated accompanying matrices. Molecularly imprinted polymer (MIP) was obtained by applying NOF as the template, β -cyclodextrin-methyl-methacrylate (β -CD-MMA) and acrylamide (AM). MIP extracted NOF selectively. The recoveries of the method was high (over 85.7 %). Because of the good validation parameters the method was proposed for the analysis of NOF in fish samples and for the preconcentration of quinolones in real samples⁵².

Reversed-phase liquid chromatography was employed for the analysis of resibufogenin and cinobufagin. The separation efficacy of the method was enhanced by adding gamma cyclodextrin to the mobile phase. The parameters influencing the validation parameters were investigated in detail (nature of cyclodextrins and organic modifiers, temperature of column). It was established that the stability of complexes decreased with increasing temperature. The method has been applied for the measurements of resibufogenin and cinobufagin in Chansu (Bufonis venenum) samples.⁵³

Thin-layer chromatographic method was applied for the separation and detection of degraded polysaccharides. The hydrolytic oligosaccharides from galactomannan or glucomannan together with pentasaccharide, tetrasaccharide, trisaccharide, and disaccharide were detected in the hydrolyzate.⁵⁴

Abbreviations

| | |
|--------|--|
| ACE-MS | affinity capillary electrophoresis mass spectrometry |
| ACN | acetonitrile |

| | |
|--------------------|--|
| CD-CSPs | cyclodextrin chiral stationary phases |
| CEC | capillary electrochromatography |
| CZE | capillary zone electrophoresis |
| DIMS | direct infusion mass spectrometry |
| EKC | electrokinetic chromatography |
| Es-GC-MS | enantioselective GC-MS |
| GCxGC | comprehensive two dimensional gas chromatography |
| GC/MS | gas chromatography/mass spectrometry |
| HCA | hierarchical cluster analysis |
| H-DAS- β -CD | Heptakis(2,3-di-O-acetyl-6-O-sulfo)- β -CD |
| H-DMS- β -CD | Heptakis(2,3-di-O-methyl-6-sulfo)- β -CD |
| HP- β -CD | hydroxypropyl- β -CD |
| HRE | heat reflux extraction |
| HSA | human serum albumin |
| HS-SPME | headspace solid phase microextraction |
| LOD | limit of detection |
| LOQ | limit of quantitation |
| MAE | microwave-assisted extraction |
| MD | in vivo microdialysis sampling |
| MDGC | heart-cut multidimensional gas chromatography |
| MDMA | 3,4-methylenedioxy-methamphetamine |
| NAIM | saccharide-naphthimidazole derivatives |
| OT-CEC | open tubular CEC |
| PCA | principal component analysis |
| p-CEC | packed-bed CEC |
| psp-CEC | pseudostationary CEC |
| QSMR | quantitative structure-mobility relationship |
| SBE- β -CD | sulfobutylether- β -cyclodextrin |
| SFC | supercritical fluid chromatography |
| TAS | Total analysis system |
| TFC | turbulent-flow chromatography |
| USE | ultrasonic extraction |

References

- Xiao, Y., Ng, S. C., Tan, T. T. Y., Wang, Y., *J. Chrom. A*, **2012**, *1269*, 52-68.
- Wang, Y., Ai, F., NG, S. C., Tan, T. T. Y., *J. Chromatogr. A*, **2012**, *1228*, 99-109.
- Kalikova, K., Riesova, M., Tesarova, E., *Centr. Eur. J. Chem.*, **2012**, *10*, 450-471.
- Wang, R. Q., Ong, T. T., Ng, S. C., *Tetrahedron Lett.*, **2012**, *53*, 2312-2315.
- Yang L., Yan, Q., H., Liu, B. G., Zhang, Y., Zhang, J. W., Fu, Q., *Asian J. Chem.*, **2012**, *24*, 3141-3144.
- Joshi, S., Sharma, A., *Acta Chrom.*, **2012**, *24*, 317-322.
- Dahlberg, C. J., Harris G., Urban, J., Tripp, M. R. Bland, J. S., Carroll, B. J., *J. Sep. Sci.* **2012**, *35*, 1183-1189.

- ⁸Mirinov, G., G., Logie, G., Okhonin, V., Renaud, J. B., Mayer, P. M., Berezowski, M. V., *J. Am. Soc. Mass Spectr.* **2012**, *23*, 1232-1240.
- ⁹Hu, C., He, M., Chen, B. B., Hu, B., *J. Agr. Food Chem.* **2012**, *60*, 10494-10500.
- ¹⁰Tao, H. Q., Meng, Q. F., Li, M. H., Yu, H., Liu, M. F., Du, D., Sun, S. L., Yang, H. C., Wang, Y. M., Ye, W., Yang, L. Z., Zhu, D. L., Jiang, C. L., Peng, H. S., *Naunyn-Schmiedeberg's Arch. Pharm.*, **2013**, *386*, 61-70.
- ¹¹Xin, G. Z., Cao, L., Shi, Z. Q., Li, H. J., Wen, X. D., Chen, J., Qi, L. W., Li, P., *J. Chromatogr. B-An. Techn. Biomed. Life Sci.*, **2012**, *899*, 127-134.
- ¹²Neves, A. R., Lucio, M., Lima, J. L. C., Reis, S., *Current Med. Chem.*, **2012**, *19*, 1663-1681.
- ¹³Dabrowska, M., Krzek, J., Miekina, M. J. P. C., *J. Planar Chrom.-Modern TLC*, **2012**, *25*, 127-132.
- ¹⁴Bi, W., Li, S., Row, K. H., *Phytochem. Anal.*, **2012**, *23*, 308-314.
- ¹⁵Ngim, K. K., Zhong, Q. Q., Mistry, K., Chetwyn, N., *J. Liq. Chrom. Rel. Technol.* **2012**, *35*, 2845-2859.
- ¹⁶Rocco, A., Maruska, A., Fanali, S., *Chemija*, **2012**, *23*, 294-300.
- ¹⁷Morales, J., Gunther, G., Zanocco, A. L., Lemp, E., *Anal. Lett.*, **2012**, *46*, 95-1016.
- ¹⁸Vozka, J., Kalikova, K., Janeckova, L., Armstrong, D. W., Tesarova, E., *Anal. Lett.*, **2012**, *45*, 2344-2358.
- ¹⁹Bezergiannidou, C., Balouktsi, M., *Fres. Env. Bull.*, **2012**, *21*, 2844-2847.
- ²⁰Cortes-Rojas, D. F., Oliveira, W. P., *Drying Technol.*, **2012**, *30*, 921-934.
- ²¹Kim, T. K., Yoo, H. H., Kim, E. J., Lee, B. Y., Park, J. H., *Arzneimitt.Forsch.-Drug Res.*, **2012**, *62*, 280-284.
- ²²Yang, H. T., Parniak, M. A., Hillier, S. L., Rohan, L. C., *J. Incl. Phenom. Macrocyclic. Chem.*, **2012**, *72*, 459-465.
- ²³Badruddoza, A. Z. M., Junwen, L., Hidajat, K., Uddin, M. S., *Coll. Surf. B.-Bioint.*, **2012**, *92*, 223-231.
- ²⁴Zhao, C. D., Guan, X. M., Liu, X. Y., Zhang, H. X. *J. Chromy. A*, **2012**, *1229*, 72-78.
- ²⁵Onuchak, L. A., Burmatnova, T. S., Spiryaeva, E. A., Kuraeva, Y. G., Belousova, Z. P., *Russ. J. Phys. Chem.* **2012**, *86*, 1308-1317.
- ²⁶Fontanay, S., Kedzierewicz, F., Duval, R. E., Clarot, I., *J. Incl. Phen. Macrocycl. Chem.* **2012**, *73*, 341-347.
- ²⁷Wang, H. S., Xie, Q. W., Wang, H. Y., Zhu, D. K., Jiang, A., *Chem. Lett.* **2012**, *41*, 730-731.
- ²⁸Wang, R. Q., Ong, T. T., Tang, W. H., Ng, S. C., *Anal. Chim. Acta.* **2012**, *718*, 121-129.
- ²⁹Machonis, P. R., Jones, M. A., Schaneberg, B. T., Kwik-Urbe, C. L., *J. AOAC Int.* **2012**, *95*, 500-507.
- ³⁰Lai, S. M., Gu, J. Y., Huang, B. H., Chang, C. M. J., Lee, W. L. *J. Chromy. B.* **2012**, *887*, 112-121.
- ³¹Rocco, A., Maruska, A., Fanali, S. *Anal. Bioanal. Chem.* **2012**, *402*, 2935-2943.
- ³²Faugeras, P. A., Boens, B., Elchinger, P. H., Brouillette, Montplaisir, D., Zerrouki, R. *Eur. J. Org. Chem.* **2012**, *22*, 4087-4105.
- ³³Xing, J. F., Chen, L. N., Song, J., Guo, C. N., Jang, G. D., Zeng, A. G., *J. Sep. Sci.*, **2012**, *35*, 1884-1892.
- ³⁴Kang, Y. F., Duan, W. P., Li, Y., Kang, J. Y., Xie, J. *Carbohydr. Polym.* **2012**, *88*, 459-464.
- ³⁵Lv, S. H., Gao, R. J., Duan, J. P., Li, D., Cao, Q. *J. Appl. Polym. Sci.* **2012**, *125*, 396-404.
- ³⁶Gierlach-Hladon, T., Lange, K., *Acta Poloniae Pharm.*, **2012**, *69*, 591-595.
- ³⁷Bi, W., Li, S., Row, K. H., *Phytochem. Anal.*, **2012**, *23*, 308-314.
- ³⁸Yang, L., Yan, Q. H., Liu, B. G., Zhang, Y., Zhang, J. W., Fu, Q., *Asian J. Chem.*, **2012**, *24*, 3141-3144.
- ³⁹Xin, G. Z., Cao, L., Shi, Z. Q., Li, H. J., Wen, X. D., Chen, J., Qi, L. W., Li, P., *J. Chrom. B. Anal. Technol. Biomed. Life Sci.*, **2012**, *899*, 127-134.
- ⁴⁰Grisales, J. O., Arancibia, J. A., Castells, C. B., Olivieri, A. C., *J. Chromy. B. Anal. Technol. Biomed. Life Sci.*, **2012**, *910*, 78-83.
- ⁴¹Feng, B. L., Jin, J. Q., Wang, C. H., Song, J., Yang, G. D., Zeng, A. G. *J. Sep. Sci.* **2012**, *35*, 3469-3476.
- ⁴²Bouabdallah, S., Trabelsi, H., Ben Dhia M. T., Ben Hamida, N., *Chromatographia*, **2012**, *75*, 1247-1255.
- ⁴³Varga, G., Fodor, G., Ilisz, I., Szeman, J., Visy, J., Szente, L., Peter, A., *J. Pharm. Biomed. Anal.* **2012**, *70*, 71-76.
- ⁴⁴Lara, A. B., Caballo, C., Sicilia, M. D., Rubio, S., *Anal. Chim. Acta* **2012**, *752*, 62-68.
- ⁴⁵Bodoki, E., Oltean, M., Bodoki, A., Stiuflu, R., *Talanta*, **2012**, *101*, 53-58.
- ⁴⁶Hu, C., He, M., Chen, B. B., Hu, B., *J. Agr. Food Chem.*, **2012**, *60*, 10494-10500.
- ⁴⁷Ward, T. J., Ward, K. D., *Anal. Chem.*, **2012**, *84*, 626-635.
- ⁴⁸Zeng, A. G., Xing, J. F., Wang, C. H., Song, J., Li, C., Yang, X., Yang, G. D., *Anal. Chim. Acta*, **2012**, *712*, 145-151.
- ⁴⁹Yong-Xue, S., Yongjin, L., Dongping, Z., Gang, W., Zhichang, L., Haiyan, Z., *J. Vet. Pharmacol. Therap.*, **2012**, *35*, 47-51.
- ⁵⁰Lee, J. H., Ryoo, J., *J. Bull. Korean Chem. Soc.*, **2012**, *33*, 4141-4144.
- ⁵¹Ilisz, I., Aranyi, A., Pataj, Z., Peter, A., *J. Chromatogr. A*, **2012**, *1269*, 94-121.
- ⁵²Rukmani, A., Sundrarajan, M., *J. Ind. Textiles*, **2012**, *42*, 132-144.
- ⁵³Zhang, B. X., Zhao, J. C., Sha, B. J., Xian, M., *Anal. Meth.*, **2012**, *4*, 3187-3192.
- ⁵⁴Xing, J. F., Chen, L. N., Song, J., Guo, C. N., Yang, G. D., Zeng, A. D. *J. Sep. Sci.* **2012**, *35*, 1884-1892.

Received: 19.07.2013.
Accepted: 22.07.2013.



ADSORPTION OF Pb(II) FROM AQUEOUS SOLUTIONS BY ACTIVATED CARBON PREPARED FROM AGRICULTURAL WASTE: MAIZE LEAVES

Uzma Nadeem

Keywords: Pb(II); Agricultural waste; Maize leaves; Activated carbon; Adsorption Isotherms; Wastewater

Adsorption of Pb(II) from the aqueous solutions was studied using activated carbon prepared by agricultural waste maize leaves. The influence of Pb(II) concentration (5-30 mg L⁻¹), pH (2-8) and contact time (0-120 min.) on adsorption have been reported. Adsorption of Pb(II) is pH dependent and the results indicate that, optimum pH for the removal was found to be 4 for maize leaves activated carbon (MLAC). The Freundlich and Langmuir isotherm models were also used to describe the adsorption of Pb(II) on MLAC. Results shows that both the isotherms were fitted well. Maximum adsorption of lead on MLAC attained was 96 %. The results suggest that MLAC can be used as adsorbent for the removal of Pb(II) from aqueous solutions as industrial wastewater.

Corresponding Authors

Tel.: (+91)(011)(9711870215)

E-Mail: uzmanadeem3@gmail.com

[a] Chemistry Department, University of Delhi, Delhi, 110007, India.

Introduction

Heavy metals present in drinking water sources and in agricultural crops can be harmful to human. Heavy metals can be toxic, e.g. they damage nerves, liver and bones and they block functional groups of vital enzymes.¹ Various chronic disorders in human beings caused by all heavy metals including lead.² Lead poisoning in humans causes severe damage to the kidneys, nervous system, reproductive system, liver and brain and can cause death. Severe exposure to lead has been associated with sterility, abortion, stillbirth and neonatal death.³ Permissible limit for lead in drinking water given by U.S.Environmental Protection Agency (U.S. EPA) is 0.015 mg L⁻¹ and for wastewaters is 0.1 mg L⁻¹, given by both the U.S. EPA and Bureau of Indian Standards (BIS).⁴ The main anthropogenic pathway through which heavy metal enters the water bodies is via wastes from industrial processes such as metal plating, mining operations, tanneries, chloralkali, radiator manufacturing, smelting, alloy industries and storage batteries industries, etc.⁵ Current treatment methods for the removal of metal ions from wastewater includes mainly reduction, ion exchange, electrodialysis, electrochemical precipitation, solvent extraction, reverse osmosis, chemical precipitation and adsorption.⁶ Most of these methods suffer from drawbacks such as high capital and operational costs or the disposal of the residual metal sludge.⁷ For example, precipitation processes cannot guarantee the metal concentration limits required by regulatory standards and produce wastes that are difficult to treat. On the other hand, ion exchange and adsorption processes are very effective but require expensive adsorbent materials for the removal of heavy metals from dilute aqueous streams. The use of low cost and waste materials of biological origins as adsorbents of dissolved metal ions has been shown to provide economic solutions to this global problem. Adsorption of heavy metal ions on to activated carbon has been applied widely as a unit

operation in the treatment of industrial wastewater. The use of commercial activated carbon may not be suitable for developing countries because of its high cost; therefore there is a need to produce activated carbon from cheaper and readily available materials, which can be used economically on a large scale. Activated carbon prepared from the rice husks, ground nut husks, coconut husks, waste fertilizer slurry, peanuts hull, jute stick, *Moringa oleifera* seed husk, coconut husk and sawdust have been used for wastewater treatment and the potential of their ultimate usage are determined through by their adsorption capacity, regeneration characteristics and physical properties of the subsequent products.^{8,9} Activated carbon with their large surface area, microporous character and chemical nature of their surface area have made them potential adsorbents for the removal of heavy metals from industrial wastewater.

In this study activated carbon prepared from agricultural waste *Zea mays* leaves was used for the adsorption of Pb(II) from aqueous solution on batch scale. The performances of adsorption of Pb(II) have been predicted using Freundlich and Langmuir equilibrium isotherms. The objective of present endeavor, therefore, is to study the adsorption behavior of Pb(II) onto maize leaves activated carbon (MLAC), an economic viable and easily available adsorbent.

Experimental

Adsorbent preparation

The maize leaves used in this study was harvested from the agricultural farm in the Kaushambi, near by 60-70 km away from Allahabad, was washed several times with deionized water and left to dry. The activated carbon was prepared by treating maize leaves with concentrated sulphuric acid (1:1 w/v). The resulted black material was activated in an air-free oven at 160 ± 5 °C for 6 h, followed by washing with deionized water until free of excess acid and MLAC was dried at 160 ± 5 °C.¹⁰ The activated carbon prepared from agricultural waste maize leaves was ground and sieved to 100 mesh and then stored in air tight container.

Reagents

Analytical grade of Pb (NO₃)₂(Qualigens) was used for making stock solution of Pb(II) (1000 mg L⁻¹) in deionized water. The stock solution was diluted by serial dilution method as per requirement. The initial pH of the solution was adjusted by using either 0.1 N NaOH or 0.1 N H₂SO₄.

Batch adsorption experiments

Batch experiments with maize leaves activated carbon (MLAC) were conducted to investigate using a certain amount of adsorbent and 50 mL solution of Pb(II) ion solution in a conical flasks. The mixture was shaken in an orbital shaker (Shivam, ISO, 900/2000) at 120 rpm at 30°C for 24 h. The following operation conditions such as pH, contact time and metal concentration were investigated. Then the solution was centrifuged and the residual concentration of Pb(II) ion in supernatant was determined by atomic absorption spectrophotometer (ECIL-4141, Hyderabad).

The effect of pH on the biosorption of Pb(II) by MLAC was determined at pH values of 2, 3, 4, 5, 6, 7 and 8. For the adsorption 0.5 g of MLAC was added to 50 mL solution of Pb(II) ion (at 30 mg L⁻¹) in seven different flasks at pH ranging from 2-8. The mixture was shaken in an orbital shaker at 120 rpm at 30°C for 24 h. The supernatant was analyzed for residual lead after contact period.

For the determination of rate of the metal adsorption by MLAC (0.5 g) were mixed with 50 mL Pb(II) ion solution at concentration of 30 mg L⁻¹. The mixture was shaken in an orbital shaker at 120 rpm at 30°C. The supernatant was analyzed for residual lead concentration after the contact period of 0, 5, 10, 20, 25, 30, 40, 60, 80, 100, and 120 min.

In order to investigate the effect of different initial metal concentration on the uptake of lead from aqueous solution, 0.5 g MLAC were mixed with 50 mL Pb(II) ion solution at concentration of 5, 10, 15, 20, 25, 30 mg L⁻¹. The mixture was shaken in an orbital shaker at 120 rpm at 30°C for 24 h. The supernatant was analyzed for residual lead concentration after the contact period.

Calculations

The percent removal of Pb(II) ion by MLAC was calculated by using the Eqn. 1.

$$R(\%) = \frac{C_i - C_f}{C_i} \times 100 \quad (1)$$

where, R is the removal, C_i is the initial metal concentration and C_f is the final concentration of the metal ion in mg L⁻¹.

The sorption capacity was calculated from Eqn. 2

$$Q_e = \frac{V(C_i - C_e)}{1000W} \quad (2)$$

where, Q_e is the adsorption capacity (mg g⁻¹), C_i is the initial metal concentration (mg L⁻¹), C_e is the equilibrium concentration of metal (mg L⁻¹), W is the adsorbent dose (g) and V is the solution volume (mL).

Fourier Transform Infrared Spectroscopy

FT-IR spectroscopy was used to determine the vibration frequency groups in the adsorbent. The spectra was collected using a model (ABB, Canada; FTLA; 2000,) with in the wave-number range 500-4000 cm⁻¹. Specimens of adsorbents were first mixed with KBr and then grounded in an agate mortar (Merck,) at an approximate ratio of 1/100 for the preparation of pellets. The resulting mixture was pressed at 10 tons for 5 min. These pellets are used in the recording of spectra.

Results and Discussion

Effect of pH

The adsorptive behavior of Pb(II) ion was studied from the aqueous solution at different pH values are the principle factor influencing the adsorptive capacities of Pb(II) ion on MLAC. The removal of lead from the solutions presents several difficulties, mainly due to the fact that a precipitation process is not possibly by simple pH regulation of the solution as in the case of polyvalent metallic cations.¹¹ The result obtained are shown in figure-1, which shows the effect of pH on the adsorption of Pb(II) ion from the aqueous solution on MLAC. It is clear that Pb(II) ion was effectively adsorbed in the pH range of 4-7 and the maximum adsorption of ion MLAC occurred at pH 4 thus, pH 4 is chosen for all experiments. The decrease in adsorption at pH greater than 7 is probably due to the formation of hydroxide. This is in agreements with the results obtained by Khalid *et al.*¹² for adsorption of lead on rice husk. The hydrolysis of cations occurs by the replacement of metal ligands in the inner coordination sphere with the hydroxyl groups.¹³ This replacement occurs after the removal of the outer hydration sphere of metal cations. Adsorption may not be related directly to the hydrolysis of the metal ion, but instead of the outer hydration sphere that precede hydrolysis.

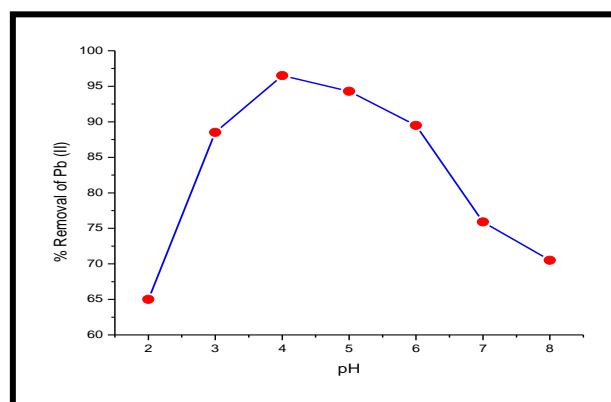


Figure 1: Effect of pH on Pb(II) removal

Most probably, the removal of lead from the aqueous solution by activated carbon involves a complex mechanism which is partly controlled by adsorption and partly by the chemical precipitation at the solid solution interface and also partly by the pore filling mechanism.¹⁴

Effect of contact time

The effect of contact time on the adsorption of lead is shown in Fig. 2. The results indicated that increase in the contact time increased the metal uptake but remained constant after an equilibrium time. The uptake of lead was rapid and the equilibrium was attained in 30 min of contact between the biosorbent and metal solution.

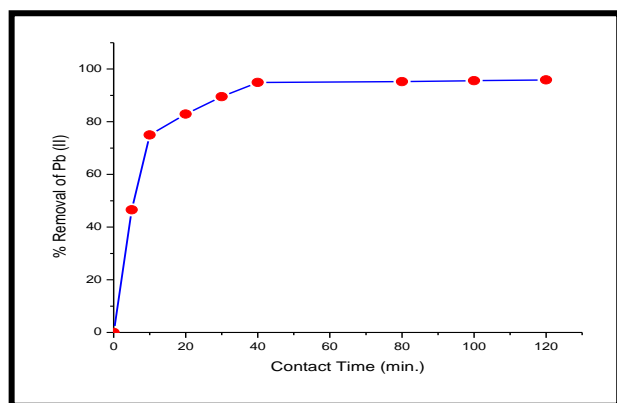


Figure 2. Effect of contact time on Pb(II) removal

Adsorption models

Modeling of equilibrium data is fundamental for the industrial application of adsorption since it gives information for comparison among different adsorbent under different operational conditions, designing and optimizing operation.¹⁵

The adsorption data were applied to the isotherm models.^{16,17} The adsorption isotherms generally used for the design of adsorption system. The Langmuir and Freundlich equations are commonly used for describing the adsorption isotherm.

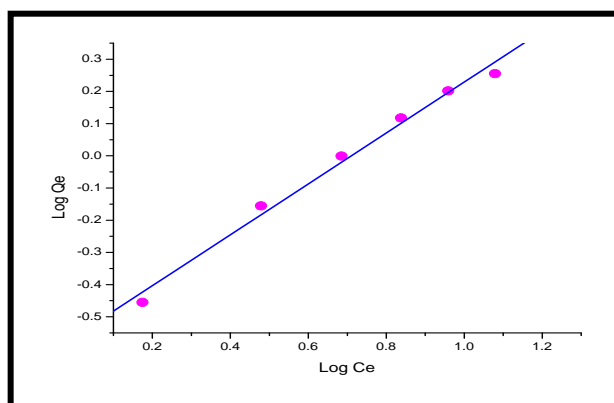


Figure 3. The linearized Freundlich adsorption isotherm of Pb(II) using maize leaves carbon

The adsorption data have been fitted to the Freundlich isotherm. Its linearised form is represented by equation.

$$\lg Q_e = \lg K + \frac{1}{n} \lg C_e \quad (3)$$

where, C_e is the equilibrium concentration (mg L^{-1}), Q_e is the amount adsorbed (mg g^{-1}) K is adsorption capacity and $1/n$ is adsorption intensity. A plot of $\log Q_e$ versus $\log C_e$ gives a straight line of slope $1/n$ and intercept K is shown in Fig. 3.

The linear equation of Langmuir represented as equation.

$$\frac{C_e}{Q_e} = \frac{1}{Q_{\max} b} + \frac{C_e}{Q_{\max}} \quad (4)$$

where, C_e is the metal concentration in the solution at equilibrium (mg L^{-1}), Q_{\max} (adsorption capacity) and b (energy of adsorption) are the Langmuir constants.

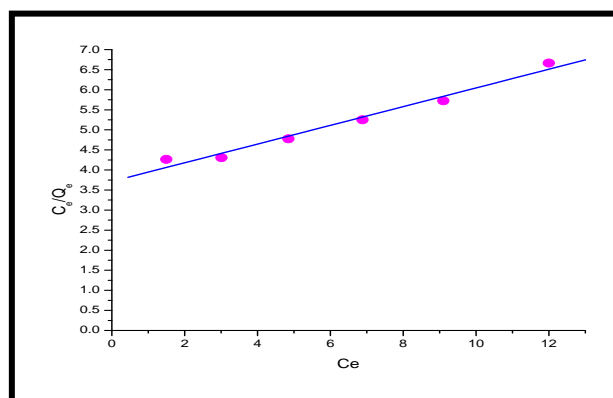


Figure 4: The linearized Langmuir adsorption isotherm of Pb(II) using maize leaves carbon

Adsorption of Pb(II) on MLAC was studied in the concentration range $5\text{--}30 \text{ mg L}^{-1}$ with 0.5 g of adsorbent in 50 mL for 24 h of equilibrium time. The plots of C_e/Q_e against C_e for adsorption of lead gave a straight line are shown in Fig. 4. It has seen that the linear fit is fairly good and enables the applicability of the Langmuir model to the Pb(II) adsorption on the maize leaf activated carbon.

The values of both Langmuir and Freundlich isotherm parameters were given in Table 1. Examination of data suggests that Freundlich isotherm is a good model for the sorption of Pb(II). The values of $1/n$ that vary between 0.1 and 1.0 indicate the favorable adsorption of heavy metals.¹⁸

Table-1: Langmuir and Freundlich adsorption parameters for the adsorption of Pb(II) ions at $30 \text{ }^\circ\text{C}$.

| Langmuir Parameters | | Freundlich Parameters | |
|------------------------------|--------|-----------------------|--------|
| $Q_{\max}, \text{mg g}^{-1}$ | 3.7136 | K | 0.2744 |
| $b \text{ L, mg}^{-1}$ | 0.6277 | $1/n$ | 0.7907 |
| R^2 | 0.9989 | R^2 | 0.9893 |

The essential characteristics of Langmuir equation can be described by dimensionless equilibrium parameter,¹⁹ R_L which is defined as;

$$R_L = \frac{1}{1 + bC_0} \quad (5)$$

where, b is the Langmuir constant, C_0 is the initial metal concentration of lead. The R_L values indicate the shape of isotherm as shown in Table 2. The R_L values between 0 and 1 indicate favorable adsorption.²⁰

Table 2. Relationship between R_L and type of isotherm

| R_L | Type of isotherm |
|-----------|------------------|
| $R_L > 1$ | Unfavourable |
| $R_L = 1$ | Linear |
| $R_L < 1$ | Favourable |
| $R_L = 0$ | Irreversible |

In the present study the R_L is shown in Fig. 5, for the initial concentration of Pb(II) ion of 5 - 30mg L⁻¹ indicating that the adsorption of Pb(II) is favorable.

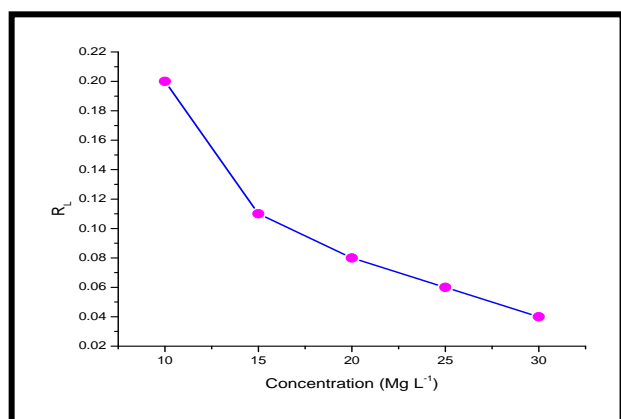


Figure 5. Plot of R_L vs initial Pb(II) concentration

The Langmuir model deals with monolayer coverage and constant adsorption energy while Freundlich equation deals with physicochemical adsorption on heterogeneous surfaces.²¹ The applicability of both these isotherms to the activated carbon, in the present study, implies that monolayer adsorption and heterogeneous surfaces conditions exist under the experimental conditions used. The adsorption properties of the adsorbent are thus likely to be complex, involve more than one mechanism.

Fourier Transform Infrared Spectroscopy

The absorption spectra of MLAC are represented in Fig. 6, reveals the functional groups that are responsible for binding the heavy metal ion. Table 3 gives the wave number with the corresponding groups. The hydroxyl and carboxyl functional groups provide the major biosorption sites for the metal binding.

Table-3. Infrared absorption bands and their corresponding groups of MLAC

| Wave numbers (cm ⁻¹) | Functional groups |
|----------------------------------|-------------------|
| 3435.935 | -OH, -NH |
| 2923.2 | -CH |
| 1515.79 | -CH |
| 1709 | C=O |
| 1630.36 | C=O, -COO |
| 1384.54 | -CH |
| 1118.84 | -C-O,C-N |

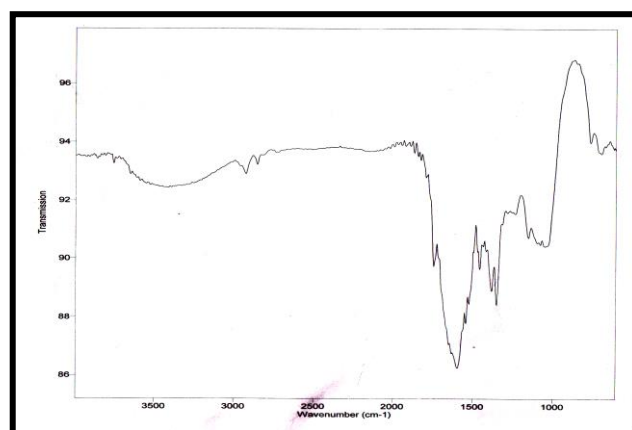


Figure 6. FTIR Spectra of activated carbon prepared from maize leaf

Conclusions

The maize leaves activated carbon is adsorbent of great potential and has proven appropriate for lead removal from aqueous solution, percentage of lead removal reach 96 %. The sorption isotherm of both Langmuir and Freundlich are obtained and they well described the sorption process indicating favorable adsorption of lead (II) onto MLAC as a monomolecular type. Removal of lead is highly pH dependent, the best results being obtained at pH 4. The sorption capacity was found to decreases lightly with increase in the adsorbate pH. The adsorption mechanism of lead(II) ion on MLAC involves either cation exchange or complexation between the metal cation and the hydroxide ion in the solution. The FT-IR of maize leaves carbon indicates the presence of several -OH and -COOH groups. Hydrogen of these groups is capable of ion exchange with metal cation. Based on the experimental conditions, it is concluded that the removal of lead ion from their aqueous solution could 96 %. This shows a new trend for using agricultural wastes for the benefit of environmental pollution control.

Acknowledgement

The authors are thankful for the financial assistance received from the University Grants Commission (UGC).

References

- ¹Evan, K. B.; Pamphlet, R.; *Neur. Tox.*, 1996, 17, 343-349.
- ²Ucun, H.; Baykan, Y.; Kaya, A.; Algur, O. F.; *Bioresource Technol.*, 2002, 85, 155-158.
- ³Goyer, R. A.; Chisolm, I. J.; *Lead in metallic contaminations and human health*. Lee DHK. (Ed.). Academic Press, New York, 1972, 57.
- ⁴Muralikrishna, K. V. S. G.; *Chemical analysis of water and soil. A laboratory manual*. Environmental Protection Society, National Institute of Ecology and Environment, Kakinada, India, 1997.
- ⁵Kadirvelu, K.; Thamaraiselvi, K.; Namasivayam, C.; *Bioresource Technol.*, 2001, 76, 63-65.
- ⁶Patterson, J. W.; *Industrial Wastewater Treatment Technology (2nd edn.)* Butterworth-Heinemann, London, 1995.
- ⁷Volesky, B.; *Hydrometallurgy*, 2001, 59, 203-216.
- ⁸Manju, G. N.; Anirudhan, T. S.; *Indian J. Environ. Health*, 1997, 4, 289-298.
- ⁹Raji, C.; Anirudhan, T. S.; *Indian J. Chem. Technol.*, 1997, 4, 228-239.
- ¹⁰Stephen Imbaraj, B.; Sulochana, N.; *Proc. Int. Conf. Water Environment (WE 2003)*, Bhopal, India, 2003, 15-18 December, 22-28.
- ¹¹Xu, M.; Liu, Y.; Tay, T.; *Bioresource Technol.*, 2006, 97, 359-363.
- ¹²Khalid, N.; Ahmad, S.; Naseer Kiani, S. and Ahmed, J.; *Sep. Sci. Technol.*, 1998, 33, 2349-2362.
- ¹³Gau, J. X.; Chen, Y. A.; Huang, S. D.; *Proc. Nat. Sci. Rep. China, Part A*, 1985, 9, 228-231.
- ¹⁴Knocke, W. R.; Hemphill, L. M.; *Water Res.*, 1981, 15, 245-250.
- ¹⁵Benguella, B.; Benaissa, H.; *Water Res.*, 2002, 36, 2463-2474.
- ¹⁶Freundlich, H.; *Z. Physik. Chem.*, 1907, 57, 385-470.
- ¹⁷Langmuir, I.; *J. Am. Chem. Soc.*, 1918, 40, 361-1403.
- ¹⁸Unnithan, M. R.; Anirudhan, T. S.; *Indian Eng. Chem. Res.*, 2001, 40, 2693-2701.
- ¹⁹Hall, K. R.; Eagleton, I. C.; Acrivos, A.; Vermeulen, T.; *Ind. Eng. Chem. Fund.*, 1996, 5, 212-219.
- ²⁰Ahalya, N.; Kanamadi, R. D.; Ramachandra, T. V.; *Ind. Jour. Chem. Technol.*, 2006, 13:122-127.
- ²¹Singh, K. K.; Singh, A. K.; Hasan, S. H.; *Bioresource Technol.*, 2006, 97, 994-1001.

Received: 30.06.2013.

Accepted: 26.07.2013.



ELECTROCHEMICAL AND SURFACE ANALYSIS STUDIES ON CORROSION INHIBITION OF MILD STEEL BY 1-(8-HYDROXY QUINOLIN-2-YLMETHYL)THIOUREA

S. S. Syed Abuthahir,^[a,b] A. Jamal Abdul Nasser,^[a] S. Rajendran^{[b]*}

Keywords: Corrosion Inhibition, mild steel, fluorescence spectra, organic inhibitors, surface analysis; 1-(8-hydroxyquinolin-2-ylmethyl)thiourea

1-(8-Hydroxyquinolin-2yl-methyl)thiourea (HTF) has been used as a corrosion inhibitor in controlling corrosion of mild steel immersed in aqueous solution containing 60 ppm of Cl⁻. Weight loss method reveals that 250 ppm of HTF + 25 ppm of Zn²⁺ provide 95% of inhibition efficiency. Polarization study indicates that the system controls anodic reaction predominantly. AC impedance spectra reveal that a protective film is formed on the metal surface. The protective film has been analyzed using Fourier Transform Infrared and fluorescence spectra.

* Corresponding Authors

E-Mail: srmjoany@sify.com

[a] Post Graduate & Research Department of Chemistry, Jamal Mohamed College, Tiruchirappalli 620 020, India. Email : syedchem05@gmail.com, ajanasser@yahoo.com

[b] Department of Chemistry, RVS School of Engineering and Technology, Dindigul-624 005, India.

Introduction

Water contains many corrosive electrolytes such as NaCl, MgCl₂ etc, Hence mild steel immersed in water containing NaCl is corroded slowly because of chemical reactions between the metal and the electrolytes.¹⁻³ Corrosion is the gradual destruction of materials usually by chemical reaction with its environment. The corrosion is severe due to the presence of Cl⁻ ions and dissolved oxygen. Water has been used as cooling fluid in various industries. Mild steel is widely used in infrastructure in marine environments.⁴ It is one of the major constituents in structural steel applications including body of a ship, offshore platforms, foundation piling, sheet piling and coastal facilities. It is also used in industry where the metal is exposed to acid corrosion. So it is imperative to study the corrosion aspect and find out suitable corrosion inhibitors to be used in water. Inhibition of corrosion and salting can be done by the applications of inhibitors which is one of the most practical and economic methods for protection against metallic corrosion.⁵⁻⁶ The use of inhibitor is one of the most practical methods to protect the metal from corrosion.⁷⁻⁸ Most of the effective inhibitors are compounds containing in their structures, nitrogen, phosphorous and sulphur. Heteroatom's such as nitrogen, phosphorous and sulphur are capable of forming coordinate covalent bond with metal owing to their free electron pairs and thus acting as inhibitor.⁷⁻⁹ This inhibitor used in protection against the corrosion of certain metals such as Ni, Co, Cu, iron and steel.¹⁰⁻¹¹ The aim of the present study was to investigate the corrosion inhibition for HTF to mild steel immersed in aqueous solution containing 60ppm Cl⁻. The corrosion inhibition efficiencies were evaluated using weight loss methods and Polarization spectra. The protective film formed on the metal surface

characterized with the help of surface analytical techniques such as fluorescence, UV-Visible and Fourier Transform Infrared Spectroscopy.

Experimental Procedure

Mild steel specimens; (0.0267% S, 0.067% P, 0.4 % Mn, 0.1 % C and the rest iron) of dimensions 1.0 cm ×4.0×0.2 cm were polished to mirrors finish and degreased with acetone and used for weight loss method.

Weight loss method

Mild steel specimens triplicate were immersed in 100 ml beaker containing 100 ml of aqueous solution containing 60 ppm of Cl⁻ containing various concentrations of the HTF-inhibitors and Zn²⁺ for one day. After one day immersion the specimens were taken out, washed in running water, dried and weighed using a Shimadzu balance, model AY62.

The corrosion inhibition efficiency (IE) was calculated using the equation:

$$IE (\%) = 100 \left(1 - \frac{W_2}{W_1} \right) \quad (1)$$

where

W₁ is the corrosion rate in the absence of inhibitor

W₂ is the corrosion rate in the presence of inhibitor.

Potentiodynamic polarization study

Polarization studies were carried out in a CHI electrochemical workstation with impedance model 643, Austin, USA. A three electrode cell assembly was used. The working electrode was mild steel. The exposed surface area was 1 cm². A saturated calomel electrode (SCE) was

Table 1. Corrosion rates (*CR*) of mild steel immersed in an aqueous solution containing 60 ppm Cl⁻ in the presence and absence of inhibitor systems at various concentrations and the inhibition efficiency (*IE*, %) obtained by weight loss method.

| Cl ⁻ | HTF, ppm | Zn ²⁺ , ppm | CR, mdd | IE, % |
|-----------------|----------|------------------------|---------|-------|
| 60 | 0 | 0 | 34.55 | - |
| 60 | 0 | 25 | 10.36 | 70 |
| 60 | 50 | 25 | 7.25 | 79 |
| 60 | 100 | 25 | 6.91 | 80 |
| 60 | 150 | 25 | 5.52 | 84 |
| 60 | 200 | 25 | 3.45 | 90 |
| 60 | 250 | 25 | 1.72 | 95 |

used as the reference electrode and a rectangular platinum foil was used as the counter electrode. The results such as Tafel slopes, I_{corr} , E_{corr} and LPR values were calculated.

Surface characterization studies

The mild steel specimens were immersed in various test solution for a period of one day. After one day the specimens were taken out and dried. The nature of the film formed on the surface of the metal specimen was analyzed by various surface analysis techniques.

FTIR studies

The FTIR spectra were recorded in a Perkin-Elmer-1600 spectrophotometer. The film formed on the metal surface was carefully removed and mixed thoroughly with KBr making the pellet.

Surface analysis by fluorescence spectroscopy

Fluorescence spectra of solutions and also the films formed on the metal surface were recorded using Jasco-F-6300 spectra fluorometer.

Results and Discussion

The corrosion rates (*CR*) of mild steel immersed in aqueous solution containing 60 ppm Cl⁻ and also inhibition efficiencies (*IE*) in the absence and presence of inhibitor (HTF) and Zn²⁺ obtained by weight loss method are given in Table 1. It is observed from Table.1 that HTF + Zn²⁺ shows good inhibition efficiency. The formulation consisting of 250 ppm of HTF and 25 ppm of Zn²⁺ has 95% inhibition efficiency.

Table 2. Corrosion parameters of mild steel in aqueous solution containing 60 ppm of Cl⁻ in the absence and presence of inhibitor obtained by polarization method.

| Systems | E_{corr} , mV vs SCE | I_{corr} , A cm ⁻² | b_a , mV/dec ⁻¹ | b_c , mV dec ⁻¹ | LPR, Ω cm ² |
|--|-------------------------------|--|------------------------------|------------------------------|------------------------|
| 60 ppm Cl ⁻ | -472 | 1.261×10^{-3} | 117 | 140 | 25.74 |
| 60 ppm Cl ⁻ + 250 ppm HTF + 25 ppm Zn ²⁺ | -459 | 8.207×10^{-4} | 096 | 144 | 30.58 |

Analysis of polarization curves

The polarization study has been used to investigate the formation of protective film on metal surface.¹²⁻¹⁶ The polarization curves of mild steel immersed in aqueous solution containing 60 ppm of Cl⁻ are shown in Figure 1. The corrosion parameters such as Corrosion potential (E_{corr}), Corrosion Current density (I_{corr}), Tafel slopes (b_c and b_a) and linear polarization curves (LPR) are given in Table 2.

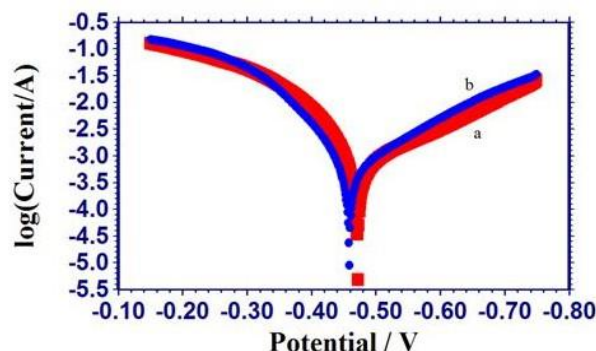


Figure 1. Polarization Curves of mild steel immersed in various test solutions: (a) Mild steel immersed in aqueous solution containing 60 ppm of Cl⁻ (b) Mild steel immersed in 250 ppm of HTF + 25 ppm of Zn²⁺.

When mild steel is immersed in aqueous solution containing 60 ppm of Cl⁻, the corrosion potential is -472 mV Vs SCE. The formulation consisting of 250 ppm of HTF + 25 ppm of Zn²⁺ shifts the corrosion potential to -459. It shows that the corrosion potential is shifted to positive side. This suggests that the anodic reaction is controlled predominantly.

The corrosion current density value and LPR value for aqueous solution containing 60 ppm of Cl⁻ are 1.261×10^{-3} A cm⁻² and 25.74 ohm cm² respectively. For the formulation of 250 ppm of HTF and 25 ppm of Zn²⁺ the corrosion density value has decreased to 8.207×10^{-4} A cm⁻² and the LPR value has increased to 30.58. The fact that the LPR value increases with decrease in corrosion current density indicates the absorption of the inhibitor on the metal surface to block the active sites and inhibit corrosion and reduce the corrosion rate with the formation of a protective film on the metal surface.

Analysis of the UV-visible spectra

The UV-Visible absorption spectrum of an aqueous solution containing HTF is shown in Figure 2. A peak appears at 450 nm. When Fe²⁺ solution is added to the solution the intensity of the UV-Visible spectra increases at 600nm. This peak is due to formation of Fe²⁺-HTF complex in solution.^{17,18}

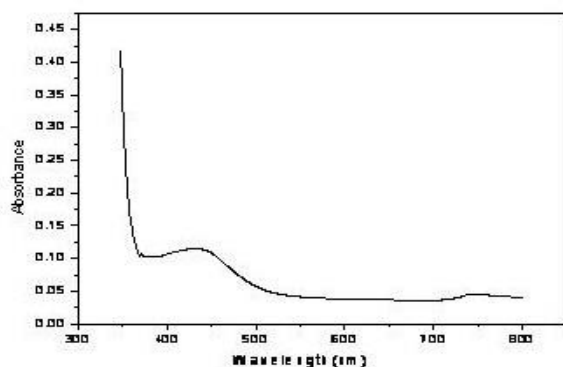


Figure 2a. UV-absorption spectrum solution containing HTF

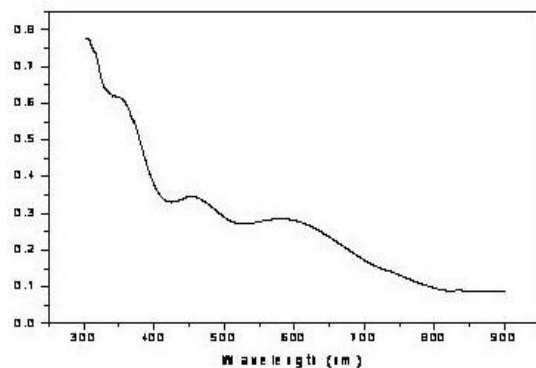


Figure 2b. UV- absorption spectra solution containing HTF-Fe²⁺

Fluorescence spectra

The emission spectrum (λ_{ex} : 460nm) of solution containing HTF-Fe²⁺ solution is shown in Figure 3a. The emission spectrum of the film formed on the metal surface after immersion in solution containing 250 ppm of HTF and 25 ppm of Zn²⁺ is shown in Figure 3b.

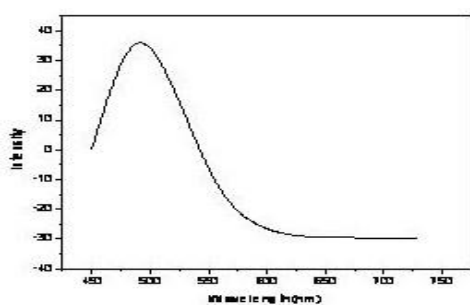


Figure 3a. Fluorescence spectrum of HTF solution

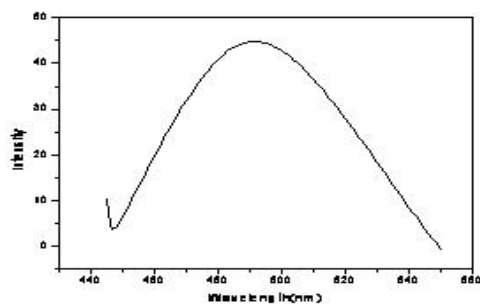


Figure 3b. Fluorescence spectra of solution containing HTF-Fe²⁺ complex.

A peak appears at 490nm. Hence it is concluded that the protective film consists of HTF-Fe²⁺ complex. The number peak obtained is only one. Hence it is confirmed that the complex of somewhat highly symmetric in solution.¹⁹

Analysis of FTIR spectrum

The FTIR spectra have been used to analyze the film formed on the metal surface.²⁰ The FTIR spectrum (KBr) of pure HTF is shown in figure 4a. The OH stretching frequency appears at 3300.34 cm⁻¹. The C=S stretching frequency appears at 1150.28 cm⁻¹. The CH stretching frequency appears at 3084.93 cm⁻¹. The peak due to secondary nitrogen (NH) appears at 3194.52cm⁻¹. The peak due to pyridine nitrogen (C=N) appears at 1490.36 cm⁻¹. The peak due to aromatic C=C appears at 1250.17 cm⁻¹.

The FTIR spectrum (KBr) of the film formed on the metal surface after immersion in the aqueous solution containing 60 ppm of Cl⁻ + 250 ppm of HTF + 25 ppm of Zn²⁺ for a period of one day is shown in Figure 4b. The phenolic OH stretching frequency has shifted from 3390.34 cm⁻¹ to 3490 cm⁻¹. The pyridine nitrogen frequency has shifted from 1490.36 cm⁻¹ to 1600 cm⁻¹. There is not much shift in other functional groups like C=S, NH and benzene ring. Thus it is concluded that oxygen atom of phenolic group and nitrogen atom of pyridine ring have coordinated with Fe²⁺ formed on the metal surface. The structure of the resulting HTF-Fe²⁺ complex is shown in Figure 5.

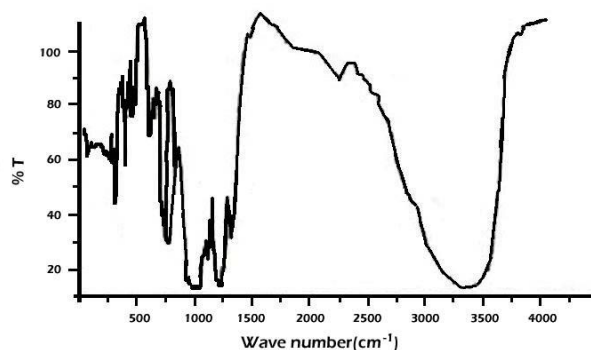


Figure 4a. FTIR spectrum of pure HTF

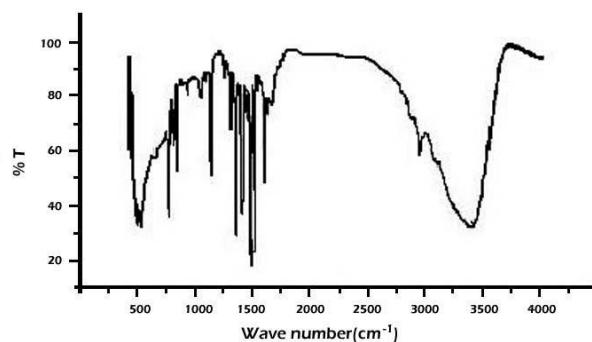


Figure 4b. FTIR spectrum of film formed on metal surface after immersion in solution containing 60 ppm Cl⁻ + 250 ppm of HTF + 25 ppm of Zn²⁺

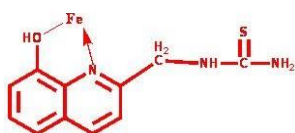


Figure 5. Structure of Fe^{2+} complex

This view is in agreement with the structure proposed by Albrecht et al. for zinc complex.²¹

Conclusion

The conclusion drawn from the results may be given as : the formulation consisting of 250 ppm of HTF and 25 ppm of Zn^{2+} has 95% inhibition efficiency. Polarization study suggests that anodic reaction is controlled predominantly. FTIR spectra show that the protective film consists of HTF- Fe^{2+} complex formed on metal surface.

References

- ¹Satyanarayana, M. G. V., Kalpana, Y., Himabindu, V. and Kumar, K., *Corros Eng Sci Technol.*, **2012**, 47(1), 38-44.
- ²Al-Baker, N., Shawabkeh, R. and Rihan, R., *Corros Eng Sci Technol.*, **2011**, 46(7), 767-776.
- ³Durodola, B. M., Olugbuyiro, J. A. O., Moshood, S. A., Fayomi, O. S. and Popoola, A. P. I., *Int. J. Electrochem Sci.*, **2011**, 6, 5605-5616.,
- ⁴Zou ,Y., Wang, J. and Zheng, Y .Y., *Corros Sci.*, **2011**, 53(1), 208-216.
- ⁵Khaled, K. F. and Hackerman, N., *Electrochim.Acta.*, **2003**, 48, 2715.
- ⁶Ali, S. A., Aseed, M. T., Rahman, S. V., *Corros.Sci.*, **2003**, 45, 253.
- ⁷Hackerman, N., *Langmuir*, **1987**, 3(6), 922-924.
- ⁸Nestle, A., "Corrosion inhibitors in petroleum production primary recovery", in *Corrosion Inhibitors*, C.C., Nathan, Ed., NACE, Houston, Tex, USA, **1973**.
- ⁹Flick, F. W., *Corrosion inhibitors: An industrial Guide*, William Andrew, 2nd edition, **1993**.
- ¹⁰Bilgic, S. and.Aksut, A. A., *British Corros. J.*, **1993**, 28(1), 59-62, .
- ¹¹Moretti, G. and Guidi, F., *Corros. Sci*, **2002**, 44(9), 1995-2011.
- ¹²Nagalakshmi. R., Rajendran. S., Sathiyabama, J., Pandiarajan, M., Lydia Christy, J., *Eur. Chem. Bull.*, **2012**, 1(17), 238.
- ¹³Sahayaraja A., Nagalakshmi, R., Rajendran. S., Angelin Thangakani, J., Pandiarajan, M., *Eur.Chem. Bull.*, **2012**, 1(3), 130.
- ¹⁴Agiladevi, S., Rajendran, S., Jeyasundari, J., Pandiarajan, M., *Eur.Chem.Bull.*, **2013**, 2(2), 503.
- ¹⁵Rajendran, S., Sridevi, S. P., Antony, N., John Amalraj, A., Sundaravadivelu, N., *Anti.Corros. Methods Mater.*, **2005**, 52, 102.
- ¹⁶Felicia Rajammal Selvarani, Santhanalakshmi, S., Wilson Sahayaraja, J., John Amalraj, A., and Rajendran, S., *Bull. Electrochem.*, **2004**, 20, 561.
- ¹⁷Rajendran, S., Maria Joany, R., Apparao, B. V. and Palaniswamy, N., *Indian J.Chem.Technol.*, **2002**, 9, 197-200.
- ¹⁸Rajendran S., Earnest John Peter, B. R., Peter Pascal Reces, A., John Amalraj, A. and Sundaravadivelu, M., *Trans. SABST.*, **2003**, 38(1), 11-15.
- ¹⁹Rajendran, S. and John Amalraj, A., *Bull. Electrochem.*, **2005**, 21, 185-191.
- ²⁰Jayasundari, J., Rajendran, S., Sayee Kannan, R., Brightson Arul Jacob, Y.,*Eur. Chem. Bull.*, **2013**, 2(9), 585-591.
- ²¹Albrecht, M., Witt, K., Weis, P., Wegelius, E., Frohlich, R., *Inorg. Chim. Acta*, **2002**, 341, 25-32.

Received: 29.05.2013.

Accepted: 22.07.2013.



BURDEN OF ORGANOCHLORINE PESTICIDE RESIDUES IN THE ROOT OF *CRYPTOLEPIS SANGUINOLENTA*, ANTIMALARIAL PLANT USED IN TRADITIONAL MEDICINE IN GHANA.

S. K. Agbeve^{[a]*}, D. Carboo^[b], G. Duker-Eshun^[a], S. Afful^[c] and P. Ofofu^[d]

Keywords: organochlorine pesticides, *Cryptolepis sanguinolenta*, anti-malarial plant, traditional medicine, bioaccumulation, pollution, gas chromatography.

The burden of organochlorine pesticides was determined in the roots of *Cryptolepis sanguinolenta*, an anti malarial plant. In all fourteen organochlorine pesticides, β -HCH, δ -HCH, γ -HCH, heptachlor, aldrin, γ -chlordane, α -endosulfan, p,p'-DDE, dieldrin, endrin, β -endosulfan, p,p'-DDD, p,p'-DDT and methoxychlor were identified and quantified using GC-ECD. Samples used for the investigation were collected from Abetifi and Pepease communities in the Kwahu-East and Apesokobi and Worawora in the Biakoye districts of Ghana. The effect of seasonal variations on the level of the organochlorine pesticide (OCPs) residues in the root of *Cryptolepis sanguinolenta* was also investigated. The mean concentrations of OCPs in the *Cryptolepis sanguinolenta* samples collected from Biakoye and Kwahu-East districts in the dry season were much higher compared to those of the wet season. The mean OCPs concentrations in dry season were found to range from 0.006 mg kg⁻¹ to 0.061 mg kg⁻¹ while the concentrations for the wet season ranged from 0.001 to 0.011 mg kg⁻¹. The sum of OCPs mean concentrations in the root *Cryptolepis sanguinolenta* also ranged from 0.033 mg kg⁻¹ to 0.354 mg kg⁻¹, with the highest mean level of 0.354 mg kg⁻¹ detected in samples collected from Biakoye district in the dry season. With the exception of residue levels obtained for the sum of aldrin and dieldrin in *Cryptolepis sanguinolenta* collected from Biakoye districts in the dry season, the mean OCP residue values obtained were generally below maximum residue limits set by the FAO/WHO Codex Alimentarius Commission and United States/European Pharmacopoeia.

*Corresponding Authors

Tel.: +233243275022

E-Mail: sagbeve@yahoo.com

- [a] Centre for Scientific Research into Plant Medicine, Ghana.
[b] Department of Chemistry, University of Ghana.
[c] Nuclear chemistry and Environmental Research Centre,
Ghana Atomic Energy Commission.
[d] Pesticide Residue Laboratory, Ghana Standards Authority,
Accra

INTRODUCTION

The increasing demand of vegetables and food crops for local consumption as well as for export has necessitated the use of various pesticides products in farming for the purpose of controlling and reducing the effect of insects in food production.¹⁻² It is estimated that 87% of farmers in Ghana use pesticides particularly in vegetable production.³ There are different types of pesticides and these may be classified as insecticides, fungicides, herbicides and antibiotics. Insecticides are mainly organochlorines, organophosphorus, carbamates and synthetic pyrethroids. All of these groups have varying effects on the environments as well as on humans.⁴⁻⁵

Organochlorine pesticides (OCPs) are a group of insecticides that came into widespread use in the late 1940's.⁶ The essential structural feature about organochlorine insecticides is the presence of carbon-chlorine bonds which are difficult to break.⁷ They therefore persist and bioaccumulate in living systems as well as biomagnified in the food chain as a result of resistant to environmental degradation through chemical, biological, and photolytic

processes.⁸⁻¹² Organochlorines have been implicated in a broad range of adverse human effects including reproductive failures and birth defects, immune system malfunction, endocrine disruptions, and cancers.¹³⁻¹⁴ It must however, be stressed that their use has now been banned by the Stockholm Convention on persistent organic pollutant. Despite being banned or prohibited, they are still detectable in the environment due to their persistence nature.¹⁵ Organochlorine pesticide once applied reach destinations other than their target species, including non-target species, air, water, soil, either by atmospheric deposition, runoff or leaching.¹⁶ Significant amount of these chemicals left on the field as residues are taken up by other biota including medicinal plants.¹⁷

Many studies of pesticide residues in herbal materials have been carried out in different countries. A study on marketed samples of passion flower (*Passiflora* spp.) from Brazil was found to contain organochlorine pesticide residues of dieldrin, lindane, α -endosulfan DDT and others at levels of 21.0 to 71.4 μ g kg⁻¹.¹⁸ A recent study by Xue and co-workers,¹⁹ also identified α -BHC, HCH, and others as the most common pesticide residues in 280 plant samples used in traditional Chinese medicine.

In Ghana *Cryptolepis sanguinolenta* is used in traditional medicine for the treatment of malaria. It is administered in dosage forms such as powders, tablets, granules in hard gelatin capsules, decoctions and tea bags. It is also used as major ingredient in the production of most gin bitters marketed in Ghana especially the popular "alomo" gin bitters by the Kasapreko Company Limited. The alcohol extract of the plant in a phyto-pharmaceutical study revealed

the present of organochlorine pesticide residues. Moreover, preparations made from this herbal plant are also administered over long periods of time especially chronic diseases requiring prolong and cheap herbal treatments.⁵ In Ghana most studies on organochlorine pesticides have focused on levels in water, sediments, fish, lean meat, breast milk, blood, fruits, vegetables and the potential health effects on farmers and consumers.²⁰⁻²⁶ However, there is paucity of data on the levels of OCP residues in medicinal plant parts used in traditional medicine in Ghana despite the wide range use of medicinal plants in Ghana.

Regarding the long term effects of low dose exposure and the public health significance of organochlorine pesticide residues.²⁷ Studies of OCP residue levels in the root of *Cryptolepis sanguinolenta* used in traditional medicine will therefore be useful in assessing the quality and safety of herbal medicine prepared from *Cryptolepis sanguinolenta* in terms of pesticide residue contamination.

The present studies therefore focused on the profile and burden of organochlorine pesticide residues in the anti-malarial plant, *Cryptolepis sanguinolenta*.

MATERIALS AND METHODS

Chemicals and reagents

All chemicals and reagents used in the study were of high quality and of analytical grade. Hexane (99% +), acetone (99.9% +), and ethyl acetate (99.8% +) were bought from Sigma-Aldrich. Florisil adsorbent material (60 - 100 mesh) was purchased from Hopkin and William Limited. The organochlorine pesticide standards used for the identification and quantification of OCPs residue were obtained from Dr. Ehrenstorfer GmbH of Augsburg, Germany. The internal standards used for the recovery experiment were obtained from United Nations Environmental Programme (UNEP) in sealed ampules.

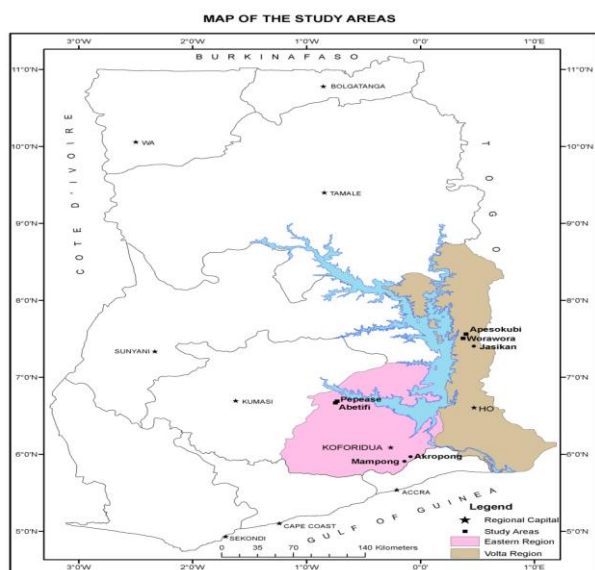


Figure 1. Map showing the study areas and sampling sites where the roots of *Cryptolepis sanguinolenta* plant were collected.

Study Area

The study was undertaken in two areas in Ghana, the Kwahu-East district in the Eastern region and the Biakoye district in the Volta region as shown in (Fig. 1). The criteria for the selection of the areas were the relatively high abundance and availability of the selected medicinal plant. The selected areas are also well known for the cultivation of vegetables, food and cash crops and therefore possible use of restricted or banned pesticides.

The sampling towns, Pepease and Abetifi in the Kwahu-East District lie between longitude 1°0'W and 0°0' and latitude 6°0'N and 7°0'N respectively as shown in (Figure 1). In terms of climate, Kwahu East lies within the west semi-equatorial region. It experiences the double maxima rainfall pattern (major and minor rainy seasons). The major rainy season starts from April and ends in July. While the minor rainy season also starts from September and end in October. Annual average rainfall is between 1580 mm and 1780 mm, with temperatures ranging between 26 °C and 30 °C. The climate in the district couple with the great irrigation potential of the Afram river favours the cultivation of food crops, fruits and vegetables. The soil belongs to the forest ochrosols. The Biakoye District with its capital Nkonya Ahenkro also forms part of the districts and municipalities created in 2008. The sampling towns, Apesokubi and Worawora lies between longitude 0°0' and 1°0'E and latitude 7°0'N and 8°0'N respectively. The district falls within the wet equatorial zone and experiences a double maxima rainfall regime in May to July and September to November with peaks in June and October. The rainfall pattern averages between 1,250 mm to 1,750 mm per annum in the mountainous areas. The dry season is mostly manifested between December and February. The vegetation supports wildlife and the major animals found are monkeys, antelopes, bush pigs, pangolins, grass-cutters, chimpanzees and reptiles.²⁸

Sample Collection

Sampling collection, extraction, clean up, and GC analysis of the pesticides were carried out according to the procedure described by other authors²⁴⁻²⁹⁻³⁰. A total of 100 of each root samples of the herbal plant from each sampling site were collected during each season. The samples which were randomly collected were put into ice chests, well sealed and labelled with unique identity and then transported to the Plant Development Department of the Centre for Scientific Research into Plant Medicine (CSRPM) at Mampong Akuapim in Ghana for identification and classification.

Sample extraction

The fresh root samples were washed thoroughly with water, air dried for two weeks and milled. Approximately 10 g of the dried-powdered and homogenized samples were each transferred into an extraction thimble that had been pre-cleaned with n-hexane and acetone and oven dried. To each sample 5 µl of isodrin used as internal standard was added and Soxhlet extracted with 160 ml of n-hexane/acetone (3:1) mixture for 12 hours. Boiling chips were added to allow smooth boiling.

The Soxhlet was also monitored occasionally during the extraction period to ensure satisfactory recycling. Extracts as well as the blank were concentrated to about 20 ml using a rotary evaporator at 40°C.

Sample cleanup

The florisil packed column which was ticked to allow the florisil to settle was conditioned by passing 12 ml n-hexane through the packed column. The sample was then transferred onto the florisil column, and eluted three times each with 10 ml portions of n-hexane using Pasteur pipette. The eluate was collected into a round bottom flask with a ground-glass stopper and evaporated to dryness using a rotary evaporator fitted to a vacuum pump. The extract was recovered with 1 ml of ethyl acetate using Pasteur pipette and then transferred into glass vials for gas chromatograph analysis.

Gas chromatographic analysis

A Varian CP-3800 Gas Chromatograph (Varian Associates Inc. USA) equipped with ^{63}Ni electron capture detector was used for the analysis. A volume of 1 μl of the extracts was injected and the separation was achieved on a 40m VF- 5ms capillary with internal diameter 0.25mm and film thickness of 0.25 μm . The oven temperature was programmed as 80°C (2min) to 180°C (1min) at 25°C min^{-1} to 300°C at 5°C min^{-1} . The carrier gas and make up gas was nitrogen at a flow rate of 1.0 and 29ml min^{-1} respectively. The injector and detector temperatures were 270°C and 300°C respectively. Sample peaks were identified by their retention times compared to the corresponding retention times of the pesticide standards.

RESULTS AND DISCUSSION

General organochlorine pesticide residues contamination

Table 1 shows the individual organochlorines, their respective mean concentrations and percentage occurrences. Margin of errors as standard deviation based on replicates determination of each organochlorine pesticide. Table 1 also shows the total residue load in the roots of *Cryptolepis sanguinolenta*. As indicated in Table 1, analysis of the samples revealed the presence of fourteen organochlorine pesticides in the roots of *Cryptolepis sanguinolenta*. The detectable compounds were β -HCH, δ -HCH, γ -HCH, heptachlor, aldrin, γ -chlordane, α -endosulfan, p,p'-DDE, dieldrin, endrin, β -endosulfan, p,p'-DDD, P,P'-DDT and methoxychlor. In generally higher concentrations of OCPs were recorded in the dry season compared to the wet season. This trend could possibly be explained from the fact that during the wet season some of the residues in the soil might have been carried away through surface run-off. The mean OCP residue concentrations in the samples collected in the dry season ranged from 0.006 mg kg^{-1} to 0.061 mg kg^{-1} (Tables 1). The highest mean concentration of 0.061 mg kg^{-1} was obtained for β -HCH in samples collected from Kwahu-East District while the lowest mean concentration of 0.006 mg kg^{-1} was recorded for p,p' DDT also in samples from

Kwahu-East District. In the wet season OCPs concentration ranged from not detected to 0.011mg kg^{-1} with the highest concentration of 0.011 mg kg^{-1} recorded for β -HCH in samples collected from Kwahu-East District. In the wet season heptachlor was not detected at Kwahu-East district while β -endosulfan and methoxychlor were also not detected at Biakoye district. Thus β -HCH was the predominant OCP in the study area with 100 % occurrences in both the dry and wet seasons. The highest total organochlorine pesticides residue load (i.e. the sum of the means of all detected organochlorine pesticides in a particular sample) ranged from 0.033 mg kg^{-1} to 0.354 mg kg^{-1} with the highest value of 0.354 mg kg^{-1} recorded for samples from Biakoye district in the dry season while a low total load of 0.033 mg kg^{-1} was obtained for samples also from the Biakoye district in the rainy season.

Variation of DDTs in the samples

Figure 2 showed the distribution of DDT and its metabolites in the samples. In Ghana DDT had been used extensively in the past for agriculture activities. However, the use of DDT in Ghana has now been limited only to malaria programs to fight the insect mosquito.³¹

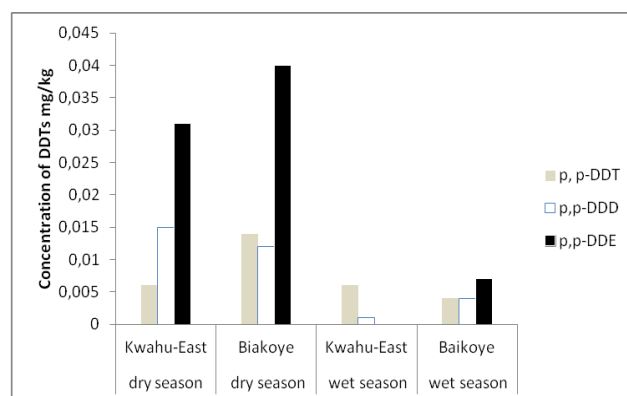


Figure 2. Distribution of DDTs in the roots of *Cryptolepis sanguinolenta* used for the investigation.

Mean concentrations of DDTs and its metabolites ranged from 0.001 mg kg^{-1} to 0.040 mg kg^{-1} . The higher concentration of 0.040 mg kg^{-1} was recorded for p,p'-DDE from the Biakoye samples in the dry season, while the lowest value of 0.001 mg kg^{-1} was recorded for p,p'-DDD from the Kwahu-East samples in the rainy season. The high mean concentrations of p,p'-DDE and p,p'-DDD compared to the parent DDT may be due to metabolic conversion and dehydrochlorination of p,p'-DDT. Additionally, the high mean values suggests the exposure of the matrices to intense sunlight experienced during the dried period and therefore possible conversions and isomerisation of p,p'-DDT by solar radiation to p,p'-DDE and p,p'-DDD.³² Also, ratios of p,p'-DDE plus p,p'-DDD/p,p'-DDT are often used as a criterion for the identification of new DDT sources. The high DDE/DDT levels suggest that current exposure levels primarily originates from previous contamination (historical use) and environmental persistency. DDE is generally more persistent in the environment than DDT and this suggests when the input levels of DDT in the environment ceases, the levels of its metabolite DDE will be higher than the parent DDT.²⁰

Table 1. Mean concentrations in mg kg⁻¹ of organochlorine pesticide residues in *C. sanguinolenta* sampled from the Kwahu-East and Biakoye Districts during the dry and rainy season and their comparison with international standards (WHO, 2007).

| Pesticide | Dry season, mg kg ⁻¹ | | | | Rainy season, mg kg ⁻¹ | | | | Limits in mg kg ⁻¹ | |
|--------------------|---------------------------------|-------|--------------|-------|-----------------------------------|-------|--------------|-------|-------------------------------|-------------------------------|
| | Kwahu-East | | Biakoye | | Kwahu-East | | Biakoye | | Ph. Eur and USP | Codex Alimentarius Commission |
| | Mean | SD | Mean | SD | Mean | SD | Mean | SD | | |
| β-HCH | 0.061 | 0.047 | 0.043 | 0.035 | 0.011 | 0.011 | 0.001 | 0.001 | ++0.300 | |
| δ-HCH | 0.017 | 0.004 | 0.032 | 0.014 | 0.002 | 0.000 | 0.001 | 0.001 | ++0.300 | |
| γ-HCH | 0.016 | 0.012 | 0.017 | 0.006 | 0.009 | 0.008 | 0.002 | 0.001 | 0.600 | |
| Heptachlor | 0.027 | 0.008 | 0.023 | 0.008 | nd | | 0.002 | 0.002 | +0.050 | |
| γ-Chlordane | 0.014 | 0.007 | 0.018 | 0.003 | 0.002 | 0.001 | 0.001 | 0.000 | +0.050 | |
| α-Endosulfan | 0.027 | 0.006 | 0.026 | 0.008 | 0.005 | 0.006 | 0.002 | 0.001 | +3.000 | +0.500 |
| β-Endosulfan | 0.010 | 0.007 | 0.029 | 0.012 | 0.005 | 0.007 | nd | | +3.000 | +0.500 |
| Aldrin | 0.012 | 0.009 | 0.020 | 0.012 | 0.003 | 0.003 | 0.001 | 0.001 | +0.050 | |
| Dieldrin | 0.032 | 0.027 | 0.046 | 0.026 | 0.009 | 0.009 | 0.006 | 0.007 | +0.050 | |
| Endrin | 0.023 | 0.010 | 0.014 | 0.008 | 0.002 | 0.000 | 0.002 | 0.001 | +0.050 | |
| p,p'-DDE | 0.031 | 0.019 | 0.040 | 0.027 | 0.003 | 0.004 | 0.007 | 0.007 | +1.000 | |
| p,p'-DDD | 0.015 | 0.007 | 0.012 | 0.006 | 0.001 | 0.001 | 0.004 | 0.006 | +1.000 | |
| p,p'-DDT | 0.006 | 0.005 | 0.014 | 0.005 | 0.006 | 0.005 | 0.004 | 0.000 | +1.000 | |
| Methoxychlor | 0.019 | 0.006 | 0.020 | 0.010 | 0.005 | 0.004 | nd | | | |
| Total Level | 0.31 | | 0.354 | | 0.063 | | 0.033 | | | |

SD = standard deviation. nd = not detected; USP = United States Pharmacopoeia; Ph.Eur = European Pharmacopoeia; + = Sum of isomers and metabolites; ++ = Sum of isomers other than γ-HCH

The mean values of methoxychlor (Table 1) may either be as a result of historical use of DDT of which technically methoxychlor contains about 88% of the p,p' isomer.³³ These values were however, lower than mean concentration of 0.03 μg g⁻¹ detected in pawpaw by.²⁵ The decreased perhaps, may be due to anaerobic biodegradation of methoxychlor which results mainly in dimethoxydiphenyl-dichloroethane (DMDD) as well as mono and dihydroxy or demethylated derivatives of methoxychlor.⁴⁻²⁶

Variation of hexachlorocyclohexane (HCHs)

1,2,3,4,5,6-hexachlorocyclohexane, the derivative of cyclohexane having one of the two hydrogen on each carbon substituted by chlorine was discovered during the Second World War to be an effective insecticides against a wide variety of insects. The pure active ingredient as well as the technical mixture has a considerable acute toxicity. Research has shown that only one of the eight isomers, the γ-isomer (the gamma isomer) has insecticidal properties and was sold as insecticide under the trade name lindane.⁴⁻⁶ The high value recorded in the studies especially in the dry season suggests photodecomposition and isomerization of HCHs (parent compound) during the transformation process in the soil, owing to the action by microorganisms. This further suggested that lindane (γ-HCH) is being used extensively in the Ghanaian agricultural sector on vegetable cultivation and on food crop production in Ghana.²⁵ This mean value of lindane also supports the findings of pesticide use in Ghana by Awumbila and Bokuma.³⁴ These pesticides were used on cocoa plantations, on vegetables farms and for the control of maize stemborers. Lindane was marketed in Ghana as Gammalin 20 and until 2007 when its use was discontinued.

Distribution of HCHs in the samples is presented in Figure 3. Three of the isomers, β, δ, γ were detected with 100 % occurrence. The α-isomeric form was not detected.

Despite the fact that γ-HCH is the main active ingredient in lindane, which had enjoyed wide application in Ghana,²⁵ the sum of β and δ- isomers far dominate the samples in terms of HCHs contamination compared to γ-HCH except in the wet season at Biakoye where percentage composition of the sum (β + δ) is the same as that of γ-HCH. The high composition of (β + δ) forms in the samples suggests wide historical used of technical mixtures of HCH in the study areas.

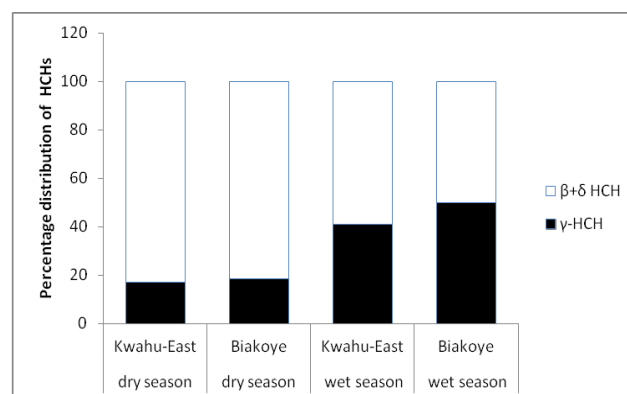
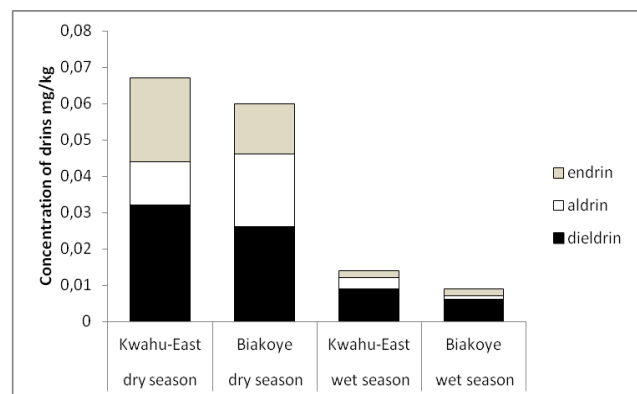


Figure 3. Profile of β, δ, γ-HCHs in the roots of *Cryptolepis sanguinolenta* sampled from Kwahu-East and Biakoye Districts in Ghana

Variation of drins

Drins is a group name used for cyclodienes insecticides aldrin, dieldrin and endrin and they are among the banned insecticides by the Stockholm Convention. Aldrin and dieldrin are chemicals that were widely applied in agricultural throughout the world to control insects in soil and in public health to control mosquitoes and tsetseflies the vectors that cause malaria and sleeping sickness respectively.⁴⁻⁶ Aldrin does break down to dieldrin in living systems but dieldrin is known to resist bacterial and

chemical breakdown processes in the environment.³⁵ Endrin had been used primarily as an insecticide on cotton as well as a rodenticide and avicide.³⁶ Figure 4 shows the profile of



the drins in the roots of *C. sanguinolenta* investigated.

Figure 4. Profile of drins in the roots of *Cryptolepis sanguinolenta* from Kwahu-East and Biakoye Districts in Ghana

It is obvious from the Figure 4 that dieldrin is the predominant drin in the samples with the highest concentration detected in samples from Kwahu-East district in the dry season. The dominance of dieldrin is not surprise at all since in the environment aldrin thus break down to dieldrin and the compound is also able to resist environmental degradation.³⁵ Aldrin on the other hand is the least significant drin in the samples. The use of aldrin in Ghana was marketed under the trade name Aldrex 40.⁴ Thus, the order of the drins in the root of *Cryptolepis sanguinolenta* was dieldrin > endrin > aldrin. In the environment endrin ketone and endin aldehyde are the degradation products of endrin through photodecomposition and microbial degradation.²⁵ The fact that endrin ketone and endrin aldehyde were not detected suggests less photodecomposition and microbial degradation of endrin in the study areas.

The study also had a high heptachlor mean concentrations of 0.023 mg kg⁻¹ and 0.027 mg kg⁻¹ as shown in (Table 1). These values were however, higher than mean concentration of 0.01 µg g⁻¹ detected in pawpaw by²⁵. Comparing the study with a similar one carried out in Romania where heptachlor concentrations in coffee samples ranged from not detected to 0.011 mg kg⁻¹,³⁷ then the medicinal plants in Ghana were highly contaminated.

Technical grade endosulfan products which consist of a mixture of two isomers, α and β-endosulfan and present in a 7:3 ratio is not on the UN list but is still in extensive use throughout the world for both domestic and agricultural applications, although its bioconcentration and environmental persistence is much lower than those of other cyclodienes. α-Endosulfan is the more thermodynamically stable of the two, thus β-endosulfan irreversibly converts to form α-endosulfan. But in this study the result suggests slow conversion (Table 1). Endosulfan was considered for restriction in December 2008 from the registered pesticides in Ghana.¹⁷ This might have accounted for relatively high concentrations of β-endosulfan and α-endosulfan detected in the study.

Comparison of pesticide residue levels to International standards

Table 1 also compares pesticide residue levels in the root of *Cryptolepis sanguinolenta* to maximum residue limit set by Codex Alimentarius Commission and United States Pharmacopoeia/European Pharmacopoeia.³⁸ Generally, the mean levels of the OCP residues in the plant species were below maximum residue limits set by FAO/WHO Codex Alimentarius Commission and United States/European Pharmacopoeia as shown in (Table 1). However, in the dry season, residue levels obtained for the sum of aldrin and dieldrin in *C. sanguinolenta* from Biakoye district were higher than WHO and FAO set limits as shown in (Table 1) below. As these chemicals are persistent and toxic and have the potential to bioaccumulate, their presence in the medicinal herbs is of great concern since increased accumulation in the food chain would pose serious health hazards to the general population.

CONCLUSIONS

The results of this study indicate that organochlorine pesticide residues are present in the roots of *Cryptolepis sanguinolenta* sampled from Kwahu-East and Biakoye Districts of Ghana. The detection of fourteen organochlorine pesticides indicates either wide use of these chemicals or environmental transport of these chemicals from other places to the study areas. The total organochlorine pesticide residues in the roots of the plant ranged from 0.033 to 0.354 mg kg⁻¹, with the highest mean level of 0.354 mg kg⁻¹ detected in the sample collected from Biakoye district during the dry season. The present investigation also gives an indication of the restricted use of DDT in Ghana. Long term persistence in the environment of this pesticide has been reported in various publications.

In the exception of the sum of aldrin and dieldrin in *Cryptolepis sanguinolenta* from Biakoye district during the dry season, the mean values obtained were generally below maximum residue limits set forth by the FAO/WHO Codex Alimentarius Commission and United States/European Pharmacopoeia. This means that traditional medicine prepared from the roots of *Cryptolepis sanguinolenta* as anti-malarial drugs may not pose health hazards in terms of organochlorine pesticide pollution. But as these chemicals are toxic and have the potential to bioaccumulate, their presence in medicinal herbs is of great concern since increased accumulation in the food chain would pose serious health hazards to the general population.

ACKNOWLEDGEMENT

We wish to extend our sincere gratitude to the following organizations for their assistance and support during this work, Centre for Scientific Research into Plant Medicine, University of Ghana, Ghana Atomic Energy Commission and Ghana Standards Authority.

REFERENCES

- ¹Clarke, E. E. K., Levy, L. S., Spurgeon, A., and Calvert, I. A., *Occup. Med.*, **1997**, *47*(5), 301-308.
- ²Taylor, M. D., Klaine, S. J., Carvalho, F. P., Barcelo, D. and Everaarts J., *Pesticide Residues in Coastal Tropical Ecosystems: Distribution, Fate and Effects* (1st edition) CRC Publishers, **2002**, 576 pp.
- ³Dinham, B., *Pest Manage. Sci.*, **2003**, *59*, 575-582.
- ⁴Nollet, L. M. L., *Handbook of Water Analysis Food Science and Technology* (1st edition). CRC, **2000**, pp. 920.
- ⁵Mukherjee, P. K., "Quality Control of Herbal Drugs ", 2002, 219-245.
- ⁶Baird, C., *Environmental Chemistry*. W. H. Freeman Company, New York, USA, 1997, 293-379.
- ⁷Stimman, M.W. Bailey, J. S. and Deal, A. S., *Study guide for agricultural pest control advisers on insects, mites and other invertebrates and their control in California*, New York Pergamon Press, 1985.
- ⁸Lars, H., *Environmental Exposure to Persistent Organohalogen and Health Risks*. In: Lennart M., (ed), *Environmental Medicine*. Ch: 12, Retrieved from: www. Envimed.com. **2000**.
- ⁹Fattore, E., Fanelli, R., and Vecchia, C. L., *J. Epidemiol. Comm. Health* 2002,*56*, 831-832.
- ¹⁰Schafer, K. S. and Kegley, S. E., *J. Epidemiol. Comm. Health*. **2002**, *56*, 813-17.
- ¹¹Kawano M., *Persistent organohalogen in environmental materials. Analytical Applications of Nuclear Techniques*, IAEA, **2004**.
- ¹²Ritter, L., Solomon K. R., Forget J., Stemeroff, M., O'Leary, C., "Persistent organic pollutants". United Nations Environment Programme, **2007**.
- ¹³Garabrant, D. H., Held, J., Langholz, B., Peter, J. M., and Mark, T. M., *J. Natl. Cancer Inst.*, **1992**, *84*(10), 764-771.
- ¹⁴Mckinney, J. D. and Waller, C. L., *Environ. Health Perspect.*, **1994**, *102*, 290 – 297.
- ¹⁵Manirakiza, P., Akimbamijo, O., Adediran, S. A., Cisse, I., Fall, S. T and Schepems, P., *J. Environ. Monitor*, **2002**, *4*, 609-617.
- ¹⁶Doong, R. A., Sun, Y. C., Liao, P. L., Peng, C. K. and Wu, S. C., *Chemosphere*, **2002**, *48*, 237 - 246.
- ¹⁷Afful, S., Anim, A. K. and Serfor-Armah, Y., *J. Environ. Earth Sci.*, **2010**, *2*(3), 133-139.
- ¹⁸Zuina, V. G, Yariwakea, J. H, Bicchi, C., *J. Chromatogr.*, **2003**, *985*, 159-66.¹⁹Xue, J., Liu, D., Chen, S., Liao, Y., Zou, Z., *Modern Tradit. Chin. Med. Mater. Med.*, **2008**, *10*, 91-6.
- ²⁰Ntow, W. J., *Res. Manag.*, **2005**, *10*, 243-248.
- ²¹Ntow, W. J., Gijzen, H. J., Drechsel, P., *Pest Manage. Sci.* **2006**, *62*(4), 356-365.
- ²²Darko, G., and Acquaaah, S. O., *Int. J. Environ. Sci. Tech.*, **2007**, *4*(4), 521-567.
- ²³Darko, G., and Acquaaah, S. O., *Chemosphere*, **2008**, *71*, 294-308
- ²⁴Darko, G., Akoto, O. and Oppong, C., *Chemosphere*, **2008**, *72*, 21-24.
- ²⁵Bempah, C. K. and Donkor, A. K., *Environ. Monit. Assess.*, **2011**, *175*(1-4), 551-61
- ²⁶Kuranchie-Mensah, H., *Studies of Organochlorine Pesticide Residues in Fish, Water and Sediment from the Densu River Basin*. M.Phil Thesis. Environmental Science Programme, University of Ghana, **2009**.
- ²⁷Lobe, J., 2006. "WHO urges DDT for malaria control Strategies," Inter Press Service. WHO. Geneva www.Commondreams.org.
- ²⁸www.ghanadistricts.com 13/02/2011
- ²⁹Ansah, C. and Gooderham, N. J., *Life Sci. Med. Toxicol. Sci.*, **2002**, *70*(2), 245-251.
- ³⁰Therdteppitak, A. and Yammeng, K., *Sci. Asia*, **2003**, *29*, 127-134.
- ³¹Environmental Protection Agency (EPA) Ghana, National Profile for Chemicals Management in Ghana, **1999**.
- ³²Barriada-Pereira, M., Gonzalez-Castro, M. J., Muniategue-Lorenzo, S., Lopez-Mahia, P., Prada-Rodriguez, D. and Fernandez-Fernandez, E., *Chemosphere*, **2005**, *58*, 1571-1578.
- ³³WHO, *Health criteria and other supporting information. guidelines for drinking-water quality*. (Vol. 2.) 2nd ed. Geneva, **1996**.
- ³⁴Awumbila, B., Bokuma, E., *Trop. Anim. Health Prod.*, **1994**, *26*, 7-12.
- ³⁵Orris, P. L., Kaatz, C., Perry, K., and Asbury, J., *Persistent organic pollutants (POPs) and human health*. World Federation of Public Health Associations (WFPHA). Washington, DC. **2000**, 45.
- ³⁶Metcalf, R. L., "Insect Control" in "Ullmann's Encyclopedia of Industrial Chemistry" Wiley-VCH, Weinheim, **2002**.
- ³⁷Stanciu, G., Dobrinas, S., Birghila, S., Popescu, M., *Environment. Eng. Manag. J.*, **2008**, *7*(6), 661-666.
- ³⁸World Health Organization (WHO), *WHO guidelines for assessing quality of herbal medicines with reference to contaminants and residue*, Geneva, **2007**.

Received: 13.07.2013.

Accepted: 28.07.2013.



IN VITRO SUSTAINED DELIVERY OF ATENOLOL, AN ANTIHYPERTENSIVE DRUG USING NATURALLY OCCURRING CLAY MINERAL MONTMORILLONITE AS A CARRIER

Seema^[a] and Monika Datta^{[a]*}

Keywords: Atenolol, Montmorillonite, Adsorption isotherm, Sustained delivery

In the present study, a naturally occurring clay mineral, Montmorillonite, (Mt) has been explored as a carrier for an antihypertensive drug, atenolol. The effect of pH, time and initial drug concentration on drug loading capacity of Mt has been evaluated. The adsorption isotherm was fitted by the Langmuir model and follows the pseudo-second-order kinetics. The synthesized Mt-atenolol complexes were characterized by XRD, FTIR, TGA, DSC etc. XRD data indicates the intercalation of atenolol within the Mt layers. The release profile of the atenolol from Mt-atenolol complexes is compared with the pure atenolol, in simulated gastric and intestinal fluids. The release behaviour of atenolol from Mt-atenolol complexes appears to be in sustained manner over a period of 24 hours and reaches upto 40% and 27% in simulated gastric and intestinal fluids respectively. As compared to pure atenolol, extended gastric retention time was observed for Mt-atenolol complexes indicative of the increased extent of absorption and bioavailability of the drug. Various kinetic models were used to elucidate the drug release mechanism, the best fitting was found for Higuchi and Korsmeyer-Peppas model. The synthesized Mt-atenolol complexes have the potential for developing in to a sustained release formulation for oral drug delivery. Thus, proposing a promising formulation for oral sustained drug delivery of atenolol.

*Corresponding Author

Fax: +91-01127666605

E-Mail: monikadatta_chem@yahoo.co.in

[a] Analytical Research Laboratory, Department of Chemistry, University of Delhi, Delhi-110 007, India

INTRODUCTION

Hypertension is one of the major causes of disability and death in the world. Today, approximately 1 billion people worldwide suffer from high blood pressure, and the number is expected to reach to 1.56 billion by the year 2025.¹ It is a chronic disease which requires treatment around the clock.

Atenolol, β -1 cardio selective adrenergic receptor blocker, is widely used in the treatment of hypertension.² The drug is orally administered as 25 mg tablets once or twice daily with total daily doses ranging from 25 to 100 mg.² Atenolol is soluble in water (26.5 mg ml⁻¹) with poor membrane permeability and reported half-life of 6-7 hours.

Administration of conventional tablets of atenolol has been reported to exhibit fluctuations in the blood plasma drug concentration, resulting either in manifestation of side effects or reduction in drug concentration at the receptor site.³⁻⁴ It is considered a drug with low jejunal permeability and a low extent of absorption; therefore it has an oral bioavailability of about 50%. Thus, it seems that an increase in gastric residence time may increase the extent of absorption and bioavailability of the drug.⁵⁻⁷ In view of these facts, this drug can be considered as a suitable candidate for preparation of controlled and sustained release dosage formulation with enhanced gastric retention time. Studies have been reported on regulation of atenolol drug release by

formulations such as mucoadhesive, extended release and floating tablets,⁵⁻⁹ nanoparticles¹⁰ hydrophilic matrices,¹¹⁻¹³ and transdermal drug delivery systems.¹⁴

Recently, natural clay mineral, especially Montmorillonite (Mt) has attracted considerable attention as a carrier for sustained drug delivery.¹⁵⁻¹⁷ Mt is a 2:1 layered smectite clay mineral composed of two SiO₄ tetrahedral layers sandwiching a central Al octahedral layer as shown in Figure 1.

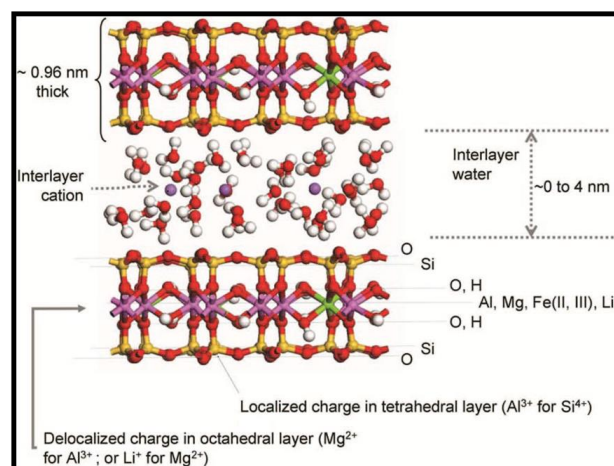


Figure 1. Structure of montmorillonite (Mt) (reproduced from the work of Jacob G., Reynolds et al. *Clays and Clay Minerals*, **2012**, 60(6), 599–609.)

Chemically montmorillonite is a hydrated sodium calcium aluminium magnesium silicate hydroxide, Na,Ca)_{0.33}(Al,Mg)₂(Si₄O₁₀)(OH)₂.nH₂O. It has large specific surface area, good adsorption ability, cation exchange

capacity, and drug-carrying capability along the (001) axis. Mt can intercalate various protonated and hydrophilic organic molecules, which can be released in a controlled manner by replacement with other kind of cations in the release media.¹⁸⁻²⁰ Drug intercalated Mt formulations offer a novel route to prepare organic and inorganic complexes that contain advantageous properties of both the inorganic host and organic guest in a single material.²¹⁻²³ Mt also known as medical clay as it is a potent detoxifier can adsorb dietary and bacterial toxins.²⁴⁻²⁶

There is no report, to the best of our knowledge on the preparation of atenolol intercalated Mt complexes for the sustained delivery. Therefore, the aim of our work was to undertake a systematic and detailed investigation on adsorption and optimization of conditions for preparing Mt-atenolol complexes for sustained release formulations. The effect of pH, time and initial drug concentration on drug intercalation capacity of Mt has been evaluated. The adsorption isotherm was better fitted by the Langmuir model and followed the pseudo-second-order kinetic model. The complexes were characterized by XRD, FTIR, TGA and DSC techniques. Atenolol was intercalated into Mt via ion exchange process increasing the basal spacing to 15.4 Å. Release of the intercalated atenolol was studied in simulated gastric and intestinal fluids at 37°C for a period of 24 hours and sustained release of atenolol from Mt-atenolol complex was observed. Drug release mechanism was found to follow the Higuchi and Korsmeyer-peppas model in simulated gastric and intestinal fluids respectively.

Thus the developed Mt-atenolol complexes have the potential to be used as an oral and sustained delivery of atenolol for the hypertension patients requiring medicinal treatment around the clock.

EXPERIMENTAL

Materials

Montmorillonite (KSF) and atenolol (purity >98%) was procured from Sigma Aldrich (USA). Analytical grade sodium hydroxide, potassium dihydrogen phosphate and potassium chloride for the preparation of drug release media were obtained from Merck Chemicals Ltd (Germany). All other reagents whether specified or not were also of analytical grade. Double distilled water filtered with 0.45 µ membrane (milipore) was used throughout the experimental work.

Study of atenolol-montmorillonite (Mt) interaction

In order to study the interaction of atenolol with Mt a batch process was selected. Initially, stability of atenolol molecule as a function of pH was evaluated in the pH range of 1-11. The obtained results indicate the stability of atenolol in the investigated pH range (Fig. 2).

In a further step, interaction of atenolol with Mt was investigated. Mt dispersion (1wt.%) was prepared by dispersing 1 g clay in 150 ml deionized water under vigorously stirring for 24 hours. 100 mg atenolol solution

(0.1% w/v) with its natural pH value of 9.6 was added drop wise into the Mt dispersion within 1 h at 25°C. The resultant Mt-atenolol dispersion shows decrease in the pH value from 9.6 to 2.3 because of the acidic nature of Mt. Therefore, the pH of the Mt-atenolol dispersion was maintained at 9.6 the actual pH of atenolol solution, with 0.1 M NaOH. The mixed reaction media was further stirred for 2 h, centrifuged, washed several times with double distilled water to remove the excess of atenolol on the surface, dried in the air and ground with mortar and pestle to obtain fine powder. The sample was designated as Mt-atenolol complex.

The encapsulation efficiency (*EE*) and drug loading (*DL*) capacity of atenolol in the Mt-atenolol complex was calculated by Eqn. 1 and 2, respectively in the supernatant recovered after centrifugation at 225 nm.

$$EE(\%) = 100 \frac{m_1 - m_2}{m_1} \quad (1)$$

where

m_1 - atenolol amount added initially

m_2 - atenolol in the supernatant

$$DL(\%) = 100 \frac{m_3}{m_4} \quad (2)$$

where

m_3 - atenolol amount within the Mt-atenolol complex

m_4 - total weight of Mt-atenolol complex obtained

The obtained UV results suggest that 73.8 mg of atenolol was intercalated within the Mt layers with drug content of 7.5% (w/w).

To investigate the interaction of atenolol with Mt XRD studies were performed on a powder X-ray diffractometer (XPRT PRO Panalytical, model PW3040160, Netherland) the measurement conditions are mentioned under characterization section.

The obtained XRD results suggest the intercalation of atenolol within the interlayer region of Mt by ion exchange process, details are provided under the appropriate section.

Batch studies for intercalation of atenolol within Mt layers

In order to achieve maximum intercalation of atenolol within the interlayer region of Mt, effect of various parameters such as, contact time, pH and initial concentration of atenolol were investigated.²⁷ Aqueous atenolol solutions (25 ml) were treated with 100 mg of Mt at different reaction conditions with continuous mechanical shaking (Khera instruments). After desired reaction time, Mt-atenolol dispersion was centrifuged with 10,000 rpm for 20 minutes at room temperature (Remi centrifuge).

The free atenolol concentration in the supernatant were determined using UV-visible spectrophotometer (Analytic Jena) at 225 nm from the Lambert-Beer's plot and the percentage of the drug adsorbed (ϕ , %), being calculated from Eq. (3).

$$\phi = \frac{C_i - C_e}{C_i} \quad (3)$$

where C_i is the initial drug concentration (mg L^{-1}) and C_e is the concentration of the drug (mg L^{-1}) in the supernatant at the equilibrium stage. The amount of drug adsorbed q_e (mg g^{-1}); was calculated via the mass-balance relationship as per the Eq. (4)

$$q_e = (C_i - C_e) \frac{V}{m} \quad (4)$$

where V is the volume of the reaction media (L) and m is the mass of Mt used for the studies (g). Influence of pH from 2-11 on the intercalation of atenolol within Mt layers were studied at 25°C for 2 hours at atenolol concentration of 200 mg L^{-1} . For adsorption kinetics in the time period of 0.25 to 18 h, all the other parameters were kept constant (pH 8, atenolol concentration of 200 mg L^{-1} at 25°C). Adsorption equilibrium studies of atenolol in the concentration range of 40 to 720 mg L^{-1} were carried out using 100 mg of Mt at 25°C for a period of 2 hours at pH 8.

Characterizations

Powder X-ray diffraction (PXRD) measurements of Mt-atenolol complex was performed on a powder X-ray diffractometer (XPRT PRO Pananalytical, model PW3040160, Netherland) the measurement conditions were Cu K α radiation generated at 40 kV and 30 mA as X-ray source 2-40° (2θ) and step angle 0.01°/second. FTIR spectra of the Mt-atenolol complex recorded with an FTIR spectrophotometer (Perkin Elmer, Spectrum BXFTIR Spectrometer) using the KBr (Merck, Germany) disc method. Thermogravimetric analysis was carried out within 30 - 800°C at 10°C min^{-1} in nitrogen flow (TGA 2050 Thermal gravimetric Analyzer). UV-Visible absorbance of atenolol solutions was measured at $\lambda_{\text{max}} = 225$ nm (UV-Visible spectrophotometer Analytic Jena) equipped with a quartz cell having a path length of 1 cm. Differential scanning calorimetric studies were conducted on DSC instrument (DSC Q200 V23.10 Build 79). The samples were purged with dry nitrogen at a flow rate of 10 ml min^{-1} and the temperature was raised at 5°C min^{-1} .

In vitro drug release profile and release kinetics

In vitro drug release studies of Mt-atenolol complex was conducted in a constant temperature bath with the dialysis bag technique.¹⁹ Buffer solution of pH 1.2 (simulated gastric fluid) was prepared by mixing 250 ml of 0.2 M HCl and 147 ml of 0.2 M KCL. Buffer solution of pH 7.4 (simulated intestinal fluid) was prepared by mixing 250 ml of 0.1 M KH_2PO_4 and 195.5 ml of 0.1 M NaOH. Dialysis sacs were

equilibrated overnight with the dissolution medium prior to experiments. Mt-atenolol complex equivalent to 25 mg of atenolol was taken in 5ml of buffer solution in the dialysis bag. Dialysis bag was dipped into the receptor compartment containing 100 ml dissolution medium, which was stirring at 37±0.5°C. The receptor compartment was closed to prevent the evaporation losses from the dissolution medium. The stirring speed was kept at 100 rpm. 5 ml of aliquots was withdrawn at regular time intervals and the same volume was replaced with a fresh dissolution medium. Samples were analyzed for released atenolol content by UV spectrophotometer at $\lambda_{\text{max}} = 225\text{nm}$ by using calibration plot of standard atenolol solutions in the same releasing media.

To analyze the in vitro release data, various kinetic models including Zero order, First-order, Higuchi and Korsmeyer – Peppas model has been used to describe the release kinetics.²⁸⁻³⁰

RESULTS AND DISCUSSION

Intercalation of atenolol at different pH values

To start with the experiment, stability of the atenolol molecule was investigated in the pH range of 1-11. It has been found that drug maintains its stability (Fig. 2) within the experimental pH range as there is no change in the absorption spectra of atenolol molecule was observed.

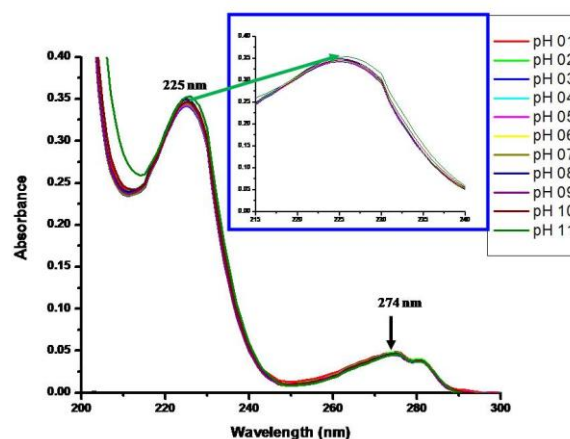


Figure 2. UV-Visible spectrum of aqueous atenolol solution (10 ppm) showing stability at various pH

The UV absorption spectra of atenolol show two absorption peaks at 225 nm and 274 nm corresponding to different electronic transitions of the molecule. In subsequent studies, wavelength of 225 nm has been selected for quantitative estimation of atenolol. The pH of the drug solution has always played a crucial role in intercalation process.²⁰⁻²² The intercalation of atenolol in Mt was found to increase from 77 % to 94% (of 200 ppm drug solution) in the pH range of 2 to 8 and remains almost constant in the pH range of 8-10 (98% of 200 ppm) (Fig. 3).

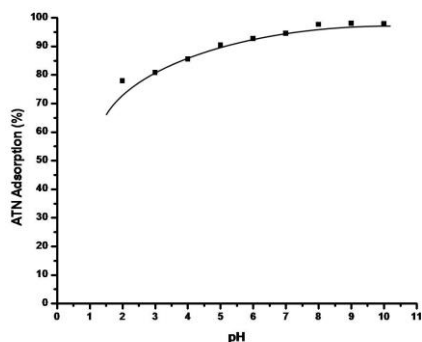


Figure 3. Atenolol intercalation within Mt layers as a function of pH

This could be explained on the basis the pK_a value of atenolol (pH 9.6) where atenolol exist as 50:50:: protonated : neutral form (Fig. 4).³¹ At lower pH, decrease in intercalation of atenolol in the Mt lattice is attributed to the competition between the cationic drug and H^+ ions present as exchangeable ion in Mt.¹⁹ However, with increase in pH, atenolol still exist in the protonated form and positive charge on the surface of the Mt decreases resulting in high adsorption of atenolol with Mt layers.

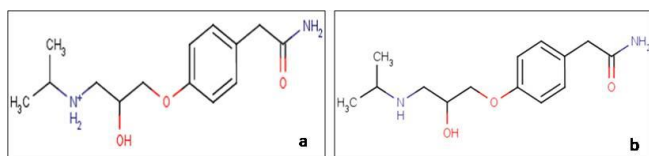


Figure 4. Protonated (a) and neutral (b) forms of atenolol

Effect of time on intercalation

Intercalation of atenolol in Mt is very rapid process, due to occurrence of ion-exchange reaction between the interlayer Na^+ ions and cationic atenolol molecules at pH 8 (Fig. 5).

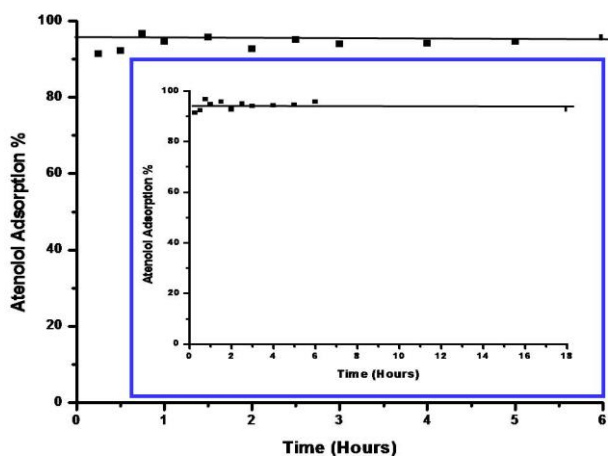


Figure 5. Effect of contact time on adsorption of atenolol on Mt, Mt = 0.1g; concentration of atenolol = 200 ppm; pH = 8; temperature = 25° C

Then, 96% of 200 ppm of atenolol was intercalated within 45 minutes of interaction time, which remained almost constant (95.6%) up to 6 hours and tends to decrease up to 92% in further 18 hours. In our studies, reaction time was set to 2 hours in order to avoid the partial intercalation in the succeeding experiments.

Kinetics of atenolol Adsorption

In order to optimize the design of an adsorption system of atenolol on Mt, it is important to establish the most appropriate correlations for the equilibrium data for the system. In this respect two kinetic models including pseudo-first order and pseudo-second order models have been applied to determine the adsorption mechanism.^{32,33}

Pseudo-first-order model

Pseudo-first-order equation can be expressed as below Eq. (5):

$$\frac{1}{q_t} = \frac{k_1}{q_1} \frac{1}{t} + \frac{1}{q_1} \quad (5)$$

where k_1 is the pseudo-first-order rate constant (min^{-1}), q_t is the amount of drug adsorbed (mg g^{-1}) at different times t , q_1 is the maximum adsorption capacity (mg g^{-1}) for pseudo-first-order adsorption.³³ Plots of $1/q_t$ versus $1/t$ for the adsorption of atenolol on Mt surface were employed to generate the intercept values of $1/q_1$ and the slope of k_1/q_1 (Fig. 6). The values of k_1 , q_1 and the correlation coefficients are given in Table 1.

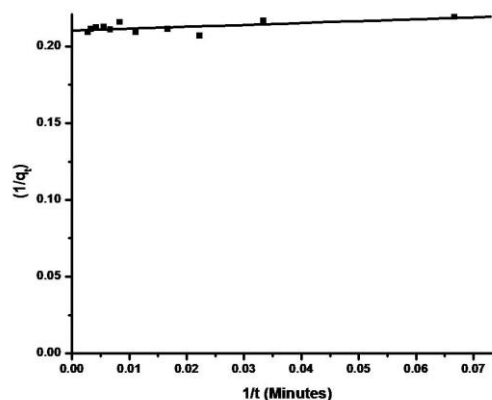


Figure 6. Pseudo first order kinetic model for atenolol adsorption on Mt surface (200 ppm, pH 8 and 25 °C)

Pseudo second order model

The pseudo-second-order kinetic equation can be represented as Eq. (6):

$$\frac{t}{q_t} = \frac{1}{k_2 q_2^2} + \frac{t}{q_2} \quad (6)$$

where k_2 is the pseudo-second order rate constant; q_2 is the maximum adsorption capacity (mg g^{-1}) for the second order adsorption process.³³ The plots of t/q_t versus t for atenolol adsorption onto Mt are given in Fig. 7. From the slope and intercept values, q_2 and k_2 values were calculated and the results are given in Table 1.

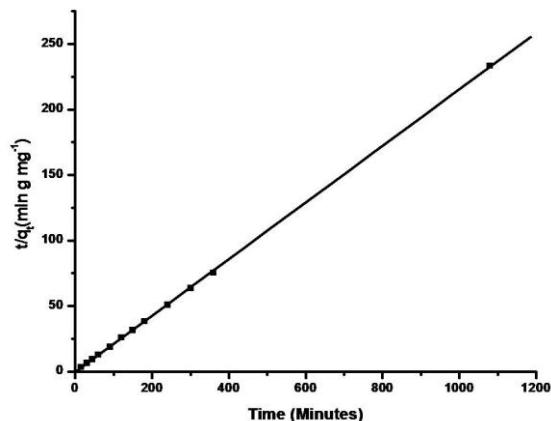


Figure 7. Pseudo second order kinetic model for atenolol adsorption on Mt (200 ppm, pH 8 and 25°C)

Table 1. Kinetic parameters for the adsorption of Atenolol on Mt surface

| Pseudo first order | | | Pseudo second order | | |
|--------------------|--------------------|---------|------------------------|--------------------|---------|
| k_1 | q_1 | R_1^2 | k_2 | q_2 | R_2^2 |
| min^{-1} | mg g^{-1} | | g mg min^{-1} | mg g^{-1} | |
| 0.5809 | 4.752 | 0.63835 | 0.082 | 4.634 | 0.99993 |

Effect of initial atenolol concentration on intercalation

At pH 8, the intercalation of atenolol within Mt layers is affected by its initial amount present in the solution. As the atenolol amount in the solution increases from 1 to 18 mg ($40 - 720 \text{ mg L}^{-1}$), the amount of atenolol intercalated within Mt layers was increases from 0.96 mg to 8.5 mg with decrease in intercalation (%) from 96.6% to 47.3% (Fig. 8).

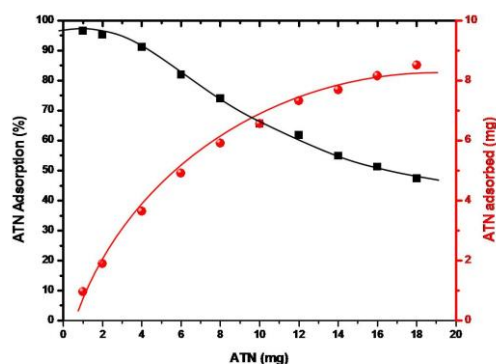


Figure 8. Effect of initial atenolol concentration on intercalation

Adsorption Isotherm for atenolol on Mt surface

The adsorption isotherm of atenolol on Mt surface obtained by plotting the atenolol amount adsorbed by Mt ($q_e \text{ mg g}^{-1}$) vs equilibrium concentration of atenolol ($C_e, \text{mg/L}$) is shown in Fig. 9.

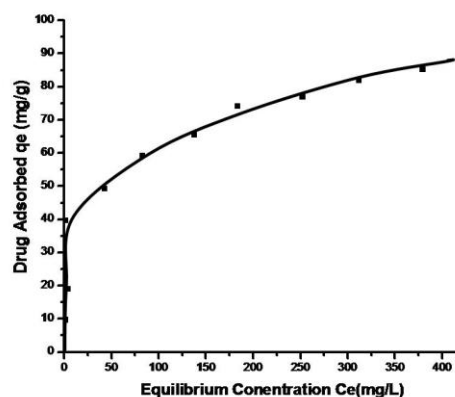


Figure 9. Adsorption isotherm of atenolol on Mt surface

The Langmuir (Eq. 7) and Freundlich (Eq. 8) adsorption isotherms were applied to evaluate the adsorption data which correspond to homogenous and heterogeneous adsorbent surfaces respectively.^{19,22,32} The equations can be expressed as follows:

$$\frac{C_e}{q_e} = \frac{1}{q_m K_L} + \frac{C_e}{q_m} \quad (7)$$

$$\ln q_e = \ln K_f + n_f \ln C_e \quad (8)$$

where q_e is the equilibrium atenolol concentration on the Mt surface (mg g^{-1}), C_e is the equilibrium atenolol concentration in solution (mg L^{-1}), q_m the monolayer adsorption capacity (mg g^{-1}), and K_L is the Langmuir adsorption constant (L mg^{-1}). In case of Freundlich adsorption isotherm, K_f (mg g^{-1}) and n_f are considered as relative adsorption capacity and adsorption intensity respectively. The values of q_m and K_L were computed from the slope and intercept of the linear plot of C_e/q_e versus C_e (Fig. 10) and are presented in Table 2. As can be seen linear form of Langmuir isotherms seems to produce a better fit in comparison with linear form of Freundlich isotherm (Fig. 11).

The essential characteristics of the Langmuir equation can be expressed in terms of a dimensionless separation factor R_L as Eq. 9:

$$R_L = \frac{1}{1 + K_L C_i} \quad (9)$$

The value of R_L indicates the shape of the isotherm to be either unfavourable ($R_L > 1$), linear ($R_L = 1$), favourable ($0 < R_L < 1$) or irreversible ($R_L = 0$). The value of the factor of separation R_L indicates the nature of the favourability adsorption process and its feasibility.

According to Freundlich equation, K_f values are 16.479 mg/g at 25°C. It can be said that the values of n_f equal to

0.2809 is smaller than 1, reflecting the favourable adsorption.

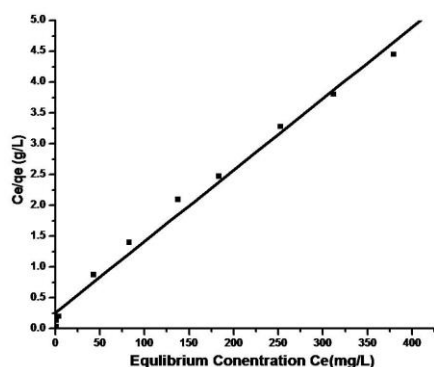


Figure 10. Linear form of Langmuir adsorption isotherm for atenolol on Mt

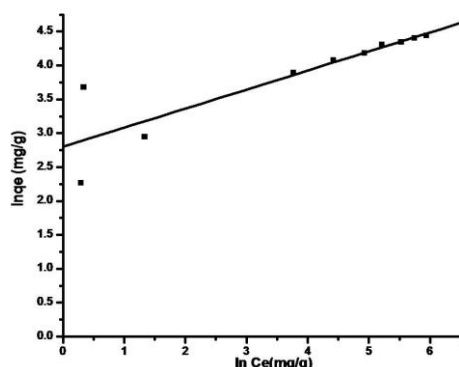


Figure 11. Linear form of Freundlich adsorption isotherm for Atenolol on Mt

XRD Studies

The XRD patterns of pristine Mt, pure atenolol and Mt-atenolol complex are shown in Fig.12. The XRD pattern of pure atenolol revealed several diffraction peaks which indicate its crystalline character.³⁵ Mt showed a distinct diffraction pattern (001 plane) at $2\theta = 6.4^\circ$ representing a 13.6 Å thickness of the Mt layer.¹⁶

Table 2. Isotherm constant for Atenolol adsorption on Mt surface

| Linear form of Langmuir | |
|---------------------------|---------|
| $q_m, \text{mg g}^{-1}$ | 86.355 |
| K_L | 0.0448 |
| R_L | 0.358 |
| R | 0.994 |
| Linear form of Freundlich | |
| $K_f (\text{mg/g})$ | 16.479 |
| n_f | 0.28094 |
| R | 0.0879 |

In case of Mt-atenolol complexes a shifting in 2θ value from A previous study,³⁶ suggest stronger intensity of the basal spacing peak occurs when the drug molecule was intercalated within the Mt layers. 6.4° to 5.7° and a stonger intensity was observed. According to Bragg's law, shifting in 2θ value from higher diffraction angle to lower diffraction angle is because of the increase in d spacing. This indicates increase in the interlayer spacing upon intercalation of atenolol in the Mt layers from 13.6Å to 15.4 Å with the replacement of interlayer cation by atenolol. Subtracting the Mt layer thickness (9.6 Å) from the d spacing (15.4 Å) of the Mt-atenolol complex, the Mt layer thickness was estimated to be 5.8 Å. Diameter of Atenolol is 6.5Å and longest crosssection dimension is 13.6 Å.^{37,38}

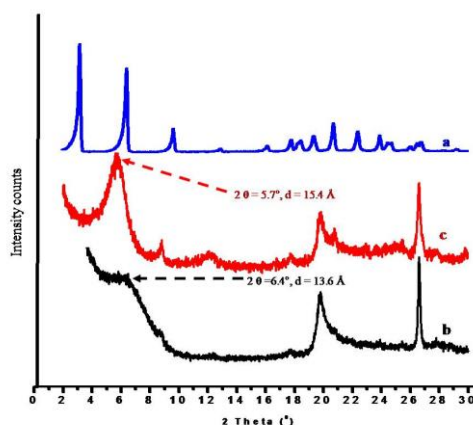


Figure 12. XRD patterns of pure atenolol (a), Pristine Mt (b) and Mt-Atenolol complex (c)

This data suggest the replacement of interlayer hydrated cations with monolayer tilted vertical orientation of the atenolol molecules parallel to the Mt layers.^{19, 21, 22}

FTIR Studies

In order to confirm the presence of atenolol within the interlayer region of the Mt, FTIR spectra were recorded in the region $500\text{--}4000 \text{ cm}^{-1}$.

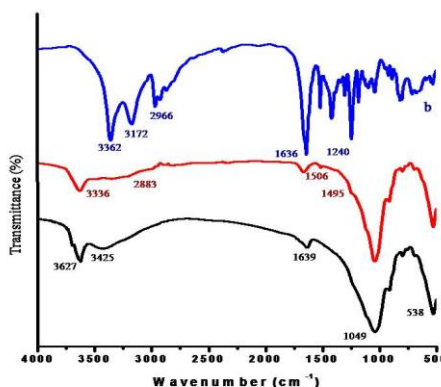


Figure 13. FTIR spectra of Mt (a), Atenolol (b) and Mt-Atenolol complex (c)

The FTIR spectrum of Pristine Mt, Pure atenolol and Mt-atenolol complex prepared by ion exchange mechanism is shown in Fig. 13. In the FTIR spectrum of Mt, the band at 3428 cm^{-1} and 3629 cm^{-1} has been assigned to H-O-H stretching vibrations from interlayer water and Si-O-H stretching vibrations of the structural OH group. The absorption band at 1639 cm^{-1} corresponds to H-O-H bending water of crystallization. The characteristic band at 1049 cm^{-1} has been assigned to Si-O stretching vibration. The absorption bands at 527 cm^{-1} are strong bending vibrations corresponding to Al-O-Si.^{20,21,23}

The IR spectrum of the pure atenolol displayed characteristic peaks at 3362 cm^{-1} , 3172 cm^{-1} and 1636 cm^{-1} due to O-H, N-H and C=O groups, respectively.^{39, 40} The peaks of 1240 cm^{-1} and 2972 cm^{-1} are due to alkyl aryl ether linkage and C-H stretching. The presence of functional groups of atenolol on the surface of Mt is verified by peaks at about 2957 cm^{-1} and 2883 cm^{-1} , characteristic of the aliphatic C-H antisymmetric and symmetric vibrations respectively from the methylene group of atenolol. The presence of these bands in Mt-atenolol complex indicates the presence of atenolol in the Mt matrix. In case of Mt-Atenolol complex the vibrational bands at 3493 cm^{-1} have been assigned to the H-O-H stretching vibrations of the interlayer water but the intensity of this peak is almost vanish compared to Mt as the intercalation of the atenolol (as confirmed by XRD) into the interlayer region displaces the water molecules. A small band at 3350 cm^{-1} and 1506 cm^{-1} corresponding to NH banding vibration and benzene ring skeletal vibration respectively from Atenolol molecule was also appeared in Mt-atenolol complex. The presence of all these bands suggests the presence of organic cations atenolol in the interlayer region of the Mt layers. Besides these, a broad hump in the region of 3400 cm^{-1} to 3100 cm^{-1} probably due to hydrogen bonding between silanol group of Mt with OH and amine functional groups of Atenolol was observed. This also indicated that Atenolol interacts with the Mt layers.

TGA Studies

The TGA thermogram of pristine Mt (Fig14 a) shows high thermal stability in the temperature region of 30-700 °C with weight loss of 10% from 30-150 °C corresponds to the evaporation of free water and water bound to the cations present within the interlayer. Weight loss in the temperature range from 600-750°C is due to the loss of hydroxyl groups in the aluminosilicate structure and at this point the structure of the Mt layers collapses,¹⁸ resulted in a strong endothermic peak in DTA curve of Mt at 80 °C and broad endothermic peak at 600 °C.²²

The thermogravimetric profile of pristine drug atenolol (Fig. 14b) represents two thermal decomposition stages. In the DTA curve for pure atenolol, a sharp endothermic peak at 182 °C was observed without any weight loss in TGA which corresponded to the melting point of atenolol.⁴¹ The drug show a sharp weight loss (~ 80%) at around 230-400 °C resulting in a strong endothermic peak in DTA curve at 297 °C followed by an small exotherm at 336 °C corresponding to decomposition of the ATN molecule.⁴² The TGA curves of Mt-atenolol complex (Fig 14c) shows the

20% weight loss with two consecutive stages due to the dehydration and decomposition in the temperature range of 20-200°C and 205-700°C, respectively.

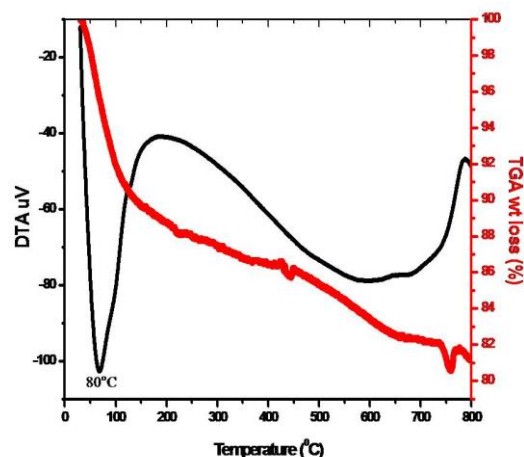


Figure 14a. TGA-DTA curves of pristine Mt

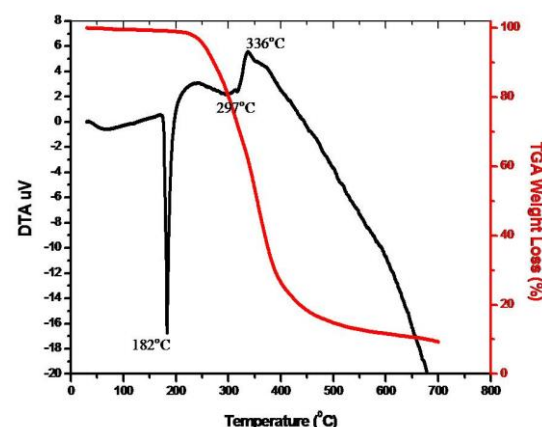


Figure 14b. TGA-DTA curves of pure atenolol

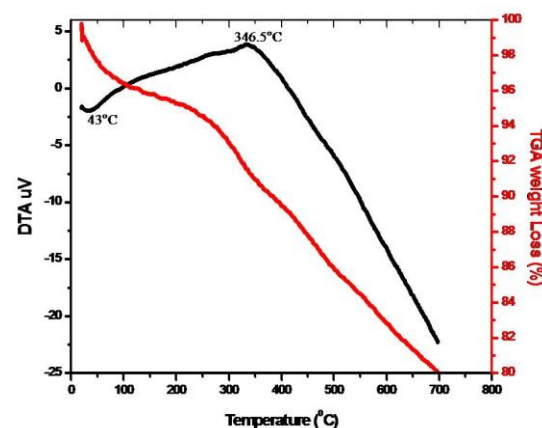


Figure 14c. TGA-DTA curves of Mt-Atenolol complex

The first weight loss (~3%) in the temperature region of 80-200°C corresponding to loss of surface adsorbed water was observed resulting in a small endotherm at 43 °C in DTA curve. The weight loss observed was smaller than the pristine Mt (~10%) because of the replacement of interlayer water with intercalated atenolol which supposed to be stable and does not show any weight loss upto 200°C.⁴¹ The second weight loss of 15% was associated in the range from 205°C to 697°C attributed to the decomposition of intercalated ATN resulting in the presence of exotherm at 346.5°C in DTA curve of Mt-atenolol complex, corresponding to the thermal degradation of atenolol.

DSC Studies

The DSC curves of pristine Mt (Fig.15a) presented a broad endothermic peak at 110°C, which was attributed to the dehydration of adsorbed water. The DSC thermograms of atenolol (Fig.15b) showed a sharp endothermic peak at 154°C indicating the melting point of atenolol.⁴¹ A broad endothermic peak at 295°C followed by an exothermic peak at 308°C represents the decomposition of atenolol.⁴²

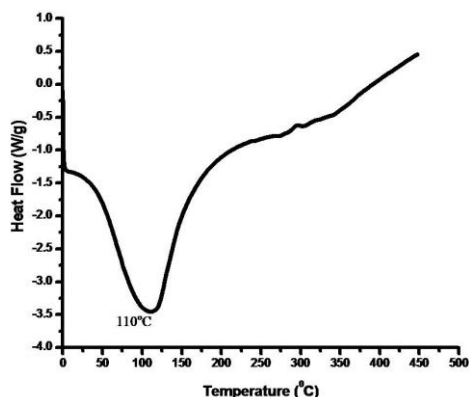


Figure 15a. DSC curves of pristine Mt

In case of Mt-atenolol complex (Fig.15c) a broad endotherm was appeared in the region of 60 °C to 140 °C which might be corresponds to the combined event for the melting of intercalated atenolol with dehydration of surface water. In the temperature region of 250 °C to 400 °C a broad endotherm might be related to the decomposition of atenolol within Mt layers was observed.

Drug Release Profile

The cumulative release profiles of pure atenolol and Mt-atenolol complex in simulated gastric fluid (HCl pH 1.2) and in simulated intestinal fluid (PBS, pH=7.4) at 37 °C for different durations are shown in Fig.16. Pure atenolol shows upto 73% and 64% release in HCl (pH 1.2) and PBS (pH 7.4) over a period of 2 hours which approaches to almost 90% over a period of 6 hours respectively.

However in case of Mt-atenolol complex a very sustained release of atenolol in HCl pH 1.2 (SGF) and PBS, pH=7.4 (SIF) was observed. Within initial 2 hours, only 18.2% and 7.3% of atenolol was released which approaches to 33.2% and 18.52% in 8 hours followed by an increase upto 47.5%

and 30.6% release over a period of 24 hours in SGF and SIF, respectively (Fig.16). Atenolol release was greatly influenced by the pH of the releasing media.

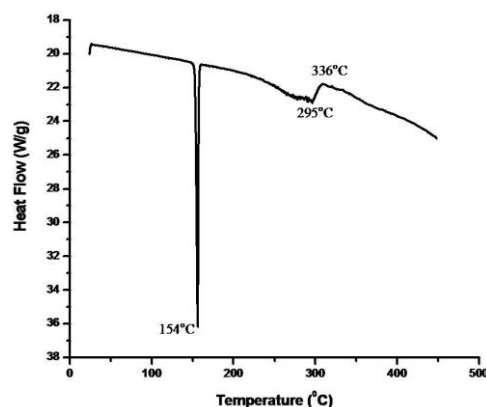


Figure 15b. DSC curves of pure atenolol

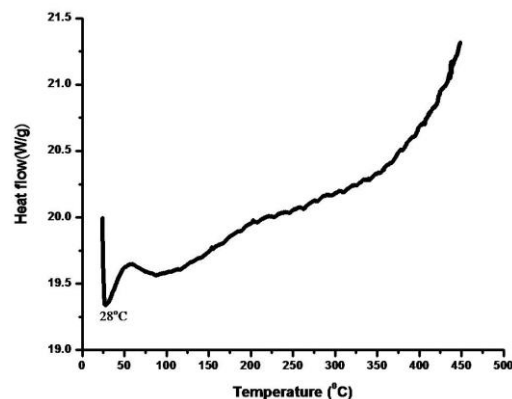


Figure 15c. DSC curves of and Mt-atenolol complex

In vitro drug release data suggest that the synthesized Mt-atenolol complex are able to retain the high amount of atenolol in gastric media (pH 1.2) (the desired site of absorption) as compared to pure drug with the advantage of gradual drug release over a longer period of time. Being a weakly basic drug with a pK_a value of 9.6 atenolol is expected to possess higher solubility and therefore a faster drug release rates at acidic pH than at basic pH media⁷.

High release in acidic media can also be because of the presence of H^+ ions in the media, being smaller in size, they can penetrate deep into the Mt layers and results in high ion exchange process as compared to the large phosphate ions in PBS.³⁵ The release data of atenolol from Mt-atenolol complex were fitted by zero order (fig 17a), first-order kinetics (fig. 17b), Higuchi (fig 17c) and Korsmeyer-Peppas models (Fig.17d) and the values of release kinetics constants in simulated gastric (HCl, pH 1.2) and intestinal (PBS pH 7.4) fluids are summarized in table 3. In SGF, the Higuchi equation gave the best representation of the release data, and the release mechanism seemed to be a diffusion process based on Fick's law.²⁸⁻³⁰ In SIF, the release kinetics was found to obey the Korsmeyer-peppas equation. Thus, the release mechanism was described as the non-Fickian anomalous transport ($n > 0.5$).

Table 3. Release kinetics of Mt-Atenolol complex in simulated gastric fluid (HCl, pH 1.2) and intestinal fluid (PBS pH 7.4)

| Release Media | Zero order $C=K_0t$ | | First order $\log C = \log C_0 - k_1t/2.303$ | | Higuchi $Q = K_H t^{1/2}$ | Korsmeyer-Peppas $M_t/M_\infty = kt^n$ | | | |
|---------------|------------------------|---------------|---|---------------|------------------------------|---|--------|--------|---------------|
| | R^2 | K_0, h^{-1} | R^2 | K_1, h^{-1} | R^2 | $K_H^{(1/2)}$ | R^2 | n | Kkp, h^{-n} |
| HCl pH 1.2 | 0.8928 | 1.1200 | 0.9299 | 1.9369 | 0.9736 | 7.5617 | 0.9717 | 0.4985 | 0.9911 |
| PBS pH 7.4 | 0.9261 | 0.7732 | 0.9416 | 0.0092 | 0.9889 | 5.2311 | 0.9914 | 0.5847 | 0.6509 |

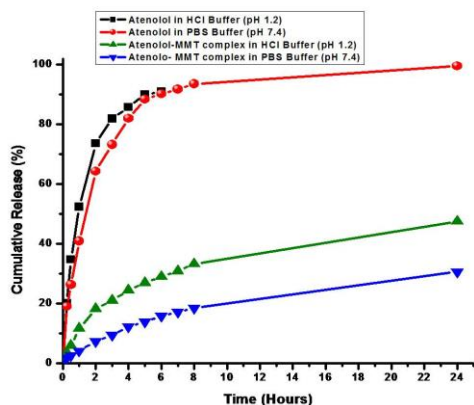


Figure 16. Release profile of pure atenolol and Mt-atenolol complex in simulated gastric fluid (HCl pH 1.2) and simulated intestinal fluid (PBS, pH 7.4)

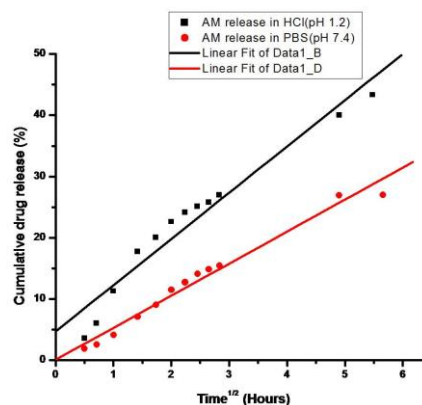


Figure 17c. Higuchi kinetic model of Mt-Atenolol complex in simulated gastrointestinal fluid

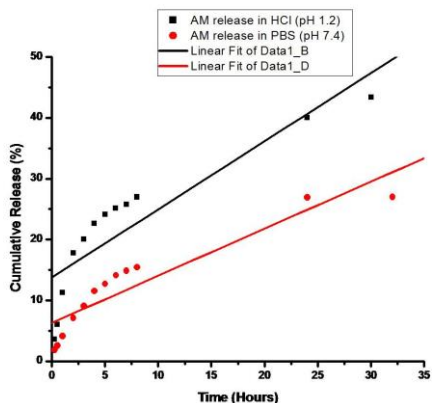


Figure 17a. Zero order kinetic model of Mt-Atenolol complex in simulated gastrointestinal fluid

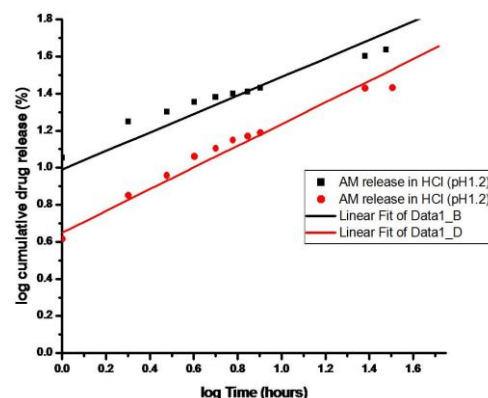


Figure 17d. Korsmeyer - Peppas kinetic model of Mt-Atenolol complex in simulated gastrointestinal fluid

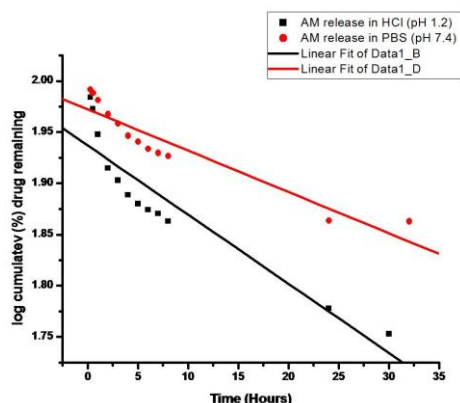


Figure 17b. First order kinetic model of Mt-Atenolol complex in simulated gastrointestinal fluid

CONCLUSION

Atenolol sustained release formulation was prepared successfully using natural clay mineral Mt as a host to retard the drug release. Intercalation of atenolol within Mt layers confirmed by XRD, FTIR and TGA analysis. The adsorption isotherms of atenolol on Mt were fitted by the Langmuir model, and the adsorption kinetics followed the pseudo-second-order kinetic model. Drug release kinetics of this formulation correspond best to Higuchi's model and Korsmeyer-Peppas model under simulated gastric and intestinal conditions respectively. In vitro drug release data suggest that the synthesized Mt-atenolol complex are able to retain the high amount of atenolol in gastric media (pH 1.2) (the desired site of absorption) as compared to pure drug with the advantage of gradual drug release over a longer

period of time, thus reducing the multiple dosing and associated drug plasma fluctuation level. Thus the obtained results are proposing a new promising formulation potentially suitable as sustained delivery carrier of atenolol.

ACKNOWLEDGEMENT

We sincerely express our thanks to the Head, Department of Chemistry, Director, USIC, University of Delhi for providing instrumentation facilities, and UGC (major research project and RGNF) for providing financial assistance.

REFERENCES

- ¹Hypertension etiology. *Hypertension statistics* [Online]. **2010** [Cited 2012 May 5]; available from: <http://www.healthstats.com/en/hypertension-statistics>.
- ²Wander G.S., Chhabra S.T., Kaur K., *Suppl. JAPI*, **2009**, *57*, 13-16.
- ³Vaithiyalingam, S. R., Sastry, S. V., Dehon, R. H., Reddy, I. K., Khan, M. A., *Pharmazie*, **2001**; *56*, 66-69.
- ⁴Sastry, S. V., Reddy, I. K., Khan, M. A., *J. Control. Release*, **1997**; *45*, 121-130.
- ⁵Barhate S. D., Patel K. M., Lokhande G. S. *Der Pharmacia Lettre*, **2011**, *3(2)*, 34-38.
- ⁶Kulkarni, A., Bhatia, M., *Iranian J. Pharm. Res.*, **2009**, *8(1)*, 15-25.
- ⁷Thomas, L. M., Khalil, Y. I., *Iraqi J. Pharm. Sci.* **2011**, *20(1)*, 70-79.
- ⁸Singh, B., Chakkal, S. K.; Ahuja, N., *AAPS Pharm. Sci. Tech.* **2006**, *7(1)*, E1-E10.
- ⁹Manivannan R., Chakole V., *Int. J. Recent Adv. Pharm. Res.*, **2011**, *3*, 25-30.
- ¹⁰Singh, A., Deep, A., *Int. J. Pharm. Res.*, **2011**, *3(4)*, 59-62.
- ¹¹Perez-Marcos, B., Iglesias, R., Gomez-Amoza, J. L., *J. Control. Release*, **1991**, *17*, 267-276.
- ¹²Rouge, N., Allemann, E., Gex-Fabry, M., *Pharm. Acta. Helv.*, **1998**, *73*, 81-87.
- ¹³Vázquez, M. J., Casalderrey, M., Duro, R., *Eur. J. Pharm. Sci.*, **1996**, *4*, 39-48.
- ¹⁴Kim, J., Shin, S. C., *Int. J. Pharm.*, **2004**, *273*, 23-27.
- ¹⁵Rodrigues L. A. S., Figueiras, A. C., Veiga, F., Freitas, R. M., Nunes, L. C. C., Filho, E. C. S., Leite, C. M. S., *Colloids Surfaces B: Biointerfaces*, **2013**, *103*, 642-651.
- ¹⁶Iliescu, R. I., Andronescu, E., Voicu, G., Ficai, F., Covaliu, C. I. R. I., *Appl. Clay Sci.*, **2011**, *52*, 62-68.
- ¹⁷Madurai, S. L., Joseph, S. W., Mandal, A. B., Tsibouklis, J., Reddy, B. S. R., *Nanoscale Res. Lett.*, **2011**, *6(15)*, 1-8.
- ¹⁸Chen, Y. M., Zhou, A. N., Liu, B., Liang, J., *Appl. Clay Sci.*, **2010**, *49(3)*, 108-112.
- ¹⁹Joshi, G. V.; Kevadiya, B.D., Patel, H. A., Bajaj, H. C., Jasra R.V., *Int. J. Pharm.*, **2009**, *374*, 53-57.
- ²⁰Meng, N., Zhou, N. L., Zhang, S. Q., Shen, J., *Int. J. Pharm.*, **2009**, *382*, 45-49.
- ²¹Joshi, G. V., Patel, H. A., Bajaj, H. C., Jasra, R. V., *Colloid. Polym. Sci.*, **2009**, *287*, 1071-1076.
- ²²Joshi, G. V., Kevadiya, B. D., Bajaj, H. C., *Microporous Mesoporous Mater.*, **2010**, *132*, 526-530.
- ²³Chen B.Y.; Lee Y.H.; Lin W.C.; Lin F.H., *Biomed. Eng. Appl., Basis Commun.*, **2006**, *18(1)*, 30-36.
- ²⁴Lee, Y. H., Kuo, T. F., Chen, B. Y., Feng, Y. K., Wen, Y. R., Lin, W. C., and Lin F. H., *Biomed. Eng. Appl., Basis Commun.*, **2005**; *17*, 72-78.
- ²⁵Feng, S. S., Mei, L., Anitha, P., Gan, C. W. and Zhou, W. *Biomater.*, **2009**; *30*, 3297-3306.
- ²⁶Dong, Y. and Feng, S. S., *Biomater.*, **2005**; *26*, 6068-6076.
- ²⁷Joshi, G. V.; Kevadiya, B. D., Bajaj, H. C., *Microporous Mesoporous Mater.*, **2010**, *132*, 526-530.
- ²⁸Suvakanta Dash, S., Murthy, P. N., Nath, L. K., Chowdhury, P., *Acta Poloniae Pharm. Drug Res.*, **2010**, *67(3)* 217-223.
- ²⁹Shoib, M. H., Tazeen, J., Merchant, H. A., Rabia Ismail Yousuf R. I., *Pak. J. Pharm. Sci.*, **2006**, *19(2)*, 119-124.
- ³⁰Paulo Costa, P., Lobo, J. M. S., *Eur. J. Pharm. Sci.*, **2001**, *13*, 123-133
- ³¹Vogelpeel, H., Welink J., Amidon, G. L., Junginger, H. E., Midha, K. K., Shah, V. P., Barends, D. M., *J. Pharm. Sci.*, **2004**, *93(8)* 1945-1956.
- ³²Yoldas Seki, Y., Yurdakoc, K., *Colloids Surfaces A: Physicochem. Eng. Aspects*, **2009**, *340*, 143-148
- ³³Ozcan, A. S., Ozcan, A., *J. Colloid Interface Sci.*, **2004**, *276*, 39-46.
- ³⁴Lata, H., Gupta, R. K., Garg, V. K., *Chem. Eng. Commun.*, **2008**, *195*, 1185-1199.
- ³⁵Shahi S. R., Shekhar D. Tribhuwan S. D., Tadwee I. K., Gupta S. K., Zadbuke N. S. And Shivanikar S.S., *Der Pharmacia Sinica*, **2011**, *2(5)*, 54-63.
- ³⁶Rojtanatanya, S., Thaned Pongjanyakul T., *Int. J. Pharm.*, **2010**, *383*, 106-115.
- ³⁷Rakic, V., Rajic, N., Dakovic, A., Aline, A., V., *Microporous Mesoporous Mater.*, **2013**, *166*, 185-194.
- ³⁸Andrade, G. F., Soares, D. C. F., Raquel Gouvea, R., Sousa E. M. B., *Microporous Mesoporous Mater.*, **2013**, *168*, 102-110
- ³⁹Nikolic, C. V., Nikolic, L. J., Stankovic, M., Kapor, A., Popsavin, M., Cvetkovic, D., *J. Serb. Chem. Soc.*, **2007**, *72*, 737-746.
- ⁴⁰Novickis, R.W., Martins, M. V. S., Miranda, L. F., Ribeiro, R. R., Silva, L., Munhoz, A. H., *Adv. Sci. Technol.*, **2013**, *86*, 102-107.
- ⁴¹Pereira R. N., Valente B. R., Cruz, A. P., Foppa T., Murkami F.S. Silva M. A. S., *Latin Am. J. Pharm.*, **2007**, *26(3)*, 382-386.
- ⁴²Wesolowski, M., Barbara, R., *J. Therm. Anal. Calorim.*, DOI 10.1007/s10973-013-3070-y

Received: 06.06.2013.

Accepted: 02.08.2013.